OPTIMISATION OF BIOENERGY SUPPLY CHAINS

Ozlem Akgul

Department of Chemical Engineering
University College London

A Thesis Submitted to University College London for the Degree of Doctor of Philosophy

2013

Declaration

I, Ozlem Akgul, confirm that the work presented in this thesis is my own. Where information has been derived from other sources, I confirm that this has been indicated in the thesis.

Signature: ……..

Date: ……..

Abstract

This thesis aims to address the optimal strategic design of bioenergy supply chains and provide insight into the future implications of these systems. Among the bioenergy supply chains, biomass-to-biofuel (as the main focus), biomass-to-bioelectricity and biomass-to-hydrogen routes are studied within the context of this thesis. To solve these problems, mathematical programming, especially mixed integer linear programming (MILP), models and solution approaches are developed.

Regarding the biofuel supply chains, deterministic, spatially-explicit, static optimisation models are developed first based on single economic objective considering first and hybrid generation systems. A "neighbourhood" flow approach is also proposed for the solution of these models. This approach provides significant computational savings when compared to similar models in literature. The single objective modelling framework is then extended to a multi-objective optimisation model which considers economic and environmental objectives simultaneously. The multi-objective model can provide insight into the trade-offs between the two conflicting objectives. Finally, the single objective static model is further developed into deterministic and stochastic multi-period modelling frameworks to incorporate temporal effects such as change of demand and biomass availability with time as well as uncertainty related to different aspects such as biomass availability.

Regarding the bioelectricity supply chains, a deterministic, spatially-explicit, static, multi-objective mathematical programming model is developed based on mixed integer nonlinear optimisation. This considers electricity generation through biomass enhanced carbon capture and storage (BECCS) systems. The model aims to address issues such as carbon tax levels required to incentivise decarbonisation in the power sector as well as the potential impacts of biomass availability and commodity (carbon and coal) prices.

The biomass-to-hydrogen route is considered as one of the possible conversion pathways within a deterministic, spatially-explicit, multi-period model developed for the optimal strategic design of future hydrogen supply chains. A two-step

hierarchical solution approach is also proposed to increase computational efficiency during the solution of the large scale problem. The model results provide insight into the optimal evolution of a hydrogen supply chain through time.

Acknowledgements

I would like to thank my supervisors Prof. Papageorgiou and Prof. Shah for their continuous support and guidance during my PhD. I would also like to thank CPSE for their financial support, my collaborators and my dear PPSE room friends.

Table of Contents

List of Figures

List of Tables

1 Introduction

This chapter provides background information on global climate change and global energy trends first and then focusses on bioenergy systems. Finally, energy systems modelling, supply chain optimisation and mathematical programming approaches used in supply chain optimisation are explained.

1.1 Global Climate Change

The concentration of greenhouse gases in the atmosphere has been significantly rising and this rise has been linked to mainly human activities. The consequence of the rising emissions is the greenhouse gas effect which leads to continuing warming of the earth and change in the climate system. The first policy response to this increase was the United Nations Framework Convention on Climate Change (UNFCCC) which was adopted in 1992. The objective of the convention was to stabilise the levels of greenhouse gas concentration in the atmosphere that would help mitigate climate change by preventing the dangerous intervention of the anthropogenic activities.

The energy sector currently accounts for 60% of the global carbon dioxide emissions (IEA, 2012c). Therefore, radical changes are required in the way we produce, transform and use energy in order to reduce these emissions. The most significant ones among the suggested changes are improving energy efficiency, reducing the use of carbon intensive fossil fuels by deploying more renewable energy resources and capturing and storing the emitted carbon dioxide.

It is highly recommended that future policies should be based on developing solutions that are based on a balanced approach that recognises the importance of environmental protection, energy security and economic efficiency. Therefore, identifying the links between climate change and energy security with the broader economy is a key issue in shaping future energy policies. For instance, a policy that aims to reduce greenhouse gas emissions without putting emphasis on maintaining a secure and reliable energy supply would have undeniably negative consequences for the energy sector. There is currently a wide range of energy policy scenarios studied

in order to gain insight into the potential evolution pathways of the future energy systems. The next section gives an overview of current and projected global energy mix under different policy scenarios considered by the International Energy Agency (IEA).

1.2 Global Energy Trends

As explained in the previous section, current and future energy policies are likely to have significant impact on the evolution of global energy trends and markets. As an important example to this, the IEA considers three different policy scenarios to study the evolution of future energy markets through to 2035:

a) **Current policies scenario** only considers the implementation of government policies and measures enacted or adopted by mid-2012. It does not take into account any possible future policy actions. This scenario provides a baseline representing the evolution of the energy markets with the current policies.

b) **New policies scenario** takes into account policy commitments that have already been implemented as well as recently announced commitments and plans. The new policies include renewable energy and energy efficiency targets as well as national targets to reduce greenhouse gas emissions and actions in the nuclear industry (phase-out or additions to be adopted). This scenario aims to provide a benchmark for the future implications of the recent energy policy developments.

c) **450 scenario:** selects policies based on a pathway that will achieve the climate change target of limiting the global average temperature increase to $2^{o}C$ in the long term (compared to pre-industrial levels). According to climate experts, the average concentration of greenhouse gases in the atmosphere needs to be limited to 450 ppm CO_2 equivalent (CO_2-eq) to achieve this target. As can be understood from the name, the goal of this scenario is to present a pathway to achieve the climate change target.

Apart from the policy side, economic and population growth, energy and carbon prices as well as technological developments are other key parameters that have an influence on energy markets. Economic and population growth rates are the important drivers that directly affect energy demand. On the other hand, energy prices affect the choice of fuel and technology to meet customer energy demand.

Finally, carbon prices (set through cap-and-trade programmes or carbon taxes) affect the composition of energy demand by changing the relative costs of using different types of fuels. Technology developments will affect energy investment decisions, therefore the cost of supply of energy and the composition and level of future energy demand (IEA, 2010c).

The projected breakdown of the supply of the estimated total global primary energy demand in 2035 between different energy resources under the three different IEA scenarios are represented in Figure 1.1 together with the actual breakdown of demand in 2010 (IEA, 2012c). As can be concluded from the figure, fossil fuels (including coal, oil and gas) remain to be the dominant source of energy across all scenarios although their share in the energy mix varies significantly. The total share of fossil fuels is highest in the current policies scenario (80%) and lowest in the 450 scenario (62%). Demand for renewables (including hydro, bioenergy and other renewables) increases across all scenarios with the highest share of 26% in the 450 scenario (IEA, 2010c).

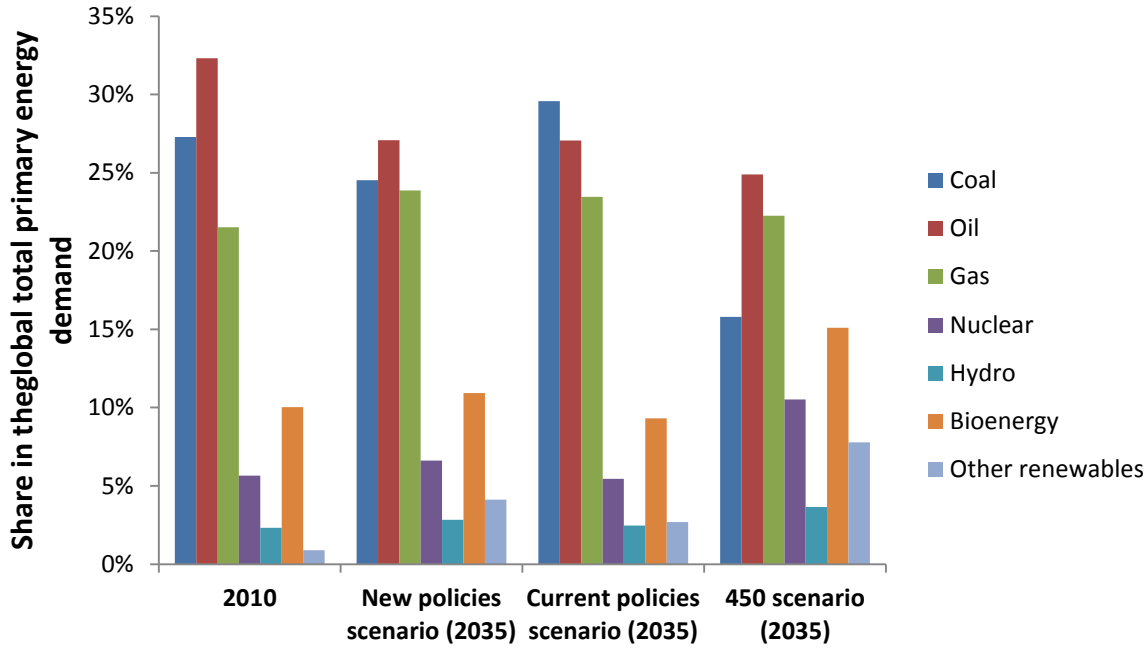

**The category "other renewables" includes wind, solar photovoltaic (PV), geothermal, concentrating solar power and marine technologies.*

Figure 1.1 The projected breakdown of the estimated total global primary energy demand in 2035 under different policy scenarios (IEA, 2012c).

As seen in Figure 1.2, the projected share of production from renewable energy resources in the power, heat and transport sectors increases significantly across all

scenarios in 2035 compared to 2010 (IEA, 2012c). This increase is an expected outcome of the increasing government support for renewables and decreasing renewable energy costs in the future. The share of renewables in electricity generation is higher than heat and transport sectors across all scenarios.

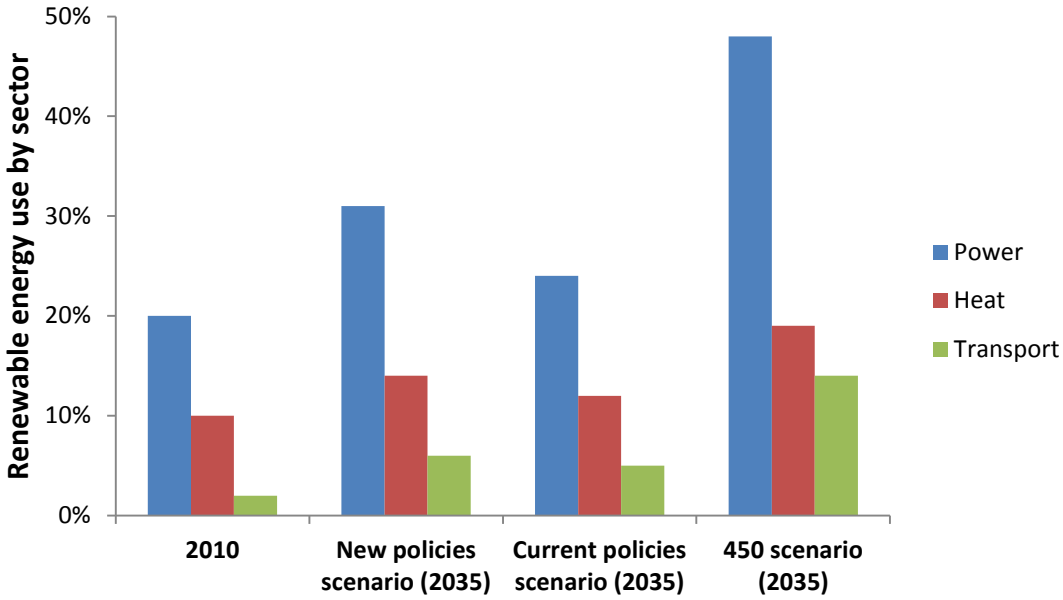

Figure 1.2 The projected share of production from renewable energy resources in the power, heat and transport sectors (% of total production in each sector) in 2035 under the three different policy scenarios of IEA (IEA, 2012c).

The projected global energy related carbon dioxide emissions under the three different scenarios is given in Figure 1.3 (IEA, 2012c). The emissions continue to rise both in new and current policies scenarios. On the other hand, by definition, the 450 scenario is designed to limit the average global temperature increase to 2^{o}C in the long term and keep the emission levels at 450 ppm for this purpose. Therefore, a significant reduction in the global emissions is observed under this scenario compared to 2010 levels.

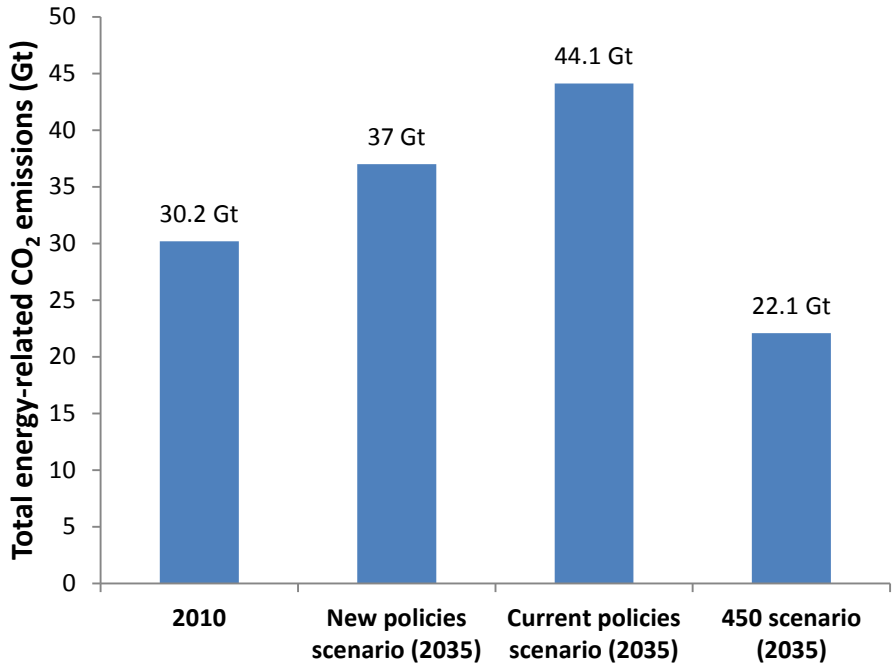

Figure 1.3 The projected energy-related CO_2 emissions in gigatonnes (Gt) in 2035 under the three different policy scenarios (IEA, 2012c).

Having presented different projections for the future global energy trends under different policy scenarios, the next section focusses on outlook for bioenergy, which is the main focus of this thesis.

1.3 Bioenergy Outlook

The term "bioenergy" refers to the energy derived from solid, liquid and gaseous products obtained from conversion of biomass feedstock (including biofuels for transport and biomass products to produce electricity and heat).

Figure 1.4 shows the projected use of bioenergy by sector in 2035 under the new policies scenario (IEA, 2012c). Apart from traditional biomass (wood, charcoal, crop residues and animal dung mainly used mainly for heating and cooking), the power sector is the largest consumer of bioenergy in 2035. It is expected that the growth of demand for bioenergy in the heat and power sectors will mainly be driven by government policies. Combined heat and power, co-firing of biomass with coal and energy from waste are considered to be the most promising technologies in this sense. Apart from that, as seen in Table 1.1, the projected use of biofuels for transport increases by more than three times in 2035 compared to 2010 levels due to the increasing blending rates set by the mandates. Bioethanol will remain to be the

main biofuel used globally (IEA, 2012c). Having presented an overview of the outlook for bioenergy in this section, the next section introduces bioenergy systems in detail.

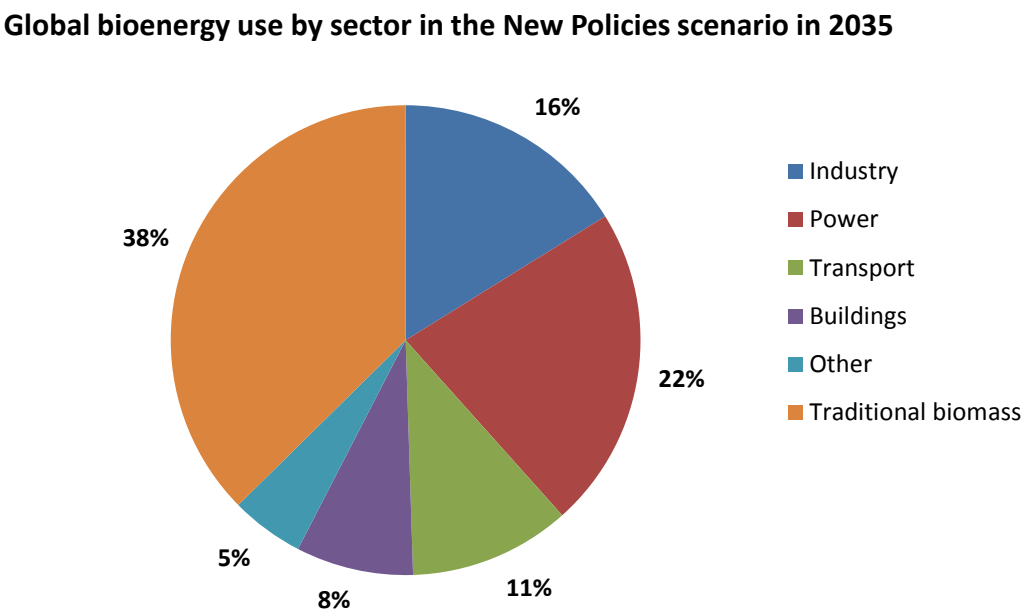

Traditional biomass refers to the use of fuel wood, charcoal, animal dung and agricultural residues in stoves with very low efficiencies.

Figure 1.4 The projected global bioenergy use by sector in 2035 under the new policies scenario (IEA, 2012c).

Table 1.1 Projected global biofuel production in 2035 under the new policies scenario (IEA, 2012c).

	Total global production (mboe/d)	
Biofuel type	2010	2035
Bioethanol	1	3.4
Biodiesel	0.3	1.1
Total	**1.3**	**4.5**

1.4 Bioenergy

As mentioned previously, bioenergy is described as the energy obtained from the conversion of biomass. It has several advantages compared to other renewable energy resources. Firstly, it is capable of producing a continuous, steady flow of

energy in contrast to intermittent wind and solar energy. In addition, it is the only source of high grade renewable heat and can also be used for the production of transport fuels resulting in lower CO_2 emissions compared to conventional fuels. Figure 1.5 shows the different bioenergy conversion pathways which can be used to produce different forms of bioenergy from a range of biomass feedstock types (DEFRA, 2012).

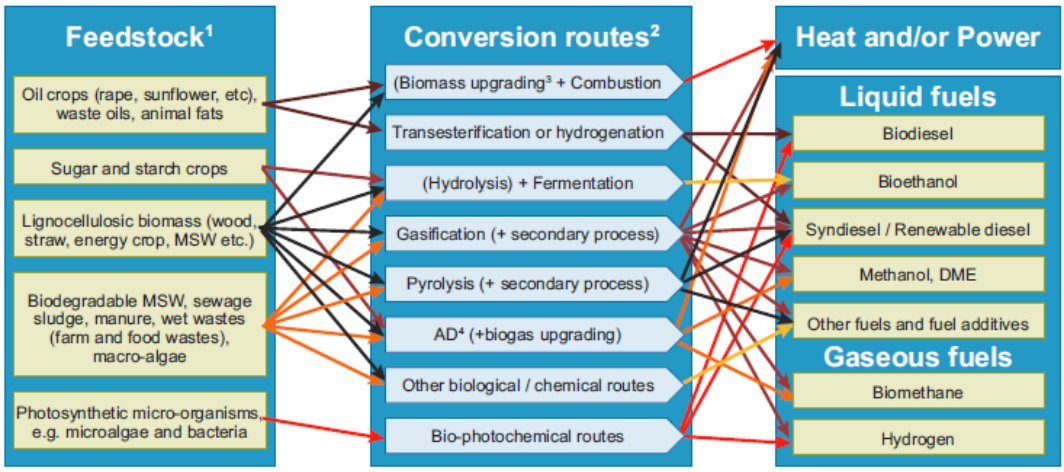

Figure 1.5 Biomass to bioenergy conversion pathways (DEFRA, 2012).

Biomass-to-bioenergy pathways cover a wide range of feedstock types, conversion technologies and end-use applications. Primary conversion processes are categorized under three main classes which are thermochemical, biochemical and mechanical conversion processes. Thermochemical processes are suitable mainly for lignocellulosic biomass with low moisture content (≤50%wb) whereas biochemical processes are mostly applied to biomass with high moisture content (≥70%wb). Mechanical processes are applied in the case of oil extraction from oilseed crops (Dunnett and Shah, 2007). Figure 1.6 shows different thermochemical conversion pathways whereas Figure 1.7 represents biochemical and mechanical conversion pathways.

Among the biomass resources shown in Figure 1.6, arboricultural arisings consist of tree and hedgerow thinnings whereas forestry includes primary fuel wood, residues, and forest industry by-products. Each of these biomass resources has different chemical composition, energy density, moisture content, and bulk handling properties. Depending on the properties of biomass and the requirements of the

conversion process, pre-treatment processes are applied between the supply of resource and conversion process (Dunnett and Shah, 2007; Clarke *et al*., 2009).

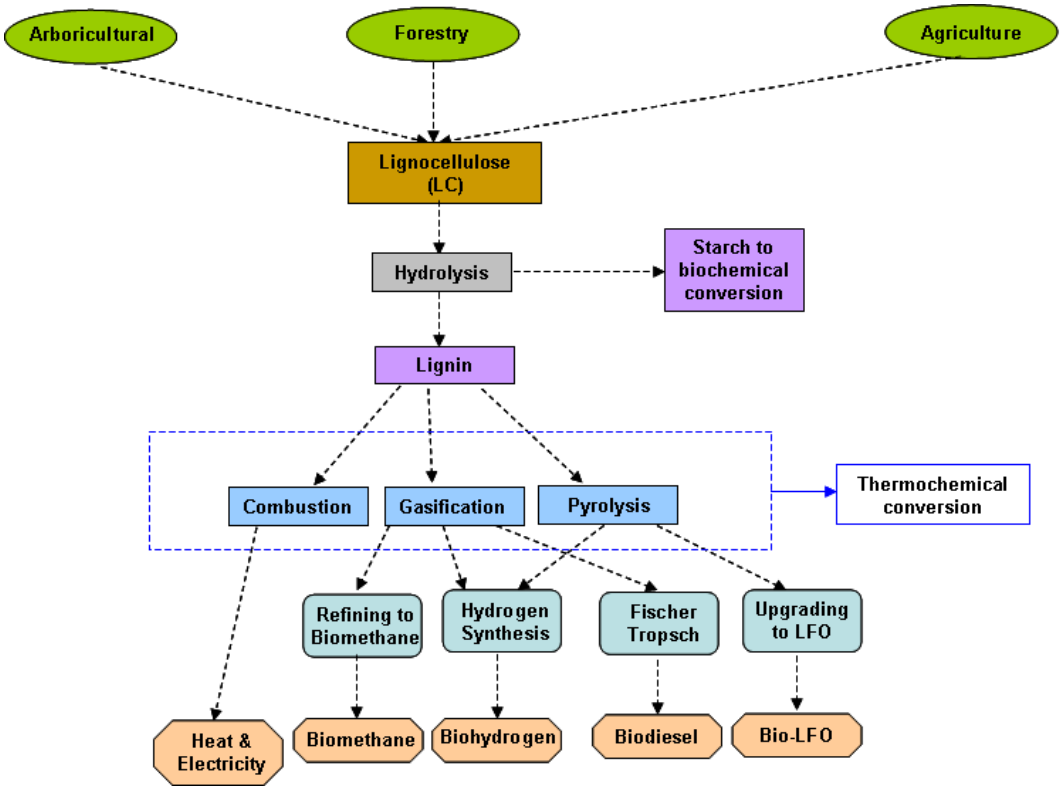

Figure 1.6 Thermochemical conversion pathways for bioenergy systems (Dunnett and Shah, 2007; Clarke *et al.*, 2009).

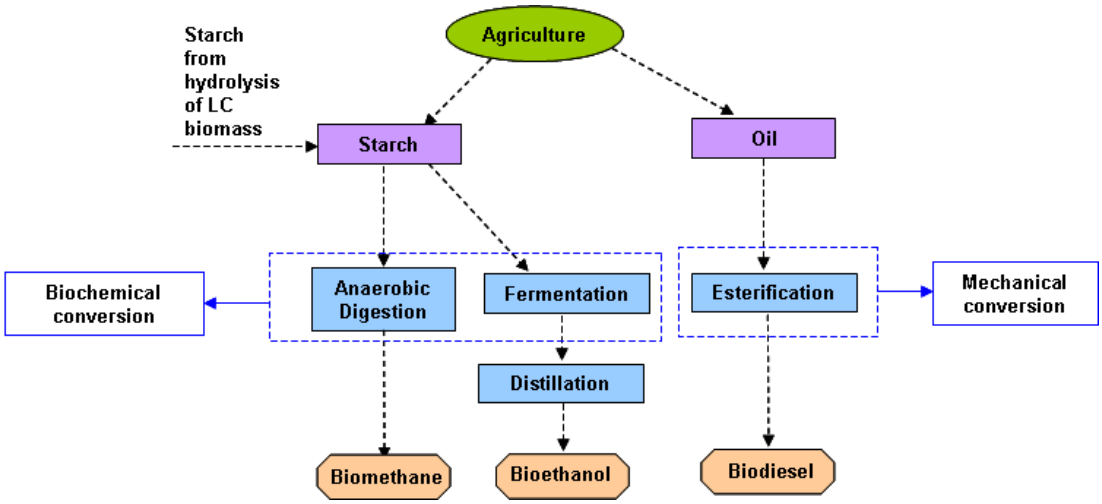

Figure 1.7 Biochemical and mechanical conversion pathways for bioenergy systems (Dunnett and Shah, 2007; Clarke *et al*., 2009).

There are many on-going R&D activities in the area of biofuels globally with the US and Brazil playing the leading roles (mainly for bioethanol production). The main concerns about bioenergy pathways include direct and indirect land use changes, lifecycle carbon reduction and other environmental impacts. Due to the negative potential impacts of the use of first generation crops on food industry, advanced biofuels technologies including second and third generation biofuel production that use non-food crops are being investigated.

Biofuels, as one of the end-use products of bioenergy and the main focus of this thesis, will be explained in detail in the next section. The topics covered include the current and projected future use of biofuels, biofuel types and production technologies, as well as controversial issues associated with their production and use.

1.5 Bioenergy for Heat and Power Generation

A wide range of biomass feedstock types can be used for heat and power generation. Among these are animal and organic wastes, agricultural and forestry residues and dedicated energy crops. Biomass has significant advantages over fossil fuels for producing heat and power. It is geographically distributed, easy to collect and has the potential to produce less carbon emissions during conversion to useful energy. On the other hand, some specific characteristics of biomass compared to fossil fuels may introduce economic and technical challenges. These characteristics include lower bulk density and calorific value, seasonal supply, requirement for more expensive and larger facilities for storing and handling, high moisture content and different chemical composition. Therefore, biomass pre-treatment becomes a crucial step before its conversion to useful energy.

Different pre-treatment processes (also applicable to biofuel production) have been developed to improve biomass characteristics for the processing step. Among these pre-treatment processes are drying, pelletisation, torrefaction, pyrolysis and hydrothermal upgrading. Drying is a basic process utilised to reduce the moisture content of biomass for easier transport and to improve its combustion efficiency. Pelletisation involves mechanically compacting bulky biomass such as sawdust and agricultural residues. In torrefaction, biomass is heated up to high temperatures of about 200-300^{o}C in the absence of oxygen and turned into char. The torrified woody

biomass is usually pelletised and has a higher bulk density as well as higher energy density compared to conventional wood pellets. In pyrolysis and hydrothermal upgrading, biomass is heated to temperatures of about 400-600^{o}C without oxygen to produce bio-oil. The improved energy density of bio-oil makes it more suitable for long distance transport (IEA, 2012d). The biomass-to-heat and biomass-to-power technologies are summarised below.

a) Biomass for Heat

One of the most traditional forms of bioenergy is the use of biomass for domestic heating and cooking. This typically involves the use of an open fire or simple stove where biomass is used as fuel to provide the energy for cooking and heating. The main problem associated with this type of energy is the unsustainable sourcing of biomass and low conversion efficiencies. More efficient biomass stoves have been developed which can provide significantly improved efficiencies.

At commercial scale, the heat generation through biomass combustion plants is a well-established technology. Modern on-site technologies include efficient woodlog, chips and pellet burning stoves, incineration of municipal solid waste (MSW) and use of biogas. Heat from biomass can also be produced in co-generation power plants with a steady heat demand.

b) Biomass for Power

One of the most well-established technologies for generating power from biomass is through a steam turbine which uses the heat produced from direct combustion of biomass in a boiler in biomass-based power plants. The generation efficiencies of biomass-based power plants are smaller than those of fossil-fuelled plants of similar scale.

Co-firing of biomass with coal in existing coal-fired power stations is regarded as one of the most cost-efficient ways of producing electricity from biomass at large scale. This technology makes use of the existing coal power generation plants and therefore requires only minor investments in biomass pre-treatment and feed-in systems. It also makes use of the higher generation efficiencies of these large scale coal plants. Solid biomass feedstocks such as pellets are mostly used for co-firing

whereas liquid and gaseous biomass such tall-oil (a by-product from pulp production) and biomethane can also be utilised.

As another technology for power production from biomass, some co-generation power plants provide an economic use of the heat produced in biomass power generation and also increase the overall efficiency of a power plant. Gas from thermal gasification or anaerobic digestion of biomass can also be utilised to produce electricity via engines or gas turbines providing increased efficiencies compared to steam cycle systems of similar scale.

There are a number of examples to existing biomass power plants in the UK. Tilbury biomass power station a capacity of 750 MWe located in Essex (though recently mothballed) is claimed to be the biggest biomass plant in the world and uses wood pellets as biomass resource. Likewise, the 14 MWe Western Wood Biomass power plant, which is the first biomass power plant in Wales, uses wood biomass to generate power. Ely power station, located in Cambridgeshire, is the world's largest straw-fired power station with a capacity of 38 MWe. There are also a number of biomass CHP plants in planning or under construction. Markins Biomass CHP is currently in the commissioning phase. The plant is designed to have net electricity generating capacity of 49.9 MWe and the capacity to supply 120 tonnes per hour (t/h) of steam.

The next section covers other bioenergy technologies apart from biofuels and biomass-to-heat and biomass-to-power technologies covered so far.

1.6 Other Bioenergy Technologies

One of the emerging bioenergy technologies is the BECCS technology where bioenergy systems are integrated with carbon capture and storage (CCS). CCS is mainly discussed in the context of avoiding the carbon emissions from fossil fuel-based energy generation but this technology could also be used in conjunction with bioenergy conversion plants. Bioenergy with carbon capture and storage could produce energy in the form of biopower, biohydrogen, bioheat and biofuels. The idea behind the bioenergy with CCS (BECCS) systems is that capture of the CO_2 emitted during bioenergy generation and its injection into a long term geological storage

provides with the possibility of removing neutral CO_2 from the atmosphere and hence leads to "negative emissions". Relatively pure CO_2 streams occurring from biomass conversion systems make CO_2 capture easier and reduces the cost of transport and storage infrastructure. The amount of CO_2 captured from bioenergy will increase with the increasing use of biomass co-firing in coal-fired power plants. It is expected that BECCS technology could significantly contribute to achieving carbon emission reduction targets (IEA, 2012d).

The biorefinery is another emerging bioenergy concept. A biorefinery is similar to an oil refinery in the sense that a variety of products can be produced from a certain feedstock, which is biomass in this case. Biorefineries can process different biomass feedstocks into intermediate and final products such as chemicals and food as well as energy. Biorefineries have significant potential to increase the sustainability and efficiency of biomass use by producing a variety of products (IEA, 2012a).

Having introduced biomass-to-heat and biomass-to-power technologies, the next section focusses on several aspects of biofuels as another bioenergy vector.

1.7 Biofuels

Biofuels are regarded to be one of the most promising options for the decarbonisation of the transportation sector, which currently accounts for approximately 23% of the global CO_2 emissions (ITF, 2010). Use of biofuels could potentially contribute to enhancement of energy security, reducing dependency on fossil fuels and also supporting rural development through creating new income opportunities.

Biofuel production started in the mid 1970s with ethanol from sugar cane in Brazil and then from corn in the USA. The fastest growth in global biofuel production has taken place during the recent 10 years mainly through biofuel targets and blending mandates. These targets and blending mandates are driven predominantly by concerns related to energy security and the greenhouse gas emissions problem resulting from the transport sector. The next section provides insight into the current and projected use of biofuels as well as the targets and blending mandates mentioned in this section.

1.1.2 Current and Projected Use of Biofuels

Support policies for biofuels are mainly in the form of blending mandates which set the proportion of biofuel use in the transport fuel mix. These mandates might sometimes be combined with other measures such as tax incentives. Currently more than 50 countries globally have adopted blending mandates or targets. Some of these mandates and targets are presented in Table 1.2 (IEA, 2011).

Table 1.2 Current and future biofuel blending mandates and targets globally (IEA, 2011).

Country/Region	Current mandates/targets	Future mandates/targets
Brazil	B5, E20-25*	
China	E10 (9 provinces)*	
EU	5.75% biofuels**	10% of transport energy from renewables
USA	48 billion litres of which 0.02 billion litres is cellulosic ethanol	136 billion litres of which 60 billion litres is cellulosic ethanol (2022)

**B: biodiesel, E: bioethanol, B5:5% biodiesel blend, E10: 10% bioethanol blend, E20-25, 20-25% bioethanol blend.*

***5.75% was a reference value for the market share of biofuels in 2010 as stated in the EC Directive on the Promotion of the Use of Biofuels or Other Renewable Fuels for Transport (2003). Each member state currently has set different targets and mandates.*

Due to the increasing support through these blending mandates and targets, global biofuel production has increased more than five-fold from 2000 (about 18 billion litres) to 2010 (about 100 billion litres) as seen in Figure 1.8 (EPI, 2011). The USA, Brazil and the EU have together accounted for 90% of global biofuel consumption in 2010. New markets such as China and India are also expected to emerge in the outlook period to 2035 (IEA, 2012c). To a significant extent, the growth of future biofuel use is likely to depend on policy support. Blending rates are expected to increase over time provided a few challenges are overcome, including concerns of consumers about the impact of the increasing blending rates on their engines. Due to the lack of targets and blending mandates for advanced biofuels, the future growth of these technologies is uncertain, which creates challenges for understanding biofuel prospects for future. Currently, the USA is the only country which has specific

targets for advanced biofuels as can be seen in Table 1.2. Financial investment support will be a key driver for these technologies to come online in future.

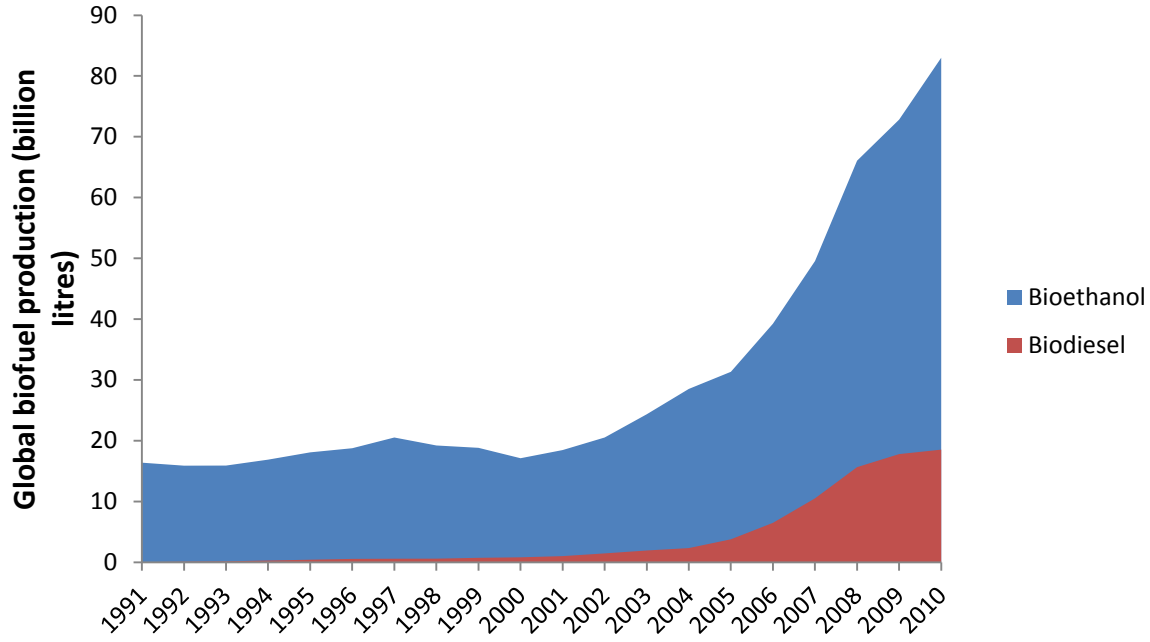

Figure 1.8 Global biofuel production in billion litres from 1991 to 2010 (EPI, 2011).

1.1.3 Types of Biofuels and Production Technologies

Biofuels used for transport are classified as first, second and third generation biofuels according to their current and potential future availability. The first generation biofuels are also named as conventional biofuels as they are produced from well-established and commercially available technologies. On the other hand, second and third generation biofuels, also named as advanced biofuels, are emerging technologies which are under development. Table 1.3 provides an overview of these technologies as well as their current status (IEA, 2011).

Table 1.3 Conventional and advanced biofuel technologies and their current status (IEA, 2011).

Biofuel	R&D	Demonstration	Early commercial	Commercial
Conventional biofuels				
Bioethanol (from sugar and starch crops)				x
Biodiesel (by transesterification)				x
Biogas (anaerobic digestion)				x
Advanced biofuels				
Cellulosic ethanol		x		
Advanced biodiesel (BtL diesel)		x		
Advanced biodiesel (HVO)			x	
Advanced biodiesel (from microalgae)	x			
Bio-synthetic gas (BioSNG)		x		
Biohydrogen (gasification with reforming)	x	x		
Biohydrogen (biogas reforming)		x		
Biohydrogen (all other novel routes)	x			
Biobutanol		x		
Biomethanol			x	
Bio-DME		x		
Pyrolysis-based fuels		X		
Novel fuels (e.g. furanics)	x			

**BtL: Biomass-to-liquids, HVO: Hydrotreated vegetable oil, DME: Dimethylether*

The three different biofuel generation technologies are explained in detail below (IEA, 2011):

a) First Generation Biofuels

First generation biofuels -also named as conventional biofuels- are produced using well-established technologies. The biomass feedstock used includes mainly food

crops such as corn, sugar cane and wheat. The most common first generation biofuel currently in use is bioethanol, followed by biodiesel, vegetable oil and biogas.

- Bioethanol (sugar or starch-based): in the sugar-based process, sucrose which is obtained from sugar crops such as sugarcane, sugar beet and sweet sorghum is fermented to ethanol. The ethanol is then recovered and concentrated. On the other hand, the starch-based process involves an additional step which involves the hydrolysis of starch into glucose. The co-products include dried distillers grains with solubles (DDGS) from maize and cereals to be used as animal feed or as fuel and sugarcane bagasse from sugarcane to be used for energy recovery.
- Biodiesel: is produced from raw vegetable oils derived from soybean, canola, oil palm or sunflower as well as animal fats and used cooking oil. The conversion process involves transesterification of oil and fats to produce fatty acid methyl ester (FAME).The co-products of the process include oilcake to be used as animal feed or energy recovery and glycerine.
- Biogas is produced from anaerobic digestion of biomass such as animal manure and sewage sludge. It can be used for heat or electricity generation or can be upgraded to biomethane and injected into the natural gas grid. It can also be used as transport fuel in natural gas vehicles. The residues from the conversion process can be used as fertiliser.

b) Second Generation Biofuels

Differently from first generation biofuels, second generation biofuels can be produced from a wide range of non-food crops such as waste biomass, stalks of wheat, corn stover and dedicated energy crops such as miscanthus. Two important second generation biofuels are:

- **Cellulosic ethanol** is produced from lignocellulosic biomass feedstock (such as wheat straw, corn stover or dedicated energy crops) using three main technologies including thermochemical conversion, biochemical conversion and a hybrid process which integrates thermochemical and biochemical conversion. Thermochemical conversion uses heat to convert biomass into liquid biofuels and utilises pyrolysis or gasification. In the biochemical conversion, cellulose and hemicellulose components of the lignocellulosic biomass are first converted into fermentable sugars and sugars are then

fermented to bioethanol as in the case of the first generation bioethanol production. Finally, the hybrid process, also called syngas fermentation, uses gasification to produce syngas from the biomass feedstock first and then syngas is fermented to cellulosic ethanol.

- **Advanced biodiesel** includes hydrotreated vegetable oil (HVO) and biomass-to-liquids diesel (BtL). HVO is produced by hydrogenation of vegetable oils or animal fats. BtL diesel (also named as Fischer-Tropsch diesel) is produced in two process steps where biomass is first converted to syngas (consisting of mainly hydrogen and carbon monoxide) through gasification of low moisture biomass and the syngas is then catalytically converted through Fischer-Tropsch synthesis to a range of hydrocarbon liquids including biodiesel.

Apart from cellulosic ethanol and advanced biodiesel, many other second generation biofuels are under development. These include biohydrogen, biomethanol and bio-dimethyl ether (bio-DME).

c) Third Generation Biofuels

Third generation biofuels, also called oilgae are produced from algae. The oil extracted from the organisms can be converted into biodiesel by transesterification. Third generation biofuels include alcohols such as biopropanol and biobutanol which are not expected to become commercially available before 2050. There are some significant challenges that must be overcome before the commercialisation of these technologies. Scaling up of production and concerns related to contamination are the major challenges in this aspect. These areas require significant research and development work (IEA 2011; Dunnett and Shah, 2007; UNEP, 2009).

Having introduced different biofuels types and production technologies, the next section provides an overview of the sustainability issues associated with biofuel production.

1.1.4 Sustainability of Biofuel Production

The sustainability issues surrounding biofuel production are mainly driven by concerns over global emissions and energy security. As an example of this, there has been a growing debate over to what extent biofuels can lead to emission reductions in greenhouse gas emissions due to direct and indirect land use changes. Considering

the close interactions of biofuel production with the agricultural and forestry sectors, it becomes essential to fully understand the environmental, economic and social sustainability of biofuel production. Several issues related to biofuel production falling under each of these three sustainability categories are represented in Figure 1.9. Some of the most significant sustainability issues are explained next.

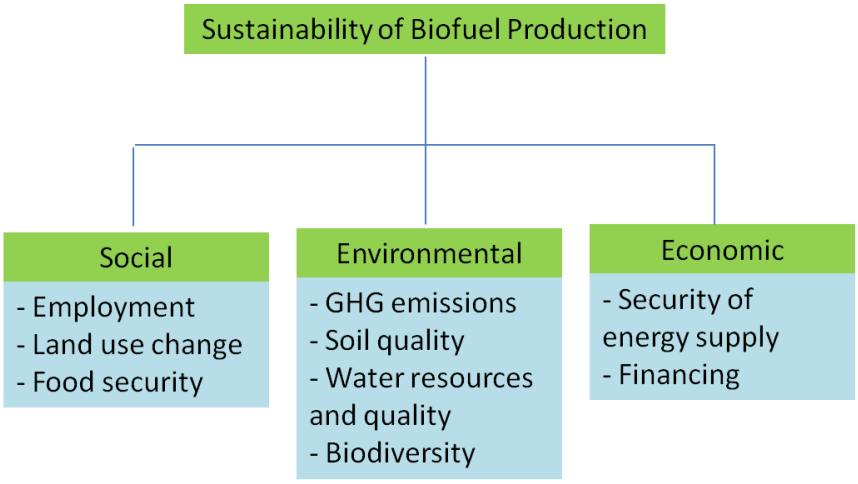

Figure 1.9 Sustainability issues associated with biofuel production (IEA, 2011).

a) Land Use Change and Its Impacts

The future land use estimates for biofuels are highly dependent on factors such as type of feedstock, geographical location and yield increases. Assuming a moderate increase in biofuel production and use, it is estimated that the global land use requirements will range between 35 Mha and 166 Mha in 2020. On the other hand, based on the highest biofuel production potentials, the land required may go up to 1,668 Mha in 2050. For comparison, total global cropland in 2005 was 1,562 Mha. This is likely to result in direct conversion of pastures, grasslands and forests. Therefore, as can be concluded, large scale deployment of biofuels also means large scale land use. This large scale land requirement may result in the clearing of natural vegetation and soil, which may affect the GHG mitigation effect of biofuels and also biodiversity, adversely. In addition, it is anticipated that continuing dependence on first generation crops for biofuels will increase the risk of deforestation**.**

Recent studies have shown that land conversion from forests and grasslands will result in significant CO_2 emissions and 'carbon debts' that might go up to hundred years. Carbon debt is described as the time necessary to counterbalance the CO_2 emissions resulting from the conversion of a native ecosystem. As a result, it is

recommended that the emissions resulting from the conversion of land should be taken into account in the net greenhouse gas balances of biofuels. The land use change can be direct when biofuels are grown on land that was previously forest and indirect when biofuel production displaces the production of other commodities, which are then produced on land converted elsewhere. It must be pointed out that there is currently no standardised approach to account for GHG emissions resulting from land use change although there are several modelling approaches being developed.

Policy makers are aiming to overcome this issue by introducing sustainability standards for biofuels. One of these standards is based on the life cycle GHG emission reduction which should be at least 35% and from 2017 and onwards, 50% for existing and 60% for new plants. However, one of the biggest challenges lies in the fact that these production specific standards cannot capture the indirect effects of land use change. Therefore, it is very important to understand and estimate the dynamics of biomass cultivation, the land requirements and their impacts to be able to foresee the effects of increasing targets and production of biofuels.

One of the largest threats to biodiversity has been identified as land use change for human activities by conversion of natural habitats. The impacts of biofuel production on biodiversity are dependent on the region and type of biofuel being produced. Conversion of protected land may lead to local or global extinctions. Many of these negative impacts could be realised instantaneously or after a short period of time. However, simple quantitative techniques are not adequate to assess these impacts of biofuel production on biodiversity.

Recent studies have shown that positive effects of biofuel production on biodiversity could only be realized when abandoned; formerly intensively used agricultural lands or degraded lands are used for biofuel crop production. These could only be realised in the longer-term after many crop rotations. Overall, the biodiversity balance depends on the land conversion for biofuel crop production and the number of years a particular biofuel crop is grown. There is a potential risk that greenhouse gas reductions from biofuel production may not compensate biodiversity losses from land conversion even in a time period of several decades.

Although there are many uncertainties about the quantification of emissions resulting from land use change due to biofuel production, it is possible to identify ways that can minimise the negative impacts such as production from wastes and residues as feedstock, use of crops with high agricultural yields to maximise efficiency of land use and cultivating perennial crops on unproductive land (IEA, 2011; IEF 2010; OFID, 2009).

b) Food Security

Another major concern about biofuel production is the potential competition with food crops for land and the risk of increasing food prices due to the use of existing food crops for biofuel production. The evidence for this is that the increase in the prices of certain food crops in recent years is mainly due to the increased demand for cereal and oilseeds for biofuel production, low global food stock and high oil and fertilizer prices (OFID, 2009).

The increasing crop prices will in turn have negative impact on food security and poverty at both national and household levels. At the national level, higher prices will affect net-food importing developing countries, especially those with low income and food deficiency. On a household level, the impacts will be realised by mainly poor urban households and poor food buyers in rural areas. However, in the longer term, it is expected that growing biofuel demand and rise in the commodity prices could enhance agricultural growth and rural development. Biofuel crop cultivation could stimulate economic growth in poor, developing countries.

According to recent studies, the prices of agricultural crops depend highly on the share of first generation biofuels in the transport energy mix and deployment of second generation biofuels could lower the risk on food security (IEA, 2011; IEF 2010; OFID, 2009).

c) Water Resources

Availability of water resources has been reported to be a limiting factor for biofuel expansion in the future. Significant amount of water is required for cultivation of biomass crops that will be used for energy or food production. The share of biofuel

crops in the total irrigation water use has been reported to be 1.7-2% in 2005. With increasing food demand and growth in biofuel production, additional strain is expected to be put on water supply.

Most of the water required for biofuel production is used in the production of feedstocks whereas only a small amount is used during processing. In addition to the potential water supply problem, biofuel production might have negative effects on water quality due to the discharge of some waste products. It has been reported that mainly expansion of first generation biofuel production will have severe impacts on both water quality and quantity. Water contamination can occur due to waste produced during biofuel production. Nitrogen contamination from fertilizers as well as eutrophication of surface water and ground water is also a major problem associated with biomass cultivation (IEA, 2006; IEA, 2011; IEF 2010).

Having explained bioenergy systems in detail so far, the next sections give background information on modelling of energy systems in general, supply chain optimisation and mathematical programming approaches used in supply chain optimisation, respectively.

1.8 Modelling of Energy Systems

A mathematical model is the use of mathematical language to describe the behaviour of a system. Mathematical models are as simplifications of real world systems which can help enhance understanding of these complex systems. As an example, modelling of energy systems is described as the application of comprehensive mathematical models to energy systems.

In the framework of energy systems modelling, a wide range of models are applied to different boundaries of the energy system. One might include transport networks whereas the other may cover only a small part of the energy system such as district heating systems. Likewise, the models can be applied to different geographical regions in the world. They can be either simulation-based or optimisation-based. Energy models developed so far can be classified under different categories according to their target group (policy makers, scientists etc.), their purpose of use

(data analysis, forecasting, simulation, optimisation), geographical coverage (regional, national, international) and conceptual framework (top-down, bottom-up).

Energy systems modelling can be utilised for policy and sensitivity analysis, decision-making as well as forecasting of future scenarios (ETSAP, 2004; NEP, 2010). It has played a key role in assessing the costs, trade-offs and pathways related to achieving long-term energy targets such as the biofuel targets described in Section 1.5.1. There are two main modelling approaches in the literature based on the energy-economic modelling of energy and climate policies, known as "bottom-up" and "top-down" models. One of the most differentiating features between the two different classes of energy models is the degree of detail employed in the representation of commodities and technologies. Other differences include economic rationale, level of disaggregation of the decision variables, time horizon over which decisions are made and geographic scope. These two modelling approaches are explained next.

1.1.5 Top-Down Models

Top-down models aim to capture the entire macroeconomy as a whole at a regional or national level by describing the relationship between labour, capital and natural resources such as energy. Energy demand is determined as a result of this relationship. They are referred to as "top-down" models as they try to describe the entire economy through a small number of aggregate variables and equations. Each sector is represented using a production function to simulate the potential substitutions between the different factors of production such as energy and labour. There are different types of top-down models including input-output models, macroeconomic models, computational general equilibrium models and system dynamics.

Input-output models consider the flow of goods and services of a country subdivided into different sectors and users described by specific input/output coefficients. A certain output from a sector such as a service or product is directly related to another sector as an input such as raw materials or energy. These models are more suitable for the evaluation of energy policies in the short term as they can only provide a current picture of the underlying economic structure based on historical data.

Computational general equilibrium (CGE) models try to capture the entire macroeconomy where the energy system is also included. These models are based on the principle that all markets for goods and services are in perfect equilibrium such that there is no excess demand or supply. Since all markets are in equilibrium, non-equilibrium cases such as account imbalances are not considered. Therefore these models do not consider the effects of market failures. Demand and supply are the results of utility maximising consumers and profit maximising producers. These models can be static or dynamic.

Macroeconomic models also try to capture the entire macroeconomy like CGE models. Differently from CGE models, they capture the effects of transitional adjustment costs due to policy changes instead of examining the economy in different states of equilibrium. As a result CGE models are well-suited for long term analysis where the economy can be assumed to be in equilibrium. On the other hand, macroeconomic models are mainly used for short to medium term analysis. One major difficulty with macroeconomic models is their heavy reliance on data which affects the credibility and adequacy of the results.

As another member of the top-down models family, the purpose of system dynamics is to describe the behaviour of an interacting social system taking into account dynamic changes over time among the various components of the system. The interconnections between the different components of the system are defined by feedback control systems or feedback loops represented by differential equations. Likewise, the development of the system over time is defined through differential analysis. One main disadvantage of these models is the validation and calibration of the feedback loops especially when modelling long horizons and when several energy technologies are considered (ETSAP, 2004; NEP, 2010).

1.1.6 Bottom-Up Models

Bottom-up models are technologically explicit models that describe the energy sector of an economy. Each technology is described by its inputs, outputs and specific technical and economic characteristics. A sector is a combination of these technologies linked together with their inputs and outputs. Energy demand is either

given or a function of factors such as energy prices and national income. These models aim to identify the optimal technologies by assessing energy policies, their costs, economic and environmental benefits and similar factors. These models can be formulated as optimisation, simulation or multi-agent models.

As a member of the bottom-up models family, partial equilibrium models are similar to CGE models. They consider a sector or subset of sectors with higher technological detail compared to CGE models. These models focus on energy supply and demand (ETSAP, 2004; NEP, 2010).

Having introduced energy systems modelling in this section, the next sections describe supply chain optimisation and mathematical modelling approaches used in supply chain optimisation.

1.9 Supply Chain Optimisation

A supply chain is described as a network of facilities and distribution mechanisms related to raw material procurement, transformation of raw material into finished products and distribution of these products to customers. Thus, a supply chain has three main components: supply, manufacturing and distribution.

Global enterprises consist of multi-site, multi-product and multi-purpose facilities operating in different geographical locations. Due to the increasing competition between these organisations, large size and complexity of the entire network, as well as strict sustainability and environmental requirements, supply chain analysis has become an essential tool for improvement of the efficiency of enterprises using a whole-system approach.

Supply chain problems can be categorised under the following three classes (Papageorgiou, 2009; Shah, 2005):

1. **Supply chain network design** mostly involves decisions at the strategic level such as where to locate new facilities, what suppliers and supply resources to use for each facility and which products to produce at each facility, which market should be served by which facility and amount of products to be produced and shipped as well as transportation decisions (mode etc.).

2. **Supply chain analysis and policy formulation** is becoming increasingly popular for policy analysis to assess the overall dynamic performance under different operating policies.
3. **Supply chain planning and scheduling** involves decisions related to the use of production, distribution and storage resources as well as timing and sequencing of operations in a fixed network structure efficiently to optimise the overall chain performance.

The possible quantitative performance measures used in supply chain analysis include cost minimisation, profit maximisation and minimisation of environmental emissions. Supply chain models can also be classified as (Papageorgiou, 2009; Shah, 2005):

- Mathematical programming approaches, which involve optimising the overall supply chain performance under unknown configurations with an aggregate view on dynamics and detail of operation,
- Simulation-based models, which are used to analyse the detailed dynamic operation of a fixed configuration under operational uncertainty.

As the main focus of this thesis, the main elements of a bioenergy supply chain can generally be described as biomass cultivation, transport of biomass from supply sites to conversion facilities, biomass-to-bioenergy conversion and production of the final product (e.g. transport fuel, heat or power generation) and finally distribution of the final product to the demand centres. All these elements must be considered simultaneously during optimisation of a bioenergy supply chain, which can then be used to assess the economic, environmental and technical implications of such future energy systems.

1.10 Mathematical Programming Approaches in Supply Chain Optimisation

As mentioned in the previous section, mathematical programming approaches are widely utilised for optimisation of supply chain performance. A mathematical programming (or optimisation) problem involves minimising or maximising an objective function subject to a set of constraints, which can be represented a follows:

$$\begin{aligned} \min \quad & f(x) \\ s.t. \quad & g(x) \le 0 \\ & h(x) = 0 \\ & x \in X \end{aligned}$$

where x is the decision variable, $f(x)$ is the objective function, $g(x)$ and $h(x)$ are the inequality and equality constraints, respectively. Based on the nature of the objective function and the constraints, mathematical programming models can be classified into the following categories:

- Linear programming (LP): the special case when the objective function, $f(x)$ and the constraints, $g(x)$ and $h(x)$ are all linear functions,
- Quadratic programming: $f(x)$ is at most a quadratic function, and $g(x)$, and $h(x)$ are linear functions,
- Mixed integer programming: the special case where both integer variables, y and continuous variables,x are considered,
- Nonlinear programming (NLP): the objective function, $f(x)$ and/or the constraint functions, $g(x)$ and $h(x)$ are nonlinear functions.

Many supply chain problems related to chemical process industries involve decision variables that can only take integer values (such as the number of trays in a distillation column) and therefore, fall under mixed integer programming. The integer variables that can only take the value of 0 or 1 (related to decisions such as building a new facility) are named as “binary variables”.

In a mixed integer programming (MIP) model, the objective function is dependent on two types of variables: x, which is a set of continuous variables and y, which denotes a set of integer variables. The MIP problems which are linear in the objective function and constraints are named as “mixed integer linear programming” (MILP) models and can be solved using linear programming approaches. On the other hand, MIP problems that include some functions which are nonlinear are named as “mixed integer nonlinear programming” (MINLP) models (Edgar *et al.*, 2001; Papageorgiou *et al.*, 2010).

Several solution methods and algorithms have been developed to provide efficient solutions for different mathematical programming problems. Among these solution methods are, branch & bound method (Land and Doig, 1960), cutting plane method

(Gomory, 1958), interior point method (Karmarkar, 1984) and quasi-Newton method (Davidon, 1959).

1.11 Scope of This Thesis

The scope of this thesis is to fill the gap in current literature work related to bioenergy supply chains, predominantly biofuels. The implications of these systems are investigated using mathematical programming approaches, mainly mixed integer linear programming-based approaches and solution procedures. The topics covered in this thesis include single and multi-objective optimisation of bioenergy systems considering economic and environmental objectives, multi-period optimisation taking into account change in demand and supply through time as well as optimisation under uncertainty regarding different supply chain aspects such as demand. By addressing these issues, this thesis aims to improve current literature on bioenergy supply chains for the existing problems as well as make novel contributions to this field.

This thesis provides important contributions to the current literature by addressing some existing gaps. The main contributions can be summarised under the three main topics covered in this thesis: biofuel supply chains, bioelectricity supply chains and hydrogen supply chains. Firstly, in the field of biofuel supply chains, the main novel contribution on the modelling side is the developed "neighbourhood flow approach" which has proven to offer significant computational efficiency when compared to similar models in literature. In addition, biofuel production in the UK has been studied in detail which has considered some important aspects such as use of dedicated energy crops for biofuel production, their cultivation on set-aside land for this purpose as well as sustainable use of this land, first generation crops and their by-products. To the best of our knowledge, implications of biofuel production in the UK have not been investigated in such detail before by any other existing literature work. Secondly, bioelectricity supply chains based on the emerging concept of bioenergy with CCS (BECCS) systems have not been considered in detail by existing literature work which has been addressed in Chapter 4 of this thesis. The developed modelling framework integrates supply chain aspects with power generation which has again not been investigated before in the context of bioelectricity production. Finally, in the field of hydrogen supply chains, the main novel contributions include the development of a "modified neighbourhood flow" approach and a hierarchical

solution procedure- which together provide significant computational savings- as well as the development of CCS network constraints.

1.12 Thesis Overview

The rest of this thesis is organised as follows:
A detailed literature review on bioenergy systems is presented in Chapter 2 which provides relevant background information for the bioenergy supply chain problems addressed in the subsequent chapters.

Chapter 3 presents the developed mixed integer linear programming (MILP) approaches for biofuel supply chains. This chapter is broken down into two main subsections including static and multi-period optimisation. The static optimisation approaches focus on single or multi-objective. The multi-period optimisation covers deterministic optimisation as well as optimisation under uncertainty.

Chapter 4 introduces a static, multi-objective mixed integer nonlinear programming (MINLP) framework for the optimisation of bioelectricity supply chains which is developed based on the approaches introduced in Chapter 3. Bioelectricity generation through biomass co-firing with coal integrated with carbon capture and storage is considered. The model provides insight into the effects of key parameters such as commodity prices (coal and carbon) and biomass availability on the economic and environmental performance of these systems.

Chapter 5 presents a multi-period MILP model for the optimal design of hydrogen supply chains taking into account a set of hydrogen production technologies where hydrogen production form biomass is considered as one possible option. The model considers carbon capture and storage and aims to provide insight into the economic feasibility of hydrogen as a transport fuel and the optimal time evolution of a hydrogen supply chain.

Finally some conclusions are drawn in Chapter 6 making link to various chapters and it also provides recommendations for future work.

2 Literature Review

Having introduced the relevant background behind energy systems focussing on bioenergy systems, energy systems modelling, supply chain optimisation and mathematical programming approaches used in supply chain optimisation in Chapter 1, this chapter presents relevant literature work on bioenergy supply chain optimisation as the main focus of this thesis. This chapter also includes a section for hydrogen supply chain optimisation for which a developed modelling framework is introduced in Chapter 5. The proposed modelling framework considers hydrogen production from biomass as one of the possible conversion pathways.

2.1 Optimisation of Bioenergy Supply Chains

This section introduces literature related to bioenergy supply chain optimisation in two subsections including biofuel supply chain optimisation and optimisation of other bioenergy supply chains.

2.1.1 Biofuel Supply Chain Optimisation

The global demand for petroleum-based fuels has been rising rapidly due to the increasing industrialisation of the world. Today, fossil fuels provide about 80% of the global primary energy demand, around one fourth of which is consumed by the transport sector. However, fossil fuel resources are becoming exhausted with the increasing consumption to satisfy the rising global demand. As explained in Chapter 1, the use of fossil fuels for energy has been found to be the major contributor to greenhouse gas (GHG) emissions, which leads to various negative impacts including climate change. As a result, the continuing depletion of the fossil fuels with increasing energy demand and GHG emissions have led to the need to shift towards alternative, sustainable, environmentally-friendly and cost-effective resources of energy.

Among the alternative resources, biofuels are regarded as a favourable replacement for fossil fuels due to their renewability and the potential to reduce greenhouse gas emissions through the absorption of CO_2 by photosynthesis during the plant life cycle. In addition, their market maturity is higher when compared to other

alternatives such as hydrogen. As explained in Section 1.5.1, minimum blending quotas and targets have been set around the globe to promote the use of biofuels. The EU Commission has set a target of 10% share of renewables in supplying transport energy by 2020. Several control measures such as tax exemptions or reductions are applied by the member countries to achieve this target. Countries around the world have adopted different measures for the use of biofuels.

The economics of each fuel type is dependent on the geographical location, biomass feedstock, technology utilised and several other factors. One of the main problems related to the use of biofuels is how to fit them into the existing transport and fuel distribution networks. Environmental and political concerns also affect the extent to which these fuels are utilised. Significant research and development activities are on-going for investigating more sustainable and environmentally-friendly feedstock and production technologies in this field.

As described in Section 1.9, supply chain optimisation is an important tool to gain insight into the implications of future bioenergy supply chains. Literature work related to the application of this mathematical programming tool to biofuel supply chains will be introduced next.

2.1.1.1 Economic Optimisation of Biofuel Supply Chains

As described previously in Section 1.9, a biofuel supply chain is a multi-echelon network consisting of biomass cultivation sites, biofuel production facilities and demand centres. Application of supply chain optimisation to such systems means consideration of all these nodes in the chain as well as transport of biomass and biofuel between these nodes simultaneously.

There are several studies in the literature that focus on the optimisation of the economic performance of biomass and biofuel supply chains. Mathematical models for supply chain optimisation can be static (steady-state) or multi-period (dynamic) depending on whether temporal effects (e.g. change of demand and supply with time) are incorporated (multi-period approach) or a snapshot in time is considered instead (static approach). Marvin *et al.* (2013) propose a mixed integer linear programming (MILP) model for the optimal biorefinery location and technology selection. The

model is applied to a case study of biofuel supply chain in the Midwestern United States. The case study considers the existing corn ethanol facilities, new candidate sites, eight types of biomass, four types of biofuel, and seven different biomass processing technologies. The different types of biomass feedstock taken into account include conventional crops, agricultural residues, forest biomass, wood waste and energy crops. The results of the case study imply that the Midwest can produce enough biofuel (including cellulosic and other advanced biofuels) to meet the 2015 mandate. Kelloway *et al.* (2012) present an MILP model for the optimisation of a distributed small scale biodiesel production system in Greater London with the objective to maximise the net present value of the system. Waste cooking oil is considered as the biomass feedstock and the results imply that small scale distributed biodiesel production is economically feasible in this region. Kim *et al.* (2011b) develop an MILP model for the optimal design of biomass processing networks for biofuel production. The model aims to determine the optimal selection of fuel conversion technologies, capacities, locations of biomass supply and logistics of transportation for delivery by maximising the overall profit. In their work, they analyse the design of both distributed and centralised conversion systems as well as their robustness to demand variations. Dyken *et al.* (2010) propose a mixed integer linear programming approach for biomass supply chains including supply, transport, storage and processing of biomass. The developed generic framework can allow for modelling of multiple biomass types and technologies. Two important aspects of this work are the representation of the relationship between moisture and energy content of different biomass types and also taking into account long term effects such as passive drying (change of quality) during storage. Zamboni *et al.* (2009a) develop a spatially-explicit, static, mixed integer linear programming model for the strategic design of a future bioethanol supply chain with the objective to minimise the overall cost. The applicability of the model is demonstrated with a case study of bioethanol production from corn in Northern Italy. They conclude that biomass importation can help support market penetration of biofuels and serve as a source to meet the increasing production targets until second generation technologies become available.

Transportation comprises an important part of the total biomass and biofuel supply chain cost. Yu *et al.* (2009) propose a discrete mathematical model for a mallee biomass supply chain in Western Australia that takes into account biomass

production, harvest, on-farm haulage and road transport to a central bioenergy plant with the objective to minimise the total delivered cost of biomass. They conclude that transportation is a significant cost component of the overall supply chain and therefore, propose some strategies for reducing this cost such as locating the biomass processing plant near areas with high biomass cultivation density. Morrow *et al.* (2006) use a linear optimisation model to determine the cost of distributing various ethanol fuel blends to all metropolitan areas in the Unites States. The results imply that transportation cost is a significant contributor to the overall cost and the transport infrastructure has to be improved to increase the competitiveness of ethanol as a fuel in the longer term.

As second-generation biofuel production is an emerging technology, opportunities might exist to integrate this emerging technology with existing first generation facilities resulting in hybrid first/second generation biofuel systems. In a wider context, biorefineries which produce a variety of useful products using different biomass resources have attracted significant attention in the recent years as the desire to use renewable sources of energy increases. In these potential systems of the future, biomass can be processed into plastics, chemicals, fuels and power. Thus, the maximum value of the biomass resources is utilised by the help of the advanced technology of biorefineries (IEA, 2012a; Naik *et al*., 2010). Some studies that focus on these newly-emerging technologies can be found in the recent literature.

Elia *et al.* (2013) develop a nationwide MILP-based optimisation framework for a biomass-to-liquids supply chain. Hardwood biomass resources in the US are utilised to produce gasoline, diesel and jet fuel. The optimisation model takes into account water resources and electricity requirement of the supply chain and provides useful insight into the optimal strategic locations of the BtL refineries. Marvin *et al.* (2012) introduce an MILP model for the economic optimisation of a lignocellulosic bioethanol supply chain in the Midwestern United States where the objective is the maximisation of the net present value. A biochemical conversion route is considered for producing ethanol from five different types of agricultural residues and a sensitivity analysis is carried out to study the impact of price uncertainty on the robustness of the supply chain design. Corsano *et al.* (2011) propose a mixed integer nonlinear optimisation model for the optimal design of a bioethanol (from sugarcane)

supply chain with the objective to maximise the net profit. The supply chain model is integrated with a detailed plant model so that plant and supply chain designs are obtained simultaneously. Sustainability issues such as residual recycle are also taken into account. Bowling *et al.* (2011) present a modelling framework for the optimal planning and facility placement for a biorefinery system. The model aims to determine the optimal supply chain configuration including the optimal selection of biomass feedstock types, and locations of the biorefinery and pre-processing hub facilities by maximising the total net profit. Bai *et al.* (2011) study a mixed integer nonlinear programming (MINLP) model for the optimal biorefinery location and supply chain planning under traffic congestion with the objective to minimise the total system cost. The total system cost accounts for costs for establishment of refineries, shipping of biomass and ethanol within the supply chain and the total travel cost for the public traffic. The proposed MINLP model is solved using a langrangian relaxation-based heuristic algorithm to obtain a near-optimum feasible solution. A branch and bound framework is also introduced to improve optimality. Leduc *et al.* (2010) develop a model for the optimal location of lignocellulosic ethanol refineries where ethanol production is integrated with combined heat and power plants. They conclude that biomass cost, availability and price of district heating are the important factors that affect the optimal location of a polygeneration plant.

Parker *et al.* (2010b) develop a mixed integer linear programming model that seeks to determine the optimal locations, technologies and scales of biorefineries by maximising the total profit. Input data to the model include spatial availability of feedstock resources, existing and potential biorefinery locations and a transportation network model. Kim *et al.* (2010) present a mixed integer linear programming model for the optimal design of biorefinery supply chains. The model aims to maximise the overall profit and takes into account different types of biomass, conversion technologies as well as several feedstock types and plant locations. In their work, they analyse both central and distributed systems.

Huang *et al*. (2010) develop a mixed integer linear programming model for the optimal multi-stage optimisation of an ethanol supply chain based on the minimisation of total system cost. They consider ethanol refineries that use different

types of biomass feedstock. The applicability of the model is investigated with a case study of ethanol production from eight different biomass waste resources in California. Tittmann *et al.* (2010) develop a spatially-explicit (where spatial distribution is taken into account explicitly in the formulation) techno-economic model for bioenergy and biofuel production in California. The model aims to maximise the profit from bioenergy production at a given market price for fuels, electricity and their co-products. The model is coupled with a geographic information system (GIS) and considers the spatially-explicit feedstock supply curves, several potential conversion technologies as well as geographical dependency of bioenergy demand. Eksioglu *et al.* (2009) propose a dynamic mathematical model for the design and management of a biomass-to-biorefinery supply chain. The model determines the optimal number, size and location of biorefineries to produce biofuel from a range of available biomass feedstock as well as the optimal amount of biomass to be processed, shipped and biomass inventory levels during a time period.

In the context of the "food vs"fuel"debate, it has been widely discussed that increasing biofuel production and the resulting land use competition will drive up the prices of agricultural products and food. As a result, it becomes crucial to gain a better understanding of the interactions between biofuel production, food industry and agricultural sector. Kretschmer *et al.* (2009) analyse the economic implications of the EU 10% biofuel target in this aspect. The results of their study show that the EU agricultural sector prices may increase by 7% in 2020 with the increasing biofuel production to meet the target. Duer and Christensen (2010) carry out a socio-economic cost analysis to investigate the costs of meeting the EU biofuel targets. The results indicate that high crude oil prices could significantly improve the economic benefits of biofuels; however the increasing demand is likely to drive up the biomass feedstock and biofuel costs. In addition, it is expected that pricing of GHG emissions can help minimise the socio-economic costs of biofuel systems.

Another important aspect that must be considered in supply chain optimisation studies is the fact that technological learning and resulting cost reductions over time can significantly affect the economic competitiveness and hence, the market share of biofuels compared to other fuels. Hettinga *et al.* (2009) assess technological learning quantitatively based on reductions in production costs and energy use in US ethanol

production. The results of their analysis show that US corn production and ethanol processing costs have declined with cumulative production over time and experience curve approach can be used to describe this trend. This approach can also be utilised to estimate future cost decline by taking into account projected production and detailed cost breakdowns. Bake *et al.* (2009) investigate the reasons behind the cost reductions of Brazilian bioethanol production and whether the experience curve concept can be used to describe the development of feedstock production and processing costs. They conclude that this approach can provide insight to the factors that lowered the costs in the past and also, can provide more accurate estimations of future cost developments. Wit *et al.* (2010) investigate the impact of different technological learning assumptions on market penetration of biofuels. An analysis is carried out using the European BioTrans model, which aims to determine the least cost biofuel route. The results imply that market share of advanced biofuels may go up to 60% by 2030.

2.1.1.2 Green Supply Chain Management (GrSCM) and Biofuels

With the increasing global industrialisation and technological developments, human society is facing important problems such as depleting natural resources and environmental pollution to tackle. The biggest challenge for enterprises is to keep the balance between economic benefits, environmental protection and sustainable utilisation of resources. As a potential way of dealing with this issue efficiently, green supply chain management (GrSCM) can be defined as the integration of environmental consciousness with supply chain management. This concept covers product design, supplier selection, material procurement, manufacturing and packaging of products and delivery of these products to consumers as well as management of the product after the end of its useful life. In this aspect, GrSCM can be considered to be quite related to to the concept of "industrial symbiosis" which is a part of industrial ecology dealing with interaction and utilisation of processes and flows such as recycling of residues for the development of new symbiosis products to increase environmental, energy and material efficiencies and reduce costs. The importance of GrSCM has been growing significantly with the exhausting natural resources, increasing levels of waste and environmental pollution (Srivastava, 2007). The studies on GrSCM in the literature can be divided into three main categories:

- Studies emphasising the importance of GrSCM (Larsen *et al.*, 2012; Ping and Zhang, 2008; Linton *et al.*, 2007; Beamon, 2005),
- Studies focussing on green design, which covers environmentally conscious design (ECD) and life-cycle analysis (LCA) (Chan *et al.*, 2013; Chunshan *et al.*, 2009; Allen and Shonnard, 2001),
- Studies on green operations that include green manufacturing and remanufacturing (to minimise energy and resource consumption), green procurement, and waste management (Diabat *et al.*, 2013; Savaskan *et al.*, 2004).

Both linear and nonlinear mathematical programming approaches have been applied to GrSCM problems. Ramudhin *et al.* (2008) propose a mixed integer programming approach for the optimal green supply chain network design by taking into consideration carbon trading. The environmental impact of the supply chain is measured in terms of total GHG emissions (t CO_2-eq) stemming from supply chain activities and the total emissions are converted to carbon credits by multiplying them with the carbon price (per t CO_2-eq) in the market. The results of their analysis show that in an environmentally-friendly world, the assessment of the total carbon footprint of supply chains will be an important factor that will have a determining effect on the way these networks will operate. Using a similar approach, Diabat and Simchi-Levi (2009) develop a mixed integer modelling framework that seeks to determine an optimal strategy for the operation of a company supply chain to meet its carbon cap by minimising the total opportunity cost. The results of the case study indicate that supply chain managers should consider potential future decreases in the carbon emission allowances when setting their carbon footprint targets.

Mostly, there are many conflicting objectives in supply chain optimisation problems. In this aspect, multi-objective optimisation can be regarded as a useful mathematical programming tool to consider these conflicting objectives simultaneously. Various solution approaches have been developed for solving such problems. The main difference between different approaches is the degree of involvement of the decision-maker during the solution process. Some may require input from the decision-maker during the solution process whereas others do not. In the *a priori* methods, the different objectives are weighed and grouped together in a single objective according

to the needs of the decision-maker. On the other hand, *a posteriori* methods provide a set of pareto optimal solutions based on the trade-off between the conflicting objectives. The decision-maker can then make a choice between different alternatives depending on his preferences and needs (Rangaiah, 2009; Zamboni *et al*., 2009b). The commonly utilised ε-constraint method, which belongs to the class of *a posteriori* methods, is based on treating all objectives except one as a constraint and solving the resulting single objective problem (Gurel and Akturk, 2007).

As an example of multi-objective optimisation in the field of green supply chain management, Hugo *et al.* (2005) develop a multi-objective mixed integer linear programming model for the strategic long range investment planning and design of future hydrogen supply chains. The two conflicting objectives considered are maximisation of net present value and minimisation of total environmental impact measured in terms of total GHG emissions. The model can identify optimal supply chain design, capacity expansion policies as well as investment strategies. Santibanez-Aguilar *et al.* (2011) propose a multi-objective optimisation model for the optimal planning of a biorefinery considering different types of feedstock, production technologies and products. The environmental impact is evaluated based on the eco-indicator-99 methodology. The model is applied to a case study of a biorefinery in Mexico. You and Wang (2011) introduce a multi-objective, multi-period, MILP model for the optimal design of biomass-to-liquids supply chains with distributed-centralised processing networks. The economic, environmental and social objectives are measured through the total annualised cost, the total life cycle greenhouse gas emissions and the total number of accrued jobs, respectively. The resulting model is solved using the ε-constraint method.

Several indicators have been used in the literature for evaluating the environmental impacts of biomass supply chains such as sustainable process index (SPI) and carbon footprint(Klemes *et al.,* 2007). Corbiere-Nicollier *et al.* (2011) propose a new global criterion based framework that aims to handle environmental, social and economic sustainability issues. The model enables the comparison of bioethanol supply chains at international level based on different sustainability indicators. Several tools have been developed and used so far to quantify the environmental impacts including life cycle assessment (LCA), the environmental fate and risk assessment tool and

thermodynamic analysis method (emergy and exergy) (Chunshan *et al.*, 2009). The environmental fate and risk assessment tool is used to quantify the environmental risk associated with industrial processes based on a global environmental risk assessment index (GERA) (Achour *et al.*, 2005). Among the thermodynamic methods, emergy (embodied enegy) is the energy used directly or indirectly to make a product or service and therefore is a measure of ecological investment and cost. On the other hand, exergy focusses on the available energy that can be converted into useful work from any product or process. Emergy and exergy analysis can together be used to assess the environmental impacts of industrial processes or products (Bakshi, 2002). LCA has proven to be one of the most efficient techniques for the assessment of the environmental impact of supply chains. Environmental LCA can be defined as a "cradle-to-grave" approach that seeks to evaluate the cumulative environmental impact resulting from all the stages in the product life cycle (EPA, 2006). Several studies in the literature focus on the assessment of environmental performance of biofuel systems adopting this approach (Acquaye *et al.*, 2011; Cherubini and Jungmeier, 2010; Iriarte *et al.* 2012).

The extent of greenhouse gas emission savings that can be achieved through biofuel production remains uncertain due to several reasons. First, emission savings are partially offset by the energy needed for cultivation, harvesting, processing and transportation steps in a biofuel supply chain. The energy requirements can differ significantly depending on the biomass crop used. Secondly, the direct and indirect land use change due to biofuel crop cultivation is likely to result in significant emissions, which can completely displace any potential environmental benefits of biofuels Therefore, it is recommended that biomass feedstock production must avoid agricultural land that is used for food production to maintain a sustainable biofuels industry and policies supporting biofuel production must ensure that biofuel crop production is directed towards idle or marginal land that is not used for food production. Otherwise, the displacement of this agricultural land may result in net greenhouse gas emissions rather than savings. (IEA, 2008; Naik *et al.*, 2010; Cherubini *et al*., 2009).

Cherubini *et al.* (2009) report key issues in LCA of bioenergy systems and provide an overview of the GHG and energy balances of the most common bioenergy

systems. It is reported that biofuel systems can contribute to the reduction of GHG emissions provided the emissions from land use change are avoided and more-environmentally-friendly production technologies are utilised. In addition, perennial grasses such as miscanthus can enhance carbon sequestration in soil if cultivated on set-aside and annual row crops land. According to the study of Singh *et al.* (2010), the social barriers for the use of first generation crops to produce biofuels (such as competition with food sector) can be partially overcome with the utilisation of second generation lignocellulosic feedstock. They also report that a lignocellulosic biorefinery system can provide up to 60% GHG emission savings compared to the fossil fuel reference system. Gnansounou *et al.* (2009) pointed out that significant variations in GHG balances on biofuel systems can occur depending on the system definition and boundaries, choice of reference systems and allocation methods.

Literature work related to environmental optimisation of biofuel supply chains is not as common as studies dealing with the economic objective. Environmental impact is mostly considered in a multi-objective framework together with the economic objective rather than as a single objective. Cucek *et. al.* (2012) study a multi-objective mixed integer nonlinear programming model for the optimisation of regional biomass supply chains which considers economic, environmental and social objectives. They analyse the trade-offs between the total profitability and the total social and environmental footprints through pareto curves. Different environmental footprints are considered including carbon, energy, water, agricultural land and water pollution footprints. Giarola *et al.* (2012b) develop a multi-objective mixed integer linear programming model for the optimal capacity planning and technology selection for bioethanol supply chains. The model aims to optimise the environmental and financial performances of the supply chain simultaneously. The results provide insight on how the optimal supply chain design and technology selection change with respect to different objectives. You *et al.* (2012) present a multi-objective mixed integer linear programming framework for the optimal design of cellulosic biofuel supply chains considering environmental, economic and social objectives. The model takes into account specific characteristics of cellulosic supply chains such as seasonality of biomass supply, biomass degradation and feedstock density. The model is applied to two different case studies where trade-offs between the different objectives are analysed through pareto curves.

Zamboni *et al.* (2011) propose a whole-systems optimisation framework for GHG emissions reduction. The results indicate that adopting an efficient crop management strategy can contribute significantly to mitigation of global warming even when utilising only first generation technologies. Giarola *et al.* (2011) present a spatially-explicit, multi-period, multi-objective mixed integer linear programming model for the strategic design and planning of hybrid first and second generation biorefineries. The model aims to optimise the environmental and financial performances simultaneously and is applied to a case study of future Italian ethanol production from corn and corn stover. Lam *et al*. (2010) develop a regional energy clustering based-algorithm to minimise the carbon footprint of regional biomass supply chains. The model offers the advantage of the development of efficient energy planning and management strategies by focussing on a simpler supply chain at regional scale. Zamboni *et al.* (2009b) develop a deterministic multi-objective, mixed integer linear programming framework that aims to optimise the economic and environmental performance of a supply chain simultaneously. The environmental impact of the supply chain is measured in terms of total GHG emissions by adopting a well-to-tank (WTT) approach and considering all the stages in the supply chain.

Having explained the extensive literature work on economic and environmental optimisation of biofuel supply chains so far, the next section deals with optimisation under uncertainty, which is another important aspect that must be taken into account when assessing the implications of biofuel supply chains.

2.1.1.3 Biofuel Supply Chain Optimisation under Uncertainty

Uncertainty has also been considered as an important issue in the field of biofuel supply chain optimisation. Chen and Fan (2012) develop a two-stage stochastic programming model for the optimal design of bioethanol supply chains under supply and demand uncertainty. The model is solved using a lagrange relaxation-based decomposition algorithm and is applied to a case study of bioethanol production from eight types of bio-waste in California. Giarola *et al.* (2012a) present a stochastic, multi-period MILP modelling framework for the optimal design of ethanol supply chains under uncertainty in biomass and carbon costs. The proposed model adopts a scenario-based approach to assess the impacts of emission

regulations and carbon trading on biofuel supply chain design and planning decisions. Tan *et al.* (2012) develop a multi-region, fuzzy input-output, linear programming (LP) optimisation model to determine the optimal bioenergy production and trades under resource availability and environmental footprint constraints. Bioenergy trades are utilised to offset the imbalance between regional supply and demand. Two different case studies including electricity generation from biomass and ethanol production are considered to represent the applicability of the LP model. Tay *et al.* (2011) develop a multi-objective MILP model based on fuzzy mathematical programming approach. The economic objective considers maximisation of the net present value whereas the environmental objective considers the minimisation of the total environmental impact evaluated through a waste reduction algorithm. The model is applied to a case study of a gasification-based biorefinery. Dal-Mas *et al.* (2011) introduce a dynamic mixed integer linear programming model for the strategic design and investment capacity planning of an ethanol supply chain under uncertainty in ethanol market prices and biomass purchase costs. The proposed model is solved using a scenario-based approach and considers optimisation of two different objectives separately: maximisation of the expected net present value and minimisation of the financial risk. They conclude that the model can be used as a helpful mathematical tool for potential investors and decision-makers. Kim *et al.* (2011a) investigate a two-stage mixed integer stochastic programming model for the optimal design of a biofuel supply chain network under the presence of uncertainty in biomass supply, biofuel market demand, biomass and biofuel market prices and processing technologies. The model aims to maximise the expected profit over the scenarios under consideration. Robustness and global sensitivity analysis of the optimised multiple-scenario design versus the single-scenario design is carried out using Monte Carlo simulation. Kostin *et al.* (2012) propose a multi-scenario mixed integer linear programming model for the optimal design and planning of integrated ethanol-sugar supply chains considering uncertainty in demand. The model seeks to optimise the economic performance of the supply chain by taking into account different financial risk measures such as value-at-risk (VaR), opportunity value (OV) and risk-area-ratio (RAR). Guillen-Gosalbez and Grossmann (2009) develop a bi-criterion stochastic mixed integer nonlinear programming framework for the optimal design and planning of sustainable supply chains under uncertainty. The model aims to maximise the net

present value and minimise the total environmental impact simultaneously. They conclude that the model can be used as a guide for the decision-makers towards the design of sustainable supply chains.

Having explained the literature work on biofuel supply chains in detail, Chapter 3 of this thesis presents the modelling frameworks for the optimal strategic design of biofuel supply chains developed under the scope of this PhD project. The main novel contributions of this thesis to the existing biofuel supply chain literature include the developed "neighbourhood flow" modelling approach, the detailed analysis of the economic and environmental implications of the future UK bioethanol production as the main case study as well as consideration of sustainability issues related to use of biomass by-products and land use for the cultivation of dedicated energy crops within this case study, The next section introduces literature work related to optimisation of other bioenergy supply chains focussing on bioelectricity for which a supply chain optimisation model is also developed as introduced in Chapter 4.

2.1.2 Optimisation of Bioelectricity Supply Chains

Motivating the large scale decarbonisation of the global economy has thus far proved elusive. Under the Kyoto Protocol, the world has been conveniently partitioned into Annex 1 and non-annex 1 countries (or developed and non-developed respectively). To date, all efforts to obtain a credible international agreement have failed; the most important non-annex 1 countries have consistently refused to adopt a carbon emission cap and perhaps the most important annex 1 country has consistently refused to ratify any binding agreement on the grounds that the most important non-annex 1 countries have not ratified any agreement. This has been referred to as a classic case of "prisoner's dilemma" (Helm, 2012). It is also a pertinent point that the rate of emission reduction for which the EU enthusiastically takes credit can be quite directly linked to deindustrialisation and economic downturn, despite the fact that carbon consumption has actually increased in the time since the Kyoto treaty.

It is also worth noting that the majority of the anthropogenic CO_2 in the atmosphere was emitted by the annex 1 countries, so the non-annex 1 countries have a point when they refuse to ratify treaties aimed at addressing concerns surrounding anthropogenic CO_2 already in the atmosphere. Therefore, if the annex 1 countries

would encourage the non-annex 1 countries to address future CO_2 emissions, it would behove the annex 1 countries to address their historical CO_2 emissions.

Both of these scenarios will depend upon the extent of deployment of CO_2 capture and storage (CCS) technologies (Mac Dowell *et al.,* 2010). Especially in the near to medium term, co-firing of biomass with coal and conversion of existing coal power plants is regarded as one of the most cost-efficient ways of switching to less carbon intensive power generation to meet the carbon emission reduction targets set by the government policies (DEFRA, 2012). In this aspect, the combination of co-firing of biomass with fossil fuels in conjunction with CCS, so-called Bio-Energy with CCS (BECCS), is a particularly promising approach which has the potential to transform the power generation industry from a carbon source into a carbon sink via the generation of carbon negative electricity (DEFRA, 2012; Fuss, 2012; Gough and Upham, 2011; McGlashan *et al.*, 2012). There is also some evidence that BECCS technologies can help reduce or eliminate the "not-in-my-backyard" (NIMBY) effect that has traditionally been an important public acceptance barrier to CCS (Wallquist *et al.*, 2012). Through BECCS systems, existing coal-fired power stations can be readily converted to co-firing fossil fuels, and if retro-fitted with CCS provide a relatively low-cost path to carbon negative energy generation (DECC, 2012c). The relevant policy instruments must be in place to promote the future deployment of these systems. (DECC, 2011b). An example of this is setting a fixed price on carbon emissions to incentivise low carbon power generation similar to the "carbon price floor" concept introduced under the UK Electricity Market Reform (DECC, 2011b).

In Chapter 4 of this thesis, a mixed integer nonlinear programming model is developed for the optimal design of BECCS supply chains. The proposed model can provide insight on what the costs associated with CO_2 emission would have to be in comparison to fuel prices, in order to incentivise the generation of carbon negative energy, and establish a backstop marginal abatement cost. The questions to be addressed involve choosing between a set of existing power stations and deciding what load factor, degree of CO_2 capture and co-firing is most appropriate, subject to a constrained supply of indigenous biomass.

There is significant literature work focussing on biofuel supply chains as introduced in Section 2.1. To the best of our knowledge, literature work related to biomass-to-heat or biomass-to-electricity is limited compared to those focussing on biomass-to-biofuels. Perez-Fortes *et al.* (2012), propose a multi-objective mixed integer linear programming model for the optimal design and planning of a regional biomass supply chain for electricity generation (through biomass gasification). They consider economic, environmental and social objectives. The model aims to determine the optimal locations and capacities of technologies, connectivity between the supply entities, biomass storage periods, transportation of materials and biomass utilisation rates. Gan and Smith (2011) propose a generic modelling framework for determining the optimal bioenergy conversion plant size and the corresponding feedstock supply radius by minimising the total bioenergy production cost. The model is applied to two different case studies including electricity generation and cellulosic ethanol production from biomass. Rentizelas *et al.* (2009) present an optimisation framework for multi-biomass tri-generation applications including electricity, cooling and heating. The model considers various technical, regulatory, social and logical constraints and applied to a case study of tri-generation application at a municipality of Greece. Dunnett *et al.* (2007) introduce a systems modelling framework for the optimal design and operations scheduling for a biomass-to-heat supply chain based on a state-task-network (STN) approach. The proposed model takes into account dynamic system influences such as harvested yield, crop moisture content, ambient drying rates and seasonal demand.

Whilst the use of biomass for energy generation is not new, the concept of co-firing biomass with fossil fuels in conjunction with CCS is a relatively new concept. One very important point to consider is the source of the biomass. Although co-firing has been proposed as a relatively cost-effective approach to mitigate CO_2 emissions, it should be highlighted that the degree to which biomass co-firing reduces the net GHG emissions depends on the methods used to produce the biomass pellets (McKechnie *et al.*, 2011; Schulze *et al.*, 2012). However, it has been suggested that, from a whole-system perspective, GHG emissions associated with co-firing are reduced at a rate slightly higher than the ratio of the biomass co-firing ratio (Mann and Spath, 2001). Apart from that, it is important to consider the additional energy penalty associated with co-firing arising from the potentially higher moisture content

of the fuel. It has been reported that the estimated heat rate degradation due to co-firing is 0.5% for every 10% input of pellets (Zhang *et al.*, 2010). Thus, this can lead to the necessity to ensure that the biomass pellets have very low moisture content - potentially raising their cost. Similarly, owing to the reduced energy density, significant quantities of pellets will be required, raising supply chain constraint questions. This obviously highlights the value in considering the exploitation of marginal land for the cultivation of bioenergy crops, although as the value of those energy crops increases, the economic incentive to produce energy crops from more productive land would be strong (Bryngelsson and Lindgren, 2013).

As can be concluded, the concept of carbon negative electricity generation via the BECCS approach is relatively new. Distinct from conventional electricity generation, carbon negative electricity is subject to the important supply chain constraints associated with the availability of sufficient biomass and also adequate processing facilities with which to convert the raw material into a fuel grade product. Therefore, the developed modelling framework introduced in Chapter 4 of this thesis aims to address the future implications of this new technological approach for carbon negative electricity generation by presenting a multi-objective optimisation-based framework which optimises the total cost and total environmental impact simultaneously taking into account production, demand and transportation constraints.

Chapter 4 of this thesis presents the developed MINLP model for the optimal design of bioelectricity supply chains. This piece of work represents a novel contribution to the existing biomass supply chain literature as it considers the newly-emerging BECCS technology and integrates supply chain aspects with the process side, which, to the best of our knowledge, have not been investigated before under the concept of bioelectricity generation. After having given detailed information about the literature studies on optimisation of bioenergy supply chains, the next section presents background work on hydrogen supply chains for which a modelling framework has been developed and is presented in Chapter 5 of this thesis. The proposed generic model can be used to account for different technology conversion pathways including hydrogen production from biomass.

2.1.3 Optimisation of Hydrogen Supply Chains

Hydrogen is widely recognised as an important option for future road transportation, but a widespread infrastructure must be developed if the potential for hydrogen is to be achieved. In recent years, a literature has developed examining the potential development of hydrogen infrastructure by modelling optimal hydrogen supply chains.

One of the main challenges against the use of hydrogen vehicles at a large scale is the lack of production and transmission infrastructure that involves production, storage, distribution and refuelling stations. Mathematical modelling is a valuable tool that can provide better understanding of these systems in different aspects including cost, environmental emissions and energy use as well as the trade-offs between these elements. Therefore, a considerable increase in using optimisation methods to model the introduction of hydrogen into the passenger transport sector has been witnessed in recent years. As discussed in Agnolucci and McDowall (2013), optimisation techniques have been employed across a number of spatial scales, notably at national scale by applying bottom-up energy system models, and regional and local scales by utilising MILP models with explicit spatial representation of the hydrogen network. Both static and dynamic optimisation techniques with different levels of complexity have been adopted for this purpose with some involving linking geographic information systems (GIS).

There are many examples of optimisation models in the literature focussing on the cost objective. Johnson and Ogden (2012) develop an MILP model which can be used for the optimal design of a hydrogen network to identify the lowest cost centralised production and pipeline transmission infrastructure within geographical regions. The model aims to minimise the total annual cost of a hydrogen network including production and pipeline transmission. In doing so, it aims to identify the optimal number, size, and location of production facilities and the diameter, length and location of transmission pipelines at a given market penetration level of hydrogen fuel cell vehicles. The model capability is demonstrated with a case study in Southwestern United States. Only pipelines are considered as a delivery mode, therefore making this model unsuitable to explore early states of transition to

hydrogen when other transport modes are expected to be competitive, as discussed in Yang and Ogden (2007). Parker *et al.* (2010a) develop a mixed integer linear programming model for the optimal design of a waste-to-hydrogen supply chain to evaluate its economic feasibility and infrastructure requirements. The proposed model aims to maximise the overall profit and takes into account a wide array of costs including production, transportation cost - both local and intercity - and refuelling stations which are then used to compute the total cost of the hydrogen supply chain. The hydrogen price is taken as input to the optimisation problem. The results of the Northern Californian case study imply that the delivery costs of hydrogen from waste can be similar to that of hydrogen production from natural gas. Transportation of both feedstock and hydrogen would incur significant costs. Almansoori and Shah (2009) present a multi-period mixed integer linear programming model for the optimal design and operation of a future hydrogen supply chain. This model is an extension of the snapshot model they developed earlier. The proposed model aims to minimise the total daily average cost of a hydrogen supply chain subject to a set of primary energy source, demand and production, transportation, storage and time evolution constraints. Han *et al.* (2012) further develop this model to consider ship and pipelines as additional delivery modes taking into account different physical forms of hydrogen with the objective to maximise the total net profit. The model is applied to a case study of Korean hydrogen supply network. Murthy Konda *et al*. (2011) introduce a spatially-explicit, multi-period mixed integer linear programming model for the optimal transition towards a large scale hydrogen infrastructure for the Dutch transport sector to investigate the implications for the environmental, economic and energetic performance of hydrogen as a transport fuel. The presented model formulation is similar to that introduced by Almansoori and Shah (2009) and aims to minimise the total cost. It can be concluded from the results of the Dutch case study that the transition towards large scale hydrogen-based transport is economically feasible under all demand scenarios and hydrogen has the potential to help alleviate Dutch energy security concerns. It is also observed that with CCS, 85% of the well-to-tank emissions can be avoided. Kamarudin *et al.* (2009) present an MILP model for the synthesis and optimisation of future hydrogen infrastructure planning in Peninsular Malaysia. The objective function is based on the minimisation of the total investment cost of the hydrogen infrastructure. The results indicate that the cost optimal supply

chain involves hydrogen production via natural gas steam reforming and delivery via tanker trucks. Ingason *et al.* (2008) present a mixed integer programming model for the optimal site selection for hydrogen production in Iceland. It is developed as part of a feasibility study which explores the idea of exporting renewable energy in the form of hydrogen from Iceland to Europe. In their work, they consider hydrogen production from electrolysis where electricity is generated from hydro and geothermal power. Lin *et al.* (2008) develop a dynamic programming approach for supplying hydrogen to California in the time period from 2010 to 2060. The developed model aims to minimise the net present value of technology, environment and fuel accessibility costs. The results imply that the optimal transition to hydrogen is likely to take place through industrial hydrogen first, then on-site SMR and biomass gasification and finally through coal gasification with CCS. Aside from the whole supply chain, some work focus on certain parts of a hydrogen supply chain such as the hydrogen stations (Bersani *et al.*, 2009; Kuby *et al.*, 2009; Lin *et al.*, 2008).

Apart from focussing on single objective, multi-objective optimisation has been adopted by several papers to identify the potential trade-offs between the conflicting objectives. Sabio *et al.* (2012) propose a multi-objective mixed integer linear programming framework that minimises the total cost and total environmental impact of a hydrogen supply chain simultaneously. Eight different LCA indicators are considered to assess the environmental impact according to the Eco-indicator 99 methodology. The corresponding pareto solutions are obtained using ε-constraint method. Guillen-Gosalbez *et al.* (2010) present a bi-criterion MILP model for the optimal design and planning of hydrogen supply chains for vehicle use with the objective to minimise the total cost and total environmental impact simultaneously. The total environmental impact is quantified based on LCA methodology and a bi-level algorithm is proposed for the efficient solution of the resulting large scale model. Kim and Moon (2008b) propose a multi-objective mixed integer linear programming model that considers the total cost and total safety risk of the supply chain simultaneously. The total risk accounts for the relative risk of production and storage sites as well as that of transportation. The relative risk is described as a measure of the chance that harmful consequences might occur from accidental events. A risk index method is utilised to evaluate the relative risk resulting from

each of these steps of the supply chain. Li *et al.* (2008) develop a multi-objective mixed integer linear programming modelling framework for the strategic dynamic investment planning and design of future hydrogen supply chains. The two objectives considered are maximisation of the net present value and minimisation of the total environmental emissions. The model is applied to a case study of China where the trade-off between the two objectives is represented through a pareto curve. Brey *et al.* (2006) study a multi-objective mixed integer programming model for designing a gradual transition to hydrogen economy in Spain based on a target of supplying minimum 15% of transport energy demand by 2010. In their work, they consider minimisation of the total cost of transition and the deviation of the energy targets set by the government simultaneously. Hydrogen production from different renewable resources including hydro, wind power, biomass, solar thermal and solar PV has been taken into account. The corresponding learning rates for each of these technologies are also considered for determining the cost reductions through time.

Apart from the deterministic studies introduced so far, some studies considered the stochastic nature of hydrogen supply chains. Almansoori and Shah (2012) present a multi-period, multi-stage stochastic mixed integer linear programming framework for the optimal design of hydrogen supply chains. The model takes into account the uncertainty in hydrogen demand using a scenario-based approach. A case study of hydrogen production in Great Britain has been examined to test the feasibility of the proposed model. The results show that uncertainty in demand can lead to significant variations in the optimal design and cost of a hydrogen supply chain network. Kim et *al.* (2008a) introduce a two-stage stochastic mixed integer linear programming model for the optimisation of a hydrogen supply chain under demand uncertainty. The proposed model is used to evaluate the future Korean hydrogen supply chain. Sabio *et al.* (2010) present a stochastic multi-objective MILP model for the optimisation of hydrogen supply chains taking into account uncertainty associated with the coefficients of the objective function including facility investment costs, variable costs and transportation costs. The model aims to minimise the total expected cost and the financial risk level of the supply chain simultaneously. A two-step sequential approach is also introduced for the solution of the proposed model.

Chapter 3 Optimisation of Biofuel Supply Chains

Having introduced the literature work on optimisation of hydrogen supply chains, Chapter 5 introduces a spatially-explicit, multi-period, mixed integer linear programming (MILP) model for the optimal design of a hydrogen supply chain, which is applied to a number of possible future scenarios for the UK.The main contributions of this work to the existing literature include the development of a “modified neighbourhood flow” approach as well as a hierachial solution procudere to increase computational efficiency for the solution of the proposed large-scale hydrogen supply chain optimisation model and detailed formulation of CCS supply chain constraints under this framework,

3 Optimisation of Biofuel Supply Chains

This chapter introduces the optimisation-based modelling frameworks developed for biofuel supply chains which are classified under two main categories including static (steady-state) and multi-period (dynamic) approaches, respectively.

3.1 Static Optimisation of Biofuel Supply Chains

This section introduces the spatially-explicit, static mixed integer linear programming models developed for the optimal strategic design of biofuel supply chains and is organised as follows. Section 3.1.1 introduces optimisation-based approaches for bioethanol supply chains based on economic (single) objective and considers first generation bioethanol production. Section 3.1.2 presents an MILP framework for the economic optimisation of an advanced biofuel supply chain, which is a further improved version of the model introduced in Section 3.1.1 and considers bioethanol production using hybrid first/second generation systems. Finally, Section 3.1.3 considers extension of the single objective approach to a multi-objective model.

3.1.1 Optimisation-Based Approaches for Bioethanol Supply Chains

This section introduces spatially-explicit, static optimisation-based approaches for the optimal design of a bioethanol supply chain with the objective to minimise the total supply chain cost and focussing on first generation biofuel production mainly from biomass food crops.

3.1.1.1 Problem Statement

There is a wide range of decisions to be obtained during the optimal design of a biofuel supply chain including the locations of biomass cultivation sites, transport system characteristics and capacity assignment of production facilities.

A biofuel supply chain network is represented in Figure 3.1. The network under consideration includes the following components: biomass cultivation and delivery to production facilities, biofuel production and distribution to demand centres.It is

worth noting that storage facilities are also part of a biomass supply chain in general but have not been considered within the proposed framework.

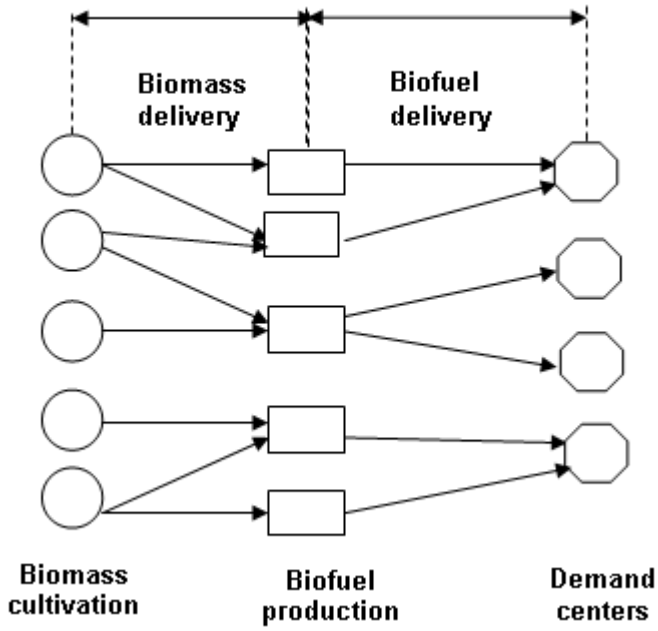

Figure 3.1 A biofuel supply chain network.

The overall problem can be stated as follows:

Given are:

- locations of biofuel demand centres and their biofuel demand,
- geographical biomass availability,
- unit biomass cultivation and biofuel production costs,
- transport logistics characteristics (cost, modes, distances and availabilities),
- capital investment costs for the biofuel production facilities,

To determine optimal:

- biomass cultivation and biofuel production rates,
- locations and scales of biofuel production facilities,
- flows of biomass and biofuel between regions and,
- modes of transport for delivery of biomass and biofuel,

So as to minimise the total supply chain network cost.

The model introduced in this work assumes steady-state conditions and adopts a "neighbourhood" flow representation. Two different configurations are considered in

this context: 4N and 8N, namely von Neumann and Moore neighbourhoods as used in geosimulation studies. These two configurations differ in the flow directions to/from a region as illustrated in Figure 3.2. In the 4N and 8N configurations, the material (biomass or biofuel) flow directions to/from a region (cell) are mutual with the four and eight neighbouring regions (cells), respectively. Material is delivered to its destination by the addition of such flows one after another as illustrated in Figure 3.3 where alternative delivery routes between two points are given according to the 4N and 8N flow representations. The proposed neighbourhood flow approach can provide significant reduction in problem size by eliminating the full connectivity between cells and therefore, lead to increase in computational efficiency for solutio n of large scale supply chain problems.

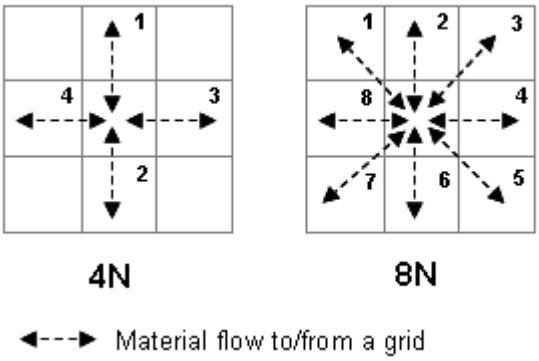

Figure 3.2 Neighbourhood flow representation with 4N and 8N configurations.

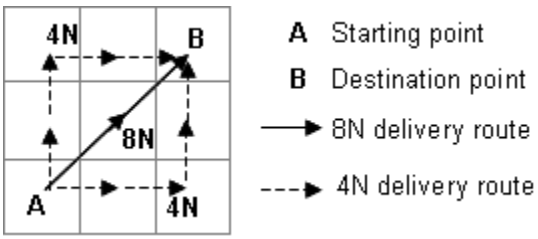

Figure 3.3 Illustration of alternative delivery routes using the neighbourhood flow representation.

3.1.1.2 Mathematical Formulation

The proposed model for the design of bioethanol supply chains is described in this section. The biofuel supply chain optimisation problem is formulated as a mixed integer linear programming (MILP) model with the following notation:

Indices:

g, g'	Square cells (regions)
i	Product (biomass, biofuel)
l	Transport mode
p	Plant size
Sets:	
G	Set of square cells (regions)
I	Set of products (biomass, biofuel)
L	Set of transport modes
P	Set of plant size intervals
$Total_{igg'l}$	Set of total transport links allowed for each product i via mode l between regions g and g'
$n_{igg'l}$	Subset of $Total_{igg'l}$ including all regions g' in the neighbourhood of region g for each product i and mode l
Parameters:	
AD_g	Arable land density of region g (km^2 arable land km^{-2} region surface)
$ADD_{gg'l}$	Actual delivery distance between regions g and g' via mode l (km)
ALD_g	Average local biomass delivery distance (km)
α	Operating period in a year (d $year^{-1}$)
BCD_g^{min}/BCD_g^{max}	Minimum/maximum biomass cultivation density in region g (km^2 cultivation km^{-2} arable land)
CCF	Capital charge factor ($year^{-1}$)
CF_g	Binary parameter for domestic biomass cultivation sites
CY_g	Cultivation yield within region g (t biomass day^{-1} km^{-2})
GS_g	Surface area of region g (km^2)
γ	Biomass to biofuel conversion factor (t biofuel t^{-1} biomass)
IC_p	Investment cost of a plant of size p (€)
$LDD_{gg'}$	Linear delivery distance between regions g and g' (km)
$NTUI^{max}$	Maximum number of units for local biomass transfer (units d^{-1})
$PCap_p^{min}/PCap_p^{max}$	Minimum/maximum biofuel production capacity of a plant of size p (t d^{-1})
$Q_{il}^{min}/Q_{il}^{max}$	Minimum/maximum flowrate of product i via mode l (t d^{-1})

$SusF$	Maximum fraction of domestic biomass allowed for biofuel production
$TCap_{il}$	Capacity of transport mode l for product i (t unit^{-1})
$TCap^{*}$	Capacity for local biomass transfer (t unit^{-1})
UCC_g	Unit biomass cultivation cost in region g (€ t^{-1})
UPC_p	Unit biofuel production cost for a plant of size p (€ t^{-1})
UTC_{il}	Unit transport cost of product i via mode l (€ t^{-1} km^{-1})
UTC^{*}	Unit transport cost for local biomass transfer (€ t^{-1} km^{-1})

Binary Variables

E_{pg}	1 if a biofuel production plant of size p is to be established in region g

Integer Variables

$NTU_{igg'l}$	Number of transport units of mode l required to transfer product i between regions g and g' (units d^{-1})

Continuous Variables

D_{ig}	Demand for product i in region g (t d^{-1})
$NTUI_g$	Number of transfer units required for local biomass transfer within region g (units d^{-1})
Pf_{pg}	Biofuel production rate at a plant of size p located in region g (t d^{-1})
P_{ig}	Production rate of product i in region g (t d^{-1})
$Q_{igg'l}$	Flow rate of product i via mode l from region g to g' (t d^{-1})
TDC	Total daily cost of a biofuel supply chain network (€ d^{-1})
TIC	Total investment cost of biofuel production facilities (€)
TPC	Total production cost (€ d^{-1})
TTC	Total transportation cost (€ d^{-1})

Neighbourhood flow representation is introduced to the mathematical formulation through a set: $n_{igg'l}$, which is a subset of the set of total feasible links between two cells denoted by $Total_{igg'l}$ and covers only the neighbouring cells of each cell g. Mathematically, this can be represented as:

$$n_{igg'l} \subset Total_{igg'l} \quad for\ LD_{gg'} \le LD_{\lim it} \tag{3.1}$$

where LD_{limit} is a distance limit whose value depends on the type of neighbourhood configuration. This distance limit represents the longest linear distance between the centres of a cell and its neighbouring cells. For 4N, the distance between a cell and its neighbours is the same in all directions. For 8N, configuration, the longest distance is between a cell and its neighbours located along the four diagonal directions as shown in Figure 3.4. Hence for a square cell of dimensions, 50x50 km as used in the illustrative example described in Section 3.1.1.3, LD_{limit} is calculated as 50 and 70.7 km, for 4N and 8N representations, respectively.

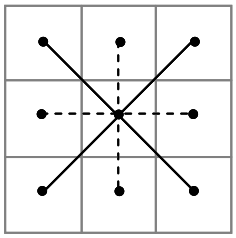

Figure 3.4 Representation of LD_{limit} for 4N and 8N configurations.

a) Objective Function

The objective function is based on the minimisation of the total daily cost and is formulated as follows:

$$TDC = \frac{TIC}{\alpha} CCF + TPC + TTC \tag{3.2}$$

As seen in equation 3.2, the total daily cost function consists of three main terms:

- *TIC* : Total investment cost of the biofuel production facilities converted to daily basis using the capital charge factor, *CCF* (year^{-1}) and the operating period (number of operating days) in a year α (d year^{-1}),
- *TPC*: Total production cost including the biomass cultivation and biofuel production costs,
- *TTC:* Total transportation cost.

The term *TIC* accounts for the total capital investment required for the establishment of new conversion facilities and is calculated by adding up the capital investment cost of each conversion plant of size *p* established in region *g*:

$$TIC = \sum_{p \in P} \sum_{g \in G} IC_p E_{pg} \tag{3.3}$$

where E_{pg} represents the binary variable for establishing a conversion plant of size p in region g and IC_p is the investment cost for that plant.

The term TPC accounts for the biomass cultivation and biofuel production costs and is calculated by:

$$TPC = \sum_{g \in G} UCC_g P_{biomass,g} + \sum_{g \in G} \sum_{p \in P} UPC_p Pf_{pg} \tag{3.4}$$

where UCC_g is the unit biomass cultivation cost in region g, $P_{biomass,g}$ is the local biomass production rate, UPC_p is the unit biofuel production cost for a plant of size p, and Pf_{pg} is the biofuel production rate at a plant of size p located in region g.

The total transportation cost, TTC is calculated by the sum of the transportation cost for delivery of products between regions and that for local biomass transfer:

$$TTC = \sum_{i \in I} \sum_{l \in L} \sum_{g \in G} \sum_{g':(i,g,g',l) \in N} \left(UTC_{il} TCap_{il} ADD_{gg'l} NTU_{igg'l} \right) + \sum_{g \in G} \left(UTC^* TCap^* ALD_g NTUI_g \right) \tag{3.5}$$

where UTC_{il} is the unit transportation cost of product i via mode l, $TCap_{il}$ is the transport capacity of mode l for product i, $ADD_{gg'l}$ is the actual delivery distance between regions g and g' via mode l, $NTU_{igg'l}$ is the number of transport units of mode l required to transfer product i between cells: g and g', UTC^* is the unit transport cost for local biomass transfer within region g, $TCap^*$ is the transport capacity for local biomass transfer, ALD_g is the average local delivery distance and $NTUI_g$ is the number of transport units required for local biomass transfer within region g. The actual delivery distance, $ADD_{gg'l}$, is calculated by the multiplication of the linear delivery distance, $LDD_{gg'l}$, and tortuosity factor for that transport mode.

b) Demand Constraints

The biomass demand in region g is related to the local biofuel production rate by the conversion factor, γ:

$$P_{biofuel,g} = \gamma D_{biomass,g} \quad \forall g \in G \tag{3.6}$$

It should be noted that the demand is considered as a single variable in this work instead of partitioning it into "local" and "imported" demand as in the model introduced by Zamboni *et al*. (2009a) (see Appendix A.1 for a brief description). This eliminates the need to take into account the related constraints in their model (equations A.2-A.4 in Appendix A.1).

c) Production Constraints

The mass balance for each product *i* and region *g* states that the production of that product in region *g* plus the total flow from other regions should be equal to the demand in that region plus the total flow from that region to other regions:

$$P_{ig} + \sum_{l \in L} \sum_{g' \in n_{ig'gl}} Q_{ig'gl} = D_{ig} + \sum_{l \in L} \sum_{g' \in n_{igg'l}} Q_{igg'l} \quad \forall i \in I, g \in G \tag{3.7}$$

The biofuel production in region *g* is equal to the sum of the biofuel production rates at the plants located within that region:

$$P_{biofuel,g} = \sum_{p \in P} Pf_{pg} \quad \forall g \in G \tag{3.8}$$

The biofuel production rate at a plant in region *g* is limited by the minimum and maximum production capacities if that plant is to be established in that region, otherwise it should be forced to zero:

$$PCap_p^{\min} E_{pg} \le Pf_{pg} \le PCap_p^{\max} E_{pg} \qquad \forall p \in P, g \in G \tag{3.9}$$

A constraint can be added to allow up to one production facility to be established in region *g*:

$$\sum_{p \in P} E_{pg} \le 1 \qquad \forall g \in G \tag{3.10}$$

The local biomass cultivation rate is also limited by the minimum and maximum local biomass availability. The local biomass availability is defined by the product of the terms: cultivation yield CY_g, arable land density AD_g, surface area GS_g and cultivation density BCD_g.

$$GS_g CY_g AD_g BCD_g^{\min} \le P_{biomass,g} \le GS_g CY_g AD_g BCD_g^{\max} \qquad \forall g \in G \tag{3.11}$$

A sustainability constraint is also introduced so that only a fraction of the total potential biomass resources is used for biofuel production to prevent the negative impacts on food production.This constraint can be applied on a global (e.g. whole country) or regional level. On a global level, this can be represented as

$$\sum_{g \in G} P_{biomass,g} \le SusF \left(\sum_{g} CF_g GS_g CY_g AD_g BCD_g^{\max} \right) \tag{3.12}$$

The left hand side of constraint 3.12 represents the total biomass production whereas the right hand side represents the product of the sustainability factor, *SusF* and the total potential biomass availability from domestic resources which are defined by the binary parameter CF_g.

On a regional level (e.g. per cell), the sustainability concept is represented as (constraint (3.11) can be replaced by):

$$SusF\,GS_g CY_g AD_g BCD_g^{\min} \le P_{biomass,g} \le SusF\,GS_g CY_g AD_g BCD_g^{\max} \quad \forall g \in G \quad (3.12a)$$

d) Transportation Constraints

The number of transfer units for product transport between regions must satisfy the minimum number of units required:

$$NTU_{igg'l} \ge \frac{Q_{igg'l}}{TCap_{il}} \qquad \forall i,l,g,g' \in n_{igg'l} \quad (3.13)$$

Similarly to constraint 3.13, the number of transfer units required for local biomass transport within region g must meet the minimum requirement:

$$NTUI_g \ge \frac{P_{biomass,g}}{TCap^*} \qquad \forall g \in G \quad (3.14)$$

It is worth noting that equations 3.13 and 3.14 have been formulated as inequality constraints rather than equality constraints as the number of transport units required must be an integer and the right hand side of the two inequality constraints must be rounded up to the nearest integer value to represent this. In addition having inequality constraints rather than equality constraints here provides more flexibility by increasing the feasible region for the problem and hence, improves computational efficiency during its solution.

An upper limit on the number of transport units required for the local transfer of biomass can also be introduced:

$$NTUI_g \le NTUI_g^{\max} \quad \forall g \in G \quad (3.15)$$

where $NTUI_g^{max}$ is simply an upper bound.

Similarly for $NTU_{igg'l}$:

$$NTU_{igg'l} \le \frac{Q_{il}^{\max}}{TCap_{il}} \qquad \forall i,l,g,g' \in n_{igg'l} \quad (3.16)$$

where Q_{il}^{max} is the maximum flowrate of product i via mode l between regions g and g'.

3.1.1.3 Computational Results

Corn-based bioethanol production in Northern Italy from the work of Zamboni *et al.* (2009a) was chosen as the case study with appropriate soil conditions, biomass yields and a wide range of transfer modes available to highlight the model applicability. Northern Italy was discretised into 59 homogeneous square regions of equal size (50 km of length) to represent the geographical dependency of biomass production. The choice of the cell size depends on the trade-off between computational time and resolution. In addition, most data were available on territorial (administrative) units with sizes ranging between 2000 and 5000 km^2. One additional cell, *g*: 60, was added to account for the option of biomass import (Eastern Europe as the potential foreign biomass supplier). It should be noted that ethanol import from foreign suppliers was not considered as an option in this work due to the national policy that aims to encourage local biofuel production for energy security.

Two different demand scenarios are considered based on the renewable fuel targets set by the European Directive. Lower heating values of fuels are used when applying the EU biofuel targets (EC, 2010). They are converted to mass fractions as explained in Appendix A.2. The target for 2011 has been calculated based on the assumption of a smooth transition from 2010 (5.75%) to 2020 (10%). Local and global sustainability constraints have been applied separately to both scenarios. In scenario 2020, it is also assumed that the domestic biomass resources are doubled in year 2020 with improved cultivation practices, yields and soil conditions.

The internal depots used for the conventional fuel storage are assumed to be the actual demand centres for biofuel as bioethanol has to be blended with gasoline just before the final distribution stage to the customers due to stability problems (Zamboni *et al.*, 2009a). The resulting demand data for both scenarios is given in Table 3.1. The operating period in a year is taken to be 365 days. All other data related to the case study is given in the Appendices A.2, A.3, A.4 and A.5 for biothenol demand, biomass cultivation, transportation and biofuel production, respectively. This data has been taken from the work of Zamboni *et al.*(2009a) where more detailed information can be found. Global and local sustainability constraints have been applied to both demand scenarios separately. Global sustainability

constraints impose restrictions on the use of first generation food crops based on the total biomass availability on a national level whereas local sustainability constraints are applied on a regional level (per cell) taking into account biomass availability in each cell.

Table 3.1 Bioethanol demand data for the demand centres in Northern Italy.

	$D_{bioethanol,g}$ (t d^{-1})	
Demand centre	**Scenario 2011**	**Scenario 2020**
22	129.71	203.70
25	193.02	303.10
27	374.54	588.15
32	193.33	303.59
37	61.56	96.67
39	192.51	302.31
41	132.62	208.26
46	121.28	190.45
52	160.20	251.57

The proposed models were solved in GAMS 22.8 using CPLEX 11.1 solver in a 3.4 GHz, 1 GB RAM machine.

Figure 3.5 and Figure 3.6 show the optimal configurations according to 8N with global and local sustainability constraints respectively for scenario 2011. For convenience, biomass and bioethanol flows have been presented in Figure 3.6a and Figure 3.6b separately. With the global sustainability constraint, there are three biofuel production plants located in cells 26, 32 and 40 with capacities of 250, 150 and 150 ktonnes/year respectively. The location of the plant in grid 32 is in accordance with one of the potential Italian industrial plans (Zamboni *et al.*, 2009a). In addition, biomass cultivation sites are mostly located within the same cell as the biofuel production plants. On the other hand, when sustainability is considered locally, these three plants are located in cells 22, 27 and 42 with capacities of 110, 250 and 200 ktonnes/year. In both optimal configurations in Figure 3.5 and Figure 3.6, rail is the preferred transport mode due to its higher capacity and lower unit cost.

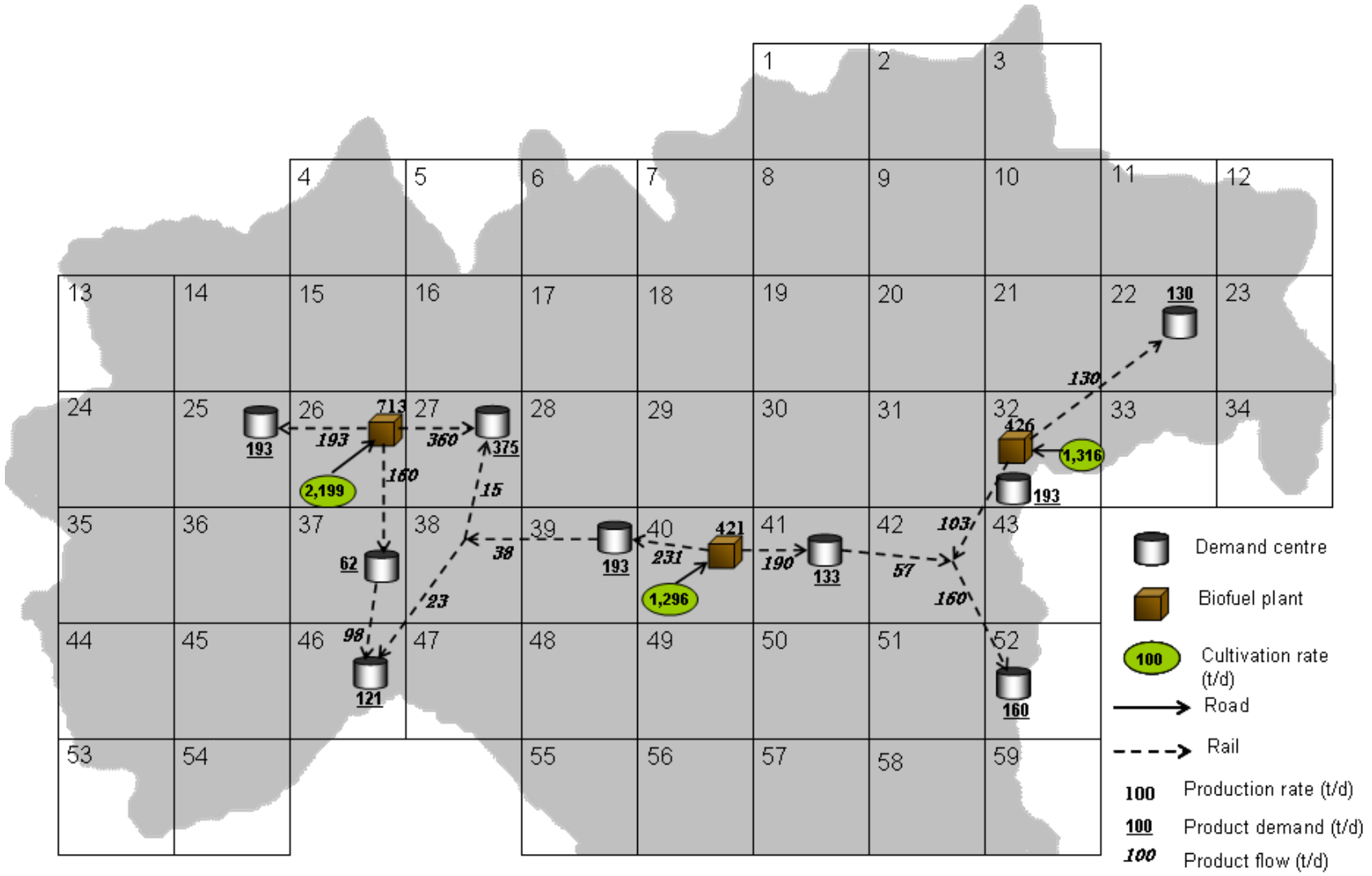

Figure 3.5 Optimal network configuration for scenario 2011 according to 8N flow representation with global sustainability constraint.

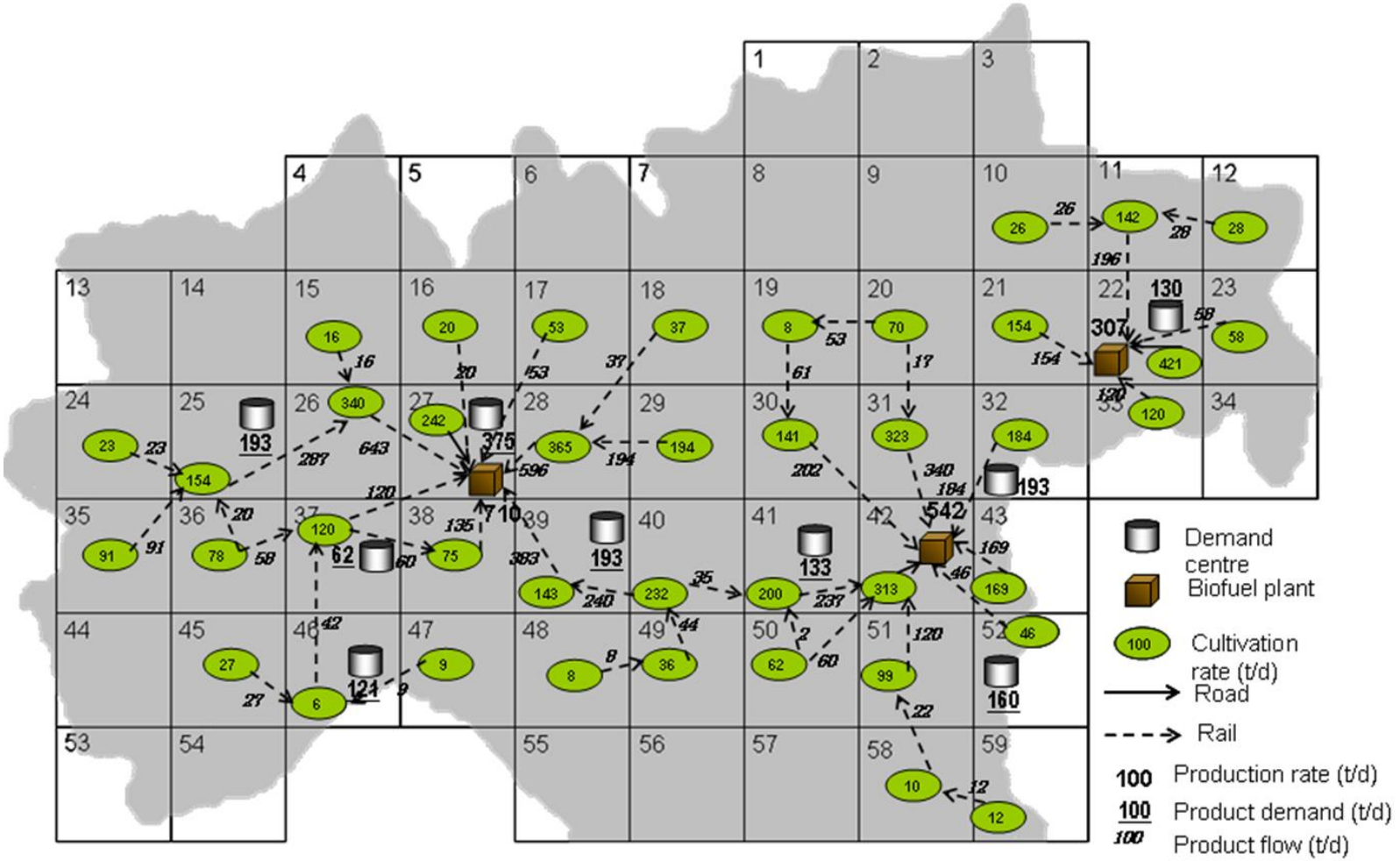

Figure 3.6a Optimal network configuration (biomass flows) for scenario 2011 according to 8N flow representation with local sustainability constraint.

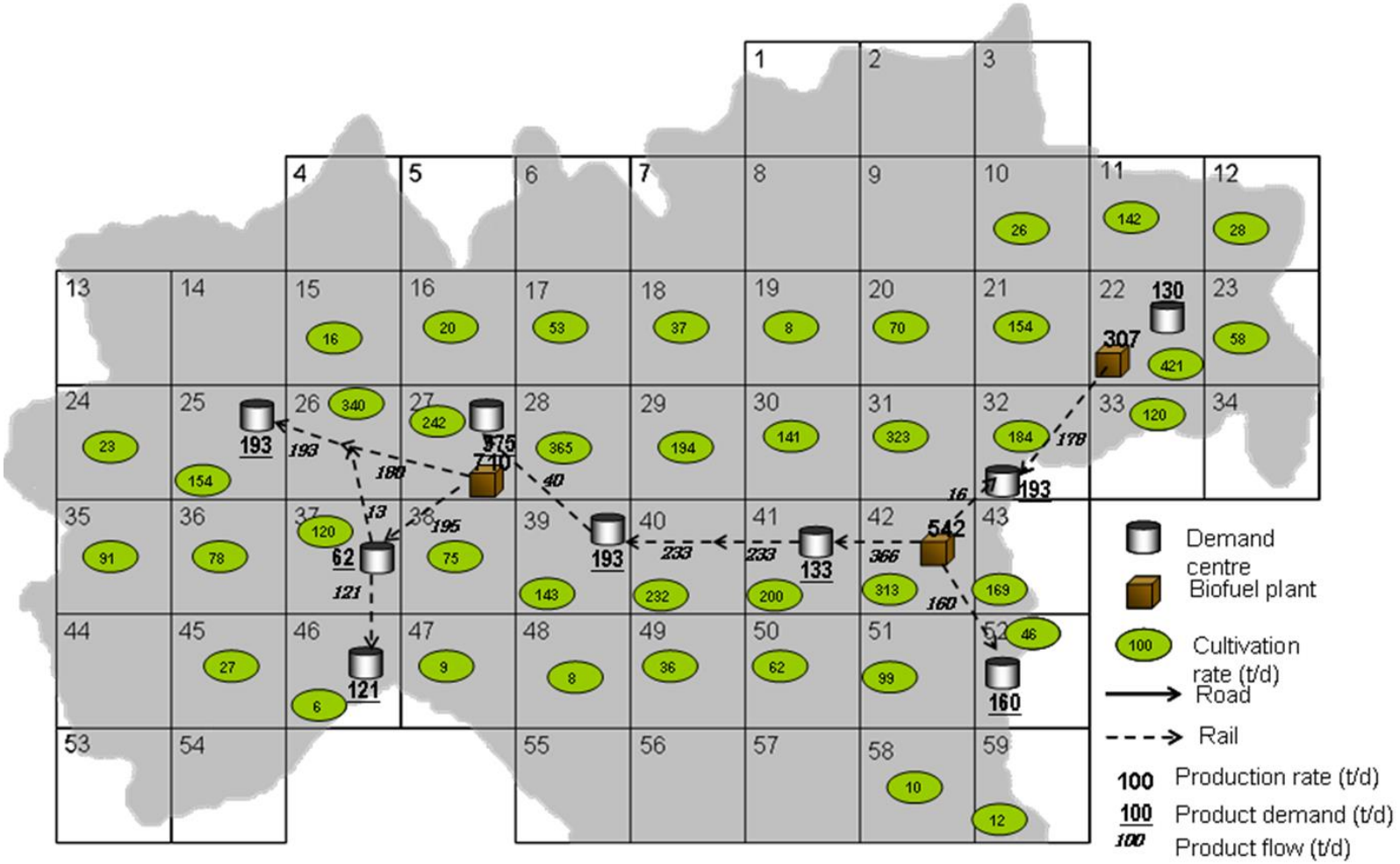

Figure 3.6b Optimal network configuration (bioethanol flows) for scenario 2011 according to 8N flow representation with local sustainability constraint.

Table 3.2 shows the breakdown of the total cost for the bioethanol supply chain for scenario 2011 with global and local sustainability constraints according to 8N representation. As it can be concluded from the table, local sustainability results in higher overall supply chain cost mainly due to the increase in biomass transport cost as more cultivation areas are activated in this case and the biomass cultivated on these sites need to be transported to the biofuel plants**.**

Table 3.2 Comparison of results for the supply chain network costs for scenario 2011 with global and local sustainability constraints according to 8N (optimality gap: 1%).

Objective function and components (€ d^{-1})	**Proposed model: 8N**	
	Global sustainability	**Local sustainability**
Total daily cost	1,225,166	1,317,733
Total investment cost	292,858	295,595
Total production cost	867,188	872,559
Biomass cultivation cost	630,670	635,822
Biofuel production cost	236,488	236,737
Total transportation cost	65,120	149,579
Biomass transport cost	35,426	118,033
Biofuel transport cost	29,694	31,546

Figure 3.7 and Figure 3.8 show the optimal configurations for scenario 2020 when global and local sustainability constraints are considered separately. With a global sustainability constraint, there are four production plants located in cells 25, 27, 33 and 41 with capacities of 250, 250, 110 and 250 ktonnes/year. On the other hand, with local sustainability, there are five production plants located in cells 22, 25, 27, 40 and 42 with capacities of 200, 110, 250, 150 and 150 ktonnes/year, respectively. In Figure 3.8a, all of the biomass produced in cell 28 is not transferred directly to cell 27, instead some of it is transferred to 39 and then to 27. This stems from transport capacity limitations.

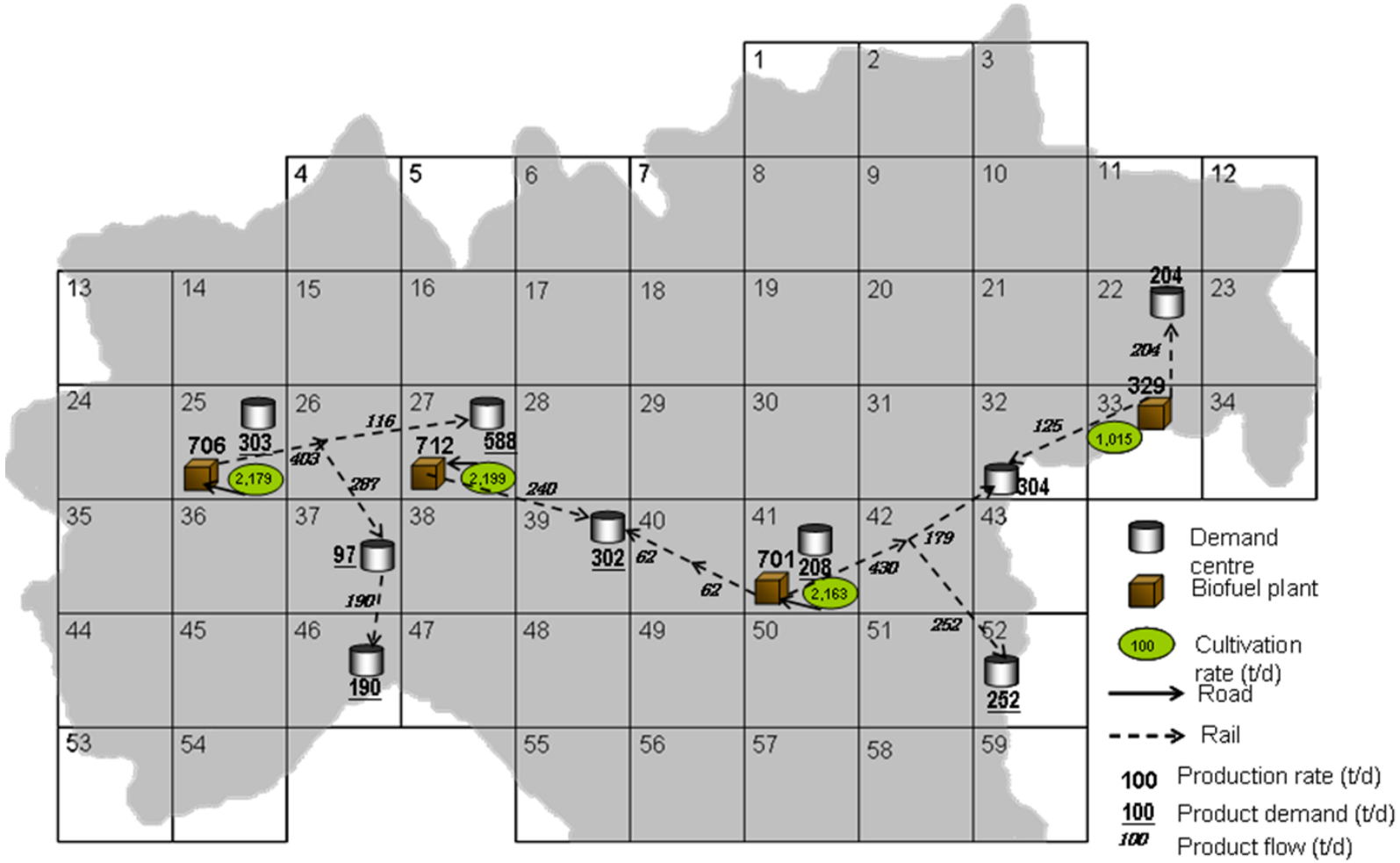

Figure 3.7 Optimal network configuration for scenario 2020 according to 8N flow representation with global sustainability constraint.

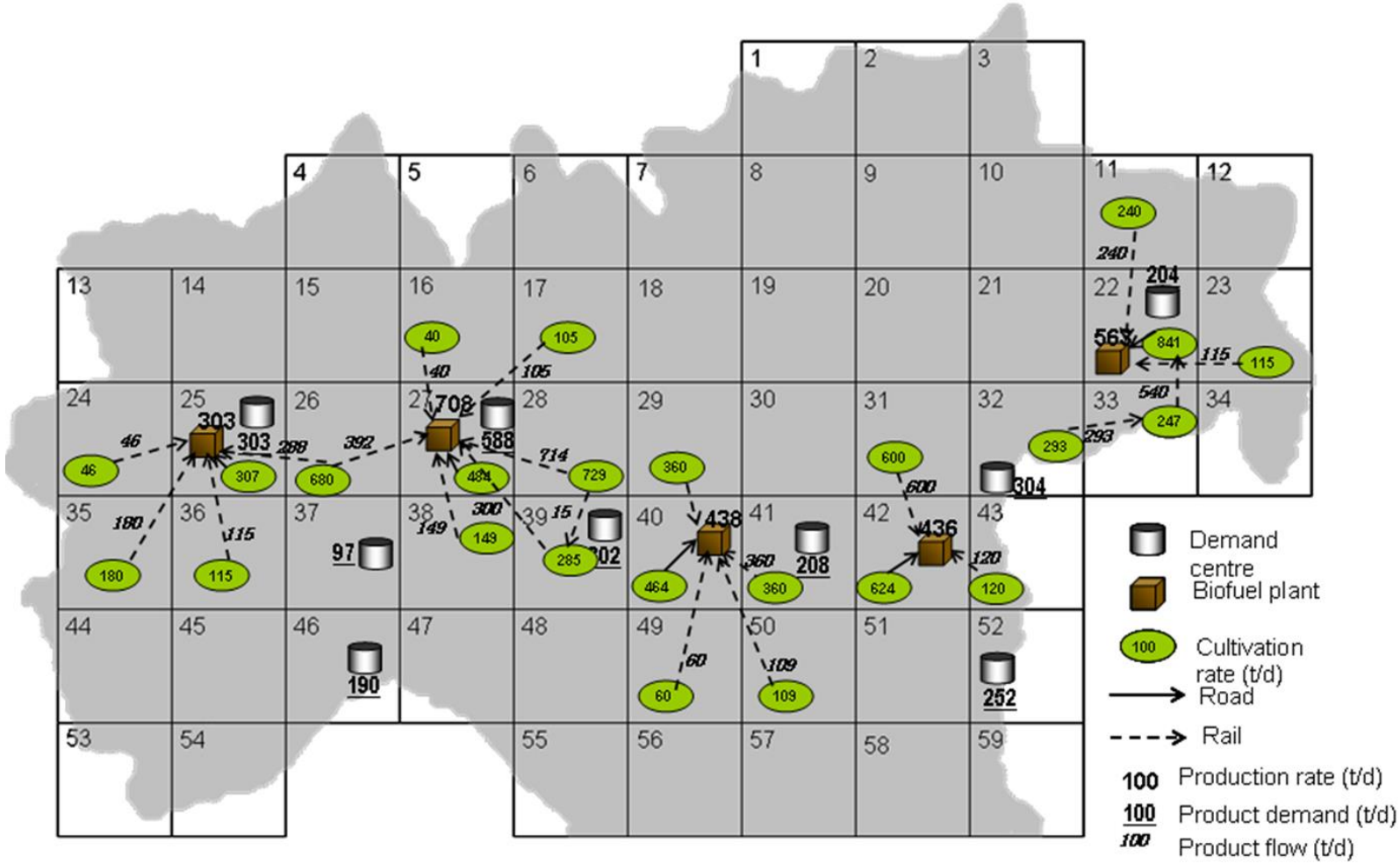

Figure 3.8a Optimal network configuration (biomass flows) for scenario 2020 according to 8N flow representation with local sustainability constraint.

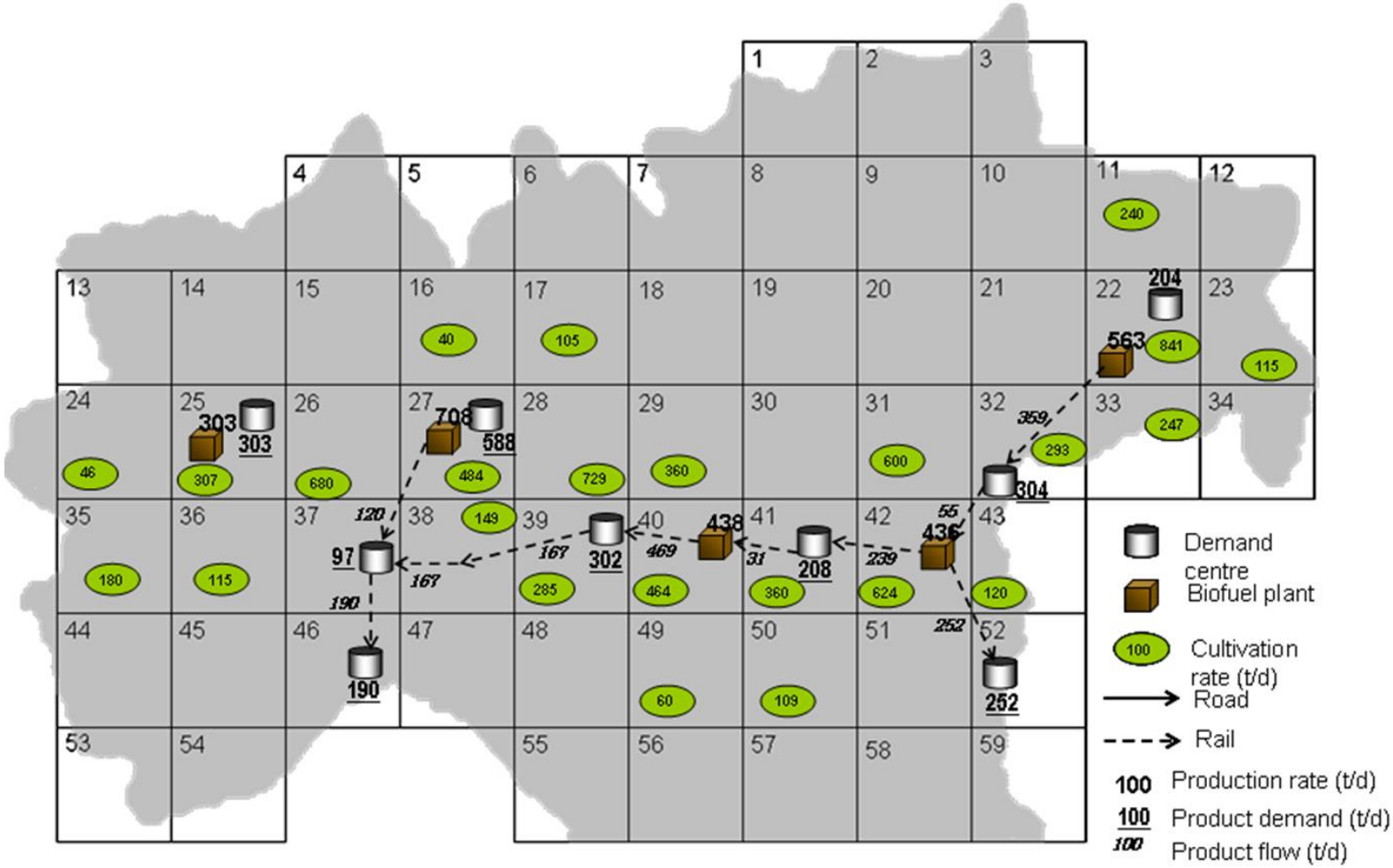

Figure 3.8b Optimal network configuration (bioethanol flows) for scenario 2020 according to 8N flow representation with local sustainability constraint.

Table 3.3 shows the optimal results for the bioethanol supply chain cost for scenario 2020 with global and local sustainability constraints according to 8N representation. Similarly to the results for scenario 2011, local sustainability results in higher overall supply chain cost compared to global sustainability. An optimality gap of 1% (being in sufficient proximity to the global optimum) has been chosen here for comparison with Zamboni *et al.* (2009a) model and reporting purposes as going down below 1% during the solution of the Zamboni *et al.* (2009a) model has proven to require significant computational time.

Table 3.3 Comparison of results for the supply chain network costs for scenario 2020 with global and local sustainability constraints according to 8N (optimality gap: 1%)

Objective function and components (€ d^{-1})	**Proposed model: 8N**	
	Global sustainability	**Local sustainability**
Total daily cost	1,892,273	1,985,121
Total investment cost	444,304	461,638
Total production cost	1,357,356	1,364,933
Biomass cultivation cost	989,216	991,383
Biofuel production cost	368,141	373,550
Total transportation cost	90,613	158,550
Biomass transport cost	55,288	126,194
Biofuel transport cost	35,324	32,356

Table **3.4** shows the comparison of computational statistics for scenarios 2011 and 2020 with global sustainability constraints according to the models: Zamboni *et al.* (2009a), 4N and 8N. As seen from the table, the proposed neighbourhood approaches provide a reduction in the problem size by a factor of 100 and achieve significant time savings when compared to the model of Zamboni *et al.* (2009a).

Table 3.4 Comparison of computational statistics for scenarios 2011 and 2020 with global sustainability.

Model statistics	**Zamboni *et al.* (2009a)**	**4N**	**8N**
No. of constraints	167,653	1,520	1,970
No. of integer variables	72,300	914	1,364
No. of continuous variables	36,789	1,222	1,674
Scenario 2011			
Total cost (€k d^{-1})	1,231	1,229	1,225
Optimality gap	1%	1%	1%
CPU time (s)	285	12	12
Scenario 2020			
Total cost (€k d^{-1})	1,899	1,896	1,892
Optimality gap	1%	1%	1%
CPU time (s)	989	1	2

Table 3.5 shows the computational statistics for both scenarios with local sustainability according to 8N and 4N representations. Similar to the case of global sustainability, the computational savings are high. It is also worth noting that apart from the very similar objective function values, the optimal supply chain configurations (including optimal plant locations, biomass consumption and biofuel production rates at each of these plants and biomass cultivation rates in each cell) under each of the three cases (models) were very similar both with global and local sustainability constraints shown in

Table **3.4** and Table 3.5, respectively.

Table 3.5 Comparison of computational statistics for scenarios 2011 and 2020 with local sustainability.

Model	**Zamboni *et al.* (2009a)**	**4N**	**8N**
Scenario 2011			
Total cost (€k d^{-1})	1,349	1,325	1,318
Optimality gap	1%	1%	1%
CPU time (s)	2,185	244	168
Scenario 2020			
Total cost (€k d^{-1})	1,991	1,989	1,985
Optimality gap	1%	1%	1%
CPU time (s)	1,152	34	42

3.1.1.4 Concluding Remarks

In this section, two new modelling approaches, 4N and 8N neighbourhood representations, have been introduced for the optimal design of bioethanol supply chains. Corn-based bioethanol production in Northern Italy has been chosen as an illustrative case study. Two different demand scenarios have been investigated for years 2011 and 2020 based on the EU biofuels target. The optimal configurations for

both scenarios have been presented. Considering sustainability per region results in a more complex network with more cultivation sites being active.

A comparison has been also made with the model introduced by Zamboni *et al.* (2009a). The results for both scenarios show that the two neighbourhood flow representations proposed provide significant reductions in problem size and computational requirements. The following sections consider extension of the proposed approaches to second-generation technologies and uncertainty aspects.

3.1.2 Economic Optimisation of a UK Advanced Biofuel Supply Chain

This section presents an MILP modelling framework for the economic optimisation of an advanced biofuel supply chain, which is a further extension of the approach introduced in the previous section. An "advanced" biofuel supply chain refers to hybrid systems where first and second generation technologies are integrated for biofuel production. In recent years, there has been significant scope to integrate the emerging second generation technologies with the well-established first generation technologies in these hybrid facilities to reduce the potential negative impacts of biofuel production on the food sector and to provide better utilisation of biomass resources.

3.1.2.1 Problem Statement

Here the problem in section Problem Statement3.1.1.1 has been extended to consider multiple biomass feedstock types and advanced production technologies.The overall problem studied in this work for the optimal design of a biofuel supply chain can be stated as follows:

Given are:

- locations of biofuel demand centres and their biofuel demand,
- biomass feedstock types and their geographical availabilities,
- unit biomass cultivation cost for each feedstock type,
- unit production cost of biofuel based on the feedstock type (hence technology) utilised,
- transport logistics characteristics (cost, modes, and availabilities),

- capital investment cost for the biofuel production facilities as a function of the production technology deployed,

Determine the optimal:

- biomass cultivation rate and location for each biomass feedstock type and biofuel production rates,
- locations and scales of biofuel production facilities,
- flows of each biomass type and biofuel between cells and biomass imports,
- modes of transport of delivery for biomass and biofuel,

So as to minimise the total supply chain cost.

The supply chain model introduced in this section adopts a "neighbourhood" flow approach with 8N configuration introduced in the previous section.

3.1.2.2 Mathematical Formulation

The problem for the optimal design of an advanced (hybrid) biofuel supply chain is formulated as a steady-state mixed integer linear programming (MILP) model. Since this model is an extension of the approach introduced in Section 3.1.1, the mathematical formulation and notation are based on those introduced in that section with some additional features. Therefore, to avoid repretition and for the purposes of clarity, the whole nomenclature and mathematical formulation are not presented once again here; but instead, the differences are highlighted. The complete mathematical formulation as well as the nomenclature is provided in Appendix B.1.

a) Objective Function

As introduced in section 3.1.1, the objective here is also the minimisation of the total supply chain cost with one additional term for outsourcing (import) cost (*TPOC*) term as follows:

$$TDC = \frac{TIC}{\alpha} CCF + TPC + TTC + TPOC \tag{3.18}$$

The total investment cost, *TIC* is evaluated as in equation 3.3 introduced in the previous section. The total production cost, *TPC* is now modified to account for different biomass types as follows:

$$TPC = \sum_{i \in BI} \sum_{g \in G} \left(UCC_{ig} P_{ig} + \sum_{p \in P} UPC_{ip} \gamma_i Df_{ipg} \right) \tag{3.19}$$

where *BI* is the set of different biomass types and Df_{ipg} is the amount of biomass *i* consumed at a plant of scale *p* located in region *g* and γ_i is the biomass-to-ethanol conversion factor for biomass type *i*.

The total transportation cost, *TTC* is now evaluated based on the total flows (for cost of transport between regions) and biomass cultivation terms (for local transport) rather than number of transportation units as introduced in Section 3.1.1 as these integer variables have been removed in this improved version of the model. Therefore, the new formulation is:

$$TTC = \sum_{i\in I}\sum_{l\in L}\sum_{g\in G}\sum_{g':(i,g,g',l)\in N}\left(UTC_{il}\,ADD_{gg'l}\,Q_{igg'l}\right)+\sum_{i\in BI}\sum_{g\in G}\left(UTC^{*}\,ALD_{g}\,P_{ig}\right) \tag{3.20}$$

The total product outsourcing cost, *TPOC* is calculated by:

$$TPOC = \sum_{i,g^{*},g,l:(i,g,g',l)\in N} IMPC_{ig^{*}}\,Q_{ig^{*}gl} \tag{3.21}$$

where g^{*} represents the foreign supplier for importing resource (or product) *i* and $IMPC_{ig^{*}}$ is the unit cost of importation of that resource from that supplier.

a) Demand Constraints

The demand constraints introduced in the previous section have now been modified to account for different biomass types. The amount of biomass *i* consumed at a plant of scale *p* located in region *g,* Df_{ipg}, is related to the biofuel production rate at that plant, Pf_{pg}, by the conversion factor, γ_i as follows:

$$Pf_{pg} = \sum_{i\in BI}\gamma_i Df_{ipg} \qquad \forall\, p\in P, g\in G \tag{3.22}$$

As a result, the total demand for biomass type *i* in region *g* is given by:

$$D_{ig} = \sum_{p\in P} Df_{ipg} \qquad \forall\, i\in BI, g\in G \tag{3.23}$$

b) Production Constraints

The mathematical constraints related to material balance, total biofuel production rate in a region as well as the total number of plants that can be established in a region introduced in equations 3.7-3.10 are included here as they are. Further differences in the production constraints are explained below.

The local biomass cultivation rate is limited by the minimum and maximum local biomass availability as follows:

$$BA_{ig}^{\min} \le P_{ig} \le BA_{ig}^{\max} \quad \forall i \in FI, g \in G \tag{3.24}$$

where FI is the set of first generation biomass crops, BA_{ig}^{min} and BA_{ig}^{max} are the minimum and maximum availability of that first generation biomass i in region g, respectively.

For second generation biomass feedstock (dedicated energy crops), competing for the set-aside land, the daily production rate in a cell g, P_{ig} is related to the land occupied by that crop, A_{ig} (ha), and its annual yield, Y_{ig} (t ha^{-1} year^{-1}), as follows:

$$P_{ig} = Y_{ig} A_{ig} / \alpha \qquad \forall i \in SI, g \in G \tag{3.25}$$

where SI is the set of second generation biomass crops and α is the network operating period in a year (d year^{-1}).

When straw is considered as a potential feedstock, the following constraint applies:

$$P_{straw,g} \le \beta P_{wheat,g} \qquad \forall g \in G \tag{3.26}$$

where β is the fraction of straw that can be recovered sustainably from the cultivated wheat. Removal of all of the straw obtained from the cultivated wheat is not sustainable as this gives rise to the need for additional fertilisers (mainly to supply carbon). Apart from biofuel production, straw can be used for other purposes including animal bedding or heat and power generation.

c) Sustainability Constraints

The constraints explained in this section mainly aim to avoid the negative impacts on food production, to avoid competition with other sectors for biomass use and to maintain the sustainable use of land.

The following constraint is introduced to the model to avoid the competition between "biomass for food" and "biomass for fuel":

$$\sum_{g \in G} P_{ig} \le SusF\left(\sum_{g} BA_{ig}^{\max} \right) \qquad \forall i \in FI \tag{3.27}$$

where as introduced in the previous section, *SusF* is a sustainability factor that allows only up to a certain fraction of total domestic first generation biomass to be used for biofuel production (Zamboni *et al.,* 2009a).

The total area occupied by second generation crops in a region *g* is limited by the maximum set-aside land availability in that region:

$$\sum_{i \in SI} A_{ig} \leq A_g^s \qquad \forall g \in G \tag{3.28}$$

where A_g^s is the total set-aside land available in cell *g*.

Likewise, the total area occupied by second generation crops should not exceed the total available set-aside land for biofuel production:

$$\sum_{i \in SI} \sum_{g \in G} A_{ig} \leq \varepsilon \sum_{g} A_g^s \tag{3.29}$$

where ε is the fraction of the total set-aside land that can be used for biofuel crop production.

d) Transportation Constraints

Due to the elimination of the variables that represent the number of transport units, equations 3.13-3.16 are not considered here. Instead, an upper limit on the flow of resource *i* between regions can be considered such that:

$$Q_{igg'l} \leq Q_{il}^{\max} \qquad \forall i, g, g', l \in n_{igg'l} \tag{3.30}$$

where Q_{il}^{max} is the maximum flowrate of resource *i* via mode *l* between regions *g* and *g'*.

3.1.2.3 Computational Results

The model described in the previous section has been applied to a case study of ethanol production in the UK. The potential feedstocks include first generation feedstocks (wheat) and second generation feedstocks (wheat straw, miscanthus and short rotation coppice (SRC). The assumed hybrid technology in this work is a lignocellulosic ethanol process technology using a biochemical route, where lignocellulose can be hydrolysed and then fermented (fed to the conventional first generation route) (NNFCC, 2008b). The UK is discretised into 34 square cells with length of 108 km each. One additional cell, 35 has been added for import of wheat from a foreign supplier. Ethanol imports have not been taken into account in this

study to support domestic production and prevent any potential negative impacts on the security of energy supply.

Two demand scenarios have been investigated based on the UK domestic target for 2011 (3.4% by energy content) (UKPIA, 2008) and the EU target for 2020 (10% by energy content) (EC, 2009) to promote the use of biofuels. Based on the current total UK gasoline demand and the biofuel targets, the total ethanol demand for 2011 and 2020 has been calculated to be 2,802 and 7,899 t/d, respectively. The total demand is distributed among six demand centres (internal depots) in the UK using the secondary distribution model of Zamboni *et al*. (2009a). The details of this model are given in Appendix B.2. All other input data for ethanol demand, biomass cultivation, transportation, ethanol production and sustainability is also given in Appendix B. The calculated ethanol demand at each depot is given in Table 3.6.

Table 3.6 Ethanol demand at six different demand centres in the UK for scenarios 2011 and 2020.

Demand centre (cell, *g*)	**Ethanol demand for 2011, $D_{ethanol,\,g}$ (t d^{-1})**	**Ethanol demand for 2020 $D_{ethanol,\,g}$ (t d^{-1})**
4	186.1	524.6
13	593.7	1,673.6
19	606.0	1,708.4
23	533.8	1,504.8
27	243.9	687.5
29	638.7	1,800.4
TOTAL	**2,802.2**	**7,899.2**

Three different instances have been studied for scenario 2011 namely: 2011A, 2011B and 2011C. In 2011A, only first generation ethanol production from wheat is considered. In 2011B, ethanol is produced using both wheat and wheat straw in hybrid first/second generation facilities. In 2011C, ethanol is produced using wheat and wheat straw as in the case of 2011B and an opportunity cost (due to competition with other uses such as animal bedding or heat and power generation) is incurred for straw. Wheat import is considered for all the three instances as an alternative source to supply the demand.

The optimal network configuration for instance 2011A is given in Figure 3.9a. For convenience, only ethanol flows are represented in all figures and optimal biomass

flows are given in separate tables. For 2011A, the optimal plant locations, ethanol production rates, biomass utilisation rates and origin cells for these biomass resources are given in Table 3.7.

As seen in Figure 3.9a and Table 3.7, there are five plants located in cells 4, 10, 18, 19 and 28 with ethanol production rates of 323, 397, 712, 712 and 658 tonnes of ethanol per day, respectively. 2,747 tonnes of wheat per day is imported, which accounts for 32% of the total domestic ethanol production. The need to import wheat is mainly due to the restriction on the use of domestic wheat for ethanol production represented by constraint 3.27 given in the previous section. The main preferred mode of transportation is rail with its lower unit cost and higher capacity compared to road transport.

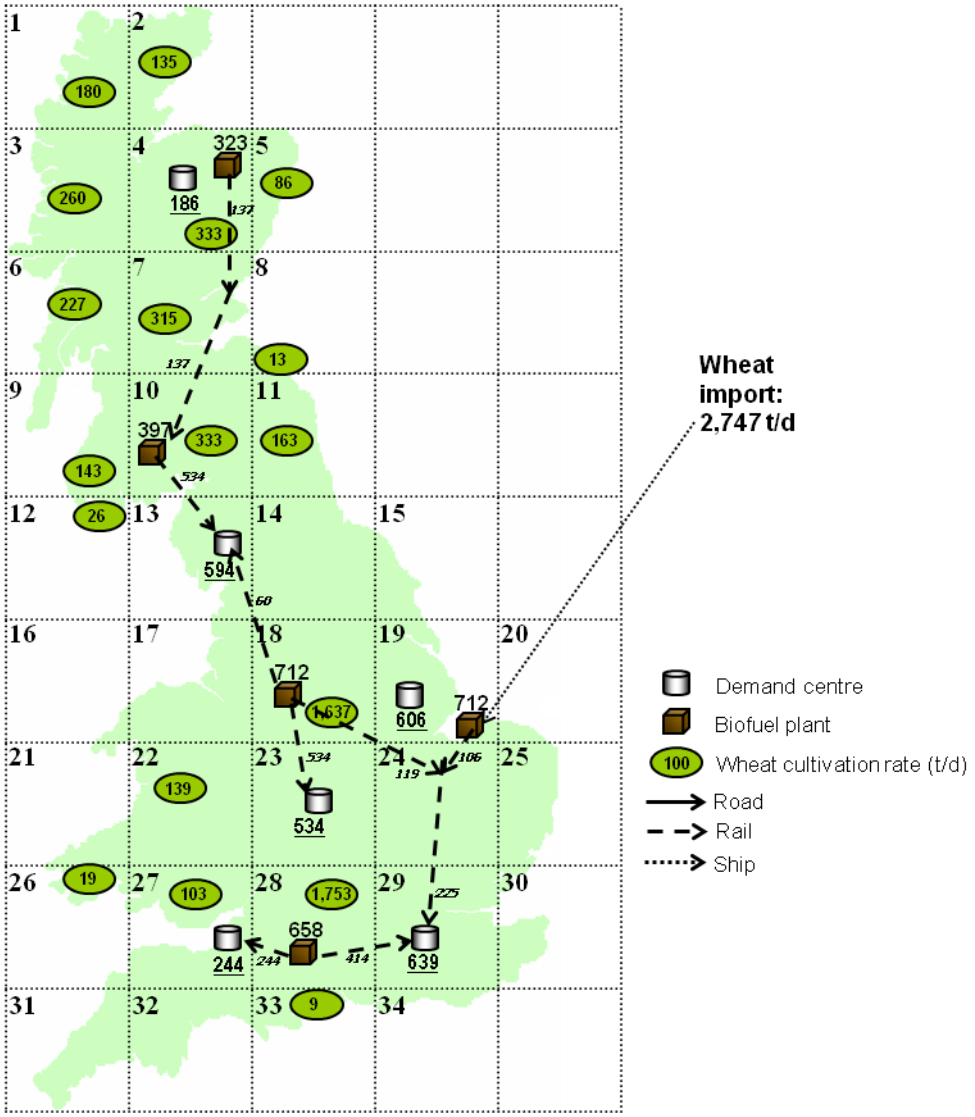

Figure 3.9a Optimal UK ethanol supply chain configuration for instance 2011A.

Table 3.7 Optimal plant locations, capacities and biomass flows for instance 2011A.

Plant Location (cell, g)	Ethanol production rate, Pf_{pg} (t d^{-1})	Biomass Feedstock	Consumed biomass, Df_{ipg} (t d^{-1})	Origin cells (g)
4	323	Wheat	995	1,2,3,4,5
10	397	Wheat	1,220	6,7,8,9,10,11,12
18	712	Wheat	2,192	18,19
19	712	Wheat	2,192	35 (import)
28	658	Wheat	2,023	22,26,27,28,33

For 2011B, the optimal network configuration is given in Figure 3.9b and the optimal flows from biomass cultivation sites to the production facilities are represented in Table 3.8. In this scenario, there are four plants located in cells 7, 18,

19 and 28 with ethanol production rates of 665, 712, 712 and 712 tonnes of ethanol per day, respectively. Differently from scenario 2011A, no wheat is imported and the total collected wheat straw accounts for 35% of the total ethanol produced. The utilisation of straw results in a less distributed network structure in terms of the number of biomass cultivation sites activated and the biomass flows. As can be concluded, hybrid production technologies offer the advantage of more efficient utilisation of biomass resources.

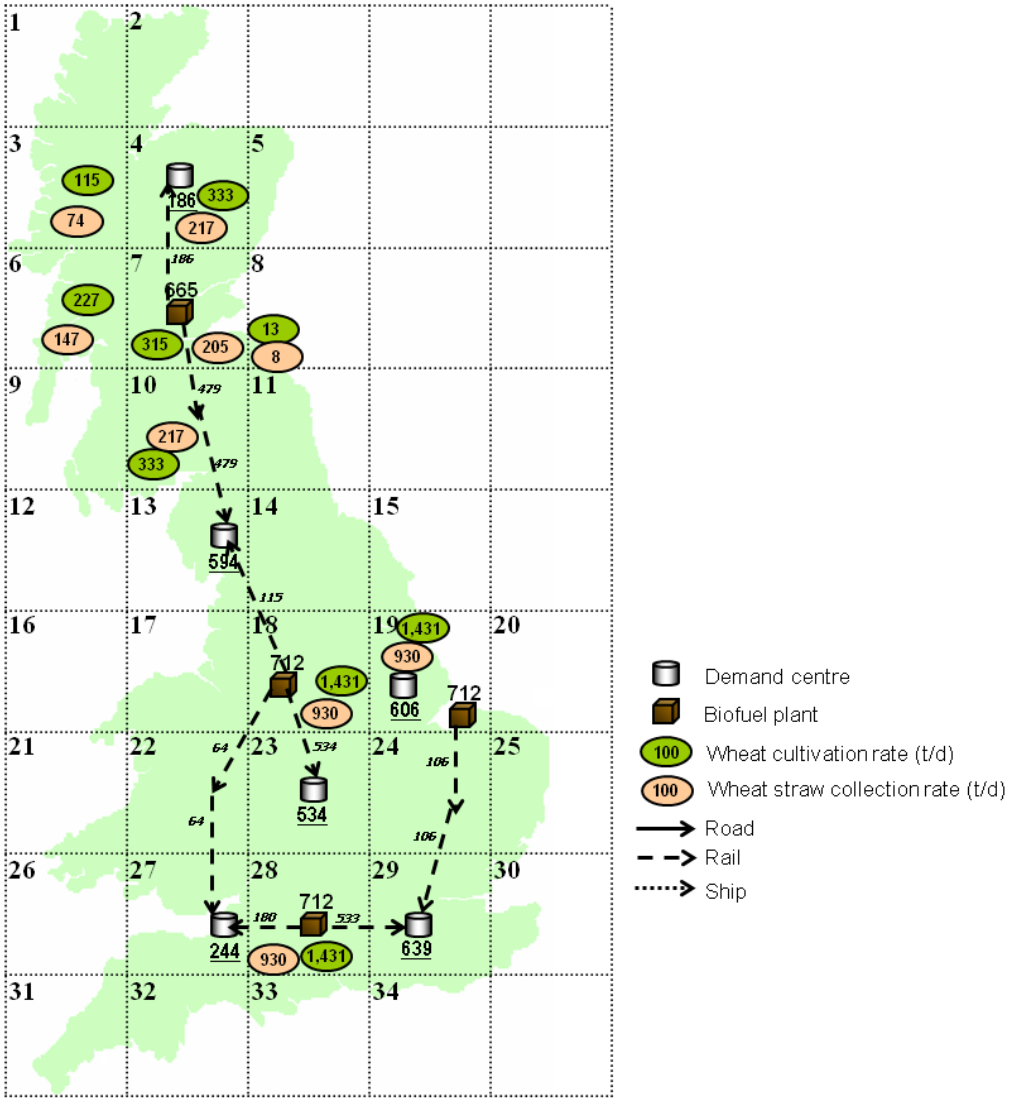

Figure 3.9b Optimal UK ethanol supply chain configuration for instance 2011B.

Table 3.8 Optimal plant locations, capacities and biomass flows for instance 2011B.

Plant Location (cell, *g*)	**Ethanol production rate, Pf_{pg} (t d^{-1})**	**Biomass Feedstock**	**Consumed biomass, Df_{ipg} (t d^{-1})**	**Origin cells (g)**
7	665	Wheat	1,336	3,4,6,7,8,10
		Straw	868	3,4,6,7,8,10
18	712	Wheat	1,431	18
		Straw	930	18
19	712	Wheat	1,431	18
		Straw	930	18
28	712	Wheat	1,431	18
		Straw	930	18

In instance 2011C, it is taken into account that wheat straw can be used for different purposes including animal bedding or heat and power generation. As a result of the competition between these sectors for the use of straw, the opportunity cost (sale price) of wheat straw can increase significantly. Based on this value as a pseudo cultivation cost for straw (35£/t as current level), the optimal configuration of the network is given in Figure 3.9c. Differently from instance 2011B where only domestic biomass resources are utilised for biofuel production, there is a total wheat import of 1,854 tonnes per day in this instance. This is mainly due to the decrease in the use of wheat straw as a feedstock compared to instance 2011B. There are four plants located in cells 7, 18, 19 and 28. The optimal biomass flows for instance 2011C are given in Table 3.9. From comparison of Table 3.8 with Table 3.9, it can be seen that the use of straw has decreased significantly in instance 2011C due to the opportunity cost incurred for its use.

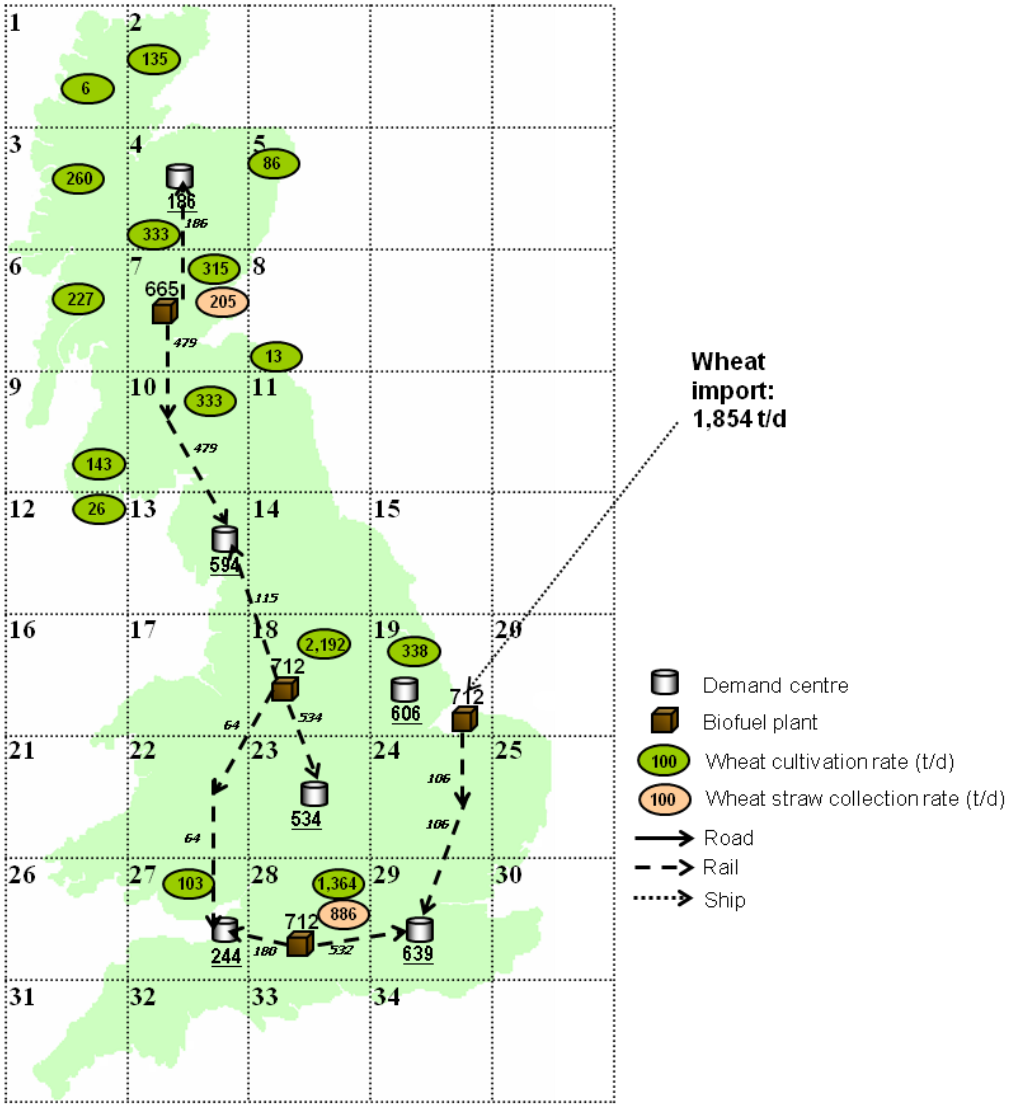

Figure 3.9c Optimal UK ethanol supply chain configuration for instance 2011C.

Table 3.9 Optimal plant locations, capacities and biomass flows for instance 2011C.

Plant Location (cell, g)	Ethanol production rate, Pf_{pg} (t d^{-1})	Biomass Feedstock	Consumed biomass, Df_{ipg} (t d^{-1})	Origin cells (g)
7	665	Wheat	1,879	1,2,3,4,5,7,8,9,10
		Straw	205	7
18	712	Wheat	2,192	18
19	712	Wheat	2,192	19,35 (import)
28	712	Wheat	1,466	27,28
		Straw	886	28

The total supply chain cost as a function of straw price (opportunity cost) for instance 2011C is shown in Figure 3.10. As the opportunity cost of the wheat straw is increased from 35£/t to 150£/t (Farmers Guardian, 2008), use of wheat straw

decreases significantly. At a price level of approximately 140£/t, no straw is used. At higher price levels, biofuel is produced using domestic and imported wheat only and therefore, the total supply chain cost remains constant after this point. This emphasises the fact that opportunity cost of straw can affect the optimal biofuel supply chain cost as well as the optimal configuration significantly.

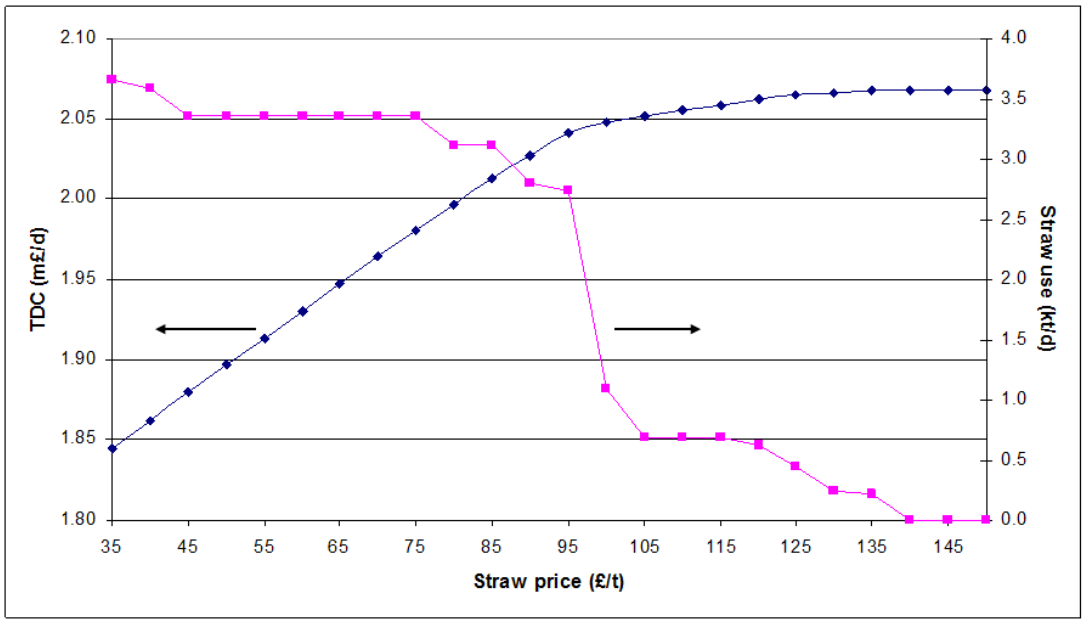

Figure 3.10 Change of total supply chain cost with straw price.

The optimal cost breakdown for scenarios 2011A, 2011B and 2011C are given in Figure 3.11a, Figure 3.11b and Figure 3.11c, respectively. As seen in all figures, total production cost, *TPC* is the most significant supply chain cost contributor. In scenario 2011A, biomass outsourcing cost accounts for 25% of the overall cost. On the other hand, no cost is incurred for import of biomass in 2011B, however the total investment cost is significantly higher due to the establishment of hybrid production facilities that require higher capital cost compared to first generation plants. Biomass cultivation, first generation biofuel and second generation biofuel production costs account for 59%, 21% and 20% of the total production cost, respectively. 73% of the total transportation cost stems from biomass transport. In scenario 2011C, due to the decrease in the use of wheat straw and corresponding increase in wheat import compared to instance 2011B, total second generation biofuel production accounts for only 6% of the overall production cost whereas total product outsourcing cost is 15% of the total supply chain cost. The total supply chain cost for scenario 2011C is 19% higher compared to scenario 2011B mainly due to increasing wheat imports. It must

be noted that the opportunity cost of straw is taken as a pseudo cultivation cost in instance 2011C, therefore it is considered as a component of the total production cost.

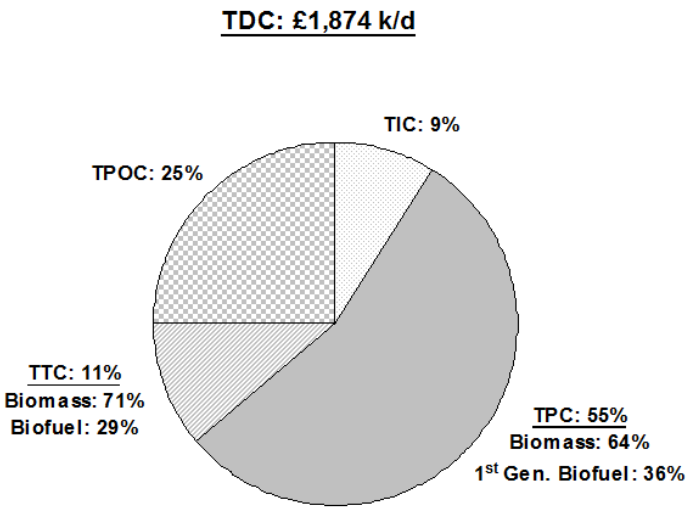

Figure 3.11a Optimal cost breakdown for instance 2011A.

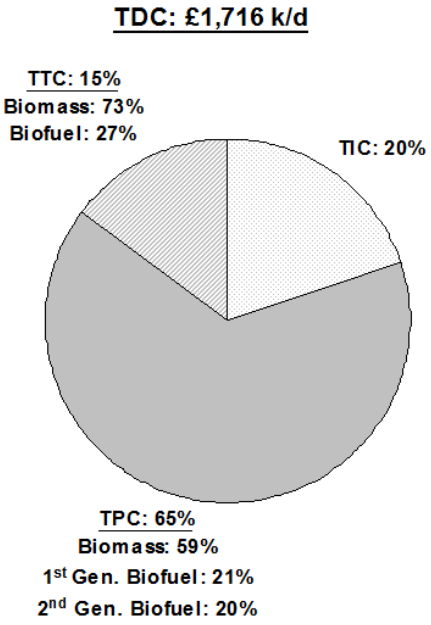

Figure 3.11b Optimal cost breakdown for instance 2011B.

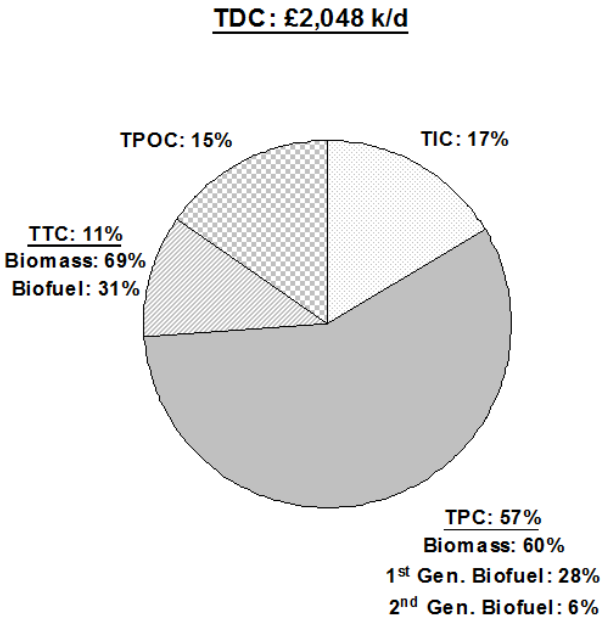

Figure 3.11c Optimal cost breakdown for instance 2011C.

Similar to scenario 2011, two instances are studied for 2020, namely: 2020A and 2020B. In both instances, ethanol can be produced using wheat from first generation and wheat straw, and miscanthus and SRC from second generation biomass crops. An important point to be emphasised is that in this case study, the annual yield estimations of the special energy crops have been based on the long-term productivity of the set-aside land. In instance 2020A, the set-aside area, which refers to the land withdrawn from production, is assumed to be fully (100%) available for cultivation of special energy crops (miscanthus and SRC). On the other hand, in 2020B, it is assumed that up to 50% of the total set-aside is available due to other uses.

The optimal configuration for scenario 2020A is given in Figure 3.12a. The optimal plant locations, capacities with biomass flows are presented in Table 3.10. The locations of plants in cells 11, 14, 15 and 19 are in agreement with the locations of the three plants that are planned to be built in Teeside, Hull, Immingham and Wissington regions, respectively, in the UK during the next few years (HGCA, 2010). There is a wheat import of 2,389 tonnes per day. Miscanthus is the preferred energy crop with its higher cultivation yield and conversion efficiency to ethanol compared to SRC. 34% of the produced ethanol comes from wheat (10% from

imported wheat and 24% from domestic wheat) whereas the remaining 66% comes from wheat straw (13%) and miscanthus (53%).

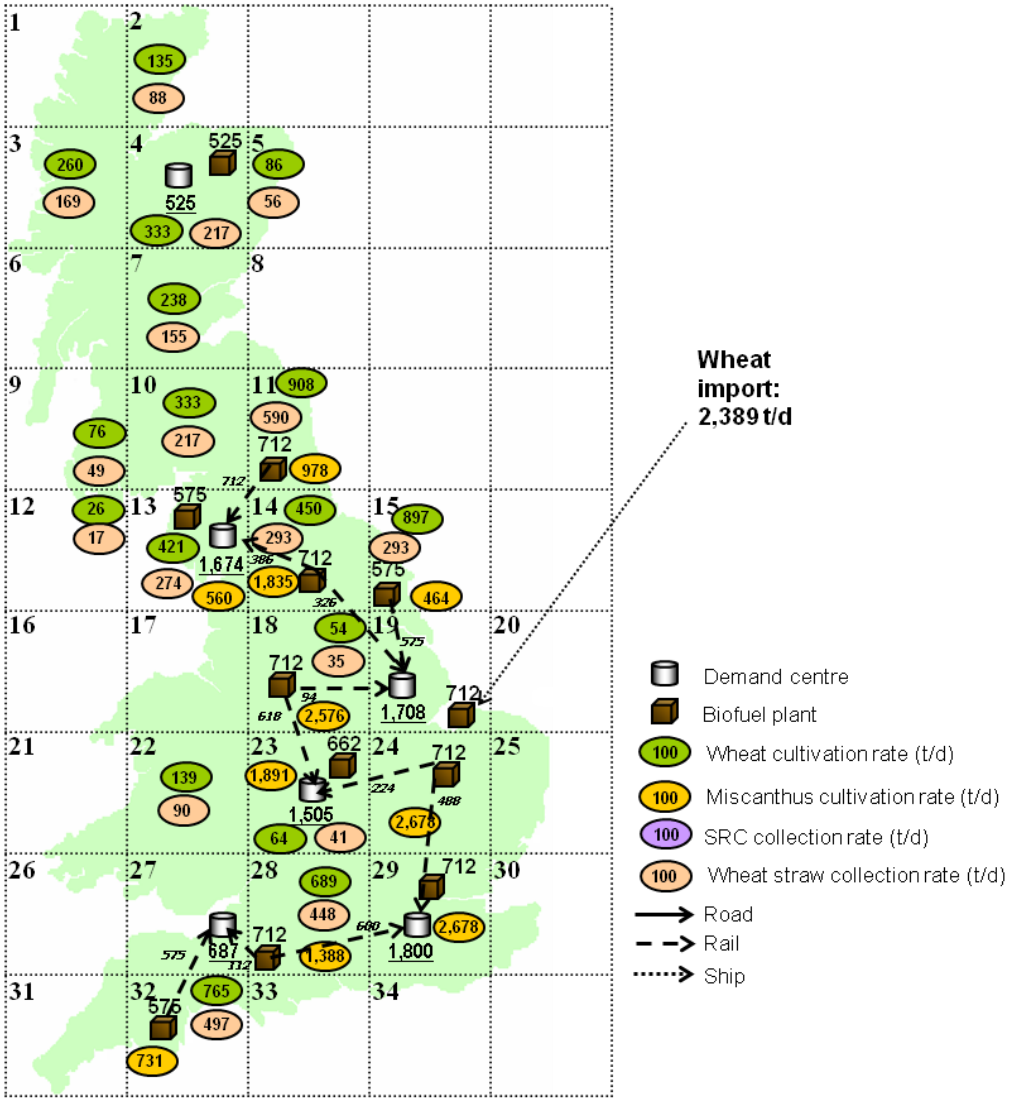

Figure 3.12a Optimal UK ethanol supply chain configuration for instance 2020A.

Table 3.10 Optimal plant locations, capacities and biomass flows for instance 2020A.

Plant Location (cell, g)	Ethanol production rate, Pf_{pg} (t d^{-1})	Biomass Feedstock	Consumed biomass, Df_{ipg} (t d^{-1})	Origin cells (g)
4	525	Wheat	1,054	2,3,4,5,7
		Straw	685	2,3,4,5,7
11	712	Wheat	908	11
		Straw	590	11
		Miscanthus	978	11
13	575	Wheat	856	9,10,12,13
		Straw	557	9,10,12,13
		Miscanthus	560	13
14	712	Wheat	450	14
		Straw	293	14
		Miscanthus	1,835	14
15	575	Wheat	914	15,19
		Straw	583	15
		Miscanthus	464	15
18	712	Wheat	54	18
		Straw	35	18
		Miscanthus	2,578	18
19	712	Wheat	2,192	19
23	662	Wheat	383	12,19,23
		Straw	131	22,23
		Miscanthus	1,891	23
24	712	Miscanthus	2,678	24
28	712	Wheat	689	28
		Straw	448	28
		Miscanthus	1,388	28
29	712	Miscanthus	2,678	29
32	575	Wheat	765	32
		Straw	497	32
		Miscanthus	731	32

The optimal configuration for instance 2020B is given in Figure 3.12b. There are twelve hybrid ethanol production plants whose locations and ethanol production rates are given in Table 3.11. 6,273 tonnes of wheat per day is imported. Similar to the case of scenario 2020A, wheat straw and miscanthus are preferred from second generation feedstocks. Wheat, wheat straw and miscanthus account for 50%, 13% and 37% of the overall ethanol production. The 50% of total ethanol production coming from first generation feedstock is further divided as 24% from domestic and 26% supplied from wheat import. The corresponding optimal biomass flows and biomass site to plant allocation are given in Table 3.11.

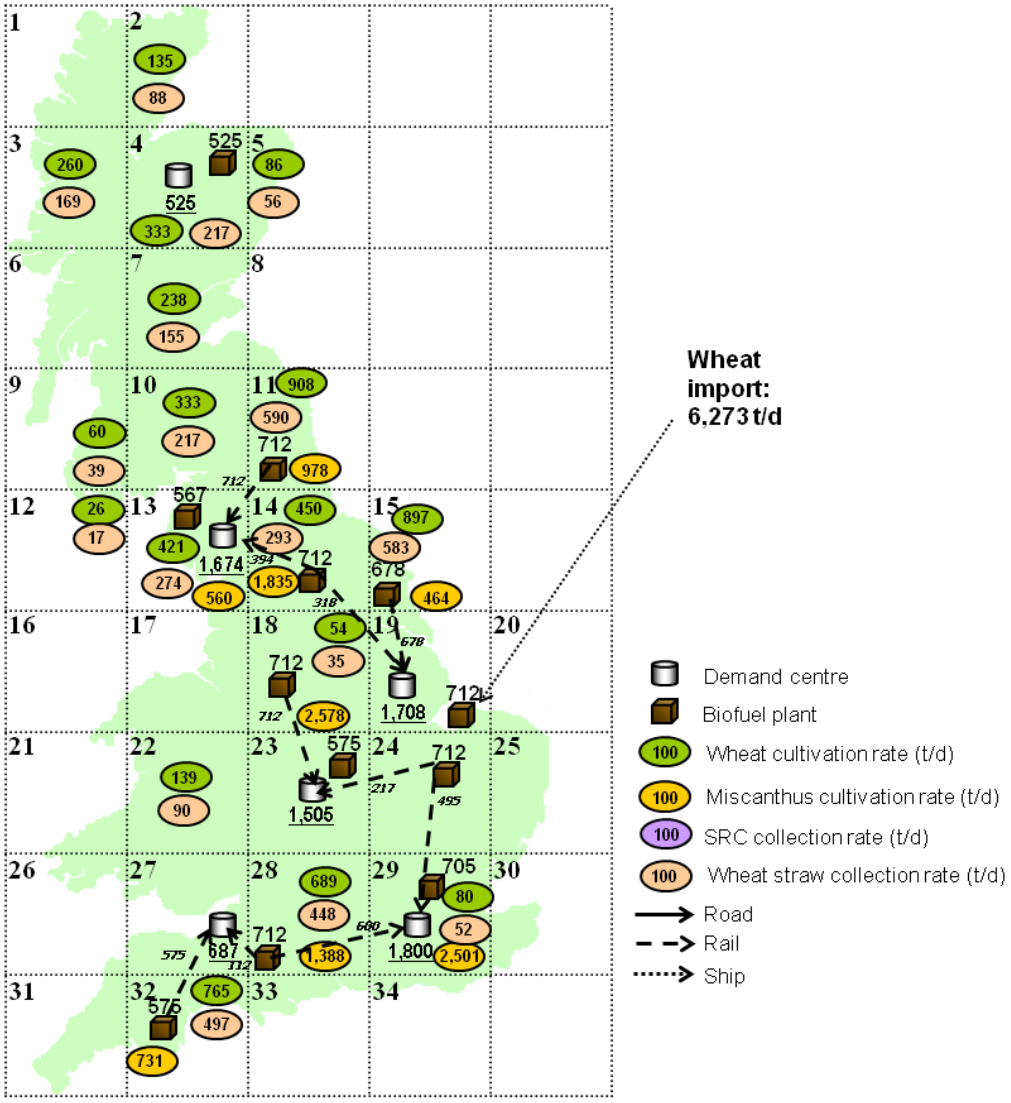

Figure 3.12b Optimal UK ethanol supply chain configuration for instance 2020B.

Table 3.11 Optimal plant locations, capacities and biomass flows for instance 2020B.

Plant Location (cell, g)	Ethanol production rate, Pf_{pg} (t d^{-1})	Biomass Feedstock	Consumed biomass, Df_{ipg} (t d^{-1})	Origin cells (g)
4	525	Wheat	1,054	2,3,4,5,7
		Straw	685	2,3,4,5,7
11	712	Wheat	908	11
		Straw	590	11
		Miscanthus	978	11
13	567	Wheat	840	9,10,12,13
		Straw	546	9,10,12,13
		Miscanthus	560	13
14	712	Wheat	450	14
		Straw	293	14
		Miscanthus	1,835	14
15	678	Wheat	1,229	15,19
		Straw	583	15
		Miscanthus	464	15
18	712	Wheat	54	18
		Miscanthus	35	18
		Straw	2,578	18
19	712	Wheat	2,192	35 (import)
23	575	Wheat	1,697	19,22
		Straw	90	22
24	712	Wheat	2,192	19
28	712	Wheat	689	28
		Straw	448	28
		Miscanthus	1,388	28
29	705	Wheat	80	29
		Straw	52	29
		Miscanthus	2,501	29
32	575	Wheat	765	32
		Straw	497	32
		Miscanthus	731	32

Figure 3.13a and Figure 3.13b show the set-aside land use for instances 2020A and 2020B respectively. In scenario 2020 A, 399.5 kha of the total available 570.2 kha set-aside land is used (corresponding to 70% utilisation of the total land). In scenario 2020B, the available 285.1 kha (50% of 570.2 kha) land is fully utilised. Utilising more set-aside area as in the case of 2020A compared to 2020B results in a reduced dependency on wheat imports and hence, enhancement of security of energy supply.

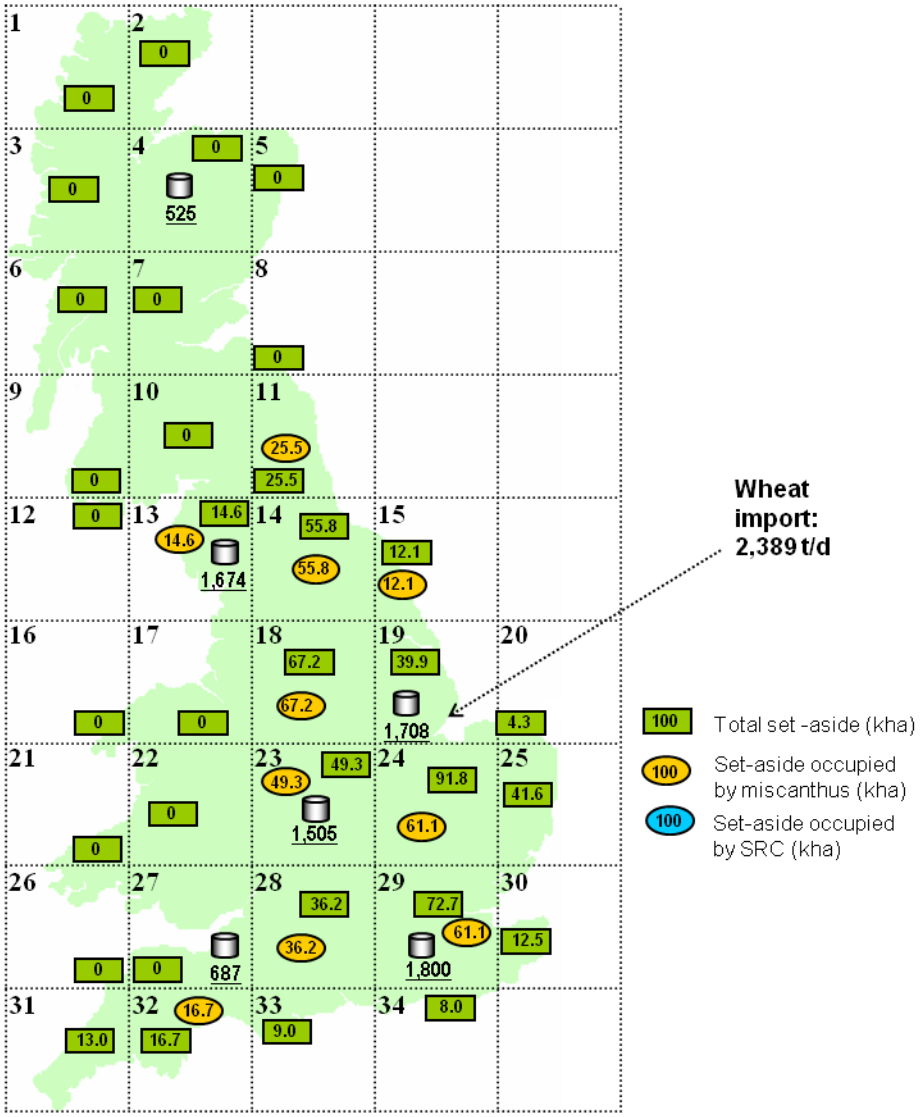

Figure 3.13a Set-aside land use for instance 2020A.

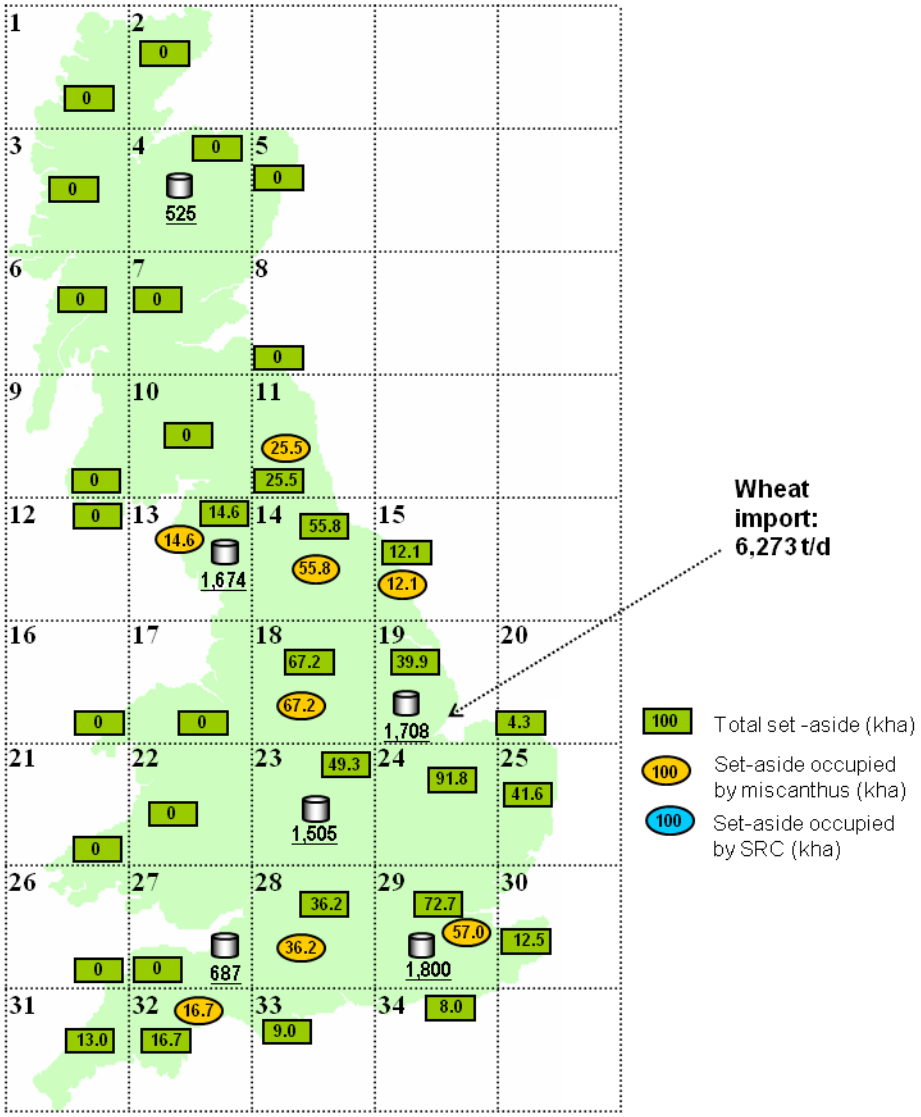

Figure 3.13b Set-aside land use for instance 2020B.

The optimal cost breakdown for instances 2020A and 2020B is given in Figure 3.14a and Figure 3.14b, respectively. Similar to the 2011 scenario, total production cost is the most important cost component. Second generation biofuel production accounts for approximately 30% of the total production cost in both instances. However, with potential cost reductions due to technological learning with time, there is scope for second generation technologies to be deployed to a greater extent.

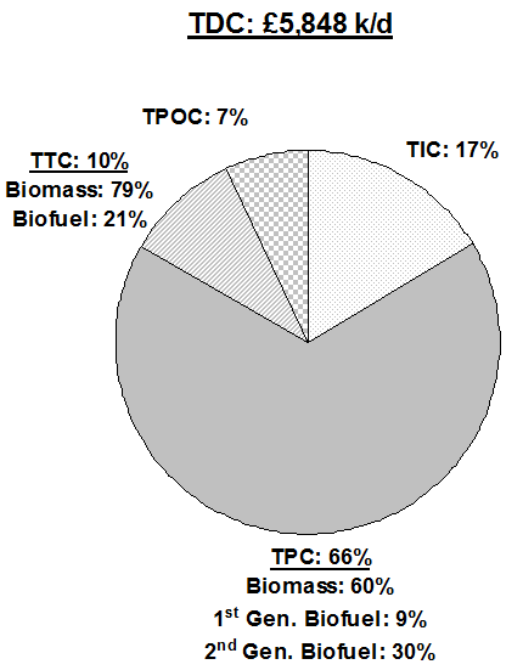

Figure 3.14a Optimal cost breakdown for scenario 2020A.

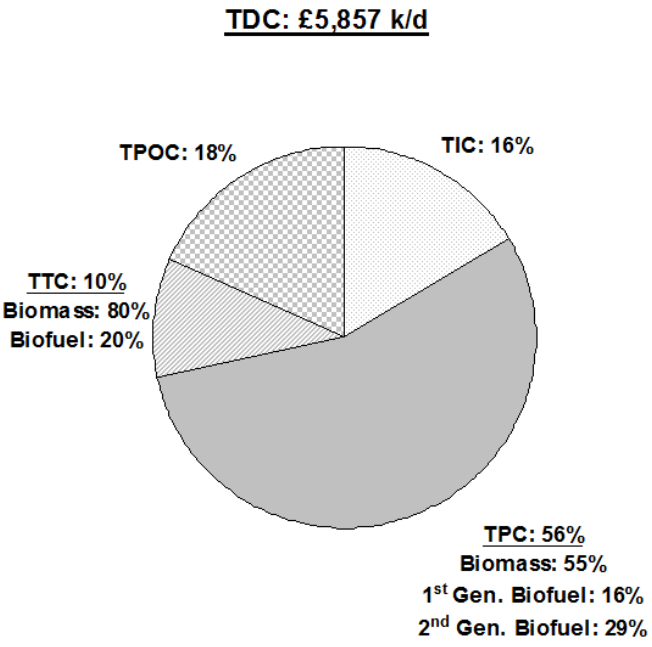

Figure 3.14b Optimal cost breakdown for scenario 2020B.

Finally, model statistics are summarized for all the scenarios in Table 3.12. The proposed models were solved in GAMS 22.8 using CPLEX 11.1 solver in a 3.2 GHz, 3.49 GB RAM machine. The global optimum was achieved for all cases in less than fifteen seconds.

Table 3.12 Summary of computational statistics.

Model Statistics	Scenario 2011 A	Scenario 2011 B	Scenario 2020A	Scenario 2020B
Number of constraints	587	691	934	935
Number of continuous variables	1,364	2,043	3,471	3,471
Number of integer variables	136	136	136	136
Optimality gap (%)	0	0	0	0
CPU time (s)	3	3	11	10

3.1.2.4 Concluding Remarks

In this work, a systems optimisation framework has been introduced for the optimal design of a UK-based hybrid first/second generation ethanol supply chain. The proposed model has been applied to a case study of ethanol production in the UK.

Different instances have been investigated for years 2011 (3.4% of transport fuel by energy content) and 2020 (10% by energy content) based on the domestic and EU biofuel targets, respectively. For 2011, first generation as well as hybrid first/second generation technologies has been studied. The results indicate that utilising wheat straw can offer reductions in the overall supply chain cost. The effect of opportunity cost of straw on the total supply chain cost and optimal network configuration has also been analysed. As seen from the results, opportunity cost can significantly affect the extent to which straw is used for biofuel production as well as the amount of wheat imported. On the other hand, in addition to straw, miscanthus and SRC crops have been considered as potential feedstocks in scenario 2020. The use of set-aside land for these two special energy crops has also been taken into account. The results show that the use of second generation technologies can reduce the dependency on biomass imports. From both scenarios, it is expected that potential future cost reductions are likely to lead to the deployment of second generation biofuel systems at a larger scale.

3.1.3 An Optimisation Framework for a Hybrid First/Second Generation Bioethanol Supply Chain

This section deals with the extension of the single-objective model introduced in Section 3.1.2 to a multi-objective modelling framework taking into account the total

environmental impact of a hybrid (advanced) biofuel supply chain as well as its total cost as the two objectives to be optimised.

3.1.3.1 Problem Statement

Definition of the system and its boundaries is the first step in evaluating the life-cycle emissions of a biofuel supply chain. Adopting a well-to-tank (WTT) approach (Winrock International, 2009), the life-cycle stages under consideration in this work consist of biomass cultivation, biomass transport to biofuel production sites, biofuel production and distribution to demand centres. The life cycle stages with the system boundary are illustrated in Figure 3.15.

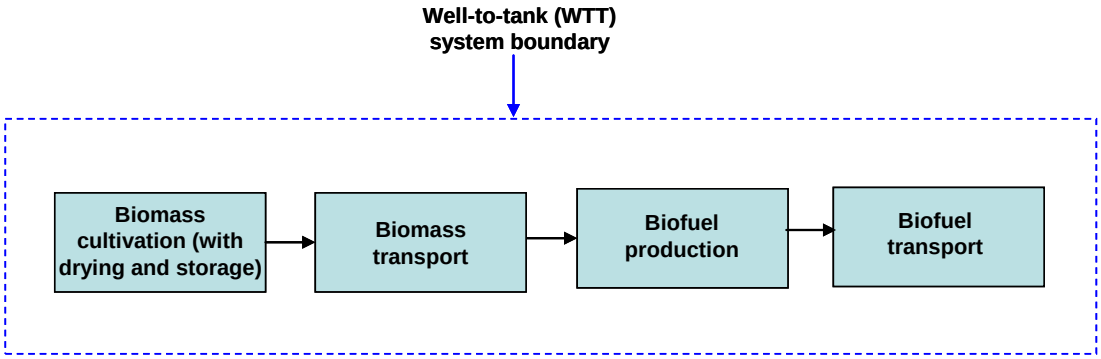

Figure 3.15 Life-cycle stages of a biofuel supply chain based on well-to-tank (WTT) approach (Winrock International, 2009).

The total GHG emissions from the supply chain are evaluated through determination of the total carbon foorprint where global warming potential (GWP) impact factors (that are used to quantify the effect of greenhouse gases in life cycle assessment analysis) are used to calculate the emissions from each life stage. The emissions resulting from a stage is calculated based on the emission factor (per unit of reference flow) and reference resource flow specific to that stage. The three main greenhouse gases emitted from the supply chain are methane (CH_4), nitrous oxide (N_2O) and carbon dioxide (CO_2). The overall GHG emissions are measured in terms of CO_2-equivalent (CO_2-eq) emissions. The global warming potentials of CH_4 and N_2O have been reported as 25 and 298 times as that of CO_2 respectively, according to the 2007 assessment report of Intergovernmental Panel on Climate Change (IPCC, 2007). The specific emission factors for each stage are given per unit of CO_2-eq emissions. Finally, the overall problem can be summarized as:

Given are:

- locations of biofuel demand centres and their biofuel demand,
- biomass feedstock types and their geographical availability,
- unit biomass cultivation cost for each feedstock type,
- unit production cost of biofuel based on the feedstock type (hence technology) utilised,
- transport logistics characteristics (cost, modes, and availabilities),
- capital investment cost for the biofuel production facilities as a function of the production technology deployed,
- specific GHG emission factors of the biofuel life cycle stages,

Determine the optimal:

- biomass cultivation rate for each biomass feedstock type and biofuel production rates,
- locations and scales of biofuel production facilities and biomass cultivation sites,
- flows of each biomass type and biofuel between cells,
- modes of transport of delivery for biomass and biofuel,

So as to minimise the total cost and the total environmental impact of the biofuel supply chain simultaneously.

3.1.3.2 Mathematical Formulation

The problem for the optimal design of a hybrid bioethanol supply chain is formulated as a static multi-objective, mixed integer linear programming (MILP) model with the following notation:

Indices:

g, g'	Square cells (regions)
i	Resource (biomass, biofuel)
l	Transport mode
p	Plant size
s	Life cycle stage of a biofuel supply chain

Sets:

BI	Set of biomass types ($BI = FI \cup CI \cup SI$)
CI	Set of first generation biomass co-products (straw)
FI	Set of first generation biomass types (wheat)

G	Set of square cells (regions)
I	Set of resources (first generation biomass, first generation biomass co-products, second generation biomass, biofuel) ($I = BI \cup PI$)
L	Set of transport modes
P	Set of plant size intervals
PI	Set of product types (biofuel)
SI	Set of second generation energy crops (miscanthus, SRC)
S	Set of life cycle stages of a biofuel supply chain

Parameters:

$EFBC_{ig}$	Emission factor for cultivation of biomass type i in region g (kg CO_2-eq t^{-1} biomass)
$EFBP_{i,}$	Emission factor for biofuel production from biomass type i (kg CO_2-eq t^{-1} biofuel)
$EFTRA_l$	Emission factor for transport mode l (kg CO_2-eq t^{-1} km^{-1})
$ADD_{gg'l}$	Actual delivery distance between regions g and g' via model l (km)
ALD_g	Average local biomass delivery distance (km)
γ_i	Biomass to biofuel conversion factor for biomass type i (t biofuel t^{-1} biomass)

Continuous Variables

Df_{ipg}	Demand for biomass i at a plant of scale p located in region g (t d^{-1})
P_{ig}	Production rate of resource i in region g (t d^{-1})
$Q_{igg'l}$	Flow rate of resource i via mode l from region g to g' (t d^{-1})
TEI	Total environmental impact of a biofuel supply chain network (kg CO_2-eq d^{-1})
EI_s	Environmental impact of life cycle stage s (kg CO_2-eq d^{-1})

a) Objective Function

Based on the ε-constraint method, one of the two conflicting objectives (environmental and economic) is treated as a constraint while the other one is optimised taking into account that constraint. Therefore, in this work, the total daily cost (TDC) of the supply chain is minimised where the total environmental impact of

the supply chain (*TEI*) must be less than or equal to the maximum allowed GHG emissions from the supply chain, denoted by: TEI^{max}. The proposed multi-objective model is derived based on an extension of the single-objective (cost minimisation) biofuel supply chain optimisation model introduced in Section 3.1.2 and therefore, considers the same constraints. As a result, the overall problem can be represented as:

Minimise TDC

$$\begin{aligned} &s.t. && TEI \le \lambda TEI^{\max} \quad (0 \le \lambda \le 1) \\ & && \textit{Production constraints} \\ & && \textit{Demand constraints} \\ & && \textit{Sustainability Constraints} \\ & && \textit{Transportation constraints} \end{aligned} \tag{3.30}$$

The total environmental impact of the supply chain is calculated by:

$$TEI = \sum_{s \in S} EI_s \tag{3.31}$$

where EI_s is the environmental impact of life cycle stage *s* (in terms of GHG emissions). Evaluation of the environmental impact of each life cycle stage is explained next.

b) Environmental Impact of Life Cycle Stages

This section describes the evaluation of the environmental impact of each life cycle stage in a biofuel supply chain. The three main stages under consideration are biomass cultivation (including drying and storage), biofuel production and transportation of resources (biomass or biofuel). The total GHG emissions for biomass cultivation are calculated by:

$$EI_{BC} = \sum_{i \in BI} \sum_{g \in G} EFBC_{ig} P_{ig} \tag{3.32}$$

where EI_{BC} denotes the total environmental impact of biomass cultivation, $EFBC_{ig}$ is the emission factor of biomass cultivation for each biomass type *i* in region *g* (per unit of biomass cultivated) and P_{ig}, which in general represents the production rate of resource *i* in region *g*, refers in this equation to the cultivation rate of biomass *i* in that region.

The environmental impact of transportation is calculated by:

$$EI_{TR} = \sum_{i,g,g',l \in n_{igg'l} I} EFTR_l Q_{igg'l} ADD_{gg'l} \quad (3.33)$$

where EI_{TR} is the environmental impact of transportation of resources within the network $EFTR_l$ is the emission factor of transportation for mode l (per unit of resource transported and per unit distance travelled), $Q_{igg'l}$ is the resource flow between regions g and g' via mode l and $ADD_{gg'l}$ is the delivery distance between these two regions via mode l.

Finally, total emissions from biofuel production are the sum of the emissions resulting from processing of each biomass type i and therefore, given by:

$$EI_{BP} = \sum_{i \in BI} \sum_{p \in P} \sum_{g \in G} EFBP_i \gamma_i Df_{ipg} \quad (3.34)$$

where EI_{BP} is the environmental impact of biofuel production, $EFBP_i$ is the emission factor of biofuel production from biomass type i (per unit of biofuel produced), γ_i is the chemical conversion factor for that biomass (unit of biofuel produced per unit of biomass consumed) and Df_{ipg} is the demand for biomass i at a plant scale of p located in region g.

3.1.3.3 Computational Results

The proposed model has been applied to the case study of bioethanol production in the UK introduced in Section 3.1.2.3. As mentioned previously, the assumed hybrid technology in this work is a lignocellulosic ethanol process technology using a biochemical route, where lignocellulose can be hydrolysed and then fermented (NNFCC, 2008b). Two different demand scenarios have been investigated for 2012 an 2020. Based on the current total UK gasoline demand (52,000 t/d) and the biofuel targets, the total bioethanol demand for 2012 and 2020 has been calculated to be 3,369 and 7,899 t/d, respectively. The demand for 2012 has been calculated assuming a regular increment from 2011 (3.4% by energy) to 2020 (10% by energy) target (UKPIA, 2008; EC, 2009). The total demand is distributed among six demand centres (internal depots) in the UK using the secondary distribution model of Zamboni *et al*. (2009a) as given in Table 3.13. The economic and environmental data for biomass cultivation, transportation and biofuel production are given in Appendix

C. Three modes of transport have been assumed to be available in this study: road, rail and ship.

Table 3.13 Bioethanol demand data for the UK in 2012 and 2020 (t/d).

Demand centre	Scenario 2012	Scenario 2020
4	223.7	524.6
13	713.7	1,673.6
19	728.5	1,708.4
23	641.7	1,504.8
27	293.2	687.5
29	767.8	1,800.4
Total	**3,368.5**	**7,899.3**

The computational results are presented in four sections. In the first section, the potential GHG savings that can be achieved through cost-optimal biofuel supply chains are analysed first. Then the impact of the consideration of carbon tax on the economic and environmental performance of the UK biofuel supply chain has been investigated. In the second section, the trade-off between the environmental and economic objectives is represented with a pareto curve obtained from solving the proposed multi-objective modelling framework based on the ε-constraint method described in the mathematical formulation section. In the third section, an instance of scenario 2020 with four different biomass types available is selected and the optimal results of this instance under three different optimisation criteria are presented and compared. These three cases include economic optimisation, economic optimisation with carbon tax and environmental optimisation. In the fourth section, the maximum ethanol throughput that can be achieved by the available domestic sources in 2020 has been analysed for different cap levels on the total cost. The proposed model was solved in GAMS 23.7 using CPLEX 12 solver on a 1.18 GHz, 3.49 GB of RAM machine at 0% optimality gap, respectively. The computational time required for the solution of the resulting MILP model was only a few seconds in all cases.

a) Potential GHG Savings and the Impact of Carbon Tax

In this section, the GHG savings that can be achieved by biofuel supply chains under economic optimisation are investigated first. Fossil fuel reference systems are used to calculate the net GHG savings resulting from the displacement of fossil fuels by biofuels through comparison of the total emissions resulting from the fossil fuel and

biofuel life cycles. According to the EU methodology, European marginal average gasoline is taken as the fossil fuel reference (Winrock International, 2009).

Two different instances have been studied for scenario 2012. Instance 1 considers bioethanol production from wheat using conventional first generation technologies whereas Instance 2 considers use of wheat and wheat straw as feedstock in hybrid first/second generation production facilities. Using the economic optimisation model introduced in Section 3.1.2, the GHG savings that can be achieved according to the fossil fuel reference have been evaluated for both instances. The results are represented in Figure 3.16. It is seen that the minimum EU GHG savings target of 35% can be met utilising first generation technologies only (Winrock International, 2009). Further reductions in overall emissions are achieved with hybrid production technologies that benefit from the lower emissions of the second generation biofuel life cycle.

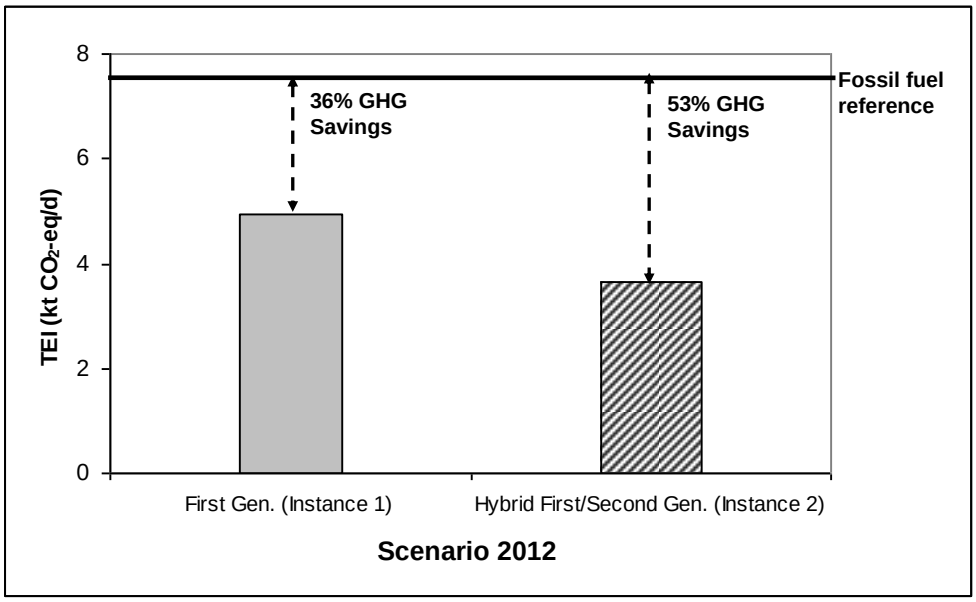

Emission savings (%) = ((Carbon intensity of fossil fuel reference- Carbon intensity of biofuel)/ Carbon intensity of fossil fuel reference)) x100 (Winrock International, 2009).

Figure 3.16 Total GHG savings for instances 1 and 2 of scenario 2012 based on the minimum cost configurations.

For 2020, three different instances have been considered. Instances 1 and 2 consider the same feedstock and production technologies as those for scenario 2012. On the other hand, instance 3 covers two dedicated energy crops: miscanthus and SRC that are cultivated on the set-aside land (allowing 100% utilisation), in addition to wheat and wheat straw. The current total set-aside land available in the UK is 570.2 kha

(DEFRA, 2007) and the distribution per cell is as given in Table B10 in Appendix B. The amount of GHG savings that can be achieved using the minimum cost configurations are given in Figure 3.17. As can be seen from the figure, the minimum 35% (short term) target cannot be met using first generation ethanol production only. When wheat straw is used in addition to wheat, the GHG savings are increased from 33% (instance 1) to 40% (instance 2). The total GHG emissions are reduced further with the use of second generation dedicated energy crops. It is clearly seen that the interim 60% GHG emissions savings target can only be met if energy crops in addition to wheat and wheat straw are used for bioethanol production (Winrock International, 2009).

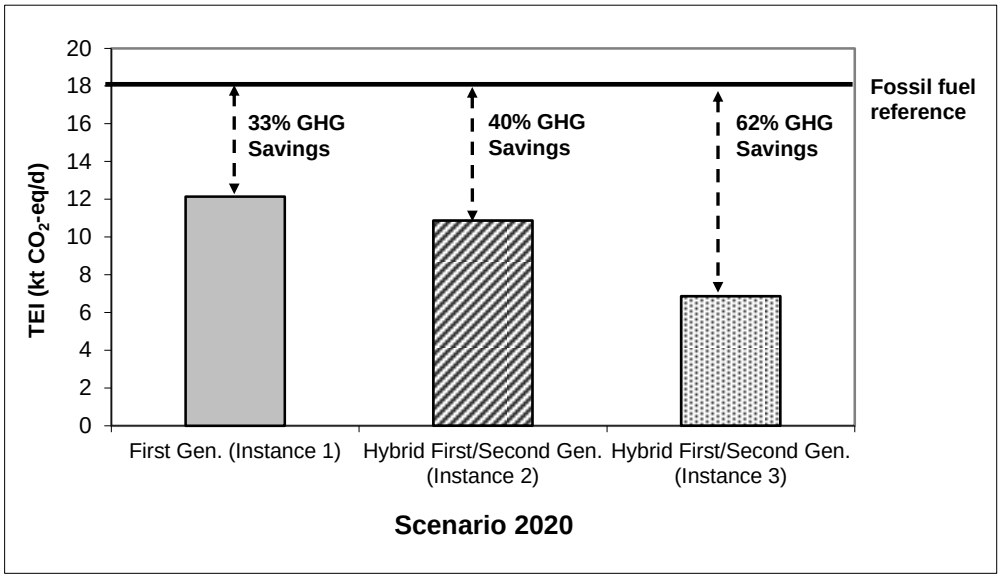

Figure 3.17 Total GHG savings for instances 1, 2 and 3 of scenario 2020 based on the minimum cost configurations.

After evaluating the GHG savings for the first and second generation biofuel supply chains with minimum overall cost, the effect of considering a carbon tax has been studied. For both 2012 instances, the currently considered tax level of 15£ per tonne (BBC, 2010) of CO_2 emitted does not improve the environmental performance of the supply chain with the cost-optimal configurations. Similarly, a maximum level of 50£/t CO_2-eq (BusinessGreen, 2010) does not have an impact on the overall emissions. This is mainly due to the system not being flexible in terms of biomass supply options.

Figure 3.18 shows the effect of considering carbon tax on the economic and environmental performances of instance 3 of scenario 2020. An important point to be made clear is that these results are for a biofuel supply chain that is required to meet the total demand as companies may decide not to operate at high carbon tax levels due to profitability reasons.The total cost of the supply chain increases linearly with carbon tax. On the other hand, the total environmental emissions are decreased remarkably up to about a carbon tax-level of 5£/t CO_2-eq by a significant reduction in biomass imports and the corresponding increase in the use of second generation crops. For tax levels between 5 and 30 £/t CO_2-eq, the total imported wheat and the total emissions remain constant. At a tax level of 35 £/t CO_2-eq, the use of second generation crops is slightly increased whereas the biomass imports are reduced further. From this tax level up to 50£/t CO_2-eq, the emission profile remains flat with no changes in the utilisation rates of domestic and imported biomass. The currently considered tax level of 15£/t CO_2-eq results in a total 64% of GHG savings compared to the fossil fuel reference, which corresponds to a 2% more savings when compared to the case with no carbon tax (Instance 3 in Figure 3.17).

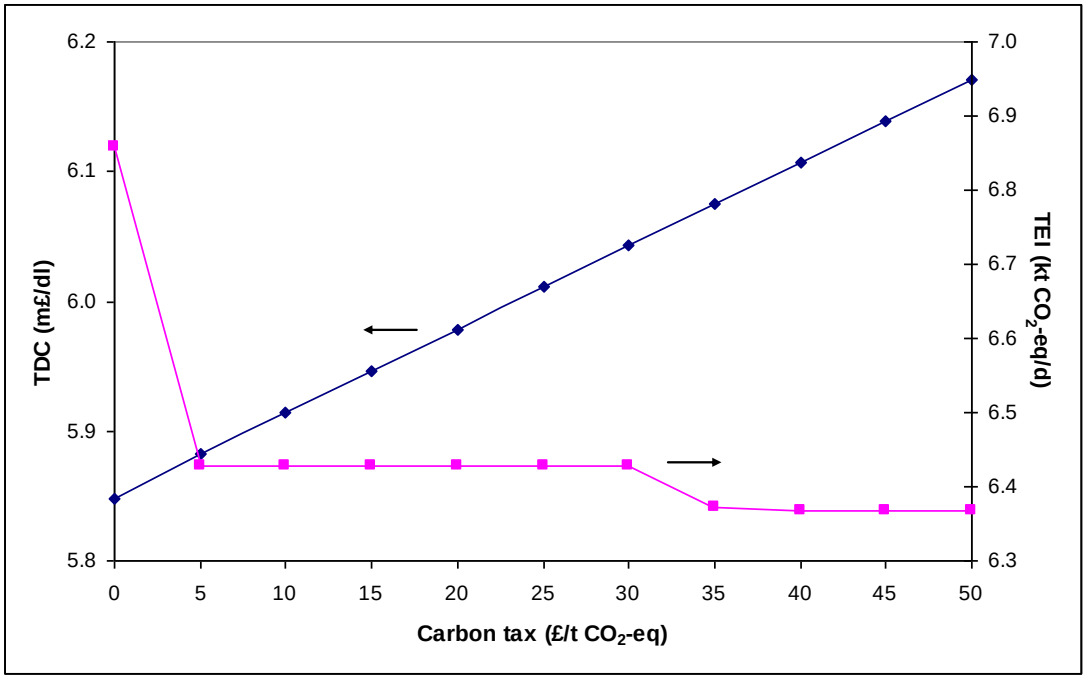

Figure 3.18 The effect of carbon tax level on the economic and environmental performances of instance 3 of 2020 scenario.

b) The Trade-off between the Economic and the Environmental Objectives

Figure 3.19 shows the trade-off between the economic and environmental objectives of instance 3 in scenario 2020. The pareto curve is obtained using the multi-objective optimisation framework explained in the mathematical formulation section. Moving from the left end to the right end to the curve, total GHG savings are increased from 62% to 69% whereas total supply chain cost increases by approximately 11%.

Proceeding along the pareto curve from configuration 1 to configuration 20, utilisation of the set-aside area increases by cultivating more energy crops as seen in Figure 3.20 and the total imported wheat amount decreases accordingly. This clearly shows the better environmental performance of second generation over first generation biofuel production systems. At point 2, no wheat is imported. From this point to 20, the overall biofuel demand is met using domestic biomass resources only and at point 20, the total available set-aside area is fully used for cultivation of energy crops. The fraction of ethanol demand met by using different biomass resources for points 1, 2, 3 and 20 is given in Table 3.14. Going from configuration 1 to 20, the increase in the use of second-generation biomass crops with the corresponding decrease in the utilisation rate of the first generation resources is clearly seen here.

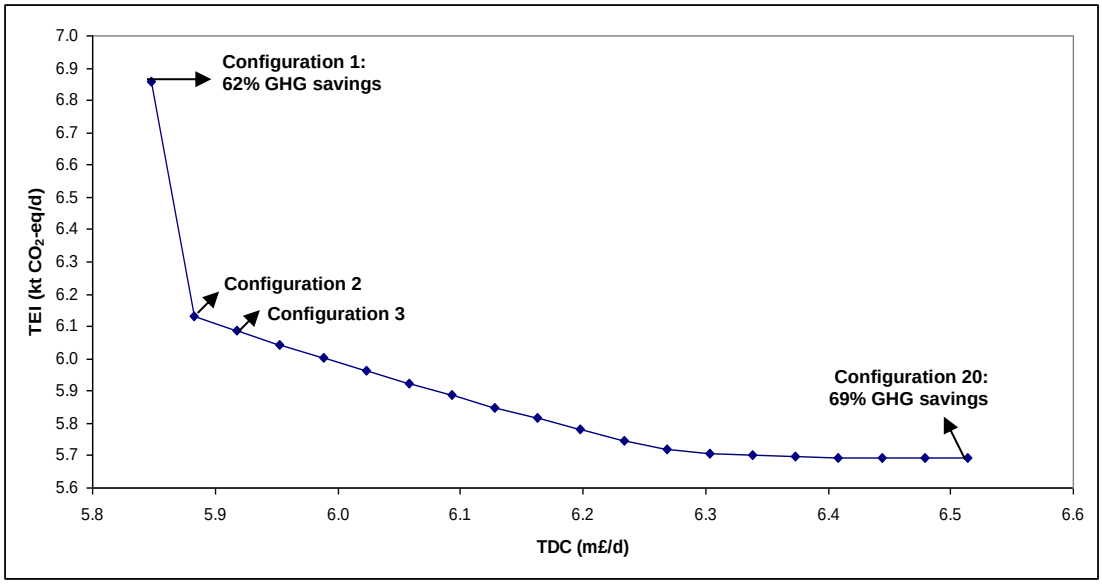

Figure 3.19 Pareto curve for instance 3 of scenario 2020 based on multi-objective optimisation.

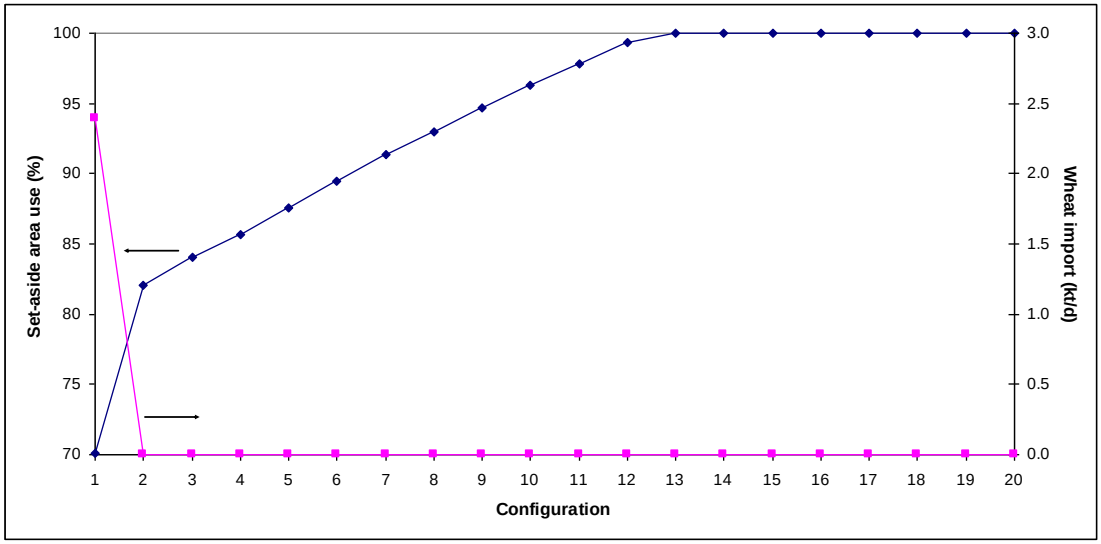

Figure 3.20 Change in use of set-aside area and imported wheat amount along the pareto curve in Figure 3.19.

Table 3.14 Breakdown of biofuel production from different biomass resources along the pareto curve.

Biofuel production (% of the overall)	Configuration 1	Configuration 2	Configuration 3	Configuration 20
Domestic wheat	24%	24%	23%	14%
Imported wheat	10%	0%	0%	0%
Wheat straw	13%	13%	12%	8%
Miscanthus	53%	63%	65%	78%

c) Comparison of the UK Biofuel Supply Chain Configurations under Different Optimisation Criteria

This section includes the comparison of the optimal UK biofuel network configurations under three different optimisation criteria, namely: economic optimisation, economic optimisation considering carbon tax and environmental optimisation.

Figure 3.21a shows the optimal configuration for instance 3 of scenario 2020. Only bioethanol flows are shown in the figure for convenience. There are twelve plants located in cells 4, 11, 13, 14, 15, 18, 19, 23, 24, 28, 29 and 32. The ethanol production rates at each plant as well as the biomass cultivation rates in each cell are

as given. Miscanthus is the preferred second generation energy crop with its higher cultivation yield and conversion efficiency to ethanol when compared to SRC. Wheat is imported at a rate of 2,389 tonnes per day, which accounts for 10% of the overall biofuel production. Domestic wheat and wheat straw are utilised to their maximum availability, meeting 24% and 13% of the overall production, respectively. The remaining 53% of the total demand is met using miscanthus, which is cultivated on 70% of the total available set-aside land.

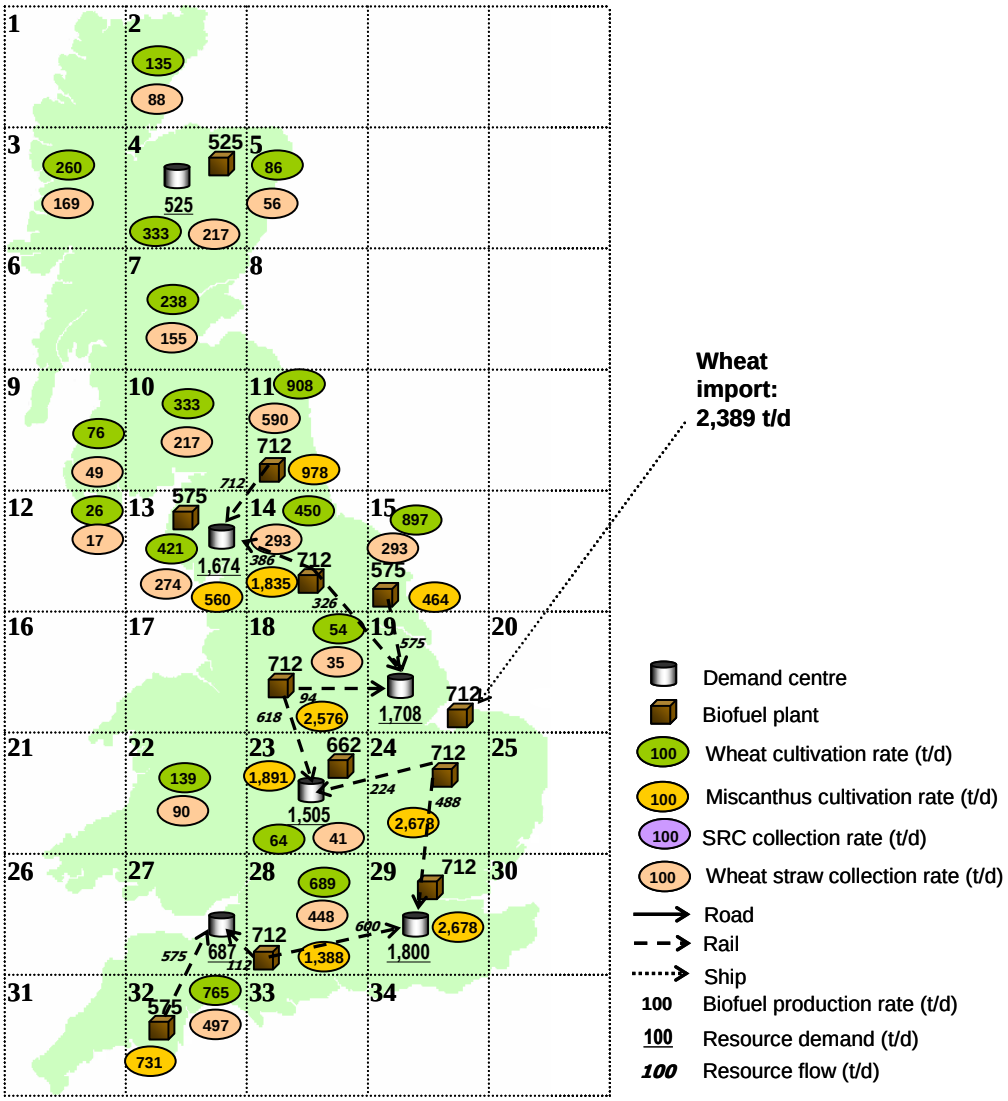

Figure 3.21a Optimal UK bioethanol supply chain configuration for instance 3 of scenario 2020 under economic optimisation.

Figure 3.21b represents the optimal UK bioethanol supply chain configuration under economic optimisation when a carbon tax is applied at the current rate of 15£/t CO_2-eq. From the comparison of Figure 3.21a and Figure 3.21b, the optimal locations and biofuel production rates remain the same whereas the biomass imports and biomass

cultivation rates in some cells (e.g. cell 19) are different. Total amount of wheat imported is decreased by 60% compared to the previous case (Figure 3.21a), whereas the use of miscanthus from second generation energy crops is increased by 11%. The optimal plant locations and biofuel production rates are given in the figure. Similar to the previous case, wheat and wheat straw are used up to their maximum availabilities where as 77% of the total available set-aside land is used for energy crop cultivation.

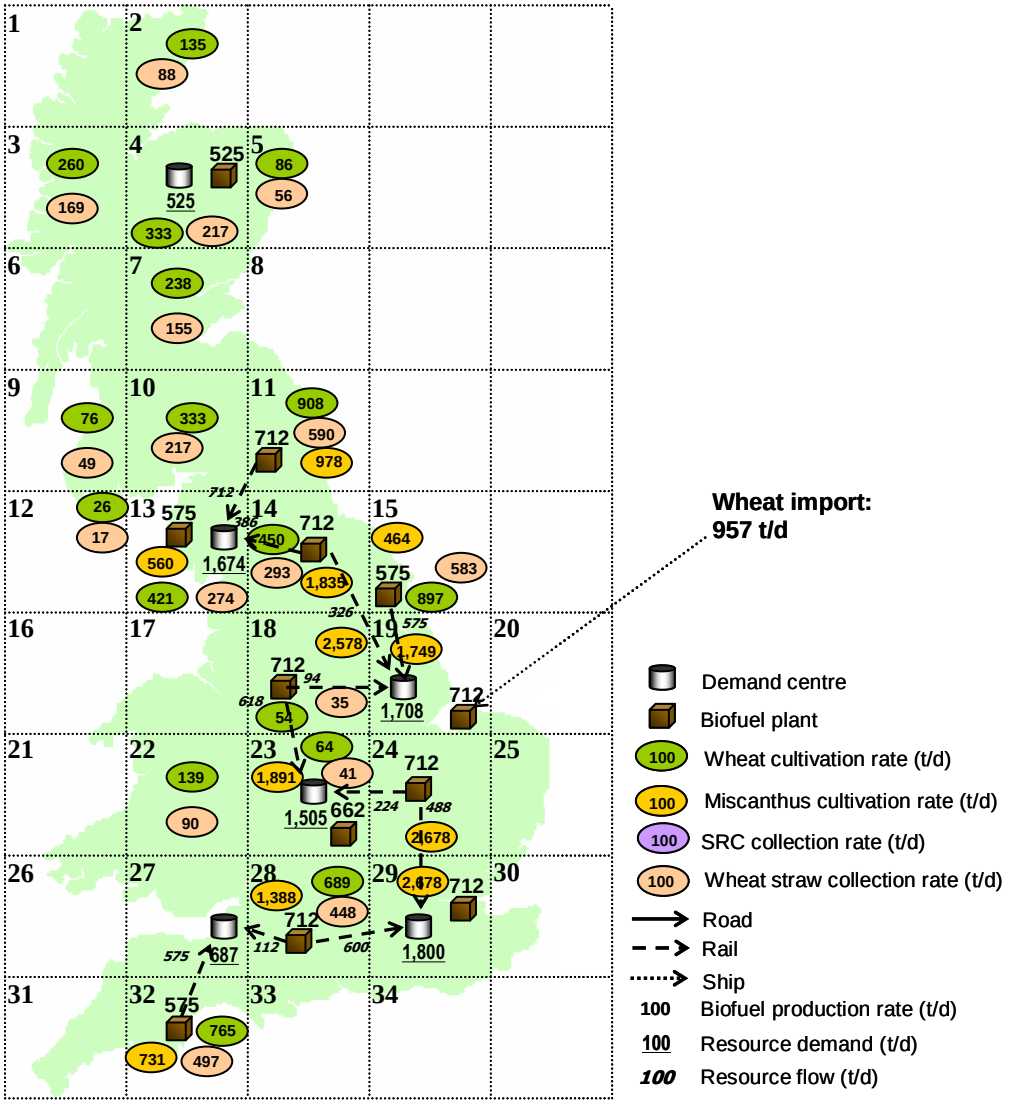

Figure 3.21b Optimal UK bioethanol supply chain configuration for instance 3 of scenario 2020 under economic optimisation with a carbon tax of 15£/t CO_2-eq.

Finally, the optimal network configuration under environmental optimisation is given in Figure 3.21c. There are 17 plants whose locations and biofuel production rates are given in the figure. To decrease the total emissions resulting from the supply chain to a minimum, no wheat is imported and miscanthus from second generation energy crops is used to its maximum availability by the full utilisation of the set-aside land

(100%). Second generation biomass crops including straw and miscanthus, account for 86% of the total biofuel production in this case.

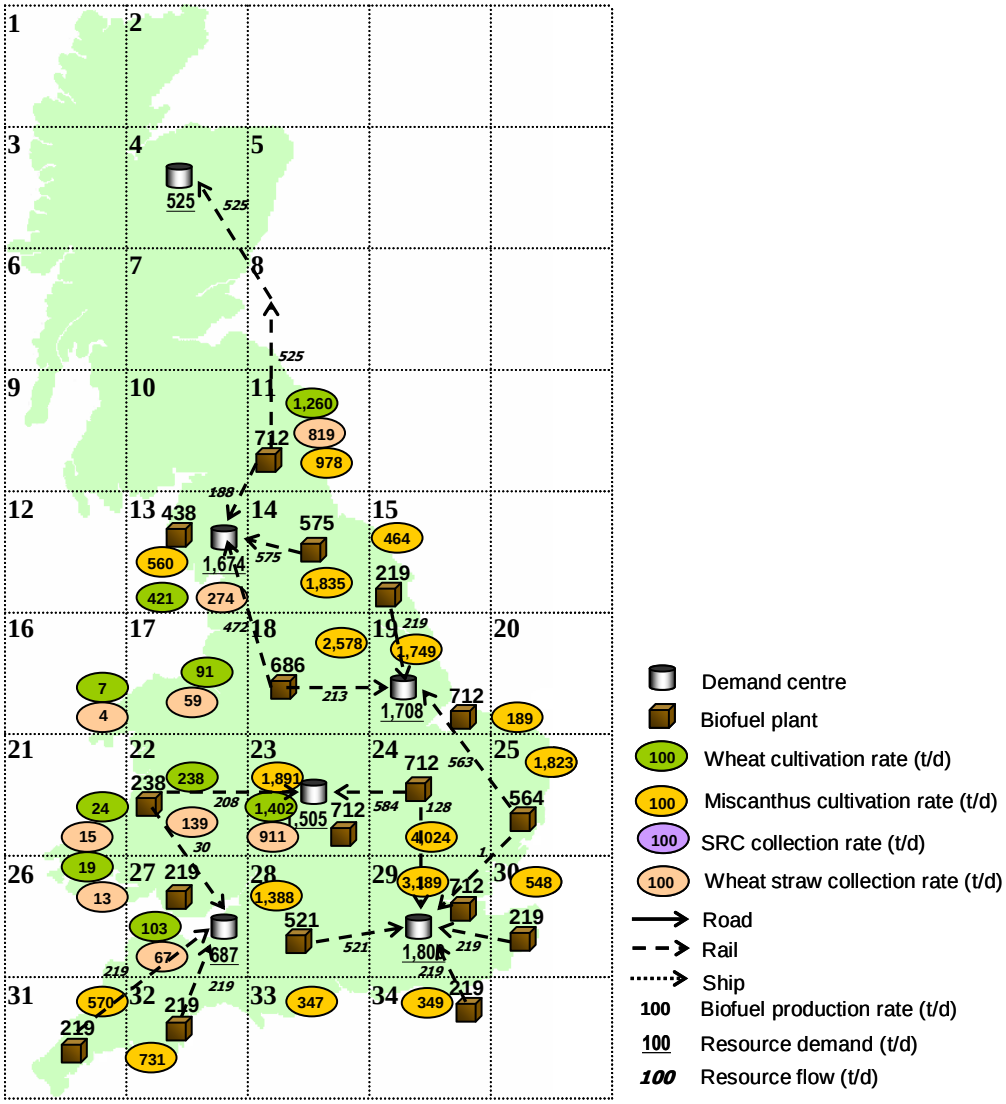

Figure 3.21c Optimal UK bioethanol supply chain configuration for instance 3 of scenario 2020 under environmental optimisation.

The optimal breakdown of the total environmental impact of the UK biofuel supply chain for instance 3 of scenario 2020 under three different optimisation criteria is shown in Table 3.15. Biofuel production, followed by biomass cultivation and transportation, is the most significant contributor to the overall GHG emissions in all cases. Under economic optimisation, biomass import accounts for 4% of the overall emissions. When a carbon tax is applied, this value is decreased to 2% as seen in the table. Going from economic to environmental optimisation, the decrease in the overall emissions and increase in the utilisation of the second generation biofuel production are clearly seen.

Table 3.15 Optimal breakdown of the total environmental impact for instance 3 of scenario 2020 under three different optimisation criteria.

Breakdown of the total environmental impact	**Economic optimisation**	**Economic optimisation with carbon tax (15£/t CO_2-eq)**	**Environmental optimisation**
TEI **(kt CO_2-eq/d)**	**6.86**	**6.43**	**5.69**
$\boldsymbol{EI_{PRO}}$ **(% of *TEI*)**	**43%**	**44%**	**47%**
1st Gen. Biofuel (% of $\boldsymbol{EI_{PRO}}$)	51%	44%	24%
2nd Gen. Biofuel (% of $\boldsymbol{EI_{PRO}}$)	49%	56%	76%
$\boldsymbol{EI_{BC}}$ **(% of *TEI*)**	**38%**	**37%**	**33%**
1st Gen. Biomass (% of $\boldsymbol{EI_{BC}}$)	66%	59%	34%
2nd Gen. Biomass (% of $\boldsymbol{EI_{BC}}$)	34%	41%	66%
$\boldsymbol{EI_{TR}}$ **(% of *TEI*)**	**15%**	**17%**	**20%**
Biomass transport (% of $\boldsymbol{EI_{TR}}$)	98%	99%	98%
Biofuel transport (% of $\boldsymbol{EI_{TR}}$)	2%	1%	2%
$\boldsymbol{EI_{IMP}}$ **(% of *TEI*)**	**4%**	**2%**	**-**

d) Analysis of the Maximum Bioethanol Throughput under Different Cap Levels for the Total Supply Chain Cost

This section presents the results of the sensitivity analysis which has been carried out to evaluate the maximum bioethanol throughput under different cap levels of the total supply chain cost. Three different values of the sustainability factor which represents the maximum fraction of domestic first generation biomass crops to be used for biofuel production have been considered. These three scenarios under consideration are named as high (20%), medium (15%) and low (10%) sustainability cases. Figure 3.22 shows the results of the sensitivity analysis. The maximum bioethanol production that can be attained without considering any cap on the total supply chain cost is about 10, 9 and 8 ktonnes per day for the high, medium and low level sustainability cases, respectively. For the medium level case (which is also the nominal value considered currently in the supply chain optimisation in this paper), up to a cap level of 7 m£/d of total supply chain cost, the total production increases with increasing cap levels. After that point, the total production remains constant regardless of the increase in the cap level as all the domestic resources including first and second generation biomass crops are used up to their maximum availabilities at

that point and the ethanol production cannot be increased further even if the cap level is increased. Analysing and understanding the relationship between the maximum bioethanol production and the total supply chain cost can have a determining effect for decision-makers as well as the government incentive plans for biofuel systems. At a cap level of about 6m£/d and current level of the sustainability factor (0.15), the maximum throughput of the supply chain is able to meet the 2020 ethanol demand (7,899 t/d). In the case where biomass is imported, a cost saving of about 0.15 m£/d is achieved through biomass imports which results in the reduction of the total daily cost to 5.85 m£/d (Figure 3.18 and Figure 3.19).

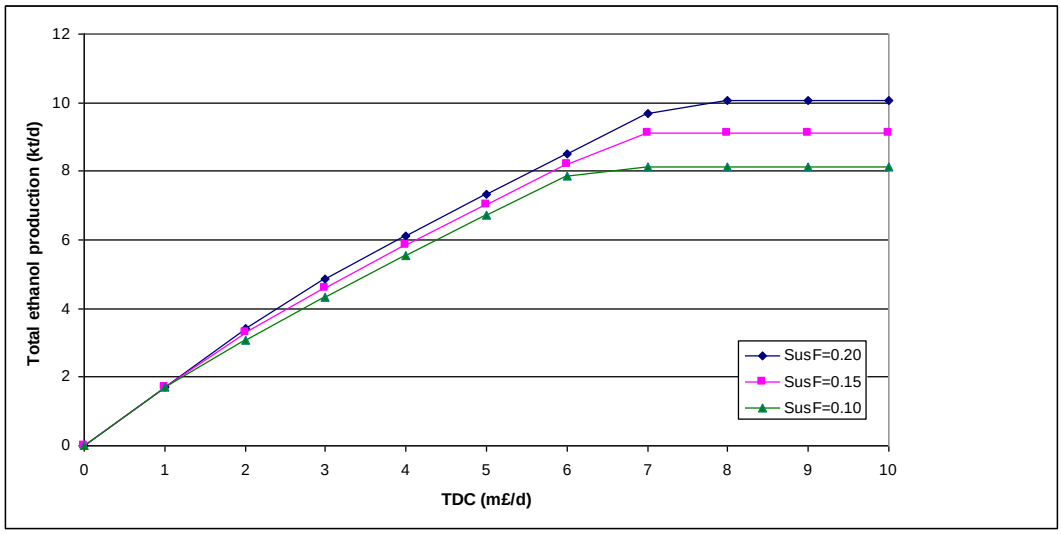

Figure 3.22 Change of maximum bioethanol throughput with different cap levels of the total supply chain cost for three different sustainability factor levels.

3.1.3.4 Concluding Remarks

In this work, the trade-off between the environmental and economic performances of the UK bioethanol supply chain has been studied using a multi-objective approach that is solved based on the ε-constraint method. The environmental impact has been evaluated using GWP impact factors. In addition, the effect of considering a carbon tax on the overall environmental emissions has also been investigated.

The results highlight the better environmental performance of the second generation biofuel production technologies compared to first generation by evaluating the potential GHG savings that can be achieved through biofuel production in hybrid facilities that integrate first and second generation technologies. The use of set-aside land for cultivation of energy crops offers significant advantages in this aspect.

Among the life cycle stages, biofuel production is the most significant source of emissions. However, with future improvements in production technologies, there is scope to reduce these emissions.

Apart from the trade-off between the economic and environmental objectives, the effect of different cap levels of the total supply chain cost on the maximum ethanol production that can be attained has been analysed for scenario 2020 where four types of different biomass feedstock were considered. The maximum ethanol production has been evaluated as approximately 9,000 tonnes per day, which is about 14% higher than the EU biofuel target for 2020 (7,899 t/d).

3.2 Multi-Period Optimisation of Biofuel Supply Chains

This section first introduces the extension of the static, single-objective MILP framework presented in Section 3.1.2 to a multi-period model to account for temporal effects such as change in bioethanol demand through time. The developed multi-period model aims to provide insight into the optimal evolution of a bioethanol supply chain through time by minimising its total net present cost. After presenting the multi-period model in the next section, Section 3.2.2 deals with incorporating uncertainty into the proposed multi-period model.

3.2.1 Deterministic Multi-Period Optimisation of Biofuel Supply Chains

A deterministic, multi-period mixed integer linear programming model is presented in this section with the objective to minimise the total (net present) cost of a biofuel supply chain taking into account temporal effects such as change of biofuel demand with time. The modelling horizon is divided into “time periods” to consider these temporal effects. The applicability of the proposed model is highlighted with a case study in Section 3.2.1.3 where the concept of technological learning is also investigated.

3.2.1.1 Problem Statement

The overall problem studied in this work for the optimal design of a biofuel supply chain can be stated as follows:
Given are:

- locations of biofuel demand centres and their biofuel demand in each time period,
- biomass feedstock types and their geographical availabilities in each time period,
- unit biomass cultivation cost for each feedstock type in each time period,
- unit production cost of biofuel based on the feedstock type (hence technology) utilised in each time period,
- transport logistics characteristics (cost, modes, and availabilities),
- capital investment cost for the biofuel production facilities as a function of the production technology deployed,

Determine the optimal:

- biomass cultivation rate and location for each biomass feedstock type and biofuel production rates in each time period,
- locations and scales of biofuel production facilities in each time period,
- flows of each biomass type and biofuel between cells and biomass imports in each time period,
- modes of transport of delivery for biomass and biofuel in each time period,

So as to minimise the total supply chain cost (net present cost).

3.2.1.2 Mathematical Formulation

The problem for the optimal design of a biofuel supply chain introduced here is formulated as a spatially-explicit, multi-period, mixed integer linear programming (MILP) model with the following notation:

Indices:

g, g'	Square cells (regions)
i	Resource (biomass, biofuel)
l	Transport mode
p	Plant size
t	Time period

Sets:

BI	Set of biomass types ($BI = FI \cup CI \cup SI$)
CI	Set of first generation biomass co-products (straw)
FI	Set of first generation biomass types (wheat)

G	Set of square cells (regions)
I	Set of resources (first generation biomass, first generation biomass co-products, second generation biomass, biofuel) ($I = BI \cup PI$)
L	Set of transport modes
P	Set of plant size intervals
PI	Set of product types (biofuel)
SI	Set of second generation energy crops (miscanthus, SRC)
T	Set of time periods
$Total_{igg'l}$	Set of total transport links allowed for each resource i via mode l between regions g and g'
$n_{igg'l}$	Subset of $Total_{igg'l}$ including all regions g' in the neighbourhood of region g for each product i and mode l

Parameters:

$ADD_{gg'l}$	Actual delivery distance between regions g and g' via model l (km)
ALD_g	Average local biomass delivery distance (km)
A_g^s	Set-aside area available in region g (ha)
α	Operating period in a year (d year^{-1})
β	Fraction of straw recovered per unit of wheat cultivated (t straw t^{-1} wheat)
$BA_{ig}^{min/max}$	Minimum/maximum availability of first generation biomass i ($i \in FI$) in region g (t biomass d^{-1})
$DFOC_t$	Discount factor for operating costs in time period t
$DFCAP_t$	Discount factor for capital costs in time period t
$\gamma_{i'i}$	Biomass to biofuel conversion factor for biomass type i' ($i' \in BI$) to biofuel type i ($i \in PI$) (t biofuel t^{-1} biomass)
IC_p	Investment cost of a plant of size p (£)
$IMPC_{ig^*t}$	Unit impost cost for importing resource i from foreign supplier g^* in time period t (£ t^{-1})
$PCap_p^{min/max}$	Minimum/maximum biofuel production capacity of a plant of size p (t d^{-1})
$Q_{il}^{min/max}$	Minimum/maximum flowrate of resource i via mode l (t d^{-1})
$SusF$	Maximum fraction of domestic first generation biomass allowed for biofuel production

UCC_{igt} Unit biomass cultivation cost of biomass type i in region g *in* time period t (£ t^{-1} biomass)

UPC_{ipt} Unit biofuel production cost of biofuel i at a plant of scale p in time period t (£ t^{-1} biofuel)

UTC_{il} Unit transport cost of product i via mode l (£ t^{-1} km^{-1})

UTC^{*} Unit transport cost for local biomass transfer (£ t^{-1} km^{-1})

Y_{ig} Yield of second generation energy crop i $(i \in SI)$ in region g (t ha^{-1} $year^{-1}$)

Binary Variables

AV_{pgt} 1 if a biofuel production plant of size p is available in region g in time period t

E_{pgt} 1 if a biofuel production plant of size p is to be established in region g in time period t

Continuous Variables

A_{igt} Land occupied by second generation crop i $(i \in SI)$ in region g in time period t (ha)

D_{igt} Demand for resource i in region g in time period t (t d^{-1})

Df_{ipgt} Demand for biomass i at a plant of scale p located in region g in time period t (t d^{-1})

Pf_{ipgt} Biofuel production rate of biofuel i $(i \in PI)$ at a plant of size p located in region g in time period t (t d^{-1})

P_{igt} Production rate of resource i in region g in time period t (t d^{-1})

$Q_{igg'lt}$ Flow rate of resource i via mode l from region g to g' in time period t (t d^{-1})

TC Total cost of a biofuel supply chain network (£)

TIC_t Total investment cost of biofuel production facilities in time period t (£)

TOC_t Total operating costs in time period t (£ $year^{-1}$)

TPC_t Total production cost in time period t (£ d^{-1})

$TPOC_t$ Total product outsourcing cost in time period t (£ d^{-1})

TTC_t Total transportation cost in time period t (£ d^{-1})

a) Objective Function

The objective is to minimise the total expected cost of the supply chain, *TC* given by:

$$TC = \sum_t \left(DFOC_t TOC_t + DFCAP_t TIC_t \right) \quad (3.35)$$

where $DFOC_t$ and $DFCAP_t$ are the discount factors for operating and capital costs in a time period *t*, respectively. TOC_t and TIC_t are the variables that represent the corresponding total operating and capital costs in that time period.

It is assumed that capital investment costs are incurred at the beginning of each time period and discounted accordingly whereas operating costs (the sum of production, transportation and import costs) are incurred and discounted an annual basis. Therefore the discount factors for the capital costs ($DFCAP_t$) and for the operating costs are given by ($DFOC_t$):

$$DFCAP_t = \frac{1}{(1+r)^{card(t)t-(card(t)-1)}} \quad \forall t \in T \quad (3.36)$$

$$DFOC_t = \sum_{a=0}^{a=card(t)-1} \frac{1}{(1+r)^{card(t)t-a}} = \frac{\sum_{a=0}^{a=card(t)-1} (1+r)^a}{(1+r)^{card(t)t}} \quad \forall t \in T \quad (3.37)$$

The total operating cost, TOC_t in a time period accounts for the total transportation cost (TTC_t), total production cost (TPC_t) and the total product outsourcing cost ($TPOC_t$) in that time period:

$$TOC_t = \alpha \left(TTC_t + TPC_t + TPOC_t \right) \quad \forall t \in T \quad (3.38)$$

where α is the number of operating days in a year.

The total transportation cost is given by:

$$TTC_t = \sum_{i \in I} \sum_{l \in L} \sum_{g \in G} \sum_{g' \in n_{igg'l}} \left(UTC_{il} ADD_{gg'l} Q_{igg'lt} \right) + \sum_{i \in BI} \sum_{g \in G} \left(UTC^* ALD_g P_{igt} \right) \quad \forall t \in T \quad (3.39)$$

where $Q_{igg'lt}$ is the flow of material *i* between regions *g* and *g'* via model in time period *t* and P_{igt}, which is a general term for production rate of material *i* in region *g* and time period *t*, refers to biomass cultivation in this equation. The other terms are as defined in section 3.1.2.

The total production cost is given by:

$$TPC_t = \sum_{i\in BI}\sum_{g\in G} UCC_{igt}P_{igt} + \sum_{i\in PI}\sum_{p\in P}\sum_{g\in G} UPC_{ipt}Pf_{ipgt} \quad \forall t \in T \tag{3.40}$$

where UCC_{igt} is the unit cultivation cost of biomass i in region g in time period t and UPC_{ipt} is the unit production cost of biofuel i at a plant scale of p in time period t. P_{igt} refers to biomass cultivation rate as in equation 3.39 and Pf_{ipgt} is the production rate of biofuel i at a plant of scale p in region g in time period t.

The total product outsourcing cost is given by:

$$TPOC_t = \sum_{i,g^*,g,l\in n_{i,g',g,l}} IMPC_{ig^*t}Q_{ig^*glt} \quad \forall t \in T \tag{3.41}$$

where $IMPC_{ig^*t}$ is the unit cost of importing material i from supplier g^* in time period t and Q_{ig^*glt} is the corresponding amount of imported material.

Finally the total investment cost is given by:

$$TIC_t = \sum_{p\in P}\sum_{g\in G} IC_p E_{pgt} \quad \forall t \in T \tag{3.42}$$

where E_{pgt} is the binary variable that represents the establishment of a biofuel plant of scale p in region g and time period t with IC_p being the investment cost of that plant.

b) Demand Constraints

The total production rate of biofuel i in a plant of scale p located in region g in time period t, Pf_{ipgt} is the sum of the production rates from all biomass types converted in that plant:

$$Pf_{ipgt} = \sum_{i'\in BI} \gamma_{i'i} Df_{i'pgt} \quad \forall i \in PI, p \in P, g \in G, t \in T \tag{3.43}$$

where $\gamma_{i'i}$ is the conversion factor for production of biofuel i from biomass type i' and $Df_{i'pgt}$ is the consumption rate of that biomass.

The total consumption rate of biomass i in a region g in time period t, D_{igt} is calculated from the sum of the consumption rates of that biomass at all the plants located in that region:

$$D_{igt} = \sum_{p\in P} Df_{ipgt} \quad \forall i \in BI, g \in G, t \in T \tag{3.44}$$

c) Production Constraints

The mass balance for material *i* in region *g* in time period *t* is given by:

$$P_{igt} + \sum_{l \in L} \sum_{g' \in n_{ig'gl}} Q_{ig'glt} = D_{igt} + \sum_{l \in L} \sum_{g' \in n_{igg'l}} Q_{igg'lt} \quad \forall i \in I, g \in G, t \in T \tag{3.45}$$

The total production rate of biofuel *i* in a region g in time period *t* is given by:

$$P_{igt} = \sum_{p \in P} Pf_{ipgt} \quad \forall i \in PI, g \in G, t \in T \tag{3.46}$$

The total biofuel production rate at a plant of scale *p* is limited by the minimum ($PCap_p^{\min}$) and maximum ($PCap_p^{\max}$) capacities of that plant as follows:

$$PCap_p^{\min} AV_{pgt} \leq \sum_{i \in PI} Pf_{ipgt} \leq PCap_p^{\max} AV_{pgt} \qquad \forall p \in P, g \in G, t \in T \tag{3.47}$$

where AV_{pgt} is the binary variable that represents the availability of a plant of scale *p* in region *g* and time period *t*.

A constraint can be added to consider establishment of at most one biofuel plant in a region *g* over the modelling horizon:

$$\sum_{p \in P} \sum_{t \in T} E_{pgt} \leq 1 \quad \forall g \in G \tag{3.48}$$

It is assumed that once a plant is established in a region *g* in time period *t*, it becomes available in that time period and remains available for the rest of the modelling horizon:

$$AV_{pgt} = AV_{pg,t-1} + E_{pgt} \; \forall p \in P, g \in G, t > 1 \in T \tag{3.49}$$

From the constraint above, when $AV_{pg,t-1}$ is zero (a plant is not available in time period *t-1*) and E_{pgt} takes the value of 1, meaning a plant is established in time period *t*, AV_{pgt}, which represents the availability of the same plant in that time period, is forced to take the value of 1. In the next time period where now *t* becomes *t-1*, $AV_{pg,t-1}$ becomes 1 which forces AV_{pgt} to be 1. The same consideration is valid for the rest of the time periods, meaning the plant stays available till the end of the modelling horizon.

Similar to the biofuel production rate, cultivation rate of a first generation biomass crop in a region *g* in time period *t* is limited by the minimum ($BA_{ig}^{\min}$) and maximum ($BA_{ig}^{\max}$) biomass availabilities in that region:

$$BA_{ig}^{\min} \le P_{igt} \le BA_{ig}^{\max} \quad \forall i \in FI, g \in G, t \in T \tag{3.50}$$

The cultivation rate of a second generation energy crop in a region *g*, which is assumed to be produced from set-aside land that has been withdrawn from production, is determined using the yield of that crop, Y_{ig} as well as the land area occupied by that crop, A_{igt}:

$$P_{igt} = Y_{ig} A_{igt} / \alpha \quad \forall i \in SI, g \in G, t \in T \tag{3.51}$$

The amount of wheat straw collection to be used for biofuel production, $P_{straw,gt}$ is limited by a factor, β which defines the maximum amount of straw that can be receovered sustainably from the cultivated wheat, $P_{wheat,gt}$ as follows:

$$P_{straw,gt} \le \beta P_{wheat,gt} \quad \forall g \in G, t \in T \tag{3.52}$$

d) Sustainability Constraints

As described previously, the total amount of first generation food crops to be used for biofuel production is constrained by a sustainability factor, *SusF* as a fraction of the total first generation biomass availability determined through the sum of maximum availabilities in each region *g*, $BA_{ig}^{\max}$:

$$\sum_{g \in G} P_{igt} \le SusF\left(\sum_{g \in G} BA_{ig}^{\max} \right) \quad \forall i \in FI, t \in T \tag{3.53}$$

The total area occupied by second generation crops in a region *g* in time period *t* is limited by the maximum set-aside land availability in that region, A_g^s :

$$\sum_{i \in SI} A_{igt} \le A_g^s \quad \forall g \in G, t \in T \tag{3.54}$$

Similar to the case of sustainable production from first generation crops, the set-aside land area that can be used for cultivation of second generation dedicated energy crops is limited by ε as a fraction of the total available set-aside land over all regions:

$$\sum_{i \in SI} \sum_{g \in G} A_{igt} \le \varepsilon \sum_{g \in G} A_g^s \quad \forall t \in T \tag{3.55}$$

e) Transportation Constraints

The flow of material i between regions *g* and *g'* via mode *l* in time period *t*, $Q_{igg'lt}$ is limited by an upper bound, $Q_{il}^{\max}$:

$$Q_{igg'lt} \le Q_{il}^{\max} \quad \forall i, g, g', l \in n_{igg'l}, t \in T \tag{3.56}$$

3.2.1.3 Computational Results

In this section, the effect of technological learning on the economic and environmental performance of a biofuel supply chain is investigated using the multi-period model introduced in the previous section. In addition, the environmental emissions profile of such a system is also studied.

The learning curve approach states that as technologies develop through time, costs decline with a fixed percentage over each doubling in cumulative production given by (Hettinga *et al.*, 2009):

$$UPC = UPC_0 P_{cum}^{\ b} \tag{3.57}$$

$$PR = 2^b \tag{3.58}$$

where UPC is the unit production cost at present, UPC_0 is the cost of the first unit of production, P_{cum} is the cumulative production at present and b is the experience index. PR is the progress ratio, which represents the rate at which costs decline for each doubling in cumulative production.

As the case study, bioethanol production from wheat and wheat straw in the UK from 2012 to 2020 has been investigated. It has been assumed that dedicated energy crops will only be ready to be utilised after 2020, therefore are not considered as potential biomass feedstock here. The planning time horizon is divided into three time periods with each consisting of three years. The bioethanol demand data for the three time periods is presented in Table 3.16. These data have been derived based on the biofuel targets for 2011 and 2020, which are 3.4% and 10% respectively (by energy content). It has been assumed that there has been a regular increment in the bioethanol demand from 2011 to 2020 and the bioethanol demand for a time period has been calculated by taking the average of the three years included by that time period. Three scenarios have been studied. In scenario A, both the unit biomass cultivation cost and unit ethanol production costs are taken to be constant with time. In scenario B, the unit biomass cultivation cost is constant with time whereas the unit ethanol production cost decreases with time based on a progress ratio. In scenario C, the biomass cultivation cost decreases 5% per year (Hettinga *et al.*, 2009) and the unit ethanol production cost decreases in the same manner as in scenario B. The biomass import cost is also assumed to decrease 5% per year in scenario C. The unit

cultivation cost per time period for scenario C is presented in Table 3.17. The figures for the first time period represent the current cost levels. On the other hand, the costs for the following time periods have been calculated based on the 5% decrease per year assumption whether or not any biomass cultivation is observed in the first time period. For all scenarios, two instances have been investigated: first with a high learning rate (PR=0.78) and a high interest rate (15%) and the other with a low learning rate (PR=0.88) and low interest rate (8%) (IEA, 2010a).

The unit bioethanol production costs for each time period are given in Table 3.18 (for scenarios B and C) for high (*PR*=0.78) and low (*PR*=0.88) learning rates, respectively. Thus, the technological learning concept has been implemented by using these progress ratios and calculating the corresponding unit production costs per time period. It has been assumed that straw is obtained from the cultivated wheat without incurring any cultivation cost. In reality, residue collection can be costly but this remains to be uncertain. Finally the discount factors for capital investment and operating costs are given in Table 3.19 for high (15%) and low (8%) interest rates, respectively.

Table 3.16 Bioethanol demand data for the UK from 2012 to 2020 (t ethanol/d).

	Time period		
Demand centre	1	2	3
4	261.3	374.2	487.0
13	833.7	1,193.6	1,553.6
19	851.0	1,218.4	1,585.9
23	749.6	1,073.2	1,396.9
27	342.5	490.3	638.2
29	896.9	1,284.1	1,671.4
Total demand	3,934.9	5,633.9	7,332.9

Table 3.17 Unit biomass cultivation and import cost for each time period (£/t wheat) (for scenario C).

Time period	$UCC_{wheat,t}$	$IMPC_{wheat,t}$
1	119	170
2	102	146
3	87	125

Table 3.18 Unit bioethanol production cost for each plant scale and each time period for a PR=0.78/0.88 (£/t ethanol) (for scenarios B and C).

	Plant scale			
Time period	1	2	3	4
1	140/140	135/135	132/132	130/130
2	123/131	119/126	116/124	114/122
3	112/125	108/120	106/118	104/116

Table 3.19 Discount factors for each time period with interest rates of 15%/8%.

	Time period		
Discount factors	1	2	3
$\boldsymbol{DFCAP_t}$	0.87/0.93	0.57/0.74	0.38/0.58
$\boldsymbol{DFOC_t}$	2.63/2.78	1.73/2.21	1.14/1.75

The change of total unit ethanol production cost of production with time for each scenario and instance is represented in Figure 3.23. The decrease in the total cost as time evolves is most remarkable in scenario C where the effect of learning curve has been considered for both biomass cultivation and bioethanol production. On the other hand, the cost profile of scenario A is relatively flat where unit biomass cultivation and bioethanol production costs remain constant through all time periods. When the two instances of any particular scenario are compared, it is seen that the instance with high learning and high interest rates result in a lower cost in all time periods than the instance with low interest and low learning rates. This is expected as high interest and high learning rates are the driving factors for decrease in costs.

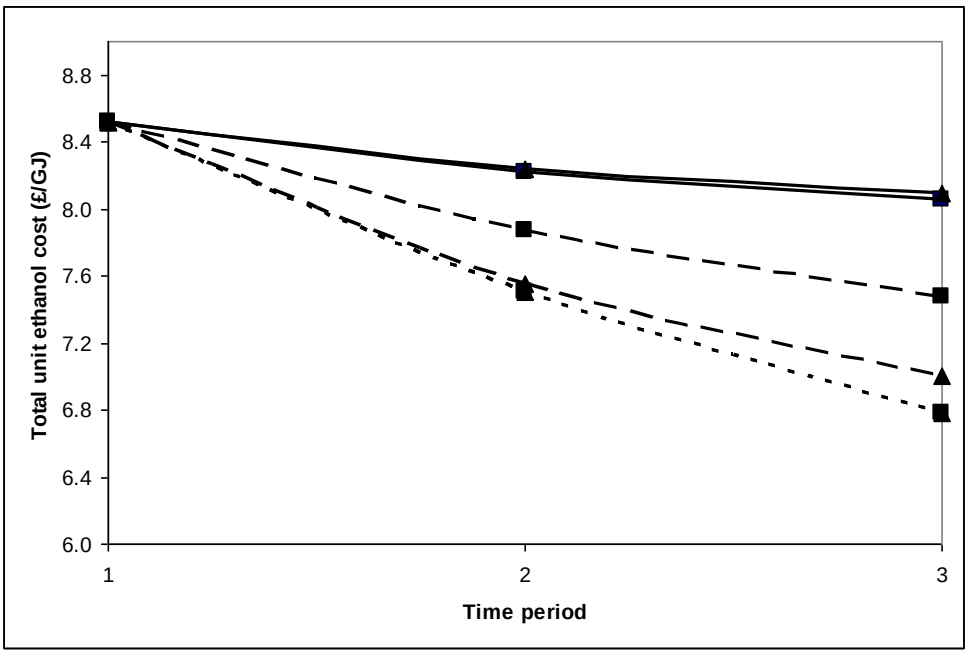

Total unit ethanol cost in a time period= Total daily cost (£/d) /(the energy content of ethanol (GJ/t)x the total production of ethanol in that period (t/d)).

Figure 3.23 Change of total unit ethanol cost with time horizon for the three scenarios.

The emissions profile of the total six instances is very similar. Figure 3.24 shows the total emissions profile as well as the total imported wheat amount per time period for scenario A. The emission savings are reduced from 49% to 41% mainly due to increasing biomass imports from the first to the last time period. The ethanol production-based average emissions are about 47.9 kg CO_2-eq/GJ ethanol through all time periods. This corresponds to an emissions reduction of 44% compared to the fossil fuel reference (Winrock International, 2009). Therefore, the minimum emissions reduction target (35%) can be met in this case whereas the interim target cannot be met (60%). This implies the need for the cultivation and use of second generation dedicated energy crops (miscanthus and SRC) for achieving and maintaining the environmental sustainability targets in the longer term.

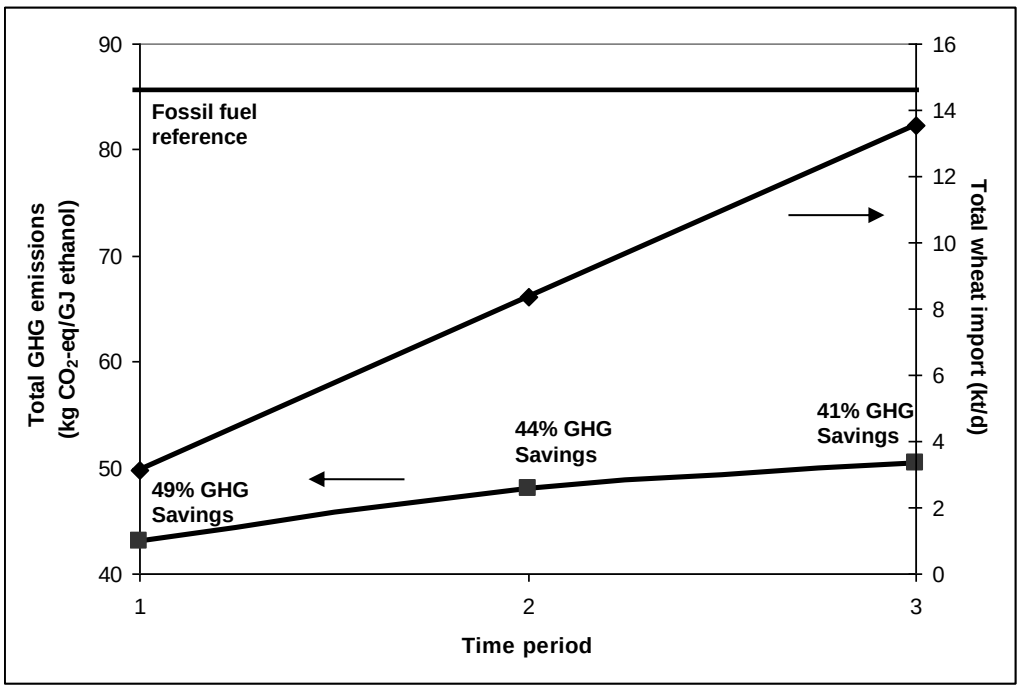

Figure 3.24 The GHG emissions profile and total imported wheat per time period in scenario A.

3.2.1.4 Concluding Remarks

In this section, a multi-period optimisation problem considering bioethanol production from wheat and wheat straw in the UK from 2012 to 2020 has been solved taking into account the reduction in unit production costs through technological learning. The results indicate that high learning and high interest rates can improve the economic performance of the supply chain by decreasing the costs remarkably. The total GHG emissions through time increase mainly due to increasing wheat imports to meet the increasing bioethanol demand. The ethanol-production based average emissions result in a 44% GHG emission savings overall, meeting the EU minimum target of 35% but not the interim target of 60%. This result emphasises the significance of second generation dedicated energy crops (miscanthus and SRC) for meeting the environmental and sustainability targets in the longer term.

3.2.2 Multi-Period Optimisation of Biofuel Supply Chains Under Uncertainty

This section considers further extension of the deterministic multi-period model introduced in the previous section to take into account uncertainty in different aspects of a biofuel supply chain such as biomass supply. The model introduced here

aims to maximise the expected net present value of a biofuel supply chain by controlling the level of financial risk simultaneously.

3.2.2.1 Problem Statement

The optimisation problem studied in this section for the optimal design of a hybrid biofuel supply chain under uncertainty can be stated as:
Given are:

- locations of biofuel demand centres and their biofuel demand in each time period,
- biomass feedstock types and their geographical availability in each time period,
- unit biomass cultivation cost for each feedstock type,
- unit production cost of biofuel based on the feedstock type (hence technology) utilised,
- transport logistics characteristics (cost, modes, and availabilities),
- capital investment cost for the biofuel production facilities as a function of the production technology deployed,
- unit bioethanol sales and import prices,
- a target net present value for the network,

Determine the optimal:

- biomass cultivation rate for each biomass feedstock type and biofuel production rates in each time period,
- locations and scales of biofuel production facilities in each time period,
- flows of each biomass type and biofuel between cells in each time period,
- modes of transport of delivery for biomass and biofuel in each time period,
- level of financial risk,

So as to maximise the expected net present value of the supply chain.

3.2.2.2 Mathematical Formulation

The problem for the optimal design of a hybrid bioethanol supply chain under uncertainty is formulated as a multi-period, two-stage stochastic mixed integer linear programming (MILP) model. The objective is the maximisation of the expected net present value of the supply chain which is described as:

$$ENPV = \sum_{s \in S} pb_s NPV_s = \sum_{s \in S} pb_s \left(REV_s - TC_s \right) \tag{3.59}$$

where pb_s is the probability of occurrence of scenario *s*. NPV_s, REV_s and TC_s are the net present value, total revenue and total cost in scenario *s* (uncertainty is time invariant here which justifies the two-stage approach).

The revenue in scenario s, REV_s is calculated by:

$$REV_s = \sum_{i \in PI} \sum_{g \in G} \sum_{t \in T} DFOP_t SPE_{is} D_{igts} \quad s \in S \tag{3.60}$$

where SPE_{is} is the sales price of biofuel *i* in scenario *s*, $DFOP_t$ is the discount factor for operating costs as introduced in Section 3.2.1.2 and D_{igts} is the sales of biofuel *i* in region *g*, time period t and scenario *s*.

The total sales of biofuel *i* in time period t and scenario *s*, D_{igts} must meet be less than or equal to the demand for that biofuel, DEM_{igt} as given by:

$$D_{igts} \leq DEM_{igt} \qquad i \in PI, g \in G, t \in T, s \in S \tag{3.61}$$

The total cost in scenario *s*, TC_s is calculated in the same manner as introduced in equation 3.35:

$$TC_s = \sum_t \left(DFOC_t TOC_{ts} + DFCAP_t TIC_t \right) \quad s \in S \tag{3.62}$$

where TOC_{ts} is the total operating costs in time period *t* and scenario *s* and TIC_t is the total investment cost in time period *t*. It must be noted that, since the plant investment decisions are first stage decisions meaning that they are the same across all scenarios, the total investment cost is only a function of time. $DFCAP_t$ is the discount factor for capital costs in time period *t* as introduced in Section 3.2.1.2.

The objective function is maximised with respect to production, demand, sustainability and transportation constraints which are as introduced in Section 3.2.1.2 and are now also considered for each scenario *s*. Therefore, these constraints are not repeated here once again, instead the differences are highlighted.

Apart from the level of the expected profit, the level of financial risk in each scenario is also important. The financial risk can be defined as the probability of not meeting a target NPV, Ω and is measured using a risk factor, *RF*. The total financial risk is defined by:

$$RF = \sum_{s \in S} pb_s \Delta_s \quad s \in S \tag{3.63}$$

where Δ_s is the positive deviation from the target NPV level. This deviation is defined through the following two equations:

$$\Delta_s \geq \Omega - NPV_s \quad s \in S \tag{3.64}$$

$$\Delta_s \geq 0 \quad s \in S \tag{3.65}$$

Through equations 3.64 and 3.65 above, when NPV_s is below the target level, Ω, Δ_s takes the value of the difference between the two (as the model will try to maximise NPV and minimise Δ_s). When NPV_s is above the target level, Ω, Δ_s takes the value of 0 which means it will not contribute to the overall financial risk.

The degree of financial risk can be controlled using a tightening factor, λ $(0 \leq \lambda \leq 1)$:

$$RF \leq \lambda RF^* \tag{3.66}$$

where RF^* is the maximum level of risk experienced without any risk constraints.

3.2.2.3 Computational Results

The proposed stochastic, multi-period model has been applied to the same case study introduced in Section 3.2.1.3, which considers bioethanol production in the UK in the time period from 2012 to 2020 using wheat (first generation feedstock) and wheat straw (second generation feedstock). The nine years from 2012 to 2020 have been divided into three time periods (2012-2014, 2015-2017, 2018-2020). The market bioethanol demand for each time period and demand centre is as given in Table 3.16 in Section 3.2.1.3. Uncertainty in biomass availability, biomass imports, bioethanol sales and import prices has been considered. The first three of these uncertain parameters is assumed to be uniformly distributed between -50% to +50% of their respective nominal values (time invariant). Bioethanol import price has been assumed to change uniformly between 1.1 to 1.5 times the sales price to account for the import tariff. 50 scenarios have been generated using these four uncertain parameters.

Without the presence of financial risk constraints, the expected net present value of the supply chain is determined as 0.96£billion for which the cumulative probability distribution function is given in Figure 3.25. Based on that, a target NPV (Ω) of 0.15 £billion has been selected. This corresponds to the 22nd percentile of the cumulative PDF, which means 22% of the 50 scenarios are below the target. To investigate the effect of imposing financial risk constraints, a risk tightening factor (λ) of 0.25 has

been applied. The resulting cumulative PDF can also be seen in Figure 3.25. The *ENPV* has decreased to 0.88 £billion in this case whereas the percentage of scenarios below the target level has decreased from 22% to 12%. As can be concluded from the comparison of the two curves, the approach of the decision maker changes from risk-taker to risk-averse as the risk tightening effect is increased. The probability distributions for the two cases are shown in Figure 3.26. It is seen that the presence of financial risk constraints results in a narrower distribution of NPV (e.g. smaller standard deviation) which also implies a reduction in the risk factor.

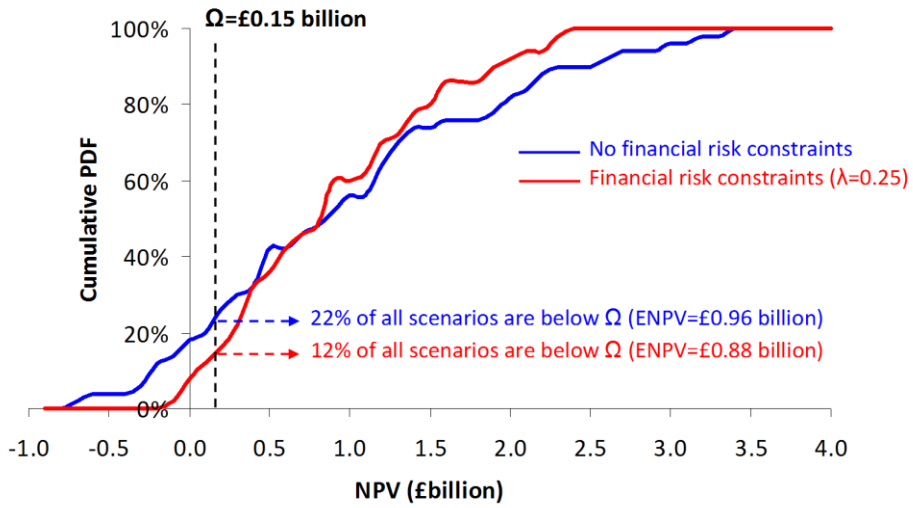

Figure 3.25 Cumulative probability distribution function of net present value for the fifty scenarios with and without financial risk constraints.

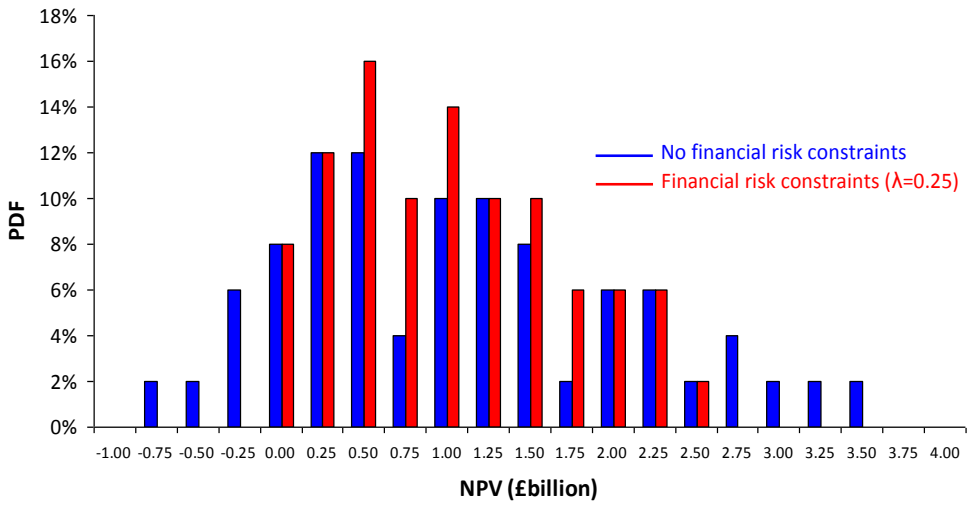

Figure 3.26 Probability distribution of net present value for the fifty scenarios with and without financial risk constraints.

Figure 3.27 shows the average fraction of ethanol and biomass imports in meeting the total ethanol sales over all time periods with and without financial risk constraints. As can be seen from the figure, both with and without financial risk constraints, imports occupy a significant fraction of the overall bioethanol sales in most of the scenarios.

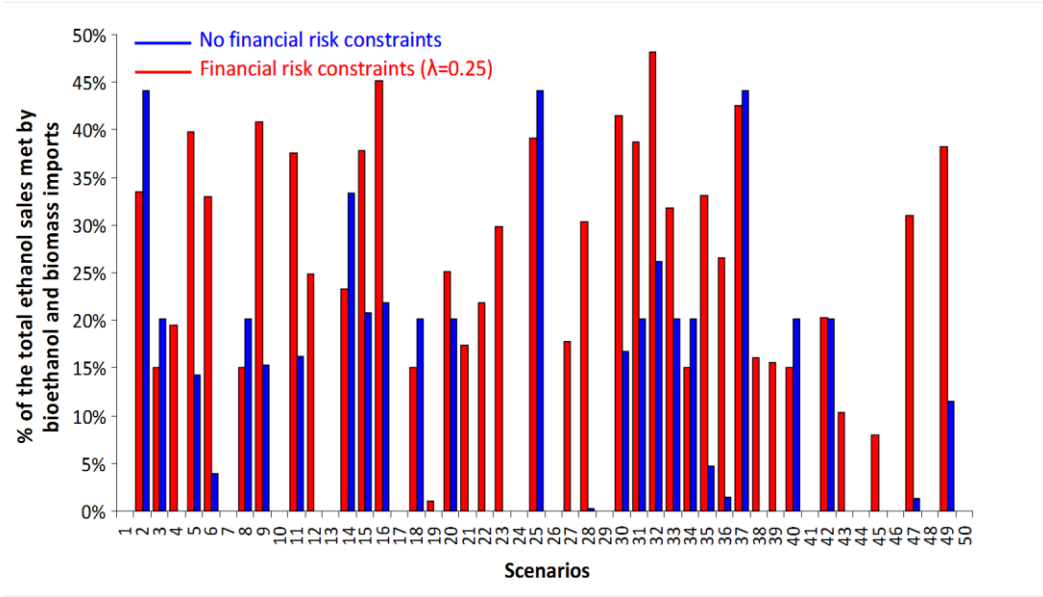

Figure 3.27 Percentage of total bioethanol production met by biomass and bioethanol imports per scenario with and without financial risk constraints.

3.2.2.4 Concluding Remarks

In this section, a stochastic, multi-period MILP modelling framework has been presented for the optimal design of a hybrid biofuel supply chain. The model has been applied to a case study of bioethanol production in the UK from wheat and wheat straw in the time horizon from 2012 to 2020. Uncertainty in biomass availability, biomass imports, bioethanol sales and import prices has been considered. The presence of financial risk constraints has also been investigated. The results indicate that incorporating financial risk constraints results in a reduction in the overall financial risk at the expense of reducing the expected net present value. In addition, biomass and bioethanol imports meet a significant portion of the total ethanol production in most of the cases.

4 Optimisation of Bioelectricity Supply Chains

As mentioned previously in Chapter 1, bioelectricity generation through biomass co-firing with coal systems integrated with carbon capture and storage is considered as a promising option for the decarbonisation of the electricity sector. Existing coal-fired power plants can be utilised for this purpose. This chapter presents a static, multi-objective mixed integer nonlinear programming model for the optimal design of such a bioelectricity supply chain which has been developed based on the optimisation-based approaches introduced in Chapter 3.

4.1 Problem Statement

The problem addressed in this work can be stated as follows:

Given:

- the geographical locations and capacities of current and potential future electricity generation plants,
- total electricity demand,
- different raw material types for pellet production and their geographical availabilities,
- unit raw material supply, pellet production, fossil fuel and electricity generation costs,
- transport logistics characteristics (costs, modes, and availabilities),
- capital investment cost for the pellet production facilities,

Determine the optimal

- raw material supply, pellet production and electricity generation rates,
- locations and scales of the pellet production facilities,
- flows of raw material and pellets between cells,
- modes of transport of delivery for raw material and pellets;
- fuel burn rates, capacity factors, generation efficiencies, extents of CCS and co-firing of pellets at each generation plant;

So as to minimise the total annual cost (*TAC*) and/or the total annual emissions (*TAE*) of the supply chain.

The supply chain model introduced in this paper adopts a "neighbourhood" flow approach with 8N configuration introduced in section 3.1.1 in detail.

4.2 Mathematical Formulation

The problem for the optimal design of a bioelectricity supply chain is formulated as a spatially-explicit, static, multi-objective, mixed integer nonlinear programming (MINLP) model with the following notation:

Indices:

elec	Bioelectricity
fossil	Fossil fuel
g, g'	Square cells (regions)
i,i'	Material (biomass, MSW, biomass pellet, SRF pellet, fossil fuel, bioelectricity)
l	Transport mode
p	Pellet production plant scale

Sets:

F	Set of fuels (biomass pellet, SRF pellet, fossil fuel)
FP	Set of final products (bioelectricity)
FI	Set of fuels that can be produced from raw material *i* (biomass pellet from biomass, SRF pellet from MSW)
I	Set of materials (biomass, MSW, biomass pellet, SRF pellet, fossil fuel, bioelectricity) ($I = R \cup F \cup FP$)
R	Set of raw material types (biomass, MSW)
$Total_{igg'l}$	Set of total transport links allowed for each material *i* via mode *l* between regions *g* and *g'*
$n_{igg'l}$	Subset of $Total_{igg'l}$ including all regions *g'* in the neighbourhood of region *g* for each material *i* and mode *l*
P	Set of pellet production plant scales

Parameters:

$ADD_{gg'l}$	Actual delivery distance between regions *g* and *g'* via model *l* (km)
ALD_g	Average local delivery distance in region *g* (km)
a_{CI}	Nameplate capacity coefficient in the carbon intensity equation

a_{η}	Nameplate capacity coefficient in the generation efficiency equation
a_{UGC}	Nameplate capacity coefficient in the unit generation cost equation
α	Annual operating hours (h year^{-1})
b_{CI}	Capacity factor coefficient in the carbon intensity equation
b_{η}	Capacity factor coefficient in the generation efficiency equation
b_{UGC}	Capacity factor coefficient in the unit generation cost equation
$BA_{ig}^{min/max}$	Minimum/maximum availability of raw material i ($i \in R$) in region g (t h^{-1})
c_{CI}	Extent of carbon capture and storage coefficient in the carbon intensity equation
c_{η}	Extent of carbon capture and storage coefficient in the generation efficiency equation
c_{UGC}	Extent of carbon capture and storage coefficient in the unit generation cost equation
$\overline{CCS}$	Reference extent of carbon capture and storage used in the carbon intensity, generation efficiency and unit generation cost equations (%)
$\overline{CI}$	Reference carbon intensity in the carbon intensity equation (kg CO_2 MWh^{-1})
CRF	Capital recovery factor (year^{-1})
d_{CI}	Extent of co-firing coefficient in the carbon intensity equation
d_{η}	Extent of co-firing coefficient in the generation efficiency equation
d_{UGC}	Extent of co-firing coefficient in the unit generation cost equation
$\overline{\delta}$	Reference capacity factor used in the carbon intensity, generation efficiency and unit generation cost equations (%)
DEM	Total electricity demand (MW)
γ_i	Conversion factor of raw material i to its pellet (t pellet t^{-1} raw material)
IC_p	Investment cost of a pellet production plant of scale p (£)
$IMPC_{ig^*}$	Unit import cost for importing material i from foreign supplier g^* (£ t^{-1})

$\overline{\varphi}$	Reference extent of co-firing used in the carbon intensity, generation efficiency and unit generation cost equations (%)
$\overline{\eta}$	Reference generation efficiency in the generation efficiency equation (%)
$PCAP_p^{min/max}$	Minimum/maximum pellet production capacity of a plant of scale p (t h^{-1})
PPC_g	Nameplate capacity of the power plant located in region g (MW)
$\overline{PPC}$	Reference nameplate capacity used in the carbon intensity, generation efficiency and unit generation cost equations (MW)
$\overline{\rho_i}$	Energy density of fuel type i $(i \in F)$ (MJ t^{-1})
Q_{il}^{max}	Maximum flowrate of material i via mode l (t h^{-1})
UFC_g	Unit fossil fuel cost at a power plant located in region g (£ t^{-1})
$UCARC$	Unit carbon cost (£ kg CO_2^{-1})
$\overline{UGC}$	Reference unit power generation cost in the unit generation cost equation (£ MWh^{-1})
UPC_{ip}	Unit pellet production cost from raw material i at a plant scale of p (£ t^{-1} pellet)
USC_{ig}	Unit supply cost of raw material i in region g (£ t^{-1})
UTC_{il}	Unit transport cost of product i via mode l (£ t^{-1} km^{-1})
UTC^*	Unit transport cost for local raw material transfer (£ t^{-1} km^{-1})

Binary Variables

E_{pg}	1 if a pellet production plant of scale p is to be established in region g

Continuous Variables

CCS_g	Extent of carbon capture and storage in a power plant located in region g (%)
CI_g	Carbon intensity of a power plant located in region g (kg CO_2 MWh^{-1})
D_{ig}	Demand for raw material i $(i \in R)$ in region g (t h^{-1})
Df_{ipg}	Demand for raw material i $(i \in R)$ at a pellet production plant of scale p located in region g (t h^{-1})
δ_g	Capacity factor of a power plant located in region g (%)
$\dot{m}_g$	The fuel mix consumption rate in a power plant located in region g (t h^{-1})

η_g Generation efficiency of a power plant located in region g (%)

Pf_{pg} Pellet production rate at a plant of size p located in region g (t h^{-1})

P_{ig} Production rate of material i in region g (t h^{-1}) $(i \neq elec)$

$P_{elec,g}$ Electricity generation rate in region g (MW)

ρ_g Energy density of the fuel mix for a power plant located in region g (MJ t^{-1})

$Q_{igg'l}$ Flow rate of material i via mode l from region g to g' (t h^{-1})

TAC Total annual cost of a bioelectricity supply chain network (£ $year^{-1}$)

TAE Total annual emissions resulting from a bioelectricity supply chain network (kg CO_2 $year^{-1}$)

UGC_g Unit power generation cost at a power plant located in region g (£ MWh^{-1})

φ_{ig} Extent of co-firing of fuel i $(i \in F)$ in a power plant located in region g (%)

a) Objective Function

The economic objective of the proposed model is the minimisation of the total annual supply chain cost (TAC) which is given by:

$$TAC = \sum_{p\in P}\sum_{g\in G} CRF\ IC_p E_{pg}$$ Total pellet production plant capital cost (4.1a)

$$+\sum_{i\in R}\sum_{g\in G}\alpha USC_{ig} P_{ig}$$ Total raw material supply cost (4.1b)

$$+\sum_{i\in R}\sum_{g\in G}\sum_{p\in P}\alpha UPC_{ip}\gamma_i\ Df_{ipg}$$ Total pellet production cost (4.1c)

$$+\sum_{g\in G}\alpha UGC_g P_{elec,g}$$ Total power generation cost (4.1d)

$$+\sum_{g\in G}\alpha UFC_g\ \dot{m}_g\varphi_{fossil,g}$$ Total fossil fuel cost (4.1e)

$$+\sum_{g\in G}\alpha UCARC\ P_{elec,g} CI_g$$ Total carbon cost (4.1f)

$$+\sum_{i,g^*,g,l\in n_{ig'gl}}\alpha\ IMPC_{ig^*}\ Q_{ig^*gl}$$ Total product outsourcing cost (4.1g)

$$\sum_{i(\neq FP),g,g',l\in n_{igg'l}}\alpha UTC_{il} ADD_{gg'l} Q_{igg'l}$$ Total material transportation cost between cells (4.1h)

$$+\sum_{i\in R}\sum_{g\in G}\alpha UTC^* ALD_g P_{ig}$$ Total local raw material transportation cost (4.1i)

Apart from the economic objective, the environmental objective of the proposed model considers the minimisation of the total annual emissions, *TAE* given by:

$$TAE = \sum_{g \in G} \alpha \, P_{elec,g} \, CI_g \tag{4.2}$$

b) Demand constraints

The amount of raw material *i* consumed at a pellet production plant of scale *p* located in region *g*, Df_{ipg}, is related to the total pellet production rate at that plant, $Pf_{i'pg}$, by the conversion factor, γ_i as follows:

$$Pf_{i'pg} = \sum_{i \in R} \gamma_i Df_{ipg} \quad \forall i' \in FI, p \in P, g \in G \tag{4.3}$$

As a result, the total consumption rate of raw material type *i* in region *g*, D_{ig} is given by:

$$D_{ig} = \sum_{p \in P} Df_{ipg} \qquad \forall i \in R, g \in G \tag{4.4}$$

c) Production constraints

The material balance for each material *i* and region *g* states that the production of a material in region *g* plus the incoming flows of that material to that region must be equal to the demand in that region plus the outgoing flows from that region.

$$P_{ig} + \sum_{l \in L} \sum_{g' \in n_{ig'gl}} Q_{ig'gl} = D_{ig} + \sum_{l \in L} \sum_{g' \in n_{igg'l}} Q_{igg'l} \quad \forall i \in I, g \in G \tag{4.5}$$

The total pellet production rate of pellet type *i* in a region *g*, P_{ig} is given by:

$$P_{ig} = \sum_{p \in P} Pf_{ipg} \quad \forall i \in FI, g \in G \tag{4.6}$$

The total pellet production rate at a plant in region *g* is limited by the minimum and maximum production capacities:

$$PCap_p^{\min} E_{pg} \le \sum_{i \in FI} Pf_{ipg} \le PCap_p^{\max} E_{pg} \qquad \forall p \in P, g \in G \tag{4.7}$$

where $PCap_p{}^{min}$ and $PCap_p{}^{max}$ are the minimum and maximum plant capacities for a pellet production plant of size *p*, respectively. E_{pg} is the binary variable that represents the establishment of a pellet production plant of size *p* in region *g*.

Similarly to the pellet production rate, the local raw material supply rate is also limited by the minimum and maximum local availabilities as follows:

$$BA_{ig}^{\min} \le P_{ig} \le BA_{ig}^{\max} \quad \forall i \in R, g \in G \tag{4.8}$$

where BA_{ig}^{min} and BA_{ig}^{max} are the minimum and maximum availabilities of raw material type i in region g, respectively.

The electricity generation rate at a power plant located in region g, $P_{elec,g}$ is related to the fuel mix burn rate, $\dot{m}_g$, the energy density of the fuel mix, ρ_g and the generation efficiency, η_g as follows:

$$P_{elec,g} = \dot{m}_g \rho_g \eta_g / 3600 \qquad \forall g \in G \tag{4.9}$$

The total electricity production must meet the total electricity demand, DEM:

$$\sum_{g \in G} P_{elec,g} = DEM \tag{4.10}$$

The energy density of the energy density of the fuel mix, ρ_g is related to the co-firing rates of the different fuel types, φ_{ig} and their energy densities, $\overline{\rho}_i$ as follows:

$$\rho_g = \sum_{i \in F} \varphi_{ig} \overline{\rho}_i \quad \forall g \in G \tag{4.11}$$

The sum of the co-firing rates of all fuel types must be equal to 1:

$$\sum_{i \in F} \varphi_{ig} = 1 \; \forall g \in G \tag{4.12}$$

The consumption rate of each fuel type i, D_{ig} in the fuel mix is related to the fuel mix burn rate and the co-firing of that fuel as follows:

$$D_{ig} = \varphi_{ig} \dot{m}_g \qquad \forall i \in F, g \in G \tag{4.13}$$

The energy balance for a power plant located in region g is written as:

$$P_{elec,g} = \delta_g \, PPC_g \qquad \forall g \in G \tag{4.14}$$

where δ_g is the variable that represents the capacity factor for a power plant located in region g and PPC_g is the parameter that represents the generation capacity of that plant.

d) Transportation constraints

An upper limit on the flow of material i between regions can be considered such that:

$$Q_{igg'l} \le Q_{il}^{\max} \qquad \forall i, g, g', l \in n_{igg'l} \tag{4.15}$$

where Q_{il}^{max} is the maximum flowrate of material *i* via mode *l* between regions *g* and *g'*.

4.2.2 Power Plant Model

As introduced in the previous section, the developed bioelectricity supply chain optimisation framework can evaluate operating cost, generation efficiency and carbon intensity of a power plant based on its name plate capacity, capacity factor, extent of co-firing of biomass and solid recovered fuels (SRF) and extent of carbon capture. To increase the computational efficiency for the solution of the optimisation problem, a meta-modelling approach has been adopted in this work instead of a detailed modelling approach to derive these mathematical relationships as illustrated in Figure 4.1 below.

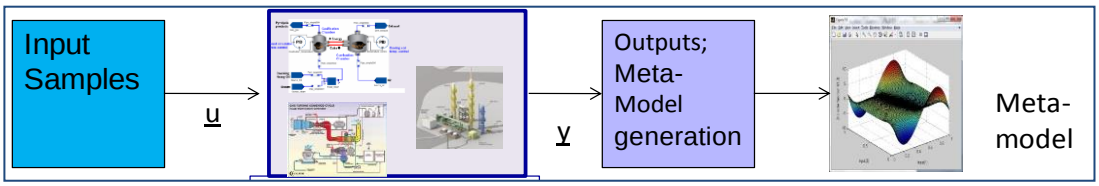

Figure 4.1 Meta modelling development process: we use a detailed modelling tool to develop a set of inputs and outputs. Subsequently the meta-model is proposed and parameters are adjusted to relate the inputs and outputs.

The meta-model is of the form:

$$y_m = \bar{y}_m(\bar{x}_n) + A_{mn}(x_n - \bar{x}_n) \tag{4.16}$$

where the output vector y_m is related to an input vector x_n through a coefficient matrix A_{mn} in a piecewise linear fashion by difference from a base input vector $\bar{x}_n$ and a base output vector $\bar{y}_m = f(\bar{x}_n)$. Using this meta-modelling approach, constraints 4.17-4.19 are derived as below.

The carbon intensity, CI_g from a power plant located in region *g*, is a linear function of the plant capacity, PPC_g, the plant capacity factor, δ_g, the extent of carbon capture and storage, CCS_g and the co-firing extent of the non-fossil fuels, φ_{ig} as follows (explained in detail in Section 4.2.1):

$$CI_g = \overline{CI} + a_{CI}\left(PPC_g - \overline{PPC}\right) + b_{CI}\left(\delta_g - \bar{\delta}\right) + c_{CI}\left(CCS_g - \overline{CCS}\right) + d_{CI}\left(\sum_{i \in FI} \varphi_{ig} - \bar{\varphi}\right) \quad \forall g \in G \tag{4.17}$$

where $\overline{CI}$, $\overline{PPC}$, $\bar{\delta}$, $\overline{CCS}$ and $\bar{\varphi}$ are the parameters that represent the reference values for carbon intensity, plant capacity, capacity factor, extent of carbon capture and storage and the co-firing extent in the base case, respectively.

Similar to the carbon intensity, the generation efficiency of a power plant located in region *g*, η_g is a linear function of the plant capacity, PPC_g, the plant capacity factor, δ_g, the extent of carbon capture, CCS_g and the co-firing extent of the non-fossil fuels, φ_{ig} as follows (explained in detail in Section 4.2.1):

$$\eta_g = \bar{\eta} + a_\eta\left(PPC_g - \overline{PPC}\right) + b_\eta\left(\delta_g - \bar{\delta}\right) + c_\eta\left(CCS_g - \overline{CCS}\right) + d_\eta\left(\sum_{i \in FI} \varphi_{ig} - \bar{\varphi}\right) \quad \forall g \in G \tag{4.18}$$

where $\bar{\eta}$ is the reference generation efficiency in the base case.

Finally, the unit generation cost in a power plant located in region *g*, UGC_g is given by (explained in detail in Section 4.2.1):

$$UGC_g = \overline{UGC} + a_{UGC}\left(PPC_g - \overline{PPC}\right) + b_{UGC}\left(\delta_g - \bar{\delta}\right) + c_{UGC}\left(CCS_g - \overline{CCS}\right) + d_{UGC}\left(\sum_{i \in FI} \varphi_{ig} - \bar{\varphi}\right) \quad \forall g \in G \tag{4.19}$$

where $\overline{UGC}$ is the reference unit generation cost in the base case.

In this work, the parameters of the meta modelling approach have been adjusted based on the Integrated Environmental Control Model (IECM) as the detailed modelling tool (CMU). IECM contains economic and technical models which are considered to be well validated, and is thus a reliable tool. An important advantage of the IECM tool is the facility for the user to define a fuel composition, in addition to the default fuel compositions. In specifying the composition and energy density of a fuel blend in this work, it has been assumed that the coal used was British bituminous coal and that the available biomass source was wood pellets. The composition and energy density of the SRF was taken from the Renewable Power Fuel product from Orchid Environmental, a UK-based SRF producer. The fuel

compositions and energy densities are provided in Table 4.1. Then the composition and energy density of the co-fired fuel blend was obtained from a mass average.

Table 4.1 Composition and energy density of the model coal and biomass used in this study.

Parameter	British bituminous coal	Biomass
GCV (MJ kg^{-1}, as received)	24.6	18.7
Moisture	12.0	7.0
C	59.6	43.5
H	3.8	4.5
N	1.5	0.2
O	5.5	42.6
S	1.8	0.01
Cl	0.2	0.01

***We note that the Orchid SRF product was given to be 80% biomass, 16% moisture and the remainder considered to be "ash". The energy density of the SRF product was given to be 12.5 MJ/kg*.**

The base case chosen for the development of the meta-models is a 500MW plant, operating at 100% capacity, co-firing 22 wt% biomass and 90% CO_2 capture. The corresponding base input and output vectors are presented in Table 4.2, the coefficient matrix, A_{ij} is given in Table 4.3and finally the operating range over which the proposed equations are valid is given in Table 4.4.

Table 4.2 Base input and output vectors obtained from IECM.

Base input vector, $\bar{x}_n$		**Base output vector, $\bar{y}_m$**	
Reference nameplate capacity, $\overline{PPC}$ (MW)	500	Reference capital Cost (k£/MW)	2,079
Reference capacity factor, $\bar{\delta}$ (%)	100	Reference unit generation cost, $\overline{UGC}$ (£/MWh)	16.57
Reference co-firing extent, $\bar{\varphi}$ (%)	22	Reference generation efficiency, $\bar{\eta}$ (%)	34.5
Reference CO_2 capture extent, $\overline{CCS}$ (%)	90	Reference carbon intensity, $\overline{CI}$ (kg CO_2/MWh)	-97

Table 4.3 Parameter values for coefficient matrix, A_{mn} (taken from the collaborators, MacDowall and Shah at Imperial College).

	Nameplate capacity, *a* (MW)	**Capacity factor, *b* (%)**	**CO_2 capture extent, *c* (%)**	**Co-firing extent, *d* (%)**
Capital cost (k£/MW)	-1.66E+00	0.00E+00	4.71E+02	1.60E+02
Unit generation cost, UGC_g (£/MWh)	-2.70E-03	0.00E+00	8.56E+00	0.00E+00
Generation efficiency, η_g (%)	6.00E-04	1.68E+00	-1.28E+01	-7.70E+00
Carbon intensity, CI_g (kg CO_2/ MWh)	-1.00E-03	2.88E+01	-7.73E+02	-1.01E+03

Table 4.4 Operating range of the meta model.

Input Parameter	**Lower bound**	**Upper bound**
Nameplate capacity (MW)	300	1,000
Capacity factor (%)	60	100
Co-firing extent (%)	0	50
CO_2 capture extent (%)	50	98

Therefore, if one wishes to calculate the generation efficiency of a 500MW plant operating at 90% capacity, with 10% co-firing and 85% CO_2 capture the corresponding equation is (equation 4.16 in the mathematical formulation section):

$$\eta_g = 34.5 + \left(6\times10^{-4}\left(500-500\right)\right) + \left(1.6758\times\left(90\%-100\%\right)\right) + \left(-12.833\times\left(85\%-90\%\right)\right) + \left(-7.7\times\left(10\%-22\%\right)\right) \approx 35.9\%$$

It can be observed that this corresponds to a slightly higher efficiency in comparison to the base case, as might be expected with a scenario corresponding to lower rates of co-firing and CO_2 capture.

The accuracy of the proposed meta models has been tested by comparing their outputs with those from the fully detailed IECM model. The average absolute relative deviation between the meta- and IECM models was 8.84%. The meta-model was therefore judged to be sufficient for inclusion in our system-scale model.

It must be noted that for the case study introduced in the next section, it has been assumed that that all power plants under consideration were composed of a number

of 500MW units, i.e., if the nameplate capacity of a given power plant as is 2,000MW, this installation is supposed to comprise 4x500MW units as is the case for the Ratcliffe-on-Soar power station operated by E.ON UK.

4.3 Computational Results

The developed modelling has been applied to a case study of bioelectricity generation in the UK. For this purpose, 10 existing UK generation assets which together provide a total generation capacity of 19 GW have been utilised. The total electricity consumption from all consumers (domestic, commercial and industrial) in the UK has been reported to be 308,034 GWh in 2011 (DECC, 2012a). Based on this total consumption and the renewables target which requires UK to supply 30% of its electricity from renewables by 2020 (DECC, 2012d), this corresponds to about 92,410 GWh of annual renewable electricity generation. The objective of this case study is to provide some insight into the costs associated with producing this renewable generation of carbon-negative energy from the existing capacity. The generation rate per hour from all the power plants required to meet the demand has been averaged throughout a year (8,000 hours of operating time per year) for the purposes of application of the proposed static model. Power generation systems where carbon capture and storage systems are combined with co-firing of biomass with fossil fuels (BECCS) have been considered. Domestic woodfuel, miscanthus as a dedicated energy crop and municipal solid waste have been considered as the potential biomass resources. As introduced previously, the UK is discretised into 34 square cells of each 108 km in length. The nameplate capacity, total annual CO_2 emissions and geographical location of each of the 10 coal-fired power plants under consideration can be found in Table D5 in Appendix D.

Some of the key inputs to the optimisation problem are the costs associated with fuel (coal, biomass and SRF) and CO_2 emissions, respectively. Three years have been chosen for the case study: 2012 (near term), 2020 (mid term) and 2050 (long term). For each of these periods, three decarbonisation scenarios are investigated corresponding to DECC's low, central and high scenarios for carbon (DECC, 2010c) and coal (DECC, 2011a) prices respectively. The scenario with low prices of carbon and coal is considered as a pessimistic decarbonisation scenario owing to weak

economic incentives to implement either fuel switching or CCS. Similarly, a scenario with both high carbon and coal prices is considered as an optimistic decarbonisation scenario owing to strong economic incentive to implement both CCS and fuel switching. The costs of both carbon and coal for each scenario are presented in Table 4.5. All the other related data related to raw materials, pellet production and power generation are given in the Appendix D. The parameters for transportation are as presented in Appendix B.4.

Table 4.5 Carbon and coal prices under the three decarbonisation scenarios for 2012, 2020 and 2050 (DECC, 2010c; DECC 2011a).

	Low scenario (pessimistic)		**Central scenario (central)**		**High scenario (optimistic)**	
	CO_2 (£/t)	Coal (£/t)	CO_2 (£/t)	Coal (£/t)	CO_2 (£/t)	Coal (£/t)
2012	13	80	22	84	28	89
2020	14	52	25	71	31	98
2050	100	52	200	71	300	100

[*] *Regarding the values for carbon and coal prices used in this work, it must be noted that DECC coal price projections are limited to an end date of 2030. Therefore it is assumed that the 2030 prices are representative of the 2050 scenario.*

From Table 4.5, it is observed that in the low and central decarbonisation scenarios, coal prices appear to be significantly reducing in the period to 2020 and beyond. It must be completely acknowledged that this is a matter of some debate, and there are good reasons to believe that this price crash may not occur. However, an exhaustive consideration of all the possible pricing scenarios is beyond the scope of this work.

4.3.1 Pareto Curve Analysis

In this section, the results for each of the three decarbonisation scenarios in each of the three years considered are presented as a series of Pareto curves (Figure 4.2, Figure 4.3 and Figure 4.4). Two main conclusions can be drawn from the comparison of these three figures. Firstly, as we move from the pessimistic decarbonisation scenario (Figure 4.2) towards the optimistic one (Figure 4.4), the carbon intensity of the system decreases at the minimum cost point. Secondly, it can be concluded that increased carbon prices and increased availability of biomass (biomass and SRF pellets) are the main drivers for reducing the carbon intensity associated with power generation; this is especially evident from the pareto curves for the 2050 scenarios

where the biomass availability and carbon prices are highest among the three years studied) in each of Figure 4.2-Figure 4.4.

It is interesting to consider how technology selection changes as we move along the pareto curve from a least cost objective to a least carbon objective. As can be seen in Figure 4.2, the trend in the optimal selection of technologies as we proceed along the pareto curve for 2012 from the minimum cost to the minimum carbon intensity point is as follows: coal only, coal + CCS, co-firing of biomass pellets with coal + CCS and co-firing of biomass and SRF pellets with coal + CCS. This is quite expected and these results are in line with those of Morrow *et al.* (2007).

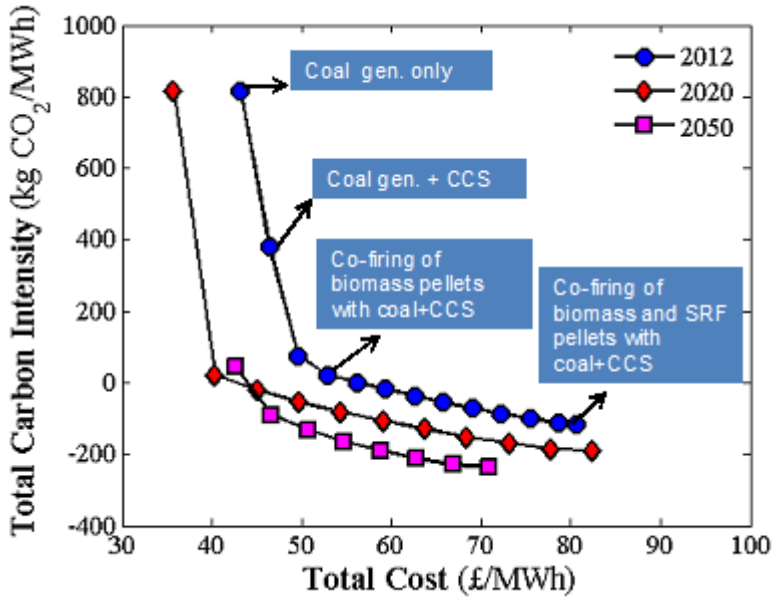

Figure 4.2 The trade-off between total cost and total carbon intensity in the pessimistic decarbonisation scenarios for years 2012, 2020 and 2050.

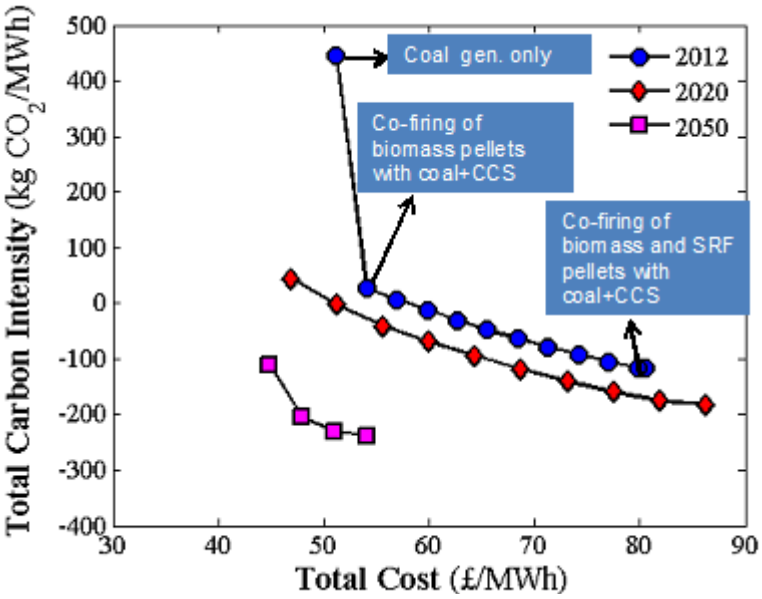

Figure 4.3 The trade-off between total cost and total carbon intensity in the central decarbonisation scenarios for years 2012, 2020 and 2050.

However, as the CO_2 and coal prices start to increase in the central scenario, we see CCS becoming the cost-optimal choice as early as 2020 (Table D7 in Appendix D). This implies that given the projected fuel and CO_2 prices, the decarbonisation of power generation in the 2020s would be a cost optimal solution. As can be concluded from the comparison of Figure 4.2 and Figure 4.3, the trend in the optimal choice of power generation technologies in this scenario as we move from one end to the other end of the Pareto curve for 2012 is similar to that observed in the pessimistic decarbonisation scenario.

Finally, in the optimistic decarbonisation scenario (high coal and CO_2 prices) – illustrated in Figure 4.4- CCS technology starts being selected in the cost optimal solution for each case.

Figure 4.4 The trade-off between total cost and total carbon intensity in the

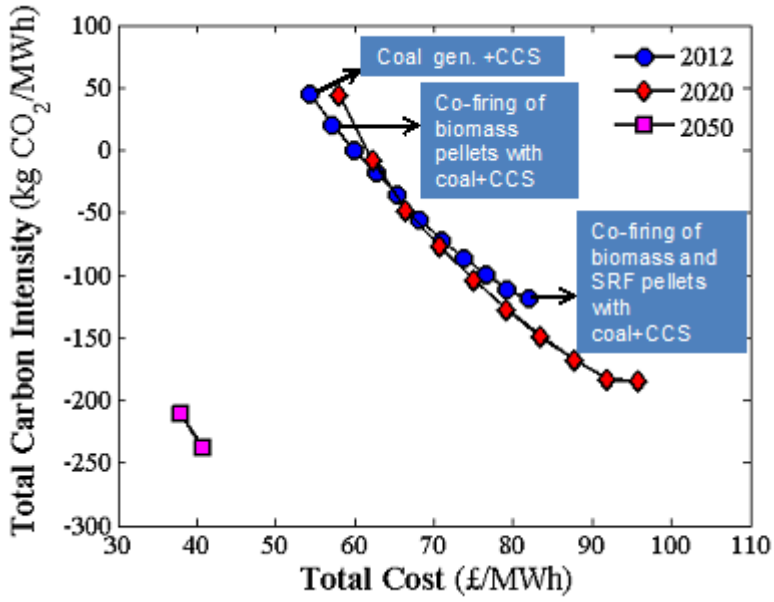

4.3.2 Optimal Network Configurations

For the representation of the optimal network configurations, the central decarbonisation scenario (with carbon and coal prices) has been selected as an average estimate of the future market conditions. The optimal minimum cost and minimum carbon intensity network configurations for 2020 with central carbon and carbon prices are shown in Figure 4.5 where the optimal solutions are presented at the regional level (including the 10 regions in the UK) for ease of visualisation. The mapping between these 10 regions and the 34 square cells is given in Table D6 in Appendix D. The corresponding detailed optimal configurations at the cell level and the optimal power generation variables can also be seen in the Figure D1-Figure D2 and Table D7-Table D10 in Appendix D. The optimal configuration figures represent the total optimal rates of biomass and MSW supply as well as the total optimal number of pellet plants established in each region (as indicated by the numbers inside the yellow squares). They also provide information on the optimal selection of co-firing plants (indicated by their locations) and the optimal electricity generation rates in these plants. As can be seen from the comparison of the two optimal configurations, in 2020 under the central decarbonisation scenario, the minimum cost configuation chooses electricity generation from coal only whereas the minimum carbon intensity configuration chooses to co-fire all the available domestic biomass and MSW resources with coal to make maximum use of the potential benefits of the non-fossil fuel resources in reducing the emissions. This leads to a

reduction of the average carbon intensity from 43 kg CO_2/MWh to -183 kg CO_2/MWh with a corresponding increase of the average cost from 47 £/MWh to 86 £/MWh. In the minimum carbon intensity configuration, the number of pellet plants established in each region is in general proportional to the availabilities of biomass and MSW in that region.

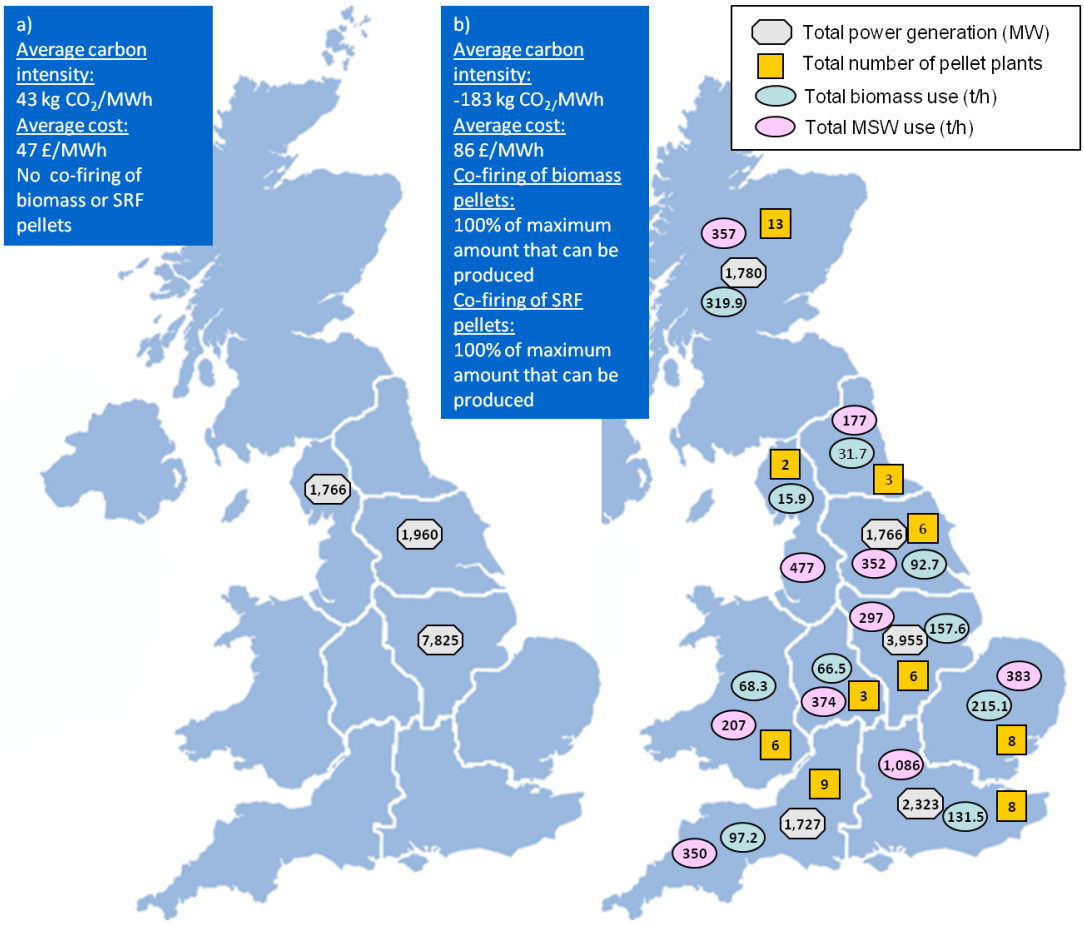

Figure 4.5 The optimal bioelectricity supply chain configuration for the a) minimum cost and b) minimum carbon intensity options for the 2020 central decarbonisation scenario. The pink and green symbols indicate the total optimal rates of MSW and biomass supply in each region. The yellow squares correspond to the total optimal number of pelletisation plants established in each region. Finally, the grey symbols represent the total optimal power generation within that region.

The minimum cost and minimum carbon intensity configurations for 2050 with central carbon and coal prices are presented in Figure 4.6. In contrast to the 2020 scenario, owing to the significantly increased cost associated with CO_2 emissions, the minimum cost configuration chooses to use the complete stock of domestic

biomass in addition to 16% of the total available MSW. This results in complete decarbonisation of the electricity sector in the cost optimal solution. Further decarbonisation can be achieved with the minimum carbon intensity configuration where all the available domestic biomass and MSW are used for co-firing with coal. This has an effect of reducing the carbon intensity from -109 kg CO_2/MWh to -238 kg CO_2/MWh with a small increase of 10 £/MWh in the average cost. Due to the higher use of biomass and MSW in the minimum carbon intensity configuration, there are more pellet plants established in that configuration compared to those in the minimum cost configuration.

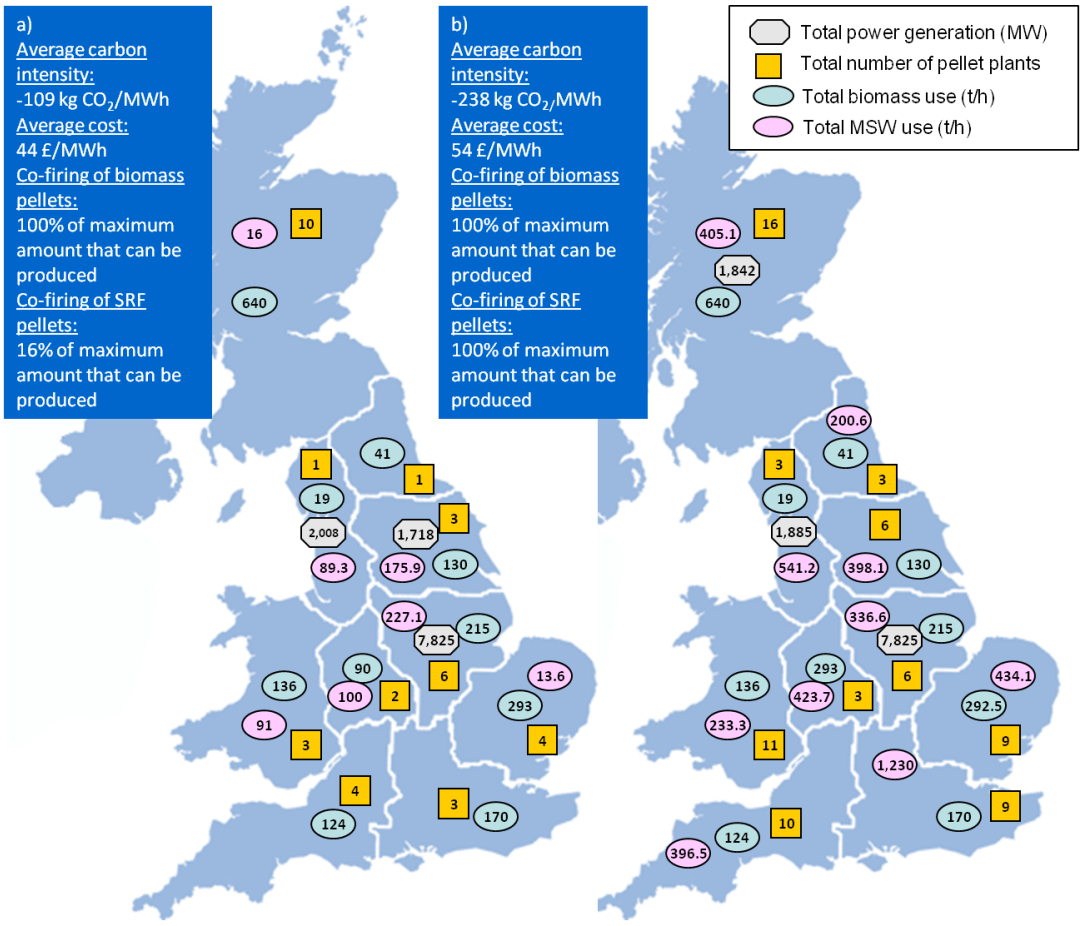

Figure 4.6 The optimal bioelectricity supply chain configuration for the a) minimum cost and b) minimum carbon intensity options for the 2050 central decarbonisation scenario. The pink and green symbols indicate the total optimal rates of MSW and biomass supply in each region. The yellow squares correspond to the total optimal number of pelletisation plants established in each region. Finally, the grey symbols represent the total optimal power generation within that region.

4.3.3 Carbon Tipping Point

One of the objectives of this work is to provide some insight into the costs associated with CO_2 emissions which would incentivise the generation of carbon negative electricity in the UK - a tipping point. In the carbon tipping point analysis, a pessimistic decarbonisation scenario where there is little incentive for decarbonisation (i.e., low carbon and low coal prices) is taken as the starting point and the CO_2 price range which will prompt the co-deployment of CCS and biomass co-firing in investigated.

Figure 4.7 shows change of the total carbon intensity of a minimum cost system with increase in the carbon price levels. As seen from the figure, there is a similar trend in the system response to the change in carbon price for the three snapshot years being studied. As can be concluded from the comparison of the figures for 2012, 2020 and 2050, the earliest switch to carbon negative electricity generation occurs in the case of 2050 at an average carbon price level of £120/t. The latest switch is in 2012 pessimistic scenario at an average price level of £175/t. This arises from the combined effect of higher coal price and lower availabilities of domestic biomass and MSW in 2012 compared to 2020 and 2050. It is, however, interesting to note that in both the 2012 and 2020 scenarios, a relatively modest price in the region of £35/tonne CO_2 is sufficient to incentivise the generation of low carbon electricity.

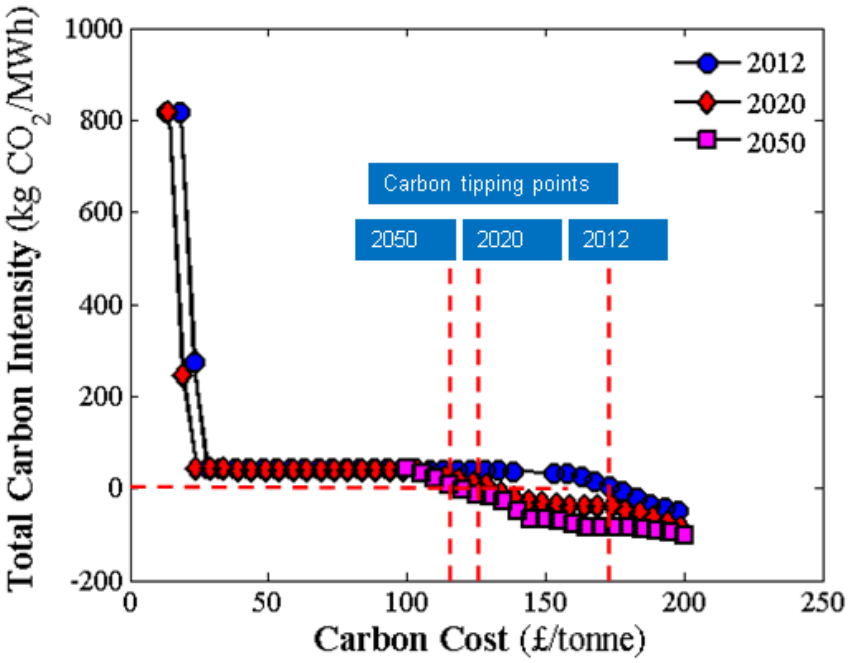

Figure 4.7 Carbon tipping point analysis for the 2012, 2020 and 2050 pessimistic decarbonisation scenarios.

4.3.4 High Biomass Availability

This section aims to investigate how an increase in biomass availability would affect the carbon intensity of a minimum cost configuration. For this purpose, three cases of biomass availability are considered: base case with the nominal biomass availability, high availability case (double the base case) and very high availability case (five times the base case). Figure 4.8 shows the lower end of the pareto curves for these three cases in the 2020 central decarbonisation scenario. In the interest of clarity, the upper portion of the pareto curves i.e., the high carbon intensity extreme, is not shown here as each of the cases has the same point of origin. As can be concluded from the comparison of the three curves, cost of decarbonisation can be reduced significantly with higher biomass availability; for example to achieve a carbon intensity of -190 kg CO_2/MWh with the base case corresponds to a cost of approximately £82/MWh, whereas with increased biomass availability, this carbon intensity can be achieved at a total cost of approximately £73/MWh and £66/MWh high biomass and very high biomass availability scenarios, respectively. Finally, at the minimum carbon intensity point, the total carbon footprint of the power plants is reduced from about -16.9MT CO_2/yr to about -27MT CO_2/yr and -31 MT CO_2/yr under the high and very high biomass availability scenarios, respectively.

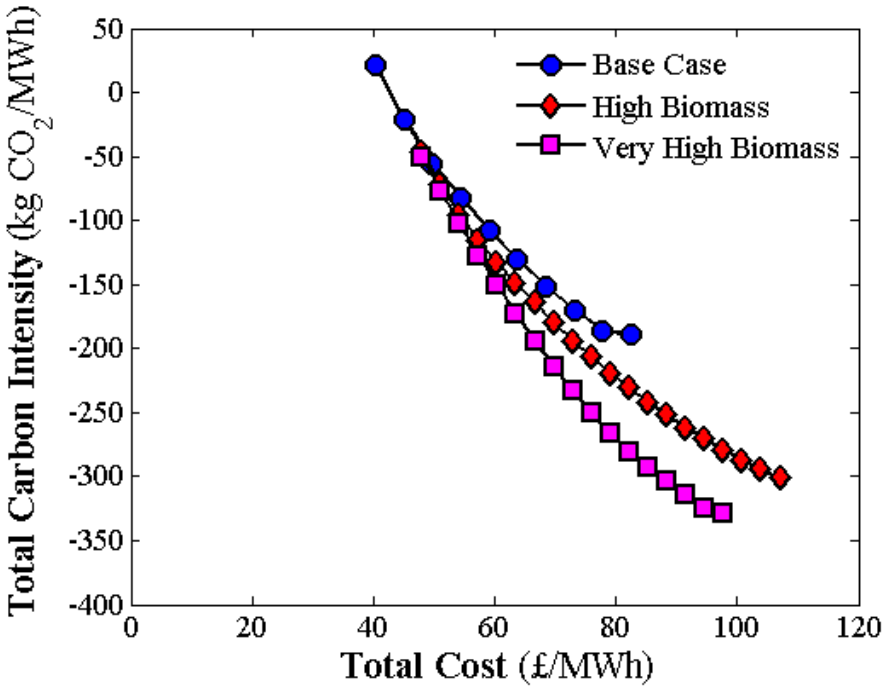

Figure 4.8 Results of the high biomass availability analysis for the 2020 central decarbonisation scenario.

4.4 Concluding Remarks

This work analyses co-firing of biomass in conjunction with CO_2 capture and storage in 10 existing coal-fired power stations in the UK. Both municipal solid waste and conventional biomass resources have been considered, which has the important advantage of increasing the biomass availability in the system. Three different decarbonisation scenarios (low, central and high prices for CO_2 and coal) have been investigated for the three snapshot years:2012, 2020 and 2050.

The levels of CO_2 price that would be required to incentivise the generation of carbon negative electricity in a low carbon and low coal price scenario have been investigated. A tipping point analysis has been carried out for this purpose where the change in the carbon intensity of a cost optimal system is analysed with an increasing CO_2 price. The results indicate that a CO_2 price in the region of £120 - 175/tonne will be necessary to incentivise the generation of carbon negative electricity. The results also imply that this cost can be reduced with increased biomass availability.

The availability of biomass has been observed an important constraint on the degree to which carbon negative energy can be generated. Thus the exploitation of waste

derived biomass as a solid recovered fuel source as well as use of dedicated energy crops can provide a useful route to at least soften this constraint. However, it has been observed previously that the promotion of the use of biomass for energy applications can cause a rapid increase in the price of biomass (Wianwiwat and Asafu-Adjaye, 2013). As the sharp increase in electricity costs associated with the transition from low carbon to carbon negative electricity arises in part from the cost of biomass, the results of the case study suggest that biomass availability is a key component to consider before ambitious targets of biomass utilisation for electricity production are established.

It can be concluded that co-firing of biomass and solid recovered fuels in conjunction with CO_2 capture provides a promising route to the near to medium term generation of carbon negative electricity. Importantly, given existing coal-fired power plants, co-firing can be implemented with relatively low capital costs within a timeframe of fewer than 5 years. The retro-fitting of CO_2 capture processes may take somewhat longer, but the relative immediacy of co-firing provides one possible route to extending the operating life of existing assets within a carbon constrained energy system. It will likely be necessary that power plants generating carbon negative electricity operate at a high load factor with similarly high rates of CO_2 capture. Achieving this could prove challenging unless coal + biomass-based CCS becomes a base-load generating technology of choice. A potential option where BECCS could become very attractive and allow it to become a base-load technology is a "carbon-bubble" concept, analogous to the "Clean Air Act" of the US Environmental Protection Agency (EPA) which allows the EPA to grant emissions permits for certain pollutants. Importantly, these permits are tradable between polluters, allowing one to pay another to reduce their emissions (the EU Emissions Trading System). This concept rests upon the specification of a geographic region – or bubble – which must reduce its total level of CO_2 emission by a given amount by a given date. The use of this bubble concept has been shown to significantly reduce the whole system cost of emission reduction and may well be attractive option in the context of CO_2 emission mitigation as well.

Finally, it must be noted that the proposed approach is sufficiently general to be extended to consider other CO_2 capture routes, e.g., oxyfuel combustion or high

temperature solids looping. This can be achived by the generation of an appropriate meta-model for the performance of a co-fired power plant equipped with an oxyfuel system and its integration with the bioelectricity supply chain optimisation model developed here. This is important because preliminary analysis indicates that the sharp “elbow” in the trade-off curve can be avoided and a much deeper decarbonisation take place once more economic “advanced” technologies (e.g. biomass gasification with CCS or biomass-based chemical looping combustion with carbon dioxide compression) are available at commercial scale.

5 A Spatial Hydrogen Infrastructure Planning Model

Hydrogen is considered as an alternative transport fuel to tacke the greenhouse gas emissions problem resulting from the transport sector. Therefore, it becomes important to study and understand the various aspects of a future hydrogen supply chain. Supply chain optimisation can be used as a valuable tool for this purpose.

This chapter presents a spatially-explicit, multi-period mixed integer linear programming model for the optimal design of a hydrogen supply chain where biomass-to-hydrogen is considered as one of the potential hydrogen conversion pathways. The model utilises a modified version of the neighbourhood approach introduced in Chapter 3.

5.1 Problem Statement

The optimal design of a hydrogen supply chain involves several decisions, including locations, technologies and scales of hydrogen production plants, storages and filling stations, and transport system characteristics. The overall hydrogen supply chain problem under consideration is stated as follows. Given:

- hydrogen demand in each region and time period,
- characteristics of hydrogen production technologies, storage, filling stations, transportation modes and CO_2 pipelines,
- carbon tax per unit of CO_2, carbon emission and capture factors,
- locations of the CO_2 collection points and reservoirs, reservoir capacities and their connections to the collection points,

To determine the optimal:

- locations, scales and types of hydrogen production plants, storage facilities, filling stations, and transport modes, as well as locations and sizes of onshore and offshore CO_2 pipes,
- hydrogen production rates and stored amounts,
- flows of hydrogen and CO_2 between regions, and CO_2 flows between collection points and reservoirs, as well as CO_2 inventory levels of the reservoirs,

So as to minimise the total supply chain network cost.

The developed model adopts a 'modified neighbourhood flow' representation for the purposes of problem size reduction and computational efficiency. In this approach, which has been developed based on the neighbourhood approach introduced in Chapter 3, a material can flow from the origin to the destination point by the addition of sequential neighbourhood flows. This approach is introduced into the mathematical formulation through a set, $N_{gg'}$ which is defined as:

$$N_{gg'}:(g,g') \quad where \quad L^R_{gg'} \le L^R_{gg''} + L^R_{g''g'} \quad \forall g \ne g' \ne g'' \in G \tag{5.1}$$

For each region g, this set includes its immediate neighbours as well as those where the direct distance from region g to g' is less than or equal to the total distance travelled when following a different route through regions g, g'' and g' with the same start point g and destination point g'. This is illustrated in Figure 5.1.

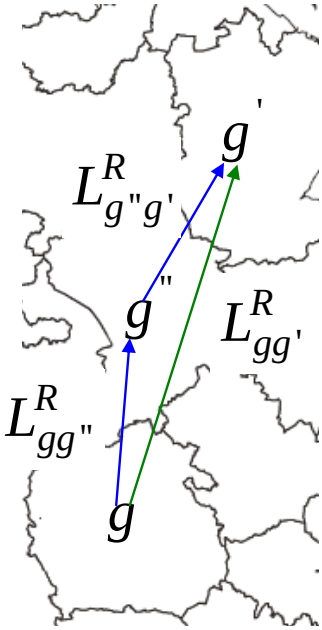

Figure 5.1 Illustration of the definition of the modified neighbourhood approach where distances between the regions g, g', and g'' are indicated by L^R.

5.2 Mathematical Formulation

The problem for the optimal design of a hydrogen supply chain is formulated as a multi-period, mixed integer linear programming (MILP) model with the following notation:

Indices:

f	Hydrogen filling station type
g	Regions
i	Physical form of hydrogen (product type)
j	Hydrogen production technology
l	Transportation mode
m	The total number of plants in a region
p	Facility size (production facility, storage facility or filling station)
s	Hydrogen storage technology
t	Time period

Sets:

F	Set of hydrogen filling station types
G	Set of regions
I	Set of physical forms of hydrogen (product types)
J	Set of hydrogen production technologies
L	Set of transportation modes
M	Set of the total number of plants in a region
$N_{gg'}$	Set of neighbouring regions g and g'
P	Set of facility sizes (production facility, storage facility or filling station)
S	Set of hydrogen storage technologies
T	Set of time periods
GR	Set of collection point (g) and reservoir (r) connections
IL	Set of product type (i) and transportation mode (l) combinations
IJP	Set of product type (i), production technology (j) and plant size (p) combinations
IFP	Set of product type (i), filling station type (f) and filling station size (p) combinations
ISP	Set of product type (i), storage type (s) and storage size (p) combinations

Parameters:

$AD^0_{gg'}$	Initial available diameter of an onshore CO_2 pipeline between regions g and g' (cm)

$\overline{ADR}_{gr}^{0}$	Initial available diameter of an offshore CO_2 pipeline between a CO_2 collection point *g* and reservoir *r* (cm)
AE_r^0	Initial activity (availability) of a reservoir *r* (0,1)
$AY_{gg'}^0$	Initial availability of an onshore CO_2 pipeline between regions *g* and *g'* (0,1)
α	Network operating period (d year^{-1})
β	Ratio of stored amount of hydrogen to hydrogen demand
CT_t	Carbon tax in time period *t* (\$ kg^{-1} CO_2)
DEM_{gt}	Total hydrogen demand in region *g* in time period *t* (kg H_2 d^{-1})
$DFCAP_t$	Discount factor for capital costs in time period *t*
$DFOC_t$	Discount factor for operating costs in time period *t*
DW_{il}	Driver wage of transportation mode *l* transporting product type *i* (\$ h^{-1})
ε	Intercept of the linear relationship between the capital cost of an onshore CO_2 pipeline and its diameter
$\bar{\varepsilon}$	Intercept of the linear relationship between the capital cost of an offshore CO_2 pipeline and its diameter
$FCAP_{fpi}^{\max}$	Maximum capacity of filling station type *f* and size *p* for product type *i* (kg H_2 d^{-1})
FE_{il}^L	Local fuel economy of transportation mode *l* transporting product type *i* within a region (km l^{-1})
FE_{il}^R	Regional fuel economy of transportation mode *l* transporting product type *i* between regions (km l^{-1})
FP_{il}	Fuel price of transportation mode *l* transporting product *i* (\$ l^{-1})
$FSCC_{fpi}$	Capital cost of filling station type *f* and size *p* for product type *i* (\$)
γc_{jpit}	CO_2 capture coefficient for producing product *i* at a plant of size *p* using technology *j* in time period *t* (kg CO_2 kg^{-1} H_2)
γe_{jpit}	CO_2 emission coefficient for producing product *i* at a plant of size *p* using technology *j* in time period *t* (kg CO_2 kg^{-1} H_2)
GE_{il}	General expenses of transportation mode *l* transporting product type *i* (\$ d^{-1})

λ	Slope of the linear relationship between the CO_2 flow in a CO_2 pipeline and its diameter
L_g^L	Local delivery distance within region g (km)
$L_{gg'}^R$	Regional delivery distance between regions g and g' (km)
$\bar{L}_{gr}$	Distance between a CO_2 collection point g and reservoir r (km)
LUT_{il}	Load/unload time of transportation mode l transporting product type i (h)
ME_{il}	Maintenance expenses of transportation mode l transporting product type i ($\$ km^{-1}$)
NF_{fpig}^0	Initial number of hydrogen filling stations of type f and size p for product type i in region g
NP_{jpig}^0	Initial number of hydrogen production plants of technology j and size p producing product type i in region g
NS_{spig}^0	Initial number of hydrogen storage facilities of type s and size p storing product type i in region g
η	Slope of the linear relationship between the capital cost of an onshore CO_2 pipeline and its diameter
$\bar{\eta}$	Slope of the linear relationship between the capital cost of an offshore CO_2 pipeline and its diameter
$PCAP_{jpi}^{\min}$ / $PCAP_{jpi}^{\max}$	Minimum/maximum production capacity of a hydrogen production plant of type j and size p producing product type i (kg H_2 d^{-1})
PCC_{jpi}	Capital cost of a production plant of type j and size p producing product type i ($)
RI_r^0	Initial CO_2 inventory in reservoir r (kg CO_2)
RVC_t	Remaining value of an onshore CO_2 pipeline in time period t ($\$ km^{-1}$)
$\overline{RVC_t}$	Remaining value of an offshore CO_2 pipeline in time period t ($\$ km^{-1}$)
RVF_{fpit}	Remaining value of a filling station of type f and size p for product type i in time period t ($)
RVP_{jpit}	Remaining value of a hydrogen production plant of type j and size p producing product type i in time period t ($)

RVS_{spit} Remaining value of a storage facility of type *s* and size *p* storing product type *i* in time period *t* ($)

$Q_{il}^{\min} / Q_{il}^{\max}$ Minimum/maximum flow rate of product type *i* via transportation mode *l* (kg H_2 d^{-1})

$SCAP_{spi}^{\min} / SCAP_{spi}^{\max}$ Minimum/maximum storage capacity of storage type *s* and size *p* for product type *i* (kg H_2)

SCC_{spi} Capital cost of storage type *s* and size *p* storing product type *i* ($)

δ Ratio of a CO_2 pipeline operating cost to its capital cost

SP_{il}^{L} Local average speed of transportation mode *l* transporting product type *i* within a region (km h^{-1})

SP_{il}^{R} Regional average speed of transportation mode *l* transporting product type *i* between regions (km h^{-1})

θ Intercept of the linear relationship between the CO_2 flow in a CO_2 pipeline and its diameter

$TCAP_{il}$ Capacity of transportation mode *l* transporting product type *i* (kg H_2 $mode^{-1}$)

TMA_{il}^{L} Local availability of transportation mode *l* transporting product *i* within a region (h d^{-1})

TMA_{il}^{R} Regional availability of transportation mode *l* transporting product *i* between regions (h d^{-1})

TMC_{il} Cost of establishing transportation mode *l* transporting product type *i* ($ $mode^{-1}$)

U Upper bound on a CO_2 pipe diameter (cm)

UPC_{jpi} Unit production cost of product type *i* by plant type *j* and size *p* ($ kg^{-1} H_2)

USC_{spi} Unit storage cost of product type *i* at storage type *s* and size *p* ($ kg^{-1} H_2 d^{-1})

W A large positive number (for the local demand constraint)

Integer Variables

IF_{fpigt} Investment of new filling stations of type *f* and size *p* for product type *i* in region *g* in time period *t*

IP_{jpigt} Investment of new plants of type *j* and size *p* producing product type *i* in region *g* in time period *t*

IS_{spigt} Investment of new storage facilities of type *s* and size *p* storing product type *i* in region *g* in time period *t*

NF_{fpigt} Number of filling stations of type *f* and size *p* for product type *i* in region *g* in time period *t*

NP_{jpigt} Number of plants of type *j* and size *p* producing product type *i* in region *g* in time period *t*

NS_{spigt} Number of storage facilities of type *s* and size *p* storing product type *i* in region *g* in time period *t*

Binary Variables

$AY_{gg't}$ 1 if an onshore CO_2 pipeline is available between regions *g* and *g'* in time period *t*, 0 otherwise

AE_{rt} 1 if a reservoir *r* is active (available) in time period *t*, 0 otherwise

U_{mgt} 1 if there are $m-1$ plants in region *g* during time period *t*, 0 otherwise

E_{rt} 1 if a reservoir *r* is activated in time period *t*, 0 otherwise

$Y_{gg't}$ 1 if an onshore CO_2 pipeline is established between regions *g* and *g'* in time period *t*, 0 otherwise

Continuous Variables

$AD_{gg't}$ Available diameter of an onshore CO_2 pipeline between regions *g* and *g'* in time period *t* (cm)

$\overline{ADR}_{grt}$ Available diameter of an offshore CO_2 pipeline between a CO_2 collection point *g* and reservoir *r* in time period *t* (cm)

CEC Carbon emissions cost ($)

D_{igt}^{L} Local demand for product type *i* in region *g* satisfied by local production in time period *t* (kg H_2 d^{-1})

D_{igt}^{I} Imported demand of product type *i* to region *g* in time period *t* (kg H_2 d^{-1})

D_{igt}^{T} Total demand for product type *i* in region *g* in time period *t* (kg H_2 d^{-1})

$Dia_{gg't}$ Diameter of an onshore CO_2 pipeline established between regions *g* and *g'* in time period *t* (cm)

$\overline{Dia}_{grt}$	Diameter of an offshore CO_2 pipeline established between a CO_2 collection point *g* and reservoir *r* in time period *t* (cm)
DM^{L}_{imgt}	Local demand of product type *i* satisfied by *m-1* number of plants in region *g* in time period *t* (kg H_2 d^{-1})
FC^{L}	Fuel cost for local transport ($)
FC^{R}	Fuel cost for regional transport ($)
LC^{L}	Labour cost for local transport ($)
LC^{R}	Labour cost for regional transport ($)
FCC	Facility capital cost ($)
FOC	Facility operating cost ($)
GC^{L}	General cost for local transport ($)
GC^{R}	General cost for regional transport ($)
MC^{L}	Maintenance cost for local transport ($)
MC^{R}	Maintenance cost for regional transport ($)
P_{jpigt}	Production rate of product type *i* produced by a plant of type *j* and size *p* in region *g* in time period *t* (kg H_2 d^{-1})
P^{T}_{igt}	Total production rate of product type *i* in region *g* in time period *t* (kg H_2 d^{-1})
PCC	Pipeline capital cost ($)
POC	Pipeline operating cost ($)
$Q_{ilgg't}$	Flowrate of product type *i* via transportation mode *l* between regions *g* and *g*' in time period *t* (kg H_2 d^{-1})
$QC_{gg't}$	Flowrate of CO_2 between regions *g* and *g'* in time period *t* via an onshore pipeline (kg CO_2 d^{-1})
$\overline{QCR}_{grt}$	Flowrate of CO_2 from a CO_2 collection point *g* to a reservoir *r* in time period *t* via an offshore pipeline (kg CO_2 d^{-1})
RI_{rt}	Inventory of CO_2 in reservoir *r* in time period *t* (kg CO_2-eq)
S_{spigt}	Average inventory of product type *i* stored in a storage facility of type *s* and size *p* in region *g* in time period *t* (kg H_2)
S^{T}_{sgt}	Total average inventory stored in storage type *s* in region *g* in time period *t* (kg H_2)
TCC	Transportation capital cost ($)

TOC Transportation operating cost ($)

a) Objective Function

The objective of the proposed model is to minimise the total supply chain cost (*TC*), which is composed of facilities capital cost (*FCC*), CO_2 pipelines capital cost (*PCC*) and transportation capital cost (*TCC*), facilities operating cost (*FOC*), CO_2 pipelines operating cost (*POC*), transportation operating cost (*TOC*) and cost of carbon emissions (*CEC*) terms as follows:

$$TC = FCC + PCC + TCC + FOC + POC + TOC + CEC \tag{5.2}$$

The facilities capital cost includes the total cost of hydrogen production plants, storage facilities and filling stations as given by:

$$\begin{aligned} FCC = & \sum_{(i,j,p)\in IJP} \sum_{g\in G} \sum_{t\in T} \left[\left(DFCAP_t\, PCC_{jpi} - RVP_{jpit} \right) IP_{jpigt} \right] + \\ & \sum_{(i,s,p)\in ISP} \sum_{g\in G} \sum_{t\in T} \left[\left(DFCAP_t\, SCC_{spi} - RVS_{spit} \right) IS_{spigt} \right] + \\ & \sum_{(i,f,p)\in IFP} \sum_{g\in G} \sum_{t\in T} \left[\left(DFCAP_t FSCC_{fpi} - RVF_{fpit} \right) IF_{fpigt} \right] \end{aligned} \tag{5.3}$$

where $DFCAP_t$ is the discount factor for capital costs in time period *t*. It is assumed that the capital costs are discounted for the initial year of each time period whereas operating costs are discounted on a yearly basis (see Appendix E for the formulation of the discount factors). PCC_{jpi} is the capital cost of establishing a production plant of technology *j* and size *p* that produces product type *i*. SCC_{spi} is the capital cost a storage facility of type *s* and size *p* for storing product *i*. $FSCC_{fpi}$ is the capital cost of a filling station of type *f* and size *p* for product *i*. RVP_{jpit}, RVS_{spit} and RVF_{fpit} are the corresponding remaining values of the production plants, storage facilities and filling stations in time period *t*, respectively. IP_{jpigt}, IS_{spigt} and IF_{fpigt} are the number of new production plants, storage facilities and filling stations that are established in region *g* in time period *t*, respectively.

The pipeline capital cost (*PCC*) is defined as:

$$\begin{aligned} PCC = & \sum_{(g,g')\in N_{gg'}} \left(\sum_{t\in T} \left(DFCAP_t \left(\varepsilon\, Y_{gg't} + \eta\, Dia_{gg't} \right) - RVC_{\ t} Y_{gg't} \right) \right) L^R_{gg'} + \\ & \sum_{g\in G} \sum_{r\in GR} \left(\sum_{t\in T} \left(DFCAP_t \left(\bar{\varepsilon}\, E_{rt} + \bar{\eta}\ \overline{Dia}_{grt} \right) - \overline{RVC}_{\ t} E_{rt} \right) \right) \bar{L}_{gr} \end{aligned} \tag{5.4}$$

The first and second terms on the right hand side of equation 5.4 represent the capital cost of onshore and offshore CO_2 pipelines, respectively. The capital cost of a pipeline per its length is linearly dependent on its diameter defined by a slope (η for onshore and $\overline{\eta}$ for offshore pipes) and intercept (ε for onshore and $\overline{\varepsilon}$ for offshore pipes). $Dia_{gg't}$ is the diameter of an onshore pipeline established between regions g and g' in time period t. On the other hand, $\overline{Dia}_{grt}$ is the diameter of an offshore pipeline established between a CO_2 collection point g and a reservoir r in time period t. RVC_t and $\overline{RVC}_t$ are the remaining values of an onshore and offshore pipeline in time period t (described the residual value of a pipeline at the end of its useful life), respectively.

Transportation capital cost (*TCC*) is a sum of the capital cost required for local and regional delivery as given by the following equation:

$$TCC = \sum_{(i,l)\in IL}\sum_{m\in M}\sum_{g\in G}\sum_{t\in T}\frac{DM^{L}_{imgt}TMC_{il}}{(m-1)TMA^{L}_{il}TCAP_{il}}\left(\frac{2L^{L}_{g}}{SP^{L}_{il}}+LUT_{il}\right)+ \sum_{(i,l)\in IL}\sum_{(g,g')\in N_{gg'}}\sum_{t\in T}\frac{Q_{igg'lt}}{TMA^{R}_{il}TCAP_{il}}\left(\frac{2L^{R}_{gg'}}{SP^{R}_{il}}+LUT_{il}\right) \quad (5.5)$$

where DM^{L}_{imgt} is the local demand of product i met by m-1 number of plants in region g and time period t. TMC_{il}, $TCAP_{il}$, SP_{il} and LUT_{il} are the cost, capacity, average speed and load/unload time of transportation mode l transporting product type i, respectively. L^{L}_{g} is the local delivery distance within region g whereas $L^{R}_{gg'}$ is the regional delivery distance between regions g and g'. $Q_{igg'lt}$ is the flowrate of product i between regions g and g' via mode l in time period t.

The facilities operating cost (*FOC*) accounts for the cost of the operating costs of the production facilities as well as those of the storage facilities as described in the following equation:

$$FOC = \sum_{(i,j,p)\in IJP}\sum_{g\in G}\sum_{t\in T}\alpha\, DFOC_t\, UPC_{jpi}P_{jpigt} + \sum_{(i,s,p)\in ISP}\sum_{g\in G}\sum_{t\in T}\alpha\, DFOC_t\, USC_{spi}S_{spigt} \quad (5.6)$$

where α *is* the number of operating days in a year and $DFOC_t$ is the discount factor for the operating costs in time period t (see Appendix E). UPC_{jpi} is the unit production cost of product type i by plant type j and size p and P_{jpigt} is the production

rate of product *i* at that plant located in region *g* in time period *t*. Likewise, USC_{spi} is the unit cost of storage of product *i* at a storage facility of type *s* and size *p*. S_{spigt} is the stored amount of product *i* in that storage type located in region *g* in time period *t*.

The CO_2 pipeline operating cost (*POC*) is assumed to be a certain fraction of its capital cost (*PCC*) as follows:

$$POC = \delta PCC \tag{5.7}$$

where δ is the parameter that defines this ratio.

The transportation operating cost (*TOC*) is composed of local and regional fuel costs (FC^L and FC^R), local and regional general costs (GC^L and GC^R), local and regional labour costs (LC^L and LC^R), and local and regional maintenance costs (MC^L and MC^R), given by:

$$TOC = FC^L + FC^R + GC^L + GC^R + LC^L + LC^R + MC^L + MC^R \tag{5.8}$$

Local fuel cost is determined by:

$$FC^L = \sum_{(i,l)\in IL} \sum_{m\in M} \sum_{g\in G} \sum_{t\in T} \alpha\, DFOC_t\, FP_{il} \left(\frac{2L_g^L DM_{imgt}^L}{(m-1) FE_{il}^L TCAP_{il}} \right) \tag{5.8a}$$

where FP_{il} is fuel price of transportation mode *l* transporting product *i* and FE_{il}^L is the local fuel economy of transportation mode *l* transporting product *i* within a region.

The regional fuel cost is given by:

$$FC^R = \sum_{(i,l)\in IL} \sum_{(g,g')\in N_{gg'}} \sum_{t\in T} \alpha\, DFOC_t\, FP_{il} \left(\frac{2L_{gg'}^R Q_{igg'lt}}{FE_{il}^R TCAP_{il}} \right) \tag{5.8b}$$

where FE_{il}^R is the regional fuel economy of that transportation mode between regions.

The local general cost is:

$$GC^L = \sum_{(i,l)\in IL} \sum_{m\in M} \sum_{g\in G} \sum_{t\in T} \alpha\, DFOC_t\, GE_{il} \left(\frac{DM_{imgt}^L}{(m-1) TMA_{il}^L TCAP_{il}} \left(\frac{2L_g^L}{SP_{il}^L} + LUT_{il} \right) \right) \tag{5.8c}$$

where GE_{il} represents the general expenses of transportation mode *l* transporting product type *i*.

The regional general cost is:

$$GC^R = \sum_{(i,l)\in IL}\sum_{(g,g')\in N_{gg'}}\sum_{t\in T}\alpha\, DFOC_t\, GE_{il}\left(\frac{Q_{igg'lt}}{TMA_{il}^R TCAP_{il}}\left(\frac{2L_{gg'}^R}{SP_{il}^R}+LUT_{il}\right)\right) \quad (5.8d)$$

The local labour cost is:

$$LC^L = \sum_{(i,l)\in IL}\sum_{m\in M}\sum_{g\in G}\sum_{t\in T}\alpha\, DFOC_t\, DW_{il}\left(\frac{DM_{imgt}^L}{(m-1)TCAP_{il}}\left(\frac{2L_g^L}{SP_{il}^L}+LUT_{il}\right)\right) \quad (5.8e)$$

where DW_{il} is the driver wage of transportation mode l transporting product type i.

The regional labour cost is:

$$LC^R = \sum_{(i,l)\in IL}\sum_{(g,g')\in N_{gg'}}\sum_{t\in T}\alpha\, DFOC_t\, DW_{il}\left(\frac{Q_{igg'lt}}{TCAP_{il}}\left(\frac{2L_{gg'}^R}{SP_{il}^R}+LUT_{il}\right)\right) \quad (5.8f)$$

The local maintenance cost is defined by:

$$MC^L = \sum_{(i,l)\in IL}\sum_{m\in M}\sum_{g\in G}\sum_{t\in T}\alpha\, DFOC_t\, ME_{il}\left(\frac{2L_g^L DM_{imgt}^L}{(m-1)TCAP_{il}}\right) \quad (5.8g)$$

where ME_{il} maintenance expenses of transportation mode l transporting product type i.

The regional maintenance cost is:

$$MC^R = \sum_{(i,l)\in IL}\sum_{(g,g')\in N_{gg'}}\sum_{t\in T}\alpha\, DFOC_t\, ME_{il}\left(\frac{2L_{gg'}^R Q_{igg'lt}}{TCAP_{il}}\right) \quad (5.8h)$$

The carbon emissions cost (*CEC)* is defined by:

$$CEC = \sum_{(i,j,p)\in IJP}\sum_{g\in G}\sum_{t\in T}\alpha\, DFOC_t\, CT_t\, \gamma e_{jpit} P_{jpigt} \quad (5.9)$$

where CT_t is the carbon tax per unit of CO_2 emitted in time period t and γe_{jpit} is the CO_2 emission coefficient for technology j of size p and producing product i in time period t.

a) Demand Constraints

The local demand for a product i in region g in time period t must be satisfied by the local production given by:

$$D_{igt}^L \le P_{igt}^T \qquad \forall\, i\in I, g\in G, t\in T \quad (5.10)$$

Distributed or small sized plants located in a region can only produce less than the local demand given by:

$$\sum_{j:(i,j,p)\in IJP} P_{jpigt} \le D^{L}_{igt} \quad \forall\, i \in I,\, p \in \{Distributed, Small\},\, g \in G, t \in T \tag{5.11}$$

The total imported amount of product *i* to a region *g* is the sum of the incoming flows of that product via all transportation modes transporting that product:

$$D^{I}_{igt} = \sum_{g'\in N_{gg'}} \sum_{l:(i,l)\in IL} Q_{ig'glt} \quad \forall\, i \in I,\, g \in G, t \in T \tag{5.12}$$

The total demand for a product *i* in a region *g* in time period *t* is the sum of the local and imported demands of that product as given by:

$$D^{T}_{igt} = D^{L}_{igt} + D^{I}_{igt} \qquad \forall\, i \in I,\, g \in G, t \in T \tag{5.13}$$

The sum of the total demands of all product types in a region *g* in time period *t* must be equal to the given total market demand of hydrogen that must be satisfied:

$$\sum_{i\in I} D^{T}_{igt} = DEM_{gt} \qquad \forall g \in G, t \in T \tag{5.14}$$

where DEM_{gt} is the parameter that represents the total market demand of hydrogen in region *g* and time period *t*.

b) Production Constraints

The mass balance for each product *i* in region *g* and time period *t* states that the production plus the incoming flows to that region must be equal to the outgoing flows from that region plus the total demand of that product as follows:

$$P^{T}_{igt} + \sum_{g'\in N_{gg'}} \sum_{l:(i,l)\in IL} Q_{ig'glt} = \sum_{g'\in N_{gg'}} \sum_{l:(i,l)\in IL} Q_{igg'lt} + D^{T}_{igt} \quad \forall\, i \in I,\, g \in G, t \in T \tag{5.15}$$

The total production of a product *i* in region *g* and time period *t* is the sum of the production rates of that product across plants of size *p* and type *j* located in that region:

$$P^{T}_{igt} = \sum_{(j,p):(i,j,p)\in IJP} P_{jpigt} \qquad \forall\, i \in I,\, g \in G, t \in T \tag{5.16}$$

The production rate of a product *i* from a certain plant type *j* and size *p* in a region *g* is limited by the number of plants of that type established in that region as well as the given minimum and maximum production capacities of that plant type as follows:

$$PCAP^{\min}_{jpi}\, NP_{jpigt} \le P_{jpigt} \le PCAP^{\max}_{jpi}\, NP_{jpigt} \;\forall (i,j,p) \in IJP,\, g \in G, t \in T \tag{5.17}$$

Once a production plant of type *j* and size *p* is established in a region *g* and time period *t*, it becomes available in the same period as well as the following time periods as given by:

$$NP_{jpigt} = NP^{0}_{jpig}\Big|_{t=1} + NP_{jpig,t-1}\Big|_{t>1} + IP_{jpigt} \quad \forall (i,j,p) \in IJP, g \in G, t \in T \tag{5.18}$$

where NP^{0}_{jpig} is the parameter that represents the initial number of plants located in region *g*. The total number of plants established in a region *g* is calculated through the sumproduct of (m-1) variable (to allow for establishment of no plants) and the binary variable, U_{mgt} as described in the work of Almansoori and Shah (2009).

c) Storage Constraints

The total stored amount of product by a storage type *s* in region *g* and time period *t* is equal to a certain fraction, β of the total demand of the type(s) of product(s) *i* stored by that storage type given by**:**

$$S^{T}_{sgt} = \beta \sum_{i:(i,s,p)\in ISP} D^{T}_{igt} \quad \forall s \in \mathrm{S}, g \in G, t \in T \tag{5.19}$$

The total stored product amount by storage type *s* is also equal to the sum of the stored amounts across product type(s) *i* and sizes *p* of that storage type:

$$S^{T}_{sgt} = \sum_{(i,p):(i,s,p)\in ISP} S_{spigt} \quad \forall s \in S, g \in G, t \in T \tag{5.20}$$

Similarly to the production rates, the stored amount of a product *i* in a storage type *s* and size *p* in a region *g* is limited by the number of storages of that type established in that region as well as the given minimum and maximum storage capacities of that storage type as follows:

$$SCAP^{\min}_{spi}\, NS_{spigt} \le S_{spigt} \le SCAP^{\max}_{spi}\, NS_{spigt} \quad \forall (i,s,p) \in ISP, g \in G, t \in T \tag{5.21}$$

Once a storage facility is established in a time period *t*, it becomes available in the same time period as well as the following time periods:

$$NS_{spigt} = NS^{0}_{spig}\Big|_{t=1} + NS_{spig,t-1}\Big|_{t>1} + IS_{spigt} \quad \forall (i,s,p) \in ISP, g \in G, t \in T \tag{5.22}$$

where NS^{0}_{spig} is the parameter that represents the initial number of storages located in region *g*.

d) Filling Station Constraints

The total maximum filling station capacity for product *i* established in region *g* and time period *t* must be sufficient to cover the demand for that product:

$$D^{T}_{igt} \le \sum_{(f,p):(i,f,p)\in IFP} FCAP^{\max}_{fpi}\, NF_{fpigt} \quad \forall i \in I, g \in G, t \in T \tag{5.23}$$

The sum of the production rates of a product *i* through distributed scale plants located in region *g* must be equal to the total filling station capacity established in that region for distributed generation of that product:

$$\sum_{j:(i,j,p)\in IJP} P_{jpigt} = FCAP_{fpi}^{\max} NF_{fpigt} \qquad \begin{array}{c}\forall i \in I,\ p \in \{Distributed\},\\ f \in (i,f,p), g \in G, t \in T\end{array} \tag{5.24}$$

As new filling stations are established in a region *g* in time period *t*, they become available for the rest of the planning horizon:

$$NF_{fpigt} = NF_{fpig}^{0}\Big|_{t=1} + NF_{fpig,t-1}\Big|_{t>1} + IF_{fpigt} \quad \forall (i,f,p) \in IFP, g \in G,\ t \in T \tag{5.25}$$

where NF_{fpig}^{0} is the parameter that represents the initial number of filling stations located in region *g*.

e) Transportation Constraints

The total number of plants located in a region *g* in time period *t* is equal to the sum of the number of plants across plant types *j* and sizes *p* producing product types *i*:

$$NP_{gt}^{T} = \sum_{(i,j,p)\in IJP} NP_{jpigt} \quad \forall g \in G, t \in T \tag{5.26}$$

The total number of plants is also related to the binary variable U_{mgt} which represents the presence of *m-1* number of plants in region *g* in time period *t* as follows:

$$NP_{gt}^{T} = \sum_{m\in M} (m-1)\, U_{mgt} \ \forall g \in G, t \in T \tag{5.27}$$

Only one of the U_{mgt} binary variables can be non-zero for a region *g* and time period *t*:

$$\sum_{m\in M} U_{mgt} = 1 \quad \forall g \in G, t \in T \tag{5.28}$$

The local demand of product *i* met by *m-1* number of plants in a region *g* must be greater than or equal to the local demand if the binary U_{mgt} is active, otherwise must be forced to be zero:

$$DM_{imgt}^{L} \geq D_{igt}^{L} - W\left(1 - U_{mgt}\right) \quad \forall i \in I, m \in M, g \in G, t \in T \tag{5.29}$$

where *W* is a sufficiently large positive number.

f) CCS Constraints

The mass balance for captured CO_2 in a region *g* in time period *t* states that the incoming flows to a region *g* plus the captured amount must be equal to the outgoing

flows from that region plus the amount sent to the reservoir *r* (in the case of a collection point *g* connected to that reservoir) as follows:

$$\sum_{g' \in N_{gg'}} QC_{g'gt} + \sum_{(i,j,p) \in IJP} \gamma c_{jpit} P_{jpigt} = \sum_{g' \in N_{gg'}} QC_{gg't} + \sum_{r \in GR} \overline{QCR}_{grt} \quad \forall g \in G, t \in T \tag{5.30}$$

The CO_2 mass balance for a reservoir *r* in time period *t* states that the sum of the incoming CO_2 flows to that reservoir from the collection points (it is connected to) plus the CO_2 inventory from the previous time period must be equal to the inventory in that time period:

$$n_t \sum_{g \in GR} QCR_{grt} + RI_r^0\Big|_{t=1} + RI_{r,t-1}\Big|_{t>1} = RI_{rt} \qquad \forall r \in R, t \in T \tag{5.31}$$

where RI_r^0 is the parameter that represents the initial CO_2 inventory in reservoir *r*.

The CO_2 inventory of a reservoir *r* in a time period must not exceed the total capacity of that reservoir defined by $RCap_r$:

$$RI_{rt} \leq E_{rt}\, RCap_r \quad \forall r \in R,\ t \in T \tag{5.32}$$

If an onshore pipeline is established between regions *g* and *g'*, the diameter of that pipe is restricted with an upper bound as follows, otherwise it must be forced to be zero:

$$Dia_{gg't} \leq U\, Y_{gg't} \quad \forall (g,g') \in N_{gg'},\ t \in T \tag{5.33}$$

where *U* is simply an upper bound on the pipe diameter.

Once an onshore CO_2 pipeline is established between regions *g* and *g*' in a time period *t*, it becomes immediately available in the same time period:

$$AY_{gg't} = AY_{gg'}^0\Big|_{t=1} + AY_{gg',t-1}\Big|_{t>1} + Y_{gg't} \qquad \forall (g,g') \in N_{gg'},\ t \in T \tag{5.34}$$

where $AY_{gg't}$ is the binary variable that represents the availability of an onshore CO_2 pipeline between regions *g* and *g'* in time period *t*. $AY_{gg'}^0$ is the parameter that represents the initial availability of an onshore pipeline between regions *g* and *g'*.

A similar constraint is written for the pipe the onshore pipe diameter:

$$AD_{gg't} = AD_{gg'}^0\Big|_{t=1} + AD_{gg',t-1}\Big|_{t>1} + Dia_{gg't} \quad \forall (g,g') \in N_{gg'},\ t \in T \tag{5.35}$$

where $AD_{gg't}$ is the variable that represents the available diameter of an onshore pipe between regions *g* and *g'* in time period *t*. $AD_{gg'}^0$ is the parameter that represents the initial available onshore pipe diameter between regions *g* and *g'* (this constraint with the time index has been added for the pipeline diameter here as a "modelling trick" to calculate the capital cost of a pipeline defined in equation 5.4 when it is first built).

The CO_2 flow between regions *g* and *g'* through an onshore pipeline is linearly dependent on the diameter of that pipe given by (this is an assumption since te exact relationship is nonlinear):

$$QC_{gg't} \le \theta AY_{gg't} + \lambda D_{gg't} \quad \forall (g,g') \in N_{gg'}, t \in T \tag{5.36}$$

where θ and λ are the intercept and slope of the linear relationship between CO_2 flow in a pipe and its diameter, respectively.

Similar to constraint (5.32), if an offshore pipeline is established between collection point *g* and reservoir *r*, the diameter of that pipe is restricted with an upper bound as follows, otherwise it must be forced to be zero:

$$\overline{Dia}_{grt} \le U\, E_{rt} \quad \forall\, g \in G, r \in GR, t \in T \tag{5.37}$$

Once a reservoir *r* is activated in a time period *t*, it becomes available from that point in time till the end of the planning horizon:

$$AE_{rt} = AE_r^0\Big|_{t=1} + AE_{r,t-1}\Big|_{t>1} + E_{rt} \quad \forall r \in R,\, t \in T \tag{5.38}$$

where AE_{rt} is the binary variable that represents the activity of a reservoir *r* in time period *t*. AE_r^0 is the parameter that represents the initial activity (availability) of a reservoir *r*.

A similar constraint is written for the onshore pipe diameter:

$$\overline{ADR}_{grt} = \overline{ADR}_{gr}^0\Big|_{t=1} + \overline{ADR}_{gr,t-1}\Big|_{t>1} + \overline{Dia}_{grt} \quad \forall\, g \in G, r \in GR,\, t \in T \tag{5.39}$$

where $\overline{ADR}_{grt}$ is thevariable that represents the available diameter of an offshore pipe established between a collection point *g* and reservoir *r* in time period *t*. $\overline{ADR}_{gr}^0$ is the parameter that represents the initial available offshore pipe diameter between a collection point *g* and reservoir *r*.

The flowrate of CO_2 from a collection point *g* to a reservoir *r* through an onshore pipeline is linearly dependent on the diameter of the CO_2 pipe established between that collection point and reservoir:

$$\overline{QCR}_{grt} \le \theta\, AE_{rt} + \lambda\, \overline{Dia}_{grt} \quad \forall\, g \in G, r \in GR,\, t \in T \tag{5.40}$$

5.2.2 Hierarchical Solution Approach

Due to the high computational requirements, the model is solved using a hierarchical approach which consists of two steps, as illustrated in Figure 5.2. In the first step, the key integer variables: U_{mgt} (binary variable that represents establishment of *m-1*

production facilities in region g in time period t), NS_{spigt} (integer variable that represents the number of storage facilities of type s and size p located in region g in time period t) and NF_{fpigt} (integer variable that represents the number of filling stations of type f and size p located in region g in time period t), which have proven to have the highest impact on the computational time, are treated as continuous variables and the model is solved to extract decisions related to location, scale and technology of production plants in the last time period, defined through the variable: $NP_{jpig,T}$. After fixing this integer variable for the last time period, $t=T$, according to the solution from the step above, the reduced original MILP model (through reduced number of variables after fixing the value of the $NP_{jpig,T}$ variable) is solved for the optimal evolution of the supply chain network configuration through time. The optimality gap is set to 5% and to 1% for the first and second steps of the proposed hierarchical approach, respectively.

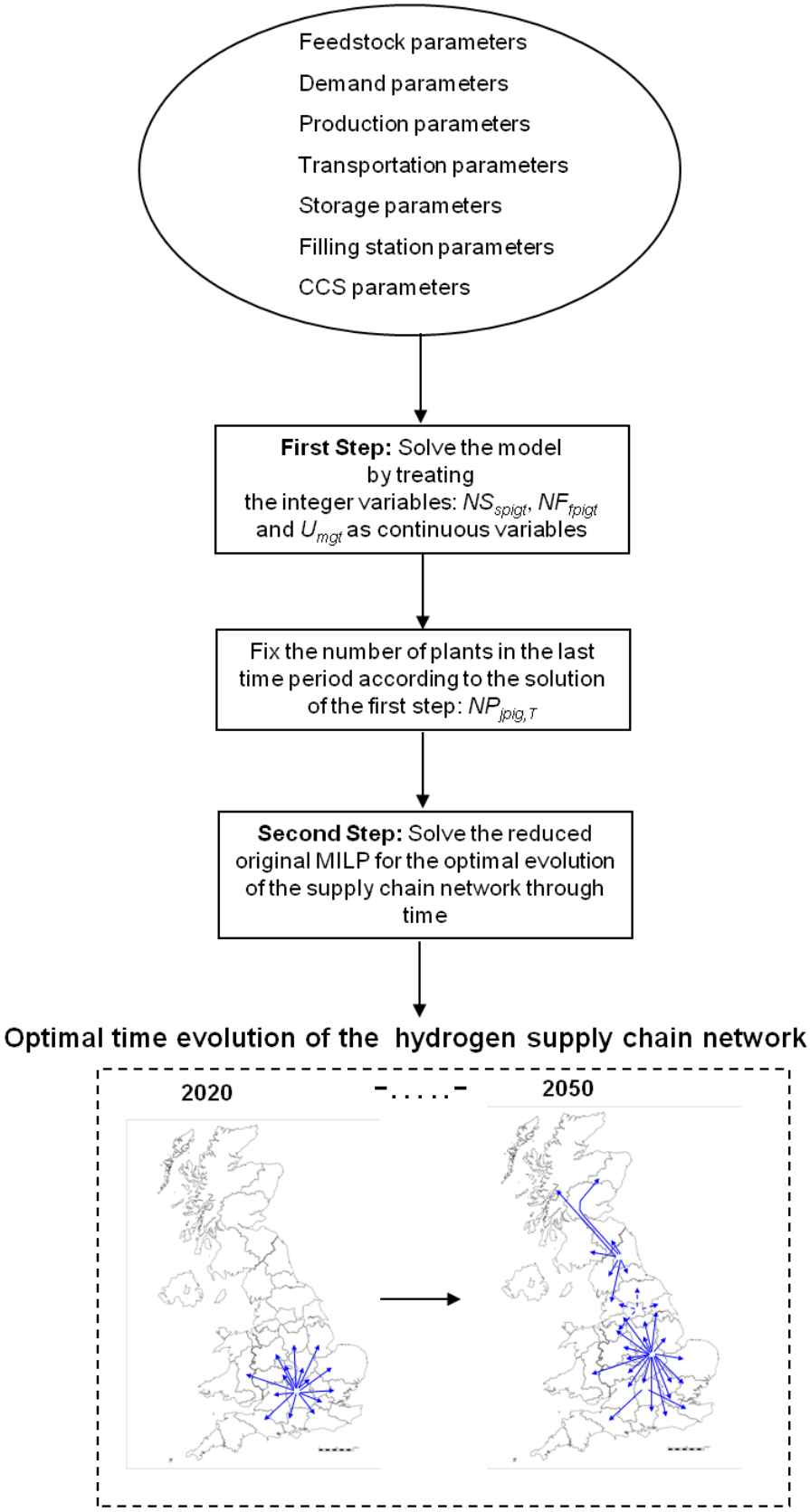

Figure 5.2 Illustration of the solution procedure through the proposed hierarchical approach.

5.3 Computational Results

The proposed spatially-explicit, multi-period hydrogen supply chain optimisation model has been applied to a case study of hydrogen production in the UK in the period from 2020 to 2050 where the modelling horizon is divided into 6 time horizons of each comprising five years.

The components of the proposed model are regions; physical forms of hydrogen, i.e. liquid (LH_2) and compressed form (GH_2); production and storage technologies allowing for different plant sizes; transportation modes to distribute hydrogen across regions; filling stations of different types and sizes; and finally CO_2 capture and infrastructure needed to dispose of it into the reservoirs. The remainder of this section briefly discusses each component of the system and explains how the relevant parameters have been obtained for the UK case study.

a) Regions

The regions in this study are based on the NUTS 2, a widespread taxonomy used by the Office for National Statistics and other governmental bodies. The list of the regions can be seen in Table E1 in Appendix E

b) Physical Forms of Hydrogen

The model presented in this chapter allows for simultaneous modelling of compressed gas (GH_2) and liquid form (LH_2) of hydrogen. LH_2 benefits from cheaper storage and transport but requires liquefaction, an expensive process both in term of capital and operational costs.

c) Production Technologies

Following a number of articles in the literature, for example the work of Almansoori and Shah (2009), four technologies for hydrogen production have been selected including steam methane reforming (SMR), coal gasification (CG), biomass gasification (BG) and electrolysis for this case study. Other production technologies including hydrogen from waste and biological hydrogen have not been included, as the implications are that the former may have only a relatively small role in the UK while the latter is at a relatively early technological stage implying considerable

uncertainty with regard to costs estimates. It is worth mentioning that different technologies which could be used in the production of electricity, in particular, wind and solar, are not considered explicitly, although they might be introduced in the developed model by having several prices for electricity, one for each technology used in the production factor. Although this would be a promising approach to take into account surplus electricity from intermitting sources which would not be used in the power system unless it can be stored by hydrogen or any other storage medium, this is not implemented in the current version of the proposed model. In the case of SMR, CG and BG the model incorporates plants with and without Carbon Capture and Sequestration (CCS). For each technology, both plants producing GH_2 and LH_2 are considered, with the obvious difference being a liquefaction plant added to the latter. Considering the additional technical component and electricity requirement, LH_2 implies higher capital costs and unit production cost than GH_2. In terms of size this article includes distributed, small, medium and large plants.

Values related to minimum and maximum production capacities of the plants are presented inTable E3 in Appendix E. The values of the capital costs in Table E2 for GH_2 are taken from NRC and NAE (2004) and NRC (2008) with the exception of the values for medium SMR and small BG which are taken from Iaquaniello *et al.* (2008) and Krewitt and Schmid (2005), respectively. The values for LH_2 comprise the capital of the production and of the liquefaction plant. Costs for liquefaction units are taken from Krewitt and Schmid (2005). All values have been scaled to the maximum capacity of each plant in Table E2 based on the size factors from NRC and NAE (2004). In terms of unit production cost (i.e. the sum of fuel and operating costs per unit production), the techno-economic analysis described in Appendix C of Almansoori (2006) has been implemented. The values in Almansoori (2006) have been updated to include the capital costs described above as well as primary sources prices which are more reflective of the current and expected future market conditions. Natural gas price used in the analysis is 1.9 p/kWh, i.e. the average price paid by UK interruptible consumers, i.e. the consumer paying the cheapest price, over the period 2008-2011 (DECC, 2012b). It must be noted that this implies a price of 8.2 $/million BTU against the 2.5 used in Almansoori (2006). The electricity price used in our computation is 5.4 p/kWh from Almansoori (2006) which implies

about 0.08 $/kWh against the 0.05 $/kWh assumed in DECC (2012b). Resulting unit production costs are shown in Table E4.

d) Transportation Modes

Two transportation modes are considered: trailers transporting GH_2 and tankers transporting LH_2. As one can see in Table E5 in Appendix E, tankers are almost twice as expensive as trailers although they are much cheaper per transported unit. Most of the parameters from Table E5 are taken from Almansoori and Shah (2009) with the exception of the price of the fuel used by trailers and tankers which is set at the dollar equivalent of 1.50 £ per litre, minimum flow rate which is set equal to the size of a single unit as described in Krewitt and Schmid (2005), and capital costs which were also sourced from Krewitt and Schmid (2005).

e) Storage Plants

Storage parameters have been sourced from the US H_2A database (Steward and Ramsden, 2008). As one can see in Table E6 in Appendix E storing GH_2 is considerably more expensive than storing LH_2, a factor which helps offset the cost of liquefaction needed to produce LH_2.

f) Filling Stations

Three types of filling stations are considered in the case study, namely stations receiving LH_2 by tanker, stations receiving GH_2 by trailer and finally stations with an on-site production plant. In all cases, hydrogen is retailed in GH_2 form for use in passenger vehicles. In the case of stations with on-site production plants we consider only large stations, while in the other two cases we consider small, medium and large stations, i.e. servicing a maximum of 72, 167 and 333 cars per day. As one can see Table E7 in Appendix E, stations receiving LH_2 are considerably pricier than stations receiving GH_2, due to the former requiring high pressure storage, LH_2 storage, evaporators and cryogenic compressors. Stations receiving hydrogen delivered by tube trailer are cheapest, as they are assumed not to require onsite storage (which is instead provided by the delivered hydrogen tubes, the cost of which is represented in the cost of tube trailers rather than in the fuelling station cost).

Stations with on-site production are more expensive due to the required onsite storage. Note that the cost of the hydrogen production technologies that must be installed adjacent to stations with on-site production is not included in the capital cost of the station, but rather in the cost of the production technologies shown in Table E2. The technical specification of the filling stations can be seen in Table E8.

g) CO_2 Emissions

CO_2 emissions from hydrogen production depend on the carbon content per MJ of the energy sources used in the production process; the efficiency of the plants - mainly sourced from NRC and NAE (2004); the electricity consumption of the plant; whether the hydrogen is produced in liquid or compressed gas form; and finally; whether CO_2 is being sequestered or not.

Table E9 in Appendix E shows the emission factors of electricity which were taken from the MARKAL scenario presented in Dodds and McDowall (2012). For each plant and technology type in this study, Figure E1 and Figure E2 display the amount of CO_2 emitted per kg of H_2. Figure E3 shows the amount of CO_2 sequestered per kg of H_2 in the plants fitted with CCS. In order to sequester CO_2, the developed model assumes that one has to build on-shore pipes from the plant up to the collection points and off-shore pipes from the collection points to the reservoirs. The capital cost of on-shore and off-shore CO_2 pipes was modelled through a linear relationship between cost per km and diameter of the pipelines which was obtained as an average of the two curves (high and low) for offshore and onshore pipes described in (IPCC, 2005). Collection points are on-shore locations near the reservoirs from where offshore pipelines reaching the reservoirs begin. Following DTI report on Industrial Carbon Dioxide Emissions and Carbon Dioxide Storage Potential in the UK (2006), this work takes into account three CO_2 reservoirs around the UK. Maximum capacity for each reservoir was sourced from (DECC, 2010b).

Table E10 shows the CO_2 reservoirs modelled in this study and the regions where collection points for each reservoir are located.

Finally, a tax on CO_2 emissions is introduced based on the results from the MARKAL runs presented in Dodds and McDowall (2012) . The level of the tax corresponds to the marginal abatement cost within a least-cost energy system transition that meets the UK‘s carbon reduction targets and is thus consistent with the carbon intensity of electricity, which is drawn from the same MARKAL scenario. This data is shown in Figure E4.

5.3.1 Total Demand for Hydrogen

In order to generate a plausible scenario of diffusion of hydrogen into the transport sector, a logistic diffusion model has been adopted (Rogers, 2003) and following the main view from the literature (i.e. Almansoori and Shah, 2009; Kim and Moon, 2008b), it is assumed that hydrogen vehicles can ultimately reach 100% of the stock. Following Agnolucci and McDowall (2013), a hydrogen demand scenario (namely the ‘high policy support, modest learning scenario‘ scenario from the HyWays (EC , 2008)) has been selected that does not postulate introduction of hydrogen unfolding at a quicker pace than those observed in historical analogies (A discussion of rates of transition for alternative fuelled vehicles can be seen in McDowall (forthcoming)).

As described in Agnolucci and McDowall (2013), an energy systems model, namely UK MARKAL, has been used to provide an indication as to when hydrogen might be introduced so that the transition is consistent with a broader analysis of cost-optimal decarbonisation trajectories. MARKAL inputs are taken from the scenario presented in Dodds and McDowall (2012), in which hydrogen fuel cell vehicles (FCVs) become cost-effective from 2040 onwards. As some consumers are likely to be less price-sensitive and eager to adopt new, innovative technologies beforehand, transitions predicted from energy system models like MARKAL are likely to be conservative (McDowall, forthcoming). As studies on the diffusion of innovations (Rogers, 2003) have suggested that around 2.5% of consumers are likely to act as ‘innovators‘, it has been assumed that a 2.5% market share (of such ‘innovators‘) can be reached in 2035 and a logistic curve is proposed with the parameter estimated from the aforementioned scenario in HyWays and passing through 2.5%

market share in 2035[1].

5.3.1.1 Spatial Distribution of Hydrogen Demand

A number of factors related to the technological specification of the vehicles and the socio-economic characteristics of the adopters are expected to be relevant in the adoption of FCVs (Ewing and Sarigollu, 2000). Among the attributes discussed in Melendez and Milbrandt (2006), access to cars, education, commuting distance and household income are considered. All of these attributes are expected to have a positive impact on the diffusion of FCVs. It is considered that the diffusion of FCVs will be facilitated by high population density, higher number of potential adopters which can be served by a given infrastructure and size of the population as it can be considered as a proxy for market size (Dunning, 1980).

Data to implement the socio-economic attributes above, which are represented in Table 5.1 below, were collected from the latest available UK Census[2]. Following Melendez and Milbrandt (2006), scores from 1 (most favourable to hydrogen) to 5 (least favourable to hydrogen) for each attribute used in the study were constructed (by using the ClassInt package in R) for each geographical area and combined into one single mark for each area by simple averaging. The results from the scoring exercise are shown in Table E1 in Appendix E and graphically in Figure 5.3. Hydrogen is expected to penetrate the passenger transport sector first in the South East of England and then develop along a corridor going from Manchester to London, including all the areas in between, with the exception of West Midlands. The third group of area in the hydrogen uptake includes Wales, some parts of Northern England and West Midlands. The next group of areas comprises large parts of Scotland, South Yorkshire in the North, Devon in the South West, and Northern Ireland. Finally, the last group of areas comprises the area at the very South West

[1] As this logistic implies over 50,000 vehicles in 2010, based on an UK vehicle fleet of 30 million vehicles (DFT, 2012), it has been assumed that 10,000 vehicles enter the market in 2020, and the number of FCVs grows linearly to 2035, at which point it reaches a 2.5% market share. From that point onward, logistic growth is assumed, until all passenger market is taken by hydrogen.

[2] Data can be found in Office of National Statistics for England and Wales, NISRA for Northern Ireland and SCROL for Scotland. As each attribute implies the use of three different variables defined in the Census, one for each group of countries comprised in the United Kingdom.

and North of the UK as well as those in the very north of England. It is interesting to notice that the score based on socio-economic factors also generates a scenario with spatial continuity in the diffusion of hydrogen although this was by no means guaranteed by the adopted approach.

Table 5.1 Socio-economic attributes thought to influence the adoption of hydrogen vehicles and related variables.

Attribute	**Variable**
Access to Cars	Percentage of households with two or more vehicles
Education	Percentage of population with higher level qualifications
Commuting Distance	Average commuting Distance per Person in miles
Household Income	Gross Disposable Household Income per head at 2001 basic
Population	Prices
Population density	Number of persons

Information from the ranking above is used to assign a set of 5 logistics to the geographical areas described above. Hydrogen is introduced in the most promising areas in 2020 and in the least promising ones 10 years later. Based on the typically faster rate of diffusion in late adopting regions (Grubler *et al.*, 1999), catching up occurs through a higher growth rate in the logistics for the area where hydrogen is introduced at a later stage. In order to compute hydrogen demand, million passenger kilometres have been estimated for each area by allocating traffic figures from DFT (2012) and DRDNI (2009) for Great Britain and Northern Ireland, respectively, on the basis of data on commuting distance. Given the traffic figures for each area, the logistics have been applied to identify the passenger kilometres travelled by using hydrogen from which hydrogen demand has been computed by using efficiency for FCVs from McDowall and Dodds (2012). The result of this procedure is shown in Figure 5.4.

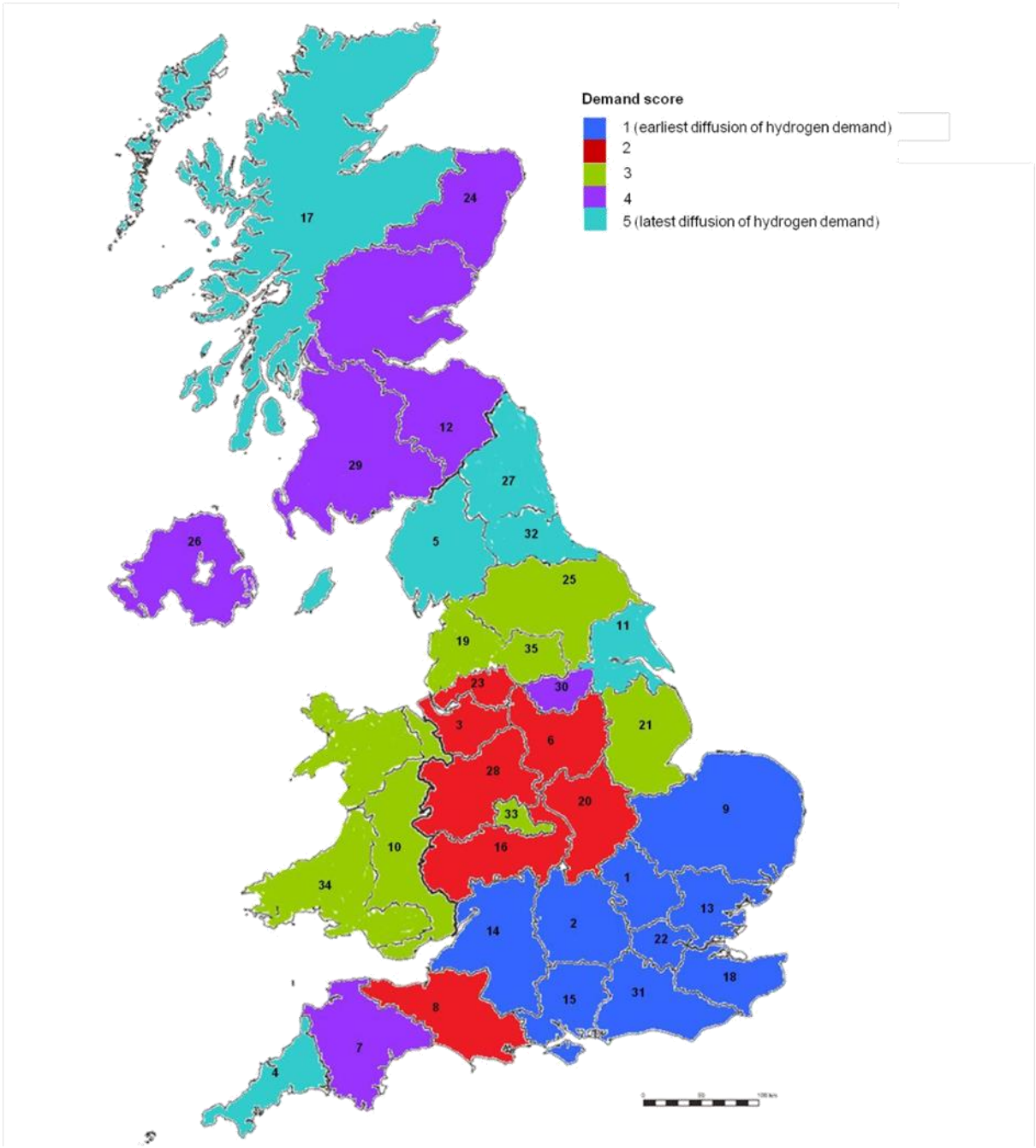

Figure 5.3 Geographical areas considered in this study. Shading indicates the demand score, while the numbers provide a key to region names, provided in Table E1.

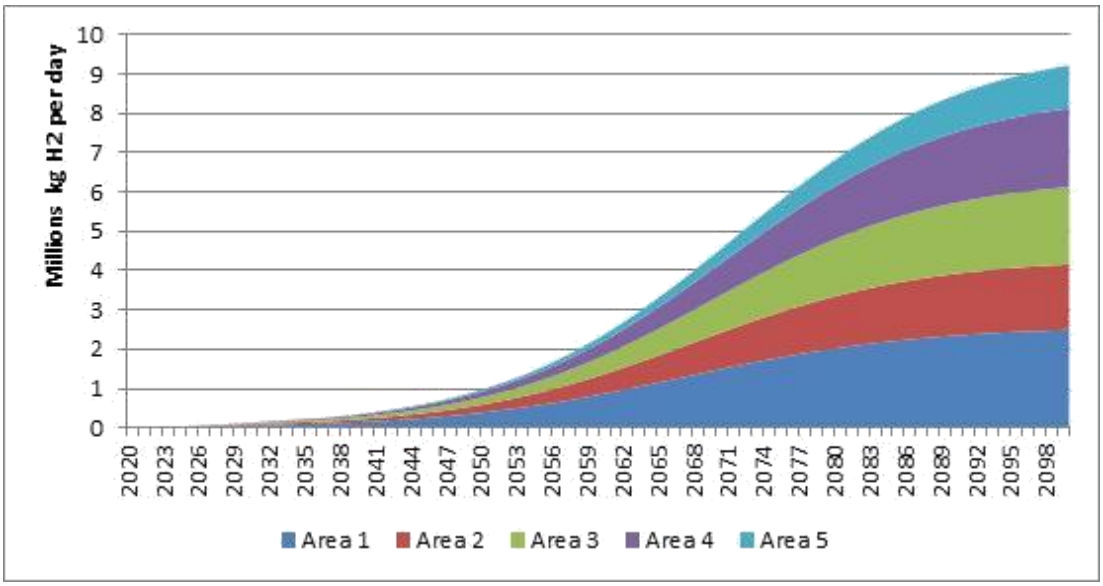

Figure 5.4 Daily demand for hydrogen split according to order of areas penetrated by hydrogen.

5.3.2 Description of Scenarios

A number of scenarios have been developed using the proposed model to test the implications of major uncertainties in the development of a hydrogen transportation system. The baseline scenario uses the hydrogen fuel demand projections, resource costs and technology characteristics outlined in the previous sections. In addition to the base case, four alternative scenarios described in Table 5.2 have been generated to examine uncertainty related to hydrogen demand characteristics and evolution, and technology and resource availability. The main driving factor to introduce hydrogen as transportation fuel is to enable its decarbonisation. In order to reach decarbonisation, hydrogen may be produced by wind and solar plants, both of them requiring electrolysis. The fact that this production technology is never selected by the model implies that renewable electricity will be cost-competitive only if power from wind and solar plants is cheaper than the power price used in this study. This may well be the case for wind from particular good locations or surplus renewable electricity which cannot find any other use in the system. Renewable electricity will generally be more competitive in the future due to technological learning, economies of scales and increased carbon price. As an extension of the current work , it would be particularly interesting to assess the electricity price at which electrolysis would be selected by the model and discuss the implications in terms of the cost of renewable electricity.

Table 5.2 Scenarios discussed in this study and their characteristics.

Scenario	Scenario characteristics	Reason for inclusion
Base case	The base case scenario is using the technologies and demand characteristics as described in Section 5.3.1	A base case against which other scenarios can be compared
Diffuse demand	Total demand for hydrogen is the same as the base case, but in this scenario it is equally apportioned to each region, based on population.	Assessing the impact of geographical dispersion of demand on the optimal configuration of the system
Clustered demand	Total demand for hydrogen is the same as the base case, but demand is spatially clustered on 'leading' regions, i.e. the four major urban regions: London, the West Midlands, Southwest Scotland, and Manchester-Merseyside. Demand outside of these regions is built up later and more slowly.	Assessing the impact of geographical dispersion of demand on the optimal configuration of the system
High demand	Demand is increased five-fold, but with the same spatial distribution as the base case. This results in a demand trajectory within the range of those discussed in the literature, but with a much faster rate of deployment than in the baseline.	Assessing the impact of the level of demand on the optimal configuration of the system
No biomass	Same as the base case, but with no biomass available for H_2 production	Assessing the optimal configuration of the system in the case of biomass not being available – included because of the observed importance of hydrogen production from biomass in model runs

5.3.3 Discussion of Results

This section presents the main messages extracted from the model results for the scenarios introduced in the previous section.

5.3.3.1 The Base Case: Production and Costs of Hydrogen

Hydrogen production in the base case is dominated by SMR with CCS and medium-sized biomass gasification plants as presented in Figure 5.5. A marginal role is

played by distributed and small SMR plant without CCS. No hydrogen is produced via electrolysis or from coal with CCS. The early phases are dominated by medium-sized biomass gasification plants although a number of distributed SMR plants are also built. In 2035, demand has risen sufficiently to support a large SMR plant with CCS. As demand grows and the model is able to benefit from scale economies arising from larger production facilities, undiscounted costs per unit hydrogen fall over time.

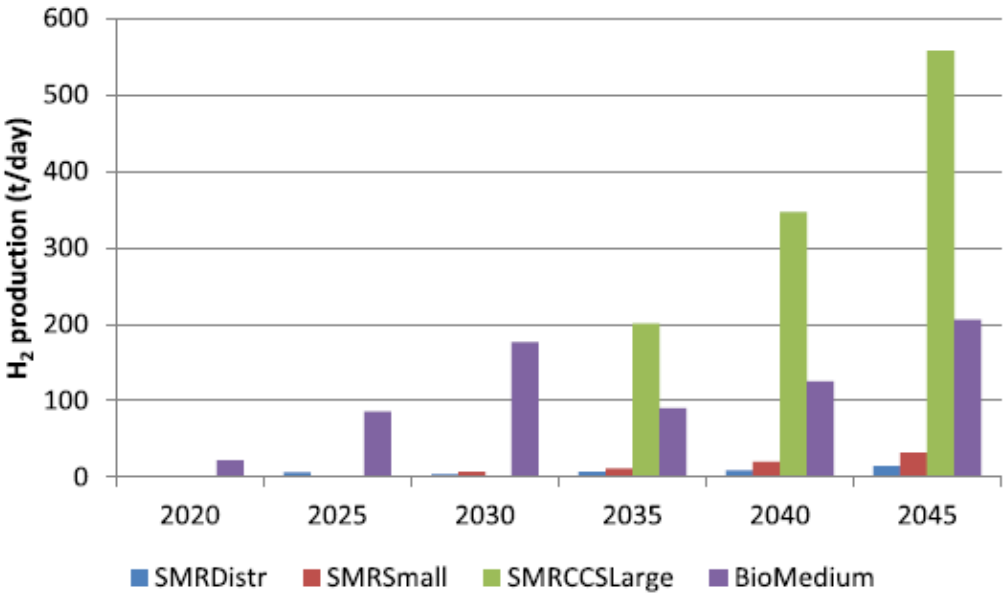

Figure 5.5 Hydrogen production in the base case scenario.

5.3.3.2 Patterns Across Space: The Trade-off Between Production Scale and Transport Costs

The spatial pattern of hydrogen demand results in trade-offs between production and transportation costs with larger plants producing hydrogen at a lower cost but incurring higher transportation costs. Faced with this trade-off, the model shows a tendency for large production facilities located in central regions in or close to regions with high demand, where they are able to service a considerable demand within relatively short distances. Small and distributed production facilities are established in peripheral regions where transport costs become prohibitive. This is clearly illustrated in the base case as can be seen in Figure 5.6 although the overall patterns of hydrogen production are similar in most scenarios with the exception of the high demand scenario where the majority of hydrogen is produced from medium-sized bio-hydrogen plants which are more cost-effective than large plants due to the

very small distribution area they need to cover due to the relatively high demand in this scenario.

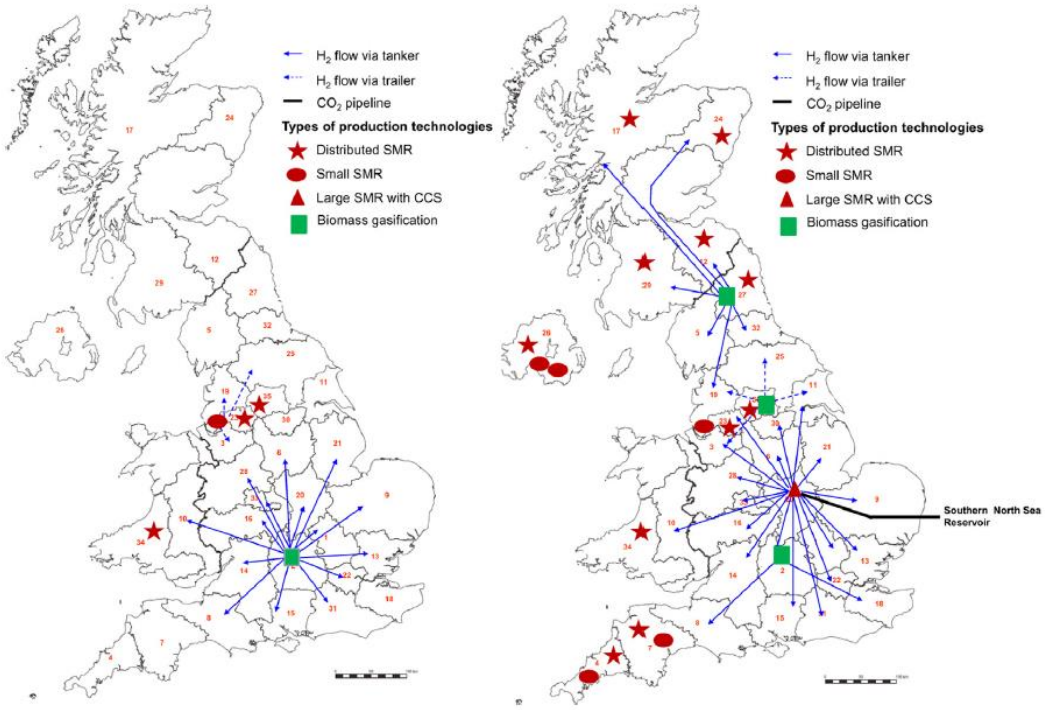

Figure 5.6 Evolution of supply in the base case scenario (first and last model period).

Examining hydrogen flows between regions as a proportion of total hydrogen production as represented by Figure 5.7 shows that most hydrogen is not produced locally but delivered to the region by tanker or trailer. The exception is the 'clustered demand' scenario, which sees no trucked hydrogen in the first period, because production facilities are located in the regions where hydrogen is first deployed, i.e. regions containing the UK's largest urban centres. The importance of distribution grows over time in this scenario, like in many of the other scenarios, with the exception of the high demand scenario where medium-sized local plants become cost-effective leading to a declining share of trucked hydrogen as time goes by.

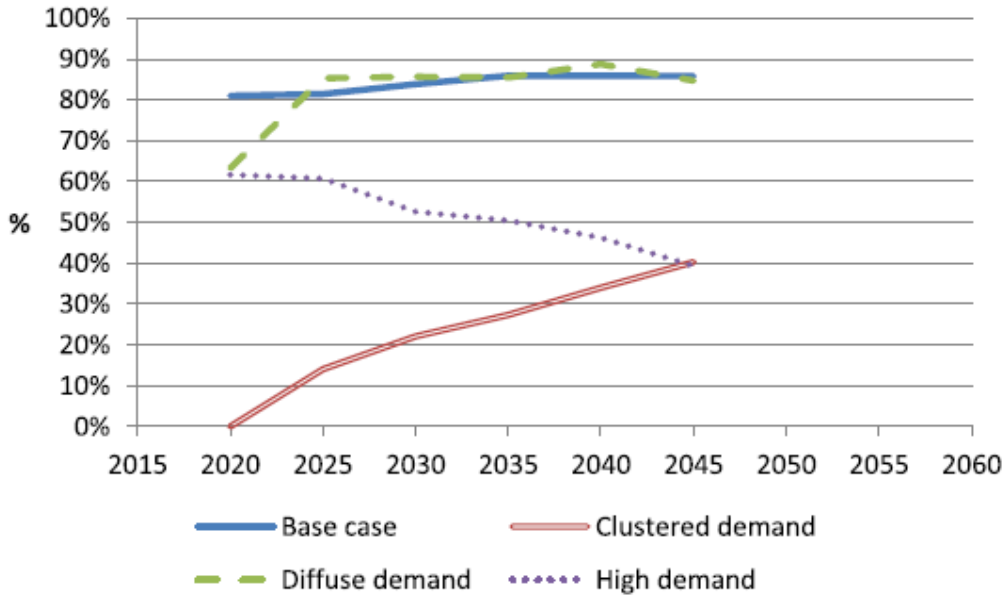

Figure 5.7 Proportion of production that is transported between regions (%) rather than produced locally, in different scenarios.

The importance of transportation - and in particular transportation costs - is also clear from an examination of the hydrogen form, LH_2 and GH_2, chosen by the model. As most scenarios are dominated by LH_2 produced in large centralised plants, the additional transportation costs of GH_2 are clearly more important than the additional liquefaction costs, with the exception of peripheral regions such as Northern Ireland and Cornwall, where small quantities of GH_2 are produced in distributed plants. Two scenarios present revealing exceptions to this overall trend. In the high demand scenario there is sufficient demand in a number of regions to support medium-sized biomass gasification plant. As imports decrease as time goes by, the model prefers to build cheaper GH_2 production plants rather than LH_2. In the clustered demand scenario, relatively cheaper GH_2 production plants are built to satisfy demand in the major demand centres. However, demand in late-comer regions is met either by local production from small distributed SMR plants, or from two LH_2 plants, one built in the North of England, another in South-central England.

The spatial pattern of demand across regions has also a strong effect on costs, as illustrated in Figure 5.8. The total discounted costs of hydrogen supply are 10% higher in the diffuse scenario compared with the clustered one. This cost differential is particularly large in the early periods, with the costs per kg of hydrogen in the diffuse scenario 25% greater than in the clustered scenario.

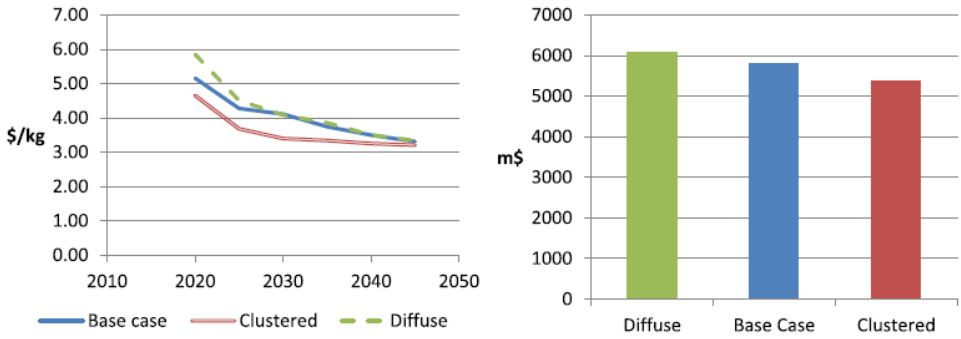

Figure 5.8 Undiscounted costs of delivered hydrogen over time in different scenarios (left) and total discounted costs across the model time horizon (right).

As a result of the trade-off between production costs and transport costs, the low level of demand and its spatial dispersion, the model leaves significant production capacity unused in all scenarios. This result is driven by scale economies associated with larger plants and the costs associated with transporting hydrogen from one region to another which prevents the model from simply building a single large plant, and using it to maximum capacity by exporting hydrogen to all the other regions. Due to the large difference between minimum and maximum production capacity, large plants may become cost effective compared to smaller plants despite leaving a considerable amount of capacity unused. As can be seen in Figure 5.9, this results in a pattern by which spare capacity falls as demand grows until a threshold is crossed for an additional investment in a large new plant, which increases the space capacity.

This high level of spare capacity is a logical feature of a system that is required to meet low and spatially diffused demands that are characteristic of the early stages of an infrastructure transition. This point tends to be well-known by those investigating the deployment of hydrogen refuelling technologies, but is often not well represented in systems models, such as the MARKAL/TIMES family of models, that lack detailed spatial disaggregation and integer variable representing investments.

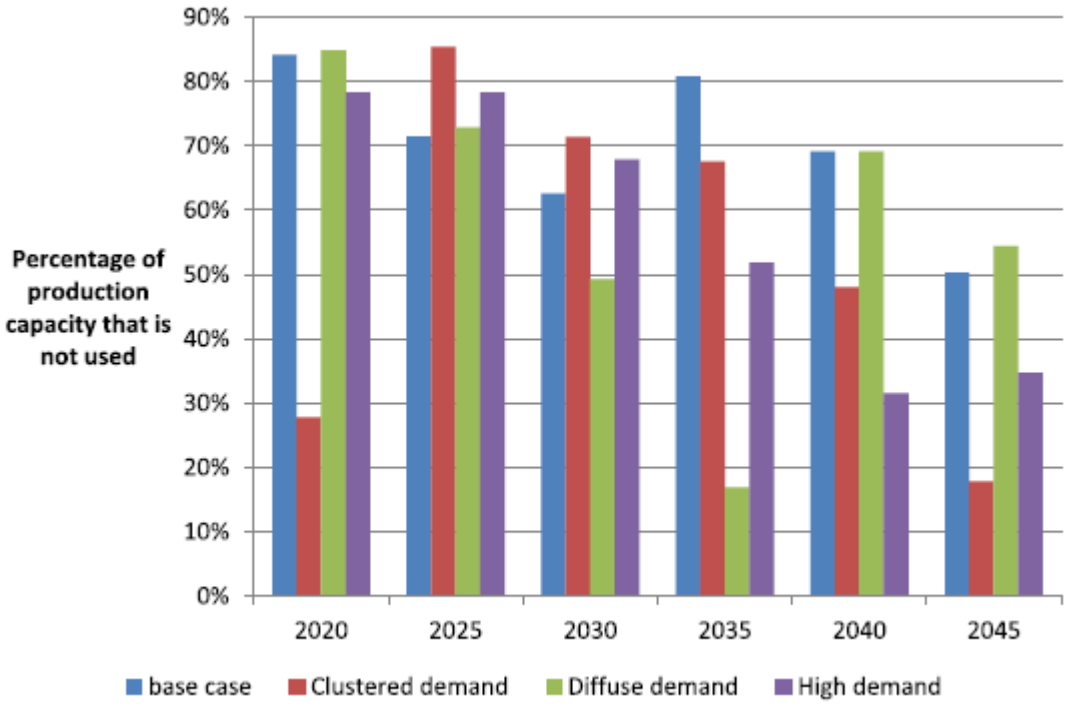

Figure 5.9 Spare capacity as a proportion of total capacity.

5.3.3.3 Technological Uncertainties: Roles of Bioenergy and CCS

The 'no biomass' scenario results in a complete reliance on natural gas for hydrogen production, with SMR plants of various sizes built across the country. In this scenario, the model introduces CCS much earlier than in other scenarios, and at a smaller scale, building two medium-sized SMR-CCS plants by 2025, as well as a single large SMR-CCS plant later on. This is unsurprising, as unabated small and medium SMR plants would incur excessive carbon costs, and electrolysis still incurs relatively high carbon costs until the grid has decarbonised from around 2030. In terms of the evolution of CCS plant and pipeline capacity, as can be seen in Figure 5.10, an initial medium SMR-CCS plant is built between major centres Birmingham and London in 2020, with a pipeline taking CO_2 to the reservoir in the southern North Sea. In 2025, an additional medium SMR-CCS plant is constructed in Lancashire. By 2035, sufficient additional demand has developed to justify a third, and now large SMR-CCS plant in central England. This additional plant makes use of the existing CO_2 pipeline capacity, and is constructed on the route of the pipeline to the southern North Sea reservoir.

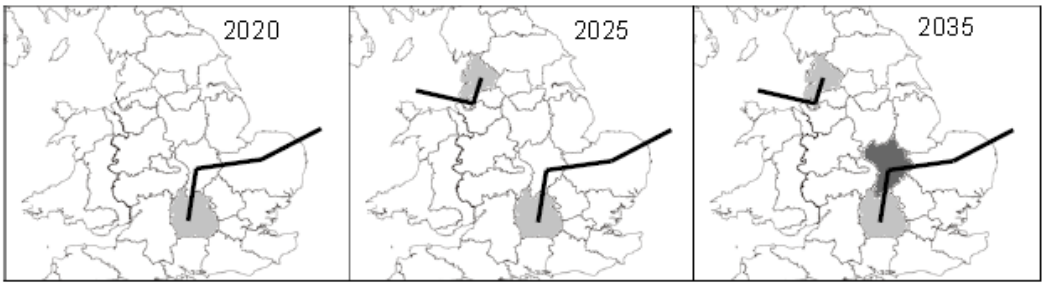

Figure 5.10 Evolution of the CCS network in the 'no biomass' scenario over the 2020-2035 time period. Black lines represent pipelines. Light shaded regions contain a medium-sized SMR-CCS plant. The dark-shaded region contains a large SMR-CCS plant.

5.4 Concluding Remarks

This chapter has presented an optimisation-based framework for the optimal design of hydrogen supply chains and CCS pipeline networks over a long planning horizon. The overall problem has been formulated as a multi-period, mixed integer linear programming model, while a hierarchical procedure has been proposed for tackling efficiently the resulting large-scale optimisation problems. A number of conclusions are drawn below.

First, despite some articles in the literature emphasising the potential for hydrogen to facilitate a decentralised energy system, the proposed model shows a tendency for large production facilities. Small and distributed production facilities are established only in peripheral regions where transport costs become prohibitive. The trade-off between production and transportation costs is an important factor determining the preference for large plants, the consequent high levels of H_2 imported into most regions and the preference for liquid hydrogen, as its lower transportation costs more than compensate the costs of liquefaction.

Secondly, the results show that varying the level and the spatial pattern of demand has significant impacts on both the optimal supply system and on the overall costs of delivered hydrogen. These are important implications because demand assumptions - particularly the spatial pattern of demand- tend to be downplayed in the literature, despite having clear implications for transition strategies of hydrogen in the

passenger vehicle sector. Highly-clustered demand which is rather cheaper to service than highly diffused demand shifts the preference of the model to gaseous hydrogen rather than liquid hydrogen, due the lower importance of transport costs caused by shorter length of the average haul. Depending on the number of clusters and their relative size, medium-sized production plants can become more cost-effective than large plants because of the decreased need for transportation. Similarly, a high level of demand makes medium-sized production become cost-effective and hydrogen tends to be produced in gaseous form because of the relatively small catchment areas for each plant.

6 Conclusions and Future Work

This thesis has addressed several problems related to bioenergy supply chains-focussing mainly on the biofuels industry, including optimal strategic design of bioenergy supply chains (taking into account spatially-explicit characteristics) based on single and multi-objective with static and multi-period design utilising deterministic optimisation as well as optimisation under uncertainty, to fill the gap in the literature work.The main novel contributions of this thesis to the existing literature are:

- Development of a "neighbourhood flow" modelling approach which has proven to offer significant computational efficiency when compared to similar models in literature;
- Investigation of potential implications of biofuel production in the UK as a case study which has not been considered by the existing literature in such a detailed fashion including the use of dedicated energy crops, their cultivation on set-aside land as well as sustainability issues associated with land use and first generation biomass crops and their by-products;
- Consideration of the emerging concept of bioenergy with CCS (BECCS) systems within a supply chain optimisation framework which has not been studied by existing literature;
- Development of a novel "modified neighbourhood flow" modelling approach and two-stage hierarchical solution procedure for the developed hydrogen supply chain optimisation model which also includes some novel aspects such as CCS constraints.

In this chapter, we aim to conclude the work presented in this thesis and provide the potential research directions for the future work.

6.1 Concluding Remarks

In this thesis, mixed integer programming (mainly MILP) based models and solution approaches have been proposed for several bioenergy supply chain optimisation problems in the process industry.

In Chapter 1, a general introduction has been given related to global climate change

and global energy trends first and then focussing on bioenergy and biofuels and finally providing background information on modelling of energy systems, supply chain optimisation as well as mathematical programming approaches used in supply chain optimsation.

In Chapter 2, a detailed literature review has been presented related to bioenergy supply chain optimisation including biofuel and bioelectricity supply chains. A section on hydrogen supply chain optimisation has also been provided.

In Chapter 3, the optimisation-based approaches developed for the optimal strategic design of biofuel supply chains have been presented. This chapter is divided into two main sections where the static approaches are presented in Section 3.1 and the multi-period approaches are presented in Section 3.2.

In Section 3.1.1, a static, spatially-explicit MILP modelling framework has been developed first with the objective to minimise the overall cost of a biofuel supply chain and taking into account first generation biofuel production. A 'neighbourhood flow' approach has also been proposed to increase the computational efficiency for the solution of the optimisation problem and this approach has proven to provide significant computational savings when compared to similar models in literature. The developed model has been applied to a case study of bioethanol production from corn in Northern Italy under two different demand scenarios for 2011 and 2020 based on the EU biofuel targets. The model results provide insight into the optimal network configurations of the future Italian bioethanol supply chain. In Section 3.1.2, the developed static model is then further developed to account for bioethanol production using hybrid (or advanced) systems where first and second generation technologies are integrated. The model has been applied to a case study of bioethanol production in the UK using wheat as first generation and wheat straw and two dedicated energy crops including miscanthus and SRC as potential biomass feedstock. The results of the case study imply that that the use of second generation technologies could potentially reduce the dependency on biomass imports and hence, contribute to security of supply. In Section 3.1.3, the developed single-objective modelling framework is further extended to a multi-objective framework that aims to minimise the total cost and total environmental impact of a biofuel supply chain

simultaneously. The total environmental impact is evaluated by calculating the total carbon footprint using GWP impact factors. The multi-objective model is solved using ε-constraint method where one of the objectives is treated as a constraint. The applicability of multi-objective MILP model has been highlighted with the UK bioethanol production case study where the trade-off between the two conflicting objectives is presented as a pareto curve. The results imply that use of second generation crops could reduce the total emissions resulting from the whole supply chain and therefore, help meet the GHG emission reduction targets.

In section 3.2, the static MILP model is developed further into a multi-period modelling framework first to account for temporal effects such as change of bioethanol demand with time. The developed multi-period model has been applied to a case study of bioethanol production in the UK in the period 2012-2020 where the modelling horizon is divided into three time periods with each consisting of three years.The concept of decrease in production costs through technological learning has also been investigated. The computational results have shown that significant cost reductions can be observed in future bioethanol production due to technological learning through increasing total cumulative production with time. This could contribute to deployment of second generation technologies to a larger extent. Finally in Section 3.2.2, a stochastic modelling framework has been proposed taking the deterministic multi-period model as basis to account for uncertainty in different supply chain aspects such as biomass supply. The developed model aims to maximise the net present value of a biofuel supply chain while controlling the overall level of financial risk simultaneously. The same case study as in Section 3.2.1 has been considered taking into account uncertainty in biomass availability, biomass imports, bioethanol sales and import prices. The results have indicated that the presence of financial risk constraints results in a reduction in the overall financial risk at the expense of reducing the expected net present value. In addition, it has been observed that biomass and bioethanol imports meet a significant portion of the total ethanol production in most of the cases.

Chapter 4 presents a static multi-objective MINLP model for the optimal design of a bioelectricity supply chain which has been developed based on the mathematical programming approaches in Chapter 3. The developed model considers electricity

generation through co-firing of biomass and fossil fuels in conjunction with CO_2 capture and storage (CCS)- so called 'bio-Energy with CCS' (BECCS) systems. The model has been applied to a case study of electricity generation in the UK to examine the potential for existing power generation assets to act as a carbon sink as opposed to a carbon source. Via a Pareto front analysis, we examine the technical and economic compromises implicit in transitioning from a dedicated fossil fuel only to a carbon negative electricity generation network. The results imply that coal and carbon prices as well as biomass availability are the key factors for decarbonisation of the power sector.

Finally in Chapter 5, a spatially-explicit multi-period MILP model has been developed for the optimal design of a hydrogen supply chain where biomass is considered as one of the potential feedstock types and capture and storage of the emitted carbon from hydrogen production is also considered. A hierarchical solution approach has been developed to increase the computational efficiency for the solution of the resulting large-scale problem. The model has been applied to a case study of hydrogen production in the UK from 2020 to 2050 where the modeling horizon is divided into six time periods with each consisting of five years. Seven different technologies has been considered in total including steam methane reforming, steam methane reforming with CCS, coal gasification, coal gasification with CCS, biomass gasification, biomass gasification with CCS and electrolysis. The results imply that varying the level and the spatial pattern of hydrogen demand could have significant impact on both the optimal supply chain configuration as well as the total cost of delivered hydrogen.

From the work presented in this thesis, the mathematical programming techniques, mainly MILP optimisation techniques, can be widely applied to the bioenergy supply chain optimisation problems. The proposed MILP approaches have successfully dealt with the supply chain problems discussed in this thesis. The work in this thesis, which not only has developed some novel approaches to literature problems, but also considered some problems that have not been investigated before, is a complement to the literature research work on the bioenergy supply chains. A number of publications have arisen from the work presented in this thesis which can be seen in Appendix F.

6.2 Future Work

The work in this thesis has covered a number of problems in the field of bioenergy supply chains, and there are still several research directions that could be deployed for future work as the extension of the current study.

Regarding the MILP models developed for the optimal design of biofuel supply chains, possible future directions could include:

İn the short term:

- Incorporating additional biomass supply chain aspects such as seasonal change in biomass yields and harvest as well as material loss during drying and storage.

In the long term:

- Further extension of the two-stage stochastic, multi-period model, to consider endogenous uncertainty as well as exogenous uncertainty which is currently considered. In this sense, endogenous uncertainty would imply that optimal investment decisions in a time period would be dependent on the optimal production and investment decisions taken in the previous time periods. This would mean a multi-stage stochastic modelling framework would be required.

As potential future work regarding the bioelectriciy supply chain optimisation model,possible directions could include:

In the short term:

- Developing the model further to capture changes in electricity demand and generation throughout a given time frame as well as change in commmodity prices;
- Incorporation of other potential low-carbon technologies such as oxyfuel combustion..

Finally, regarding the spatial multi-period hydrogen infrastructure planning MILP model,

In the short term:

- Improving the model to consider pipelines to deliver hydrogen;
- Utilising an LCA analysis to evaluate the degree of decarbonisation that can be achieved by promoting hydrogen as a transport fuel.

In the long term:

- Linking the proposed model with an energy system model in order to systematically assess the effect of different level of hydrogen demands resulting from an optimised energy system on the infrastructure required to meet that demand;
- Incorporation of uncertainty..

Appendix A Optimisation of Biofuel Supply Chains

A.1 Summary of Zamboni Et Al. (2009a) Model

The mathematical formulation for the bioethanol supply chain optimisation model introduced by Zamboni *et al.* (2009a) is summarised below. The symbols used for indices, sets and parameters are the same as those introduced in Section 3.1.1.

Nomenclature

Parameters

$TPot$	Total potential domestic biomass production rate (t d^{-1})

Binary Variables

$X_{igg'l}$	1 if product i is to be shipped via mode l from region g to region g'
Y_{pg}	1 if a biofuel production plant of size p is to be established in region g

Integer Variables

$NTU_{igg'l}$	Number of transport units of mode l to transfer product i between regions g and g'
$NTUI_g$	Number of transfer units for local biomass transfer within region g

Continuous Variables

D^L_{ig}	Local demand for product i in region g (t d^{-1})
D^i_{ig}	Imported demand for product i in region g (t d^{-1})
D^T_{ig}	Total demand for product i in region g (t d^{-1})
FCC	Total capital costs of facilities (€)
PC	Total production cost (€ d^{-1})
Pf_{pg}	Biofuel production rate of a plant of size p located in region g (t d^{-1})
P^T_{ig}	Production rate of product i in region g (t d^{-1})
$Q_{igg'l}$	Flow rate of product i via mode l from region g to g' (t d^{-1})
TC	Total transportation cost (€ d^{-1})
TDC	Total daily cost for the biofuel supply chain network (€ d^{-1})
TD_i	Total demand for product i (t d^{-1})
TP_i	Total production rate of product i (t d^{-1})

$$Min\ TDC = \sum_{p,g} PCC_p Y_{pg} \times (CCF/\alpha) + \sum_{g} \left(UPCb_g P^T{}_{biomass,g} + \sum_{p} UPCf_p Pf_{pg} \right) + \sum_{i,l} \left(UTC_{il} TCap_{il} ADD_{gg'l} NTU_{igg'l} \right) + UTC^* \sum_{g} TCap^* ALD_g NTUI_g \quad (A.1)$$

Subject to:

Demand Constraints:

$$D^T{}_{ig} = D^L{}_{ig} + D^I{}_{ig} \quad \forall i \in I, g \in G \quad (A.2)$$

$$D^L{}_{ig} \le P^T{}_{ig} \quad \forall i \in I, g \in G \quad (A.3)$$

$$D^I{}_{ig} \le \sum_{l,g'} Q_{ig'gl} \quad \forall i \in I, g \in G \quad (A.4)$$

$$P^T{}_{biofuel,g} = \gamma D^T{}_{biomass,g} \quad \forall g \in G \quad (A.5)$$

$$TP_i \ge TD_i \quad \forall i \in I \quad (A.6)$$

$$TD_i = \sum_{g} D^T{}_{ig} \quad \forall i \in I \quad (A.7)$$

$$TP_i = \sum_{g} P^T{}_{ig} \quad \forall i \in I \quad (A.8)$$

Production Constraints:

$$P^T{}_{ig} = D^T{}_{ig} + \sum_{l,g'} \left(Q_{igg'l} - Q_{ig'gl} \right) \quad \forall i \in I, g \in G \quad (A.9)$$

$$P^T{}_{biofuel,g} = \sum_{p} Pf_{pg} \quad \forall g \in G \quad (A.10)$$

$$PCap_p^{\min} Y_{pg} \le Pf_{pg} \le PCap_p^{\max} Y_{pg} \quad \forall p \in P, g \in G \quad (A.11)$$

$$\sum_{p} Y_{pg} \le 1 \quad \forall g \in G \quad (A.12)$$

$$GS_g CY_g AD_g BCD_g^{\min} \le P^T{}_{biomass,g} \le GS_g CY_g AD_g BCD_g^{\max} \quad \forall g \in G \quad (A.13)$$

$$TP_{biomass} \le SusF\ TPot \quad (A.14)$$

$$TPot = \sum_{g \in G} GS_g CY_g AD_g BCD_g^{\max} \quad (A.15)$$

Transportation Constraints:

$$NTU_{igg'l} \ge \frac{Q_{igg'l}}{TCap_{il}} \quad \forall i \in I, g, g' \in G, l \in L \quad (A.16)$$

$$NTUI_g \geq \frac{P_{biomass,g}}{TCap^*} \quad \forall g \in G \tag{A.17}$$

$$Q_{il}^{\min} X_{igg'l} \leq Q_{igg'l} \leq Q_{il}^{\max} X_{igg'l} \quad \forall i \in I, g, g' \in G, l \in L \tag{A.18}$$

$$\sum_l X_{igg'l} + \sum_l X_{ig'gl} \leq 1 \qquad \forall i \in I, g, g' \in G \tag{A.19}$$

$$\sum_i \sum_l X_{iggl} = 0 \qquad \forall g \in G \tag{A.20}$$

$$\sum_{i,g,g',l \notin Total_{igg'l}} X_{igg'l} = 0 \tag{A.21}$$

A.2 Bioethanol Demand

The biofuel targets are converted to mass fraction for the gasoline-bioethanol fuel mixture using the following formula:

$$X^e_{bioethanol} = \frac{LHV_{bioethanol} X^m_{bioethanol}}{LHV_{bioethanol} X^m_{bioethanol} + LHV_{gasoline} X^m_{gasoline}} \tag{A.22}$$

where X^e and X^m represent the fraction of a component in the transport fuel mix on the basis of energy and mass contents, respectively whereas *LHV* is the lower heating value of each component. The lower heating values for ethanol and gasoline are 26,952 MJ t^{-1} and 43,448 MJ t^{-1}, respectively (Hydrogen Analysis Resource Center, 2008).

A.3 Biomass Cultivation Parameters

The input data for biomass cultivation is given in Table A1-Table A5 including the following parameters specific to each region respectively: cultivation yield (CY_g), maximum cultivation density (BCD_g^{max}), surface area (GS_g), biomass production cost (UCC_g) and arable land density (AD_g). The value of the sustainability factor, SusF has been set to 15% as taken from the work of Zamboni *et al.* (2009a) where more detailed information can be found.

Table A1 Cultivation yield in each cell of Northern Italy.

Region (*g*)	CY_g (t d^{-1} km^{-2})	Region (*g*)	CY_g (t d^{-1} km^{-2})
1	1.9	31	3.0
2	1.9	32	2.7
3	1.9	33	2.9
4	2.0	34	2.4

5	2.2	35	3.1
6	2.3	36	2.3
7	2.2	37	1.7
8	1.2	38	2.6
9	1.4	39	3.2
10	2.1	40	3.1
11	2.9	41	2.9
12	2.9	42	2.4
13	1.8	43	2.4
14	2.1	44	2.3
15	2.5	45	2.0
16	2.4	46	1.8
17	4.0	47	2.2
18	2.8	48	2.9
19	1.4	49	2.9
20	2.5	50	2.7
21	2.5	51	2.3
22	2.9	52	2.2
23	2.7	53	0.0
24	3.4	54	0.5
25	3.0	55	1.8
26	2.7	56	2.8
27	3.1	57	2.5
28	3.7	58	2
29	3.3	59	2
30	2.6	60	3

Table A2 Maximum cultivation density in each cell of Northern Italy.

Region (*g*)	BCD_g^{max} **(km^2 km^{-2})***	**Region (*g*)**	BCD_g^{max} **(km^2 km^{-2})***
1	0.00	31	0.44
2	0.00	32	0.50
3	0.00	33	0.54
4	0.00	34	0.00
5	0.05	35	0.22
6	0.00	36	0.23
7	0.07	37	0.23
8	0.00	38	0.21
9	0.01	39	0.19
10	0.18	40	0.24
11	0.56	41	0.27

12	0.55	42	0.46
13	0.00	43	0.46
14	0.04	44	0.17
15	0.12	45	0.17
16	0.12	46	0.10
17	0.15	47	0.10
18	0.19	48	0.05
19	0.08	49	0.07
20	0.25	50	0.11
21	0.39	51	0.17
22	0.56	52	0.20
23	0.37	53	0.00
24	0.24	54	0.01
25	0.34	55	0.02
26	0.45	56	0.08
27	0.31	57	0.08
28	0.32	58	0.06
29	0.28	59	0.06
30	0.31	60	1.00

km^2 cultivation km^{-2} arable land

Table A3 Surface area of each cell of Northern Italy.

Region	GS_g (km^2)	Region (g)	GS_g (km^2)
1	1,875	31	2,500
2	2,500	32	1,500
3	1,500	33	750
4	1,250	34	250
5	1,000	35	2,500
6	1,250	36	2,500
7	2,000	37	2,500
8	2,500	38	2,500
9	2,500	39	2,500
10	2,500	40	2,500
11	2,500	41	2,500
12	1,250	42	2,500
13	2,000	43	1,500
14	2,250	44	2,500
15	2,500	45	2,500
16	2,000	46	1,750
17	2,500	47	2,000
18	2,500	48	2,500

19	2,500	49	2,500
20	2,500	50	2,500
21	2,500	51	2,500
22	2,500	52	1,000
23	1,250	53	1,000
24	2,000	54	1,500
25	2,500	55	1,500
26	2,500	56	2,500
27	2,500	57	2,500
28	2,500	58	2,500
29	2,500	59	1,750
30	2,500	60	210,000

Table A4 Unit biomass cultivation cost in each cell of Northern Italy.

Region	UCC_g (€ t^{-1})	**Region**	UCC_g (€ t^{-1})
1	145.6	31	130.2
2	145.6	32	131.3
3	145.6	33	130.5
4	141.6	34	135.1
5	137.2	35	130.2
6	136.2	36	135.3
7	137.1	37	152.8
8	195.2	38	132.3
9	174.4	39	130.3
10	141.3	40	130.2
11	130.4	41	130.5
12	130.4	42	134.0
13	151.3	43	133.8
14	140.0	44	135.5
15	132.7	45	142.7
16	134.7	46	151.4
17	134.8	47	138.4
18	130.8	48	130.4
19	170.1	49	130.6
20	133.1	50	131.7
21	133.4	51	135.8
22	130.4	52	138.6
23	131.1	53	195.2
24	130.7	54	197.3
25	130.3	55	151.3

26	131.5	56	131.1
27	130.2	57	133.0
28	132.0	58	142.4
29	130.4	59	142.4
30	131.8	60	114.6

The value of the binary parameter CF_g was set to 1 for domestic cultivation sites and 0 for the foreign cultivation sites. The minimum cultivation density, BCD_g^{min} was set to 0 for all regions.

Table A5 Arable land density of each cell in Northern Italy.

Region (*g*)	AD_g **(km^2 km^{-2})***	**Region (*g*)**	AD_g **(km^2 km^{-2})***
1	0.10	31	0.70
2	0.10	32	0.65
3	0.10	33	0.75
4	0.10	34	0.10
5	0.10	35	0.38
6	0.10	36	0.42
7	0.15	37	0.58
8	0.20	38	0.39
9	0.20	39	0.67
10	0.20	40	0.89
11	0.25	41	0.73
12	0.10	42	0.81
13	0.10	43	0.73
14	0.10	44	0.29
15	0.15	45	0.28
16	0.25	46	0.13
17	0.25	47	0.15
18	0.20	48	0.15
19	0.20	49	0.50
20	0.32	50	0.60
21	0.45	51	0.72
22	0.74	52	0.75
23	0.33	53	0.20
24	0.10	54	0.10
25	0.43	55	0.15
26	0.80	56	0.15
27	0.72	57	0.20

28	0.88	58	0.25
29	0.60	59	0.40
30	0.50	60	1.00

* *km^2 arable land km^{-2} regional surface*

A.4 Transportation Parameters

The available modes of transport are trucks, rail, barge and ships. In addition, small trucks are used for local transfer of biomass within each cell element and trans-ships can be used for biomass and ethanol import from foreign suppliers. However, as mentioned previously, ethanol import is not considered in this work, hence the capacity for trans-shipping of bioethanol is set to 0. The input parameters for these modes of transport are given in Table A6.

Table A6 Unit transport costs and transportation capacities for each transfer mode.

Transport	UTC_{il} (€ t^{-1} km^{-1})		$TCap_{il}$ (€ t^{-1} km^{-1})	
	Ethanol	**Corn**	**Ethanol**	**Corn**
Small truck		0.27 (*UTC**)		5 (*TCAP**)
Truck	0.500	0.540	23.3	21.5
Rail	0.210	0.200	59.5	55
Barge	0.090	0.120	3247	3,000
Ship	0.059	0.064	8658	8,000
Trans-ship		0.005		10,000

The tortousity factors for road and rail are taken as 1.4 and 1.2 respectively. Local roads are assumed to exist between all elements. Trans-shipping is considered for biomass import from foreign suppliers (region *g*:60). The data for other transport modes are given in Table A7. The average local delivery distance, ALD_g is assumed to be proportional to the actual surface area of each region *g*, GS_g.

Table A7 Tortousity factor for barge and ship transport modes.

Element linkages	**Transport mode**	**Tortousity factor**
38-39	Barge	1.9
39-40	Barge	1.0
40-42	Barge	1.4
42-43	Barge	1.8
32-34	Ship	0.85
32-43	Ship	1.18
32-52	Ship	1.06

34-43	Ship	0.66
34-52	Ship	0.68
43-52	Ship	1.54

A.5 Bioethanol Production Parameters

The input data related to ethanol production is given in Table A8. The biomass-to-bioethanol conversion factor (γ) is taken as 0.324 t bioethanol t^{-1} biomass.

Table A8 Input parameters for ethanol production.

Plant size *p*	$PCap_p$ **(kt year^{-1})**	$PCap_p^{max}$ **(kt year^{-1})**	$PCap_p^{min}$ **(kt year^{-1})**	***PCC*** **(€m)**	UPC_p **(€ t^{-1})**
1	110	120	80	70	160
2	150	160	140	91	154
3	200	210	190	115	151
4	250	260	240	139	149

Appendix B Economic Optimisation of a UK Advanced Biofuel Supply Chain

B.1 Mathematical Formulation

The problem for the optimal design of a hybrid ethanol supply chain is formulated as a steady-state mixed integer linear programming (MILP) model with the following notation:

Indices:

g, g'	Square cells (regions)
i	Resource (biomass, biofuel)
l	Transport mode
p	Plant size

Sets:

BI	Set of biomass types ($BI = FI \cup CI \cup SI$)
CI	Set of first generation biomass co-products (straw)
FI	Set of first generation biomass types (wheat)
G	Set of square cells (regions)
I	Set of resources (first generation biomass, second generation biomass, biofuel) ($I = BI \cup PI$)
L	Set of transport modes
P	Set of plant size intervals
PI	Set of product types (biofuel)
SI	Set of second generation energy crops (miscanthus, SRC)
$Total_{igg'l}$	Set of total transport links allowed for each resource *i* via mode *l* between regions *g* and *g'*
$n_{igg'l}$	Subset of $Total_{igg'l}$ including all regions g' in the neighbourhood of region *g* for each product *i* and mode *l*

Parameters:

$ADD_{gg'l}$	Actual delivery distance between regions *g* and *g'* via model *l* (km)
ALD_g	Average local biomass delivery distance (km)
A_g^s	Set-aside area available in region *g* (ha)
α	Operating period in a year (d year^{-1})
β	Fraction of straw recovered per unit of wheat cultivated

	(t straw t^{-1} wheat)
$BA_{ig}^{min/max}$	Minimum/maximum availability of first generation biomass i ($i \in FI$) in region g (t biomass d^{-1})
CCF	Capital charge factor ($year^{-1}$)
ε	Fraction of set-aside land that can be used for biofuel crop production
γ_i	Biomass to biofuel conversion factor for biomass type i (t biofuel t^{-1} biomass)
IC_p	Investment cost of a plant of size p (£)
$IMPC_{ig*}$	Unit impost cost for importing resource i from foreign supplier g^* (£ t^{-1})
$PCap_p^{min/max}$	Minimum/maximum biofuel production capacity of a plant of size p (t d^{-1})
$Q_{il}^{min/max}$	Minimum/maximum flowrate of resource i via mode l (t d^{-1})
$SusF$	Maximum fraction of domestic first generation biomass allowed for biofuel production
UCC_{ig}	Unit biomass cultivation cost of biomass type i in region g (£ t^{-1} biomass)
UPC_{ip}	Unit biofuel production cost from biomass type i at a plant of scale p (£ t^{-1} ethanol)
UTC_{il}	Unit transport cost of product i via mode l (£ t^{-1} km^{-1})
UTC^*	Unit transport cost for local biomass transfer (£ t^{-1} km^{-1})
Y_{ig}	Yield of second generation energy crop i ($i \in SI$) in region g (t ha^{-1} $year^{-1}$)

Binary Variables

E_{pg}	1 if a biofuel production plant of size p is to be established in region g

Continuous Variables

A_{ig}	Land occupied by second generation crop i ($i \in SI$) in region g (ha)
D_{ig}	Demand for resource i in region g (t d^{-1})
Df_{ipg}	Demand for biomass i at a plant of scale p located in region g (t d^{-1})
Pf_{pg}	Biofuel production rate at a plant of size p located in region g (t d^{-1})
P_{ig}	Production rate of resource i in region g (t d^{-1})
$Q_{igg'l}$	Flow rate of resource i via mode l from region g to g' (t d^{-1})
TDC	Total daily cost of a biofuel supply chain network (£ d^{-1})
TIC	Total investment cost of biofuel production facilities (£)

TPC Total production cost (£ d^{-1})

$TPOC$ Total product outsourcing cost (£ d^{-1})

TTC Total transportation cost (£ d^{-1})

$$Min\ \ TDC = \frac{TIC}{\alpha} CCF + TPC + TTC + TPOC \tag{B.1}$$

$$TIC = \sum_{p \in P} \sum_{g \in G} IC_p E_{pg} \tag{B.2}$$

$$TPC = \sum_{i \in BI} \sum_{g \in G} \left(UCC_{ig} P_{ig} + \sum_{p \in P} UPC_{ip} \gamma_i Df_{ipg} \right) \tag{B.3}$$

$$TTC = \sum_{i \in I} \sum_{l \in L} \sum_{g \in G} \sum_{g' \in n_{igg'l}} \left(UTC_{il} ADD_{gg'l} Q_{igg'l} \right) + \sum_{i \in BI} \sum_{g \in G} \left(UTC^{*} ALD_g P_{ig} \right) \tag{B.4}$$

$$TPOC = \sum_{i, g^{*}, g, l \in n_{i, g', g, l}} IMPC_{ig^{*}} Q_{ig^{*}gl} \tag{B.5}$$

Subject to:

Demand constraints

$$Pf_{pg} = \sum_{i \in BI} \gamma_i Df_{ipg} \qquad \forall\, p \in P, g \in G \tag{B.6}$$

$$D_{ig} = \sum_{p \in P} Df_{ipg} \qquad \forall\, i \in BI, g \in G \tag{B.7}$$

Production constraints

$$P_{ig} + \sum_{l \in L} \sum_{g' \in n_{ig'gl}} Q_{ig'gl} = D_{ig} + \sum_{l \in L} \sum_{g' \in n_{igg'l}} Q_{igg'l} \qquad \forall\, i \in I, g \in G \tag{B.8}$$

$$P_{ig} = \sum_{p \in P} Pf_{pg} \qquad \forall\, i \in PI, g \in G \tag{B.9}$$

$$PCap_p^{\min} E_{pg} \le Pf_{pg} \le PCap_p^{\max} E_{pg} \qquad \forall\, p \in P, g \in G \tag{B.10}$$

$$\sum_{p \in P} E_{pg} \le 1 \qquad \forall\, g \in G \tag{B.11}$$

$$BA_{ig}^{\min} \le P_{ig} \le BA_{ig}^{\max} \qquad \forall\, i \in FI, g \in G \tag{B.12}$$

$$P_{ig} = Y_{ig} A_{ig} / \alpha \qquad \forall\, i \in SI, g \in G \tag{B.13}$$

$$P_{straw,g} \le \beta P_{wheat,g} \qquad \forall\, g \in G \tag{B.14}$$

Sustainability Constraints

$$\sum_{g \in G} P_{ig} \le SusF \left(\sum_{g} BA_{ig}^{\max} \right) \qquad \forall\, i \in FI \tag{B.15}$$

$$\sum_{i \in SI} A_{ig} \leq A_g^s \qquad \forall g \in G \tag{B.16}$$

$$\sum_{i \in SI} \sum_{g \in G} A_{ig} \leq \varepsilon \sum_{g} A_g^s \tag{B.17}$$

B.2 Summary of Zamboni Et Al. (2009a) Secondary Distribution Model

The mathematical formulation for the slightly modified version of the ethanol supply chain optimisation model introduced by Zamboni *et al.* (2009a) is summarised below. It must be pointed out that the binary variable which determines which cell is served by which internal depot as used in the formulation by Zamboni *et al.* (2009a) has been removed in this version. The symbols used for indices, sets and parameters are as introduced in the work of Zamboni *et al*. (2009a).

Nomenclature

Indices

d	Depot (terminal)
g, g'	Square cells (regions)

Sets

D	Set of depots (terminals)
g, g'	Set of square cells (regions)

Parameters

α	Network operating period in a year (d year^{-1})
CCF	Capital charge factor (year^{-1})
CCT	Capital cost of a truck (£)
DD_{dg}	Delivery distance between depot *d* and cell *g* (km)
DEM_g	Local gasoline demand in cell *g* (t d^{-1})
DW	Driver wage for tankers (£ h^{-1})
FD	Fuel demand of tankers (km L^{-1})
FP	Fuel price (£ L^{-1})
GE	General expenses of tankers (£ d^{-1})
LUT	Load/unload time of tankers (h trip^{-1})
ME	Maintenance expenses of tankers (£ km^{-1})
SP	Average speed of tankers (km h^{-1})
TCap	Capacity of tankers (t trip^{-1})
THR_d^{max}	Maximum terminal throughput (t d^{-1})

TMA	Availability of tankers (h d^{-1})

Integer Variables

NTU_{dg}	Number of transport units required to transport fuel from depot *d* to region *g* (units d^{-1})

Continuous Variables

FC	Fuel costs for blended fuel delivery (£ d^{-1})
GC	General costs for blended fuel delivery (£ d^{-1})
LC	Labour costs for blended fuel delivery (£ d^{-1})
MC	Maintenance costs for blended fuel delivery (£ d^{-1})
Q_{dg}	Flow rate of fuel from depot *d* to cell *g* (t d^{-1})
TCC	Transport capital cost for blended fuel delivery (£ d^{-1})
TOC	Transportation operating costs for blended fuel delivery (£ d^{-1})

$$Min\ TOC = FC + LC + MC + GC + TCC \tag{B.18}$$

$$FC = 2\sum_{d\in D}\sum_{g\in G} FP \cdot DD_{dg} \cdot Q_{dg} / (FD \cdot TCap) \tag{B.19}$$

$$LC = \sum_{d\in D}\sum_{g\in G} DW\left(Q_{dg} / TCap\right)\left(\left(2DD_{dg} / SP\right) + LTU\right) \tag{B.20}$$

$$MC = 2\sum_{d\in D}\sum_{g\in G} ME\left(DD_{dg} Q_{dg} / TCap\right) \tag{B.21}$$

$$GC = \sum_{d\in D}\sum_{g\in G} GE\left(Q_{dg} / \left(TCap \cdot TMA\right)\right)\left(2DD_{dg} / SP + LTU\right) \tag{B.22}$$

$$TCC = \sum_{d\in D}\sum_{g\in G} NTU_{dg} \cdot CCT \cdot CCF / \alpha \tag{B.23}$$

Subject to:

$$\sum_{g\in G} Q_{dg} \le THR_d^{\max} \qquad \forall\, d \in D \tag{B.24}$$

$$\sum_{d\in D} Q_{dg} = DEM_g \qquad \forall\, g \in G \tag{B.25}$$

$$NTU_{dg} = \left(Q_{dg} / \left(TMA \cdot TCap\right)\right)\left(2LUT + \left(2DD_{dg} / SP\right)\right) \quad \forall\, d \in D, g \in G \tag{B.26}$$

The values of the input parameters are given in Table B1 (Zamboni *et al.*, 2009a). As another input parameter, the fuel demand in each cell *g*, DEM_g is given in Table B2. The demand for each cell has been determined based on the total UK gasoline demand (UKPIA, 2008) and population density per region (Almansoori and Shah, 2006).

Table B1 Input data for the secondary distribution model (Zamboni *et al*., 2009a).

Parameter	Value
α	365 d year^{-1}
CCF	0.12 year^{-1}
CCT	84,200 £
DW	8.5 £ h^{-1}
FD	2.55 km L^{-1}
FP	1.056 £ L^{-1}
GE	23.67 £ d^{-1}
LUT	2 h trip^{-1}
ME	0.0891 £ km^{-1}
SP	50 km h^{-1}
TCap	44 t trip^{-1}
TMA	18 h d^{-1}

Table B2 Local gasoline demand in each cell *g* (UKPIA, 2008; Almansoori and Shah, 2006).

Cell (g)	DEM_g (t d^{-1})	Cell (g)	DEM_g (t d^{-1})
1	396.2	18	3,873.0
2	310.8	19	1,930.7
3	613.8	20	159.3
4	769.2	21	244.7
5	159.3	22	2,424.0
6	505.0	23	4,067.3
7	672.1	24	3,344.7
8	27.2	25	1,383.0
9	330.2	26	244.7
10	1,227.6	27	1,530.6
11	1,495.6	28	3,414.6
12	0.0	29	10,593.5
13	2,466.8	30	730.3
14	3,504.0	31	808.0
15	555.5	32	978.9
16	93.2	33	718.7
17	1,899.6	34	528.3

B.3 Bioethanol Demand

The biofuel target for 2011 based on the volumetric fractions of components has been converted to mass fraction using the following formula:

$$X^{m}_{bioethanol} = \frac{\rho_{bioethanol} X^{v}_{bioethanol}}{\rho_{bioethanol} X^{v}_{bioethanol} + \rho_{gasoline} X^{v}_{gasoline}} \quad \text{(B.27)}$$

where $\rho_{ethanol}$ and $\rho_{gasoline}$ are the densities of ethanol (0.79 g cm^{-3}) and gasoline (0.73 g cm^{-3}) (BFIN), respectively. X^{v} denotes the volumetric fraction of a component in the transport fuel mix.

The target for 2020 based on the energy content of the fuel mix has been converted to mass fraction using equation A.22.

B.4 Biomass Cultivation Parameters

The square cells covered by each region in the UK are given in Table B3. The daily wheat availability in each cell based on the regional cultivation data in the UK is given in Table B4. This corresponds to a total wheat availability of 39,170 t d^{-1} (DEFRA, 2010). This figure must be multiplied by the corresponding sustainability factor to determine the available amount for ethanol production. The minimum wheat availability, $BA^{\min}_{wheat,g}$ has been set to 0. The data for the sustainability parameters are given in Appendix B.7. The β parameter, which represents the amount of straw that can be recovered sustainably per unit of wheat cultivated, is taken as 0.65 (DTI, 2003).

The regional yields of special energy crops: miscanthus and SRC are given in Table B5 (NNFCC, 2008a). The unit cultivation costs for wheat, miscanthus and SRC are presented in Table B6 (Ericsson *et al.*, 2009; Savills Research, 2009).

Table B3 Discretisation of the UK into square cells**.**

Region	Cell (g)
North East	11
North West and Merseyside	13
Yorkshire & The Humber	14,15
East Midlands	18,19
West Midlands	23
Eastern	20,24,25
South East and London	29,30,34
South West	28,31,32,33
Scotland	1,2,3,4,5,6,7,8,9,10,12
Wales	16,17,21,22,26,27

Table B4 Daily cultivable wheat in each cell *g* in the UK (DEFRA, 2010).

Cell (g)	Daily cultivable wheat, $BA^{max}_{wheat,g}$	Cell (g)	Daily cultivable wheat, $BA^{max}_{wheat,g}$
1	179.71	18	4,821.52
2	135.43	19	2,862.78
3	260.45	20	325.58
4	333.38	21	23.82
5	85.95	22	138.57
6	226.59	23	3,147.17
7	315.14	24	6,945.68
8	13.02	25	3,147.26
9	143.25	26	19.49
10	333.38	27	102.85
11	1,259.62	28	1,753.46
12	26.04	29	4,011.19
13	420.79	30	689.42
14	4,138.91	31	630.15
15	896.76	32	808.24
16	6.50	33	438.37
17	90.94	34	438.72

Table B5 Miscanthus and SRC yields per cell in the UK (NNFCC, 2008a).

		Y_{ig} (t ha^{-1} year^{-1})			
Cell (g)	**Miscanthus**	**SRC**	**Cell (g)**	**Miscanthus**	**SRC**
1	14	12	18	14	12
2	14	12	19	16	10
3	14	12	20	16	10
4	12	8	21	16	10
5	14	12	22	14	8
6	14	12	23	14	10
7	12	8	24	16	10
8	14	12	25	16	10
9	14	12	26	16	10
10	12	8	27	16	10
11	14	12	28	14	10
12	14	12	29	16	10
13	14	8	30	16	10
14	12	10	31	16	8
15	14	10	32	16	10

16	16	10	33	14	10
17	14	9	34	16	10

Table B6 Unit cultivation costs of wheat, miscanthus and SRC crops per cell in the UK (Ericsson *et al.*, 2009; Savills Research, 2009).

	UCC_{ig} (£ t^{-1})		
Cell (g)	**Wheat**	**Miscanthus**	**SRC**
1	87.3	68	61
2	87.3	68	61
3	87.3	68	61
4	87.3	68	61
5	87.3	68	61
6	87.3	68	61
7	87.3	68	61
8	87.3	68	61
9	87.3	68	61
10	87.3	68	61
11	117.2	91.3	82
12	87.3	68	61
13	117.2	91.3	82
14	120.9	94.2	85
15	120.9	94.2	85
16	106.0	82.6	74
17	106.0	82.6	74
18	124.6	97.1	87
19	124.6	97.1	87
20	143.0	111.4	100
21	106.0	82.6	74
22	106.0	82.6	74
23	154.2	120.2	108
24	143.0	111.4	100
25	143.0	111.4	100
26	106.0	82.6	74
27	106.0	82.6	74
28	131.2	102.2	92
29	148.4	115.6	104
30	148.4	115.6	104
31	131.2	102.2	92
32	131.2	102.2	92
33	131.2	102.2	92

34	148.4	115.6	104

B.5 Transportation Parameters

The unit transportation cost data is given in Table B7. This data has been converted from the equivalent data given in Table A6 in Appendix A using the related currency exchange rate. The tortousity factors for road, rail and ship are 1.4, 1.2 and 1, respectively. More information on the assumptions for determining these factors can be found in the work of Zamboni *et al.* (2009a). Road and rail modes are assumed to exist between all elements whereas ship is used for the transport of imported biomass between elements 19 and 35.

Table B7 Unit transportation cost for each mode and resource.

	UTC_{il} (£ t^{-1} km^{-1})	
Transport mode	**Biomass**	**Ethanol**
Road	0.47	0.44
Rail	0.17	0.18
Ship	0.06	0.05

B.6 Bioethanol Production Parameters

The parameters related to first generation and hybrid production facilities are given in Table B8 (NNFCC, 2008b). The bioethanol production parameters for first generation are the same as those given in Appendix A. The unit cost of ethanol production from each biomass type and for each plant size is given in Table B9 (DTI, 2003). The unit production costs are based on the total cost of staff, maintenance and consumables of the processes.

The biomass-to-ethanol conversion factors, γ_i (t ethanol t^{-1} biomass) are 0.324, 0.266, 0.266 and 0.235 for wheat, straw, miscanthus and SRC respectively (NNFCC, 2008b).

Table B8 Minimum/maximum plant capacities and capital costs (NNFCC, 2008b).

Plant size (p)	$PCap_p^{max}$ (ktons $year^{-1}$)	$PCap_p^{min}$ (ktons $year^{-1}$)	***PCC*** **(m£) for a first gen. facility**	***PCC*** **(m£) for a hybrid facility**
1	120	80	61	145
2	160	140	80	180
3	210	190	101	220

4	260	240	122	257

Table B9 Unit ethanol production cost for each biomass type and plant scale (DTI, 2003).

	***UPC* (£ t^{-1})**			
Plant size *(p)*	**Wheat**	**Wheat straw**	**Miscanthus**	**SRC**
1	140	252	252	232
2	135	243	243	224
3	132	238	238	219
4	130	234	234	216

B.7 Sustainability Parameters

The value of the sustainability factor, *SusF* for the use of first generation crops to produce biofuel is 0.15 as given in Appendix A. The availability of set-aside land per region in the UK is given in Table B10 (DEFRA, 2007). The fraction of this land that can be used for biofuel production, ε is taken as 1 and 0.5 for scenarios 2020A and 2020B, respectively.

Table B10 The distribution of set-aside land per cell in the UK (DEFRA, 2007).

Cell (g)	**Available set-aside land, A_g^s (kha)**	**Cell (g)**	**Available set-aside land, A_g^s (kha)**
1	0.0	18	53.6
2	0.0	19	53.6
3	0.0	20	45.9
4	0.0	21	0.0
5	0.0	22	0.0
6	0.0	23	49.3
7	0.0	24	45.9
8	0.0	25	45.9
9	0.0	26	0.0
10	0.0	27	0.0
11	25.5	28	18.7
12	0.0	29	31.1
13	14.6	30	31.1
14	34.0	31	18.7
15	34.0	32	18.7
16	0.0	33	18.7
17	0.0	34	31.1

Appendices

Appendix C An Optimisation Framework for a Hybrid First/Second Generation Bioethanol Supply Chain

C.1 Biomass Cultivation Parameters

The economic parameters for biomass cultivation are given in the related section in Appendix B. The emission factors for biomass cultivation for each biomass type *i* and region *g* has been calculated based on the average values obtained and the distribution of these average values through cells in proportion to the cultivation yields (RFA, 2011). The resulting data for wheat, wheat straw, miscanthus and SRC are given in Table C1 (RFA, 2011).

Table C1 Emission factor data for cultivation of each biomass type in each cell of the UK (RFA, 2011).

	$EFBC_{ig}$ (kgCO_2-eq t^{-1} biomass)			
Cell (g)	**Wheat**	**Wheat straw**	**Miscanthus**	**SRC**
1	217.7	25.5	48.4	52.1
2	217.7	25.5	48.4	52.1
3	217.7	25.5	48.4	52.1
4	217.7	25.5	41.4	34.8
5	217.7	25.5	48.4	52.1
6	217.7	25.5	48.4	52.1
7	217.7	25.5	41.4	34.8
8	217.7	25.5	48.4	52.1
9	217.7	25.5	48.4	52.1
10	217.7	25.5	41.4	34.8
11	190.8	22.3	48.4	52.1
12	217.7	25.5	48.4	52.1
13	134.4	15.7	48.4	34.8
14	217.7	25.5	41.4	43.4
15	217.7	25.5	48.4	43.4
16	190.8	22.3	55.3	43.4
17	190.8	22.3	48.4	39.1
18	220.4	25.8	48.4	52.1
19	220.4	25.8	55.3	43.4
20	215.0	25.1	55.3	43.4
21	190.8	22.3	55.3	43.4
22	190.8	22.3	48.4	34.8
23	198.9	23.3	48.4	43.4
24	215.0	25.1	55.3	43.4

25	215.0	25.1	55.3	43.4
26	190.8	22.3	55.3	43.4
27	190.8	22.3	55.3	43.4
28	212.3	24.8	48.4	43.4
29	220.4	25.8	55.3	43.4
30	220.4	25.8	55.3	43.4
31	212.3	24.8	55.3	34.8
32	212.3	24.8	55.3	43.4
33	212.3	24.8	48.4	43.4
34	220.4	25.8	48.4	43.4

C.2 Transportation Parameters

The economic parameters for transportation are given in the related section in Appendix B. The emission factor for each transport mode is given in Table C2 (Zamboni *et al.*, 2009b; EC Joint Research Centre, 2006). It should be noted that small trucks are used for local biomass transport.

Table C2 Emission factor data for transportation (Zamboni *et al.*, 2009b; EC Joint Research Centre, 2006).

Transport Mode	$EFTRA_l$ (kg CO_2-eq t^{-1} km^{-1})
Small truck	0.5910
Road	0.1231
Rail	0.0228
Ship	0.0139

C.3 Bioethanol Production Parameters

The economic parameters for bioethanol production are given in the related section in Appendix B. The emission factor data for biofuel production from each biomass type is given in Table C3 (RFA, 2011).

Table C3 Emission factor data for biofuel production (RFA, 2011).

Biomass type	$EFBP_i$ (kg CO_2-eq t^{-1} ethanol)
Wheat	562.96
Wheat straw	145.95
Miscanthus	311.74
SRC	311.74

Appendix D Optimisation of Bioelectricity Supply Chains

D.1 Raw Material Parameters

The biomass availability data is presented in Table D1. It must be noted that it is assumed that only woodfuel is assumed to be available as biomass resource in 2012 whereas miscanthus will also be available by 2020 and 2050 as an additional biomass resource apart from woodfuel. Therefore, the biomass availability data for 2012 corresponds to the availability of woodfuel only whereas those for 2020 and 2050 represent the total availabilities of both miscanthus and woodfuel (CEBR, 2010; NNFCC, 2008a; DEFRA, 2007).

Table D1 UK Biomass availability data per cell for years 2012, 2020 and 2050 (CEBR, 2010; NNFCC, 2008a; DEFRA, 2007).

$BA_{biomass,g}^{max}$ (t h^{-1})							
Cell	**2012**	**2020**	**2050**	**Cell**	**2012**	**2020**	**2050**
1	5.2	28.0	56.0	18	6.5	82.7	118.5
2	3.9	21.1	42.2	19	3.9	74.9	96.2
3	7.5	40.6	81.2	20	0.4	48.3	50.7
4	9.6	52.0	104.0	21	0.8	4.3	8.6
5	2.5	13.4	26.8	22	4.5	24.7	49.4
6	6.5	35.3	70.6	23	4.3	66.5	89.9
7	9.1	49.1	98.2	24	9.4	97.5	149.1
8	0.4	2.0	4.0	25	4.3	69.3	92.7
9	4.1	22.3	44.6	26	0.6	3.5	7.0
10	9.6	52.0	104.0	27	3.4	18.4	36.8
11	1.7	31.7	41.1	28	2.4	29.4	42.4
12	0.7	4.1	8.2	29	5.4	60.9	90.7
13	0.6	15.9	19.0	30	0.9	36.2	41.3
14	5.6	56.2	86.9	31	0.9	23.4	28.1
15	1.2	36.5	43.2	32	1.1	24.7	30.7
16	0.2	1.2	2.4	33	0.6	19.7	23.0
17	3.0	16.2	32.4	34	0.6	34.4	37.7
TOTAL 2012				121			
TOTAL 2020				1,196			
TOTAL 2050				1,858			

The municipal solid waste availability for 2012, 2020 and 2050 is given in Table D2. This data has been derived based on the fact that the UK produces 0.5 tonnes of

waste per person per year on average. The current and projected populations are used to calculate the total availability of municipal solid waste and this total value is distributed between different cells in the UK based on their population densities (Eurostat; Almansoori and Shah, 2006).

Table D2 UK MSW availability data per cell for years 2012, 2020 and 2050 (Eurostat; Almansoori and Shah, 2006).

$BA_{MSW,g}^{max}$ (t h^{-1})							
Cell	**2012**	**2020**	**2050**	**Cell**	**2012**	**2020**	**2050**
1	30.2	31.3	35.5	18	179.7	186.3	211.2
2	22.8	23.6	26.7	19	106.7	110.6	125.4
3	43.8	45.4	51.4	20	11.5	12.0	13.6
4	56.0	58.1	65.8	21	12.4	12.8	14.5
5	14.4	15.0	17.0	22	72.0	74.7	84.6
6	38.1	39.5	44.7	23	360.6	373.7	423.7
7	53.0	54.9	62.2	24	246.3	255.3	289.4
8	2.2	2.3	2.6	25	111.6	115.7	131.1
9	24.1	25.0	28.3	26	10.1	10.5	11.9
10	56.0	58.1	65.8	27	53.5	55.4	62.8
11	170.8	177.0	200.6	28	163.0	168.9	191.5
12	4.4	4.5	5.1	29	817.3	847.0	960.2
13	460.6	477.4	541.2	30	140.5	145.6	165.0
14	278.5	288.6	327.2	31	58.6	60.7	68.8
15	60.3	62.5	70.9	32	75.1	77.9	88.3
16	3.4	3.5	4.0	33	40.8	42.2	47.9
17	47.3	49.0	55.5	34	89.4	92.6	105.0
TOTAL 2012				3,915			
TOTAL 2020				4,058			
TOTAL 2050				4,600			

Table D3 shows the unit supply cost of biomass per region in the UK. This data has been derived based on the fact that the average biomass price is 50 £/t (DECC, 2010a) and the cost variation is assumed to be the same as that of wheat prices per region in the UK. The cost of MSW has been taken as 50 £/t for all regions (Eunomia; DEFRA, 2009).

Table D3 Unit supply cost of biomass per cell in the UK (DECC, 2010a).

$USC_{biomass,g}$ (£ t^{-1})			
Cell	**2012**	**Cell**	**2012**
1	38.3	18	54.7
2	38.3	19	54.7
3	38.3	20	62.7
4	38.3	21	46.5
5	38.3	22	46.5
6	38.3	23	67.7
7	38.3	24	62.7
8	38.3	25	62.7
9	38.3	26	46.5
10	38.3	27	46.5
11	51.4	28	57.6
12	38.3	29	65.1
13	51.4	30	65.1
14	53	31	57.6
15	53	32	57.6
16	46.5	33	57.6
17	46.5	34	65.1

D.2 Pellet Production Parameters

The cost parameters for different scales of pellet production plants as well as the corresponding minimum and maximum plant capacities are given in Table D4 (McCartney, 2007). The conversion factors for pellet production from biomass and MSW are taken to be 1/3 and 1/5, respectively (Harvard Green Campus Initiative).

Table D4 Pellet production parameters used in this study (Harvard Green Campus Initiative).

Plant size (*p*)	$PCap_p^{min}$ (t h^{-1})	$PCap_p^{max}$ (t h^{-1})	UPC_{ip} (£ t^{-1})	IC_p (£)
1	1	10	105	94,575
2	11	20	98	182,831
3	21	30	90	248,405

D.3 Power Generation Parameters

The characteristics of the power plants considered in this study are given in Table D5 below.

Table D5 Name plate capacity, average annual emissions and geographical location of each of the power plants considered in this study.

Name of power plant	Fuel	Nameplate capacity (MW)	Average emissions ($MtCO_2$/ year)	Longitude	Latitude	Cell
Drax	COAL	3,870	21.6	-1	53.73	19
Cottam	COAL	2,008	9.4	-0.78	53.31	13
Ratcliffe	COAL	2,000	8.6	-1.25	52.86	18
West Burton	COAL	1,972	8.7	-0.81	53.36	10
Eggborough	COAL	1,960	7.3	-1.13	53.71	14
Kingsnorth	COAL	1,940	7.1	0.6	51.42	30
Didcot A	COAL	1,925	5.3	-1.26	51.62	28
Tilbury B	COAL	750	4.2	0.39	51.45	29
Ferrybridge C	COAL	1,955	6.7	-1.29	53.72	18
Rugeley	COAL	1,006	4.2	-1.91	52.75	23

D.4 Optimal Configurations

This mapping between the 10 UK regions and the 34 cells is given in Table D6. The detailed optimal configurations at cell level are given in Figure D1-Figure D2 whereas the corresponding optimal power generation variables are given in Table D7-Table D10.

Table D6 Discretisation of the UK into square cells.

UK region	Cell
North East	11
North West and Merseyside	13
Yorkshire & The Humber	14,15
East Midlands	18,19
West Midlands	23
Eastern	20,24,25
South East and London	29,30,34
South West	28,31,32,33
Scotland	1,2,3,4,5,6,7,8,9,10,12
Wales	16,17,21,22,26,27

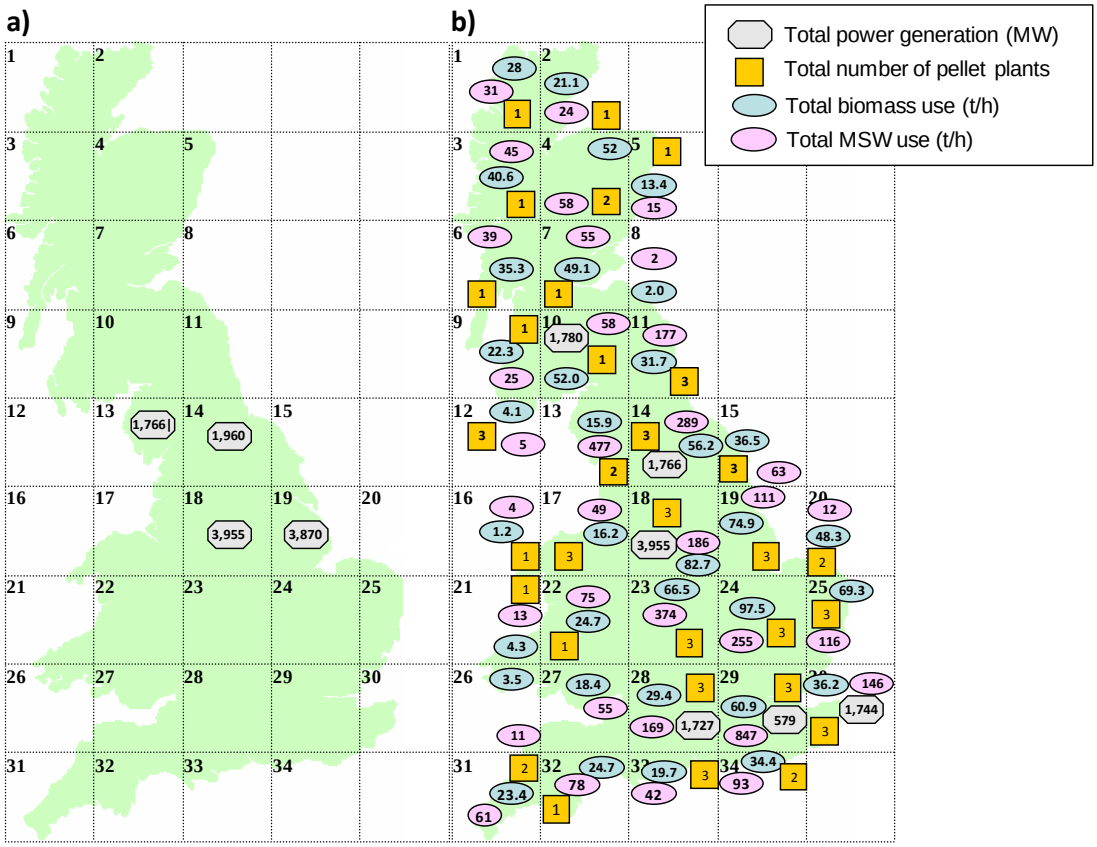

Figure D1 The optimal bioelectricity supply chain configuration for the a) minimum cost and b) minimum carbon intensity options for the 2020 central decarbonisation scenario. The pink and green symbols indicate the optimal rates of MSW and biomass supply in each cell. The yellow squares correspond to the optimal number of pelletisation plants established in each cell. Finally, the grey symbols represent the total optimal power generation within that cell, e.g., in cell 18 the number 3,995 represents the combined generation capacity of the Ferrybridge C and Rattcliffe power plants operating at 100% of their capacity.

.

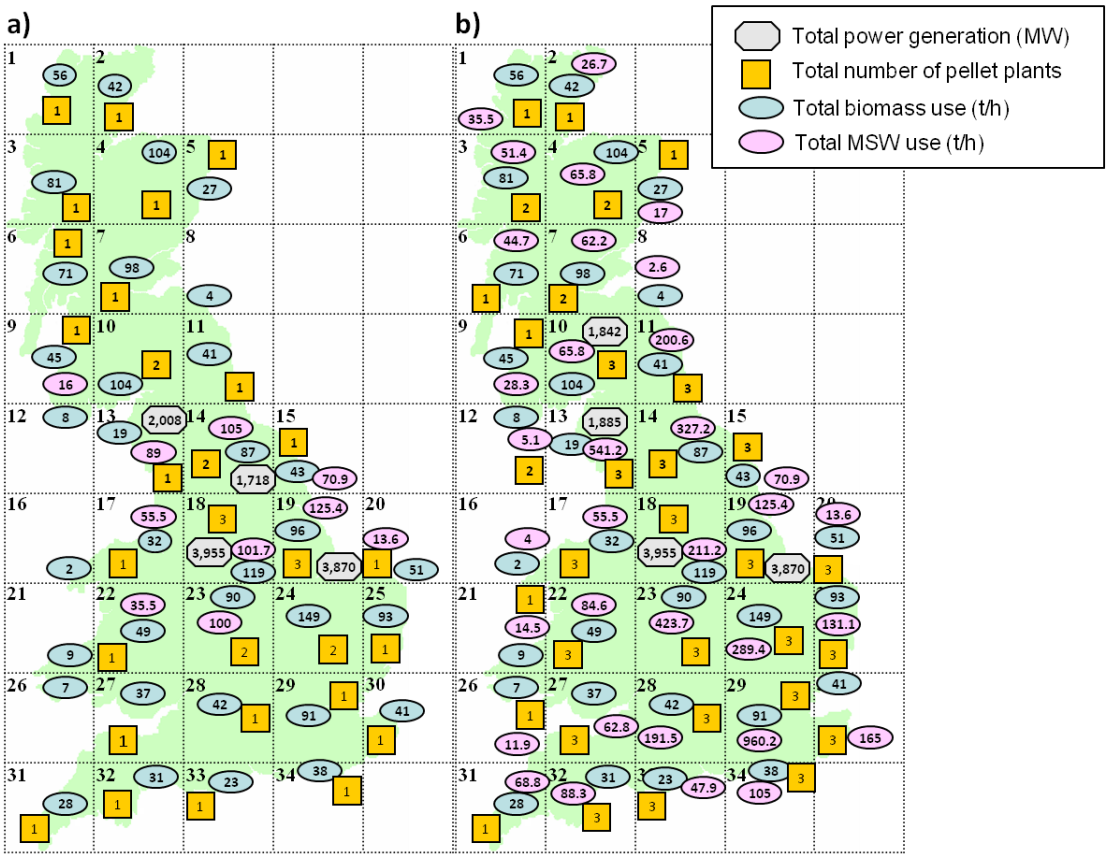

Figure D2 The optimal bioelectricity supply chain configuration for the a) minimum cost and b) minimum carbon intensity options for the 2050 central decarbonisation scenario. The pink and green symbols indicate the optimal rates of MSW and biomass supply in each cell. The yellow squares correspond to the optimal number of pelletisation plants established in each cell. Finally, the grey symbols represent the total optimal power generation within that cell, e.g., in cell 18 the number 3,995 represents the combined generation capacity of the Ferrybridge C and Rattcliffe power plants operating at 100% of their capacity.

Table D7 Optimal power plant variables for the 2020 central decarbonisation scenario (minimum cost). In this scenario, there is no co-firing of biomass or solid recovered fuels and electricity is generated using coal in conjunction with CO_2 capture. This results a CO_2 footprint of approximately 4 MT/CO_2 per year.

Cell	$P_{elec,g}$ (MW)	δ_g (%)	η_g (%)	$\dot{m}_g$ (t/h)	φ_{ig} (%) (*i*:biomass pellet)	φ_{ig} (%) (*i*:MSW pellet)	CCS_g (%)	CI_g (kg CO_2/ MWh)
13	1,766	88%	36%	726	0%	0%	100%	42
14	1,960	100%	36%	802	0%	0%	100%	45
18	3,955	100%	37%	1,565	0%	0%	100%	43
19	3,870	100%	37%	1,533	0%	0%	100%	43

Table D8 Optimal power plant variables for the 2020 central decarbonisation scenario (minimum carbon intensity). In this scenario, a combination of co-firing biomass or solid recovered fuels with coal in conjunction with CO_2 capture results in a CO_2 footprint of approximately -16.9 MT/CO2 per year.

Cell	$P_{elec,g}$ (MW)	δ_g (%)	η_g (%)	$\dot{m}_g$ (t/h)	φ_{ig} (%) (*i*:biomass pellet)	φ_{ig} (%) (*i*:MSW pellet)	CCS_g (%)	CI_g (kg CO_2/ MWh)
10	1,780	90%	34%	849	0%	20%	100%	-161
14	1,766	90%	34%	842	0%	20%	100%	-161
18	3,955	100%	35%	1,795	22%	5%	100%	-227
28	1,727	90%	34%	824	0%	20%	100%	-160
29	579	77%	33%	280	0%	18%	100%	-144
30	1,744	90%	34%	832	0%	20%	100%	-161

Table D9 Optimal power plant variables for the 2050 central decarbonisation scenario (minimum cost). In this scenario, a combination of co-firing biomass or solid recovered fuels in conjunction with CO_2 capture results in a CO_2 footprint of approximately -10 MT/CO_2 per year.

Cell	$P_{elec,g}$ (MW)	δ_g (%)	η_g (%)	$\dot{m}_g$ (t/h)	φ_{ig} (%) (*i*:biomass pellet)	φ_{ig} (%) (*i*:MSW pellet)	CCS_g (%)	CI_g (kg CO_2/ MWh)
13	2,008	100%	34%	896	19%	0%	100%	-145
14	1,718	88%	34%	763	12%	3%	100%	-109
18	3,955	100%	36%	1,689	9%	5%	100%	-97
19	3,870	100%	36%	1,651	12%	3%	100%	-104

Table D10 Optimal power plant variables for the 2050 central decarbonisation scenario (minimum carbon intensity). In this scenario, a combination of co-firing biomass or solid recovered fuels in conjunction with CO_2 capture results in a CO_2 footprint of approximately -22 MT/CO_2 per year.

Cell	$P_{elec,g}$ (MW)	δ_g (%)	η_g (%)	$\dot{m}_g$ (t/h)	φ_{ig} (%) (*i*:biomass pellet)	φ_{ig} (%) (*i*:MSW pellet)	CCS_g (%)	CI_g (kg CO_2/ MWh)
10	1,842	93%	34%	901	0%	24%	100%	-195
13	1,885	94%	34%	922	0%	24%	100%	-196
18	3,955	100%	35%	1,890	0%	26%	100%	-223
19	3,870	100%	34%	1,794	34%	0%	100%	-294

Appendix E A Spatial Hydrogen Infrastructure Planning Model

E.1 Demand Parameters

Table E1 Number, name and order of penetration of hydrogen for the areas considered in this study.

Number	Area	Order	Number	Area	Order
1	Bedfordshire and Hertfordshire	1	19	Lancashire	3
2	Berkshire, Buckinghamshire and Oxfordshire	1	20	Leicestershire, Rutland and Northamptonshire	2
3	Cheshire	2	21	Lincolnshire	3
4	Cornwall and Isles of Scilly	5	22	London	1
5	Cumbria	5	23	Manchester and Merseyside	2
6	Derbyshire and Nottinghamshire	2	24	North Eastern Scotland	4
7	Devon	4	25	North Yorkshire	3
8	Dorset and Somerset	2	26	Northern Ireland	2
9	East Anglia	1	27	Northumberland and Tyne and Wear	5
10	East Wales	3	28	Shropshire and Staffordshire	2
11	East Yorkshire and Northern Lincolnshire	5	29	South Western Scotland	4
12	Eastern Scotland	4	30	South Yorkshire	4
13	Essex	1	31	Surrey, East and West Sussex	1
14	Gloucestershire, Wiltshire and Bristol/Bath area	1	32	Tees Valley and Durham	5
15	Hampshire and Isle of Wight	1	33	West Midlands	3
16	Herefordshire, Worcestershire and Warwickshire	2	34	West Wales and The Valleys	3
17	Highlands and Islands	5	35	West Yorkshire	3
18	Kent	1			

E.2 Production, Transportation, Storage and Filling Station Parameters

Table E2 Capital costs of hydrogen production plants (NRC and NAE, 2004).

		PCC_{jpi} ($m)						
		Production technology (*j*)						
Product type (*i*)	**Plant size (*p*)**	**SMR**	**SMR CCS**	**CG**	**CG CCS**	**BG**	**BG CCS**	**Electro**
LH_2	Distr	-	-	-	-	-	-	-
	Small	50	-	-	-	93	-	64
	Medium	280	330	-	-	329	379	553
	Large	860	910	1,587	1,637	1,572	1,622	-
GH_2	Distr	4.9	-	-	-	-	-	7.1
	Small	14.5	-	-	-	48.2	-	29
	Medium	127	177	-	-	175	225	399
	Large	453	503	1,152	1,202	1,165	1,215	-

Table E3 Minimum/maximum production capacities for hydrogen production plants (NRC and NAE, 2004; NRC, 2008; Iaquaniello *et al.*, 2008; Krewitt and Schmid, 2005)

		$PCAP^{min}_{jpi}$ / $PCAP^{max}_{jpi}$ (thousand kg d^{-1})						
		Production technology (*j*)						
Product type (*i*)	**Plant size (*p*)**	**SMR**	**SMR CCS**	**CG**	**CG CCS**	**BG**	**BG CCS**	**Electro**
LH_2	Distr	-	-	-	-	-	-	-
	Small	1.6/10	-	-	-	1.6/14	-	1.6/10
	Medium	10/150	-	-	-	15/ 150	-	10/150
	Large	200/ 1,100	200/ 1,100	200/ 1,200	200/ 1,200	200/ 1,100	200/ 1,100	-
GH_2	Distr	0/1.5	-	-	-	-	-	0/1.5
	Small	1.6/10	-	-	-	1.6/14	-	1.6/10
	Medium	10/150	-	-	-	15/150	-	10/150
	Large	200/ 1,100	200/ 1,100	200/ 1,200	200 / 1,200	200 / 1,100	200/ 1,100	-

Table E4 Unit production costs for hydrogen production plants (Almansoori, 2006; DECC, 2012b).

		UPC_{jpi} ($ kg^{-1})						
		Production technology (*j*)						
Product type (*i*)	**Plant size (*p*)**	**SMR**	**SMR CCS**	**CG**	**CG CCS**	**BG**	**BG CCS**	**Electro**
LH_2	Distr	-	-	-	-	-	-	-
	Small	6.09	-	-	-	-		8.94
	Medium	2.94	3.17	-	-	2.98	3.18	6.37
	Large	2.36	2.45	2.11	2.18	2.3	2.38	-
GH_2	Distr	3.87	-	-	-	-	-	5.86
	Small	3.28	-	-	-	-	-	5.62
	Medium	1.94	2.17	-	-	1.89	2.09	5.09
	Large	1.79	1.88	1.42	1.5	1.64	1.71	-

Table E5 Parameters for transportation modes (Almansoori and Shah, 2009; Krewitt and Schmid, 2005).

Parameter	**Unit**	**LH_2 Tanker**	**GH_2 Trailer**
Driver wage (DW_{il})	$ h^{-1}	23.00	23
Fuel economy (FE_{il}^{L} , FE_{il}^{R})	km l^{-1}	2.30	2.3
Fuel price (FP_{il})	$ l^{-1}	2.25	2.3
General expenses (GE_{il})	$/d^{-1}	8.22	8.2
Load/Unload time (LUT_{il})	h	2.00	0.25
Maintenance expenses (ME_{il})	$ km^{-1}	0.1	0.1
Minimum/maximum flow rate ($Q_{il}^{\min}$ / $Q_{il}^{\max}$)	kg d^{-1}	3370/ 1,100,000	250/ 1,100,000
Average speed (SP_{il}^{L} , SP_{il}^{R})	km h^{-1}	55	55
Capacity ($TCAP_{il}$)	kg mode^{-1}	3370	250
Local availability (TMA_{il}^{L})	h d^{-1}	15	15
Regional availability (TMA_{il}^{R})	h d^{-1}	18	18
Capital cost (TMC_{il})	$ mode^{-1}	775,000	460,000

Table E6 Parameters for storage facilities (Steward and Ramsden, 2008).

Parameter	**Size**	**Unit**	**LH_2**	**GH_2**
Minimum Capacity ($SCAP_{spi}^{min}$)	Small	kg d^{-1}	0	0
	Medium		10,000	380
	Large		200,000	5,010
Maximum Capacity ($SCAP_{spi}^{max}$)	Small	kg d^{-1}	9,500	370
	Medium		150,000	5,000
	Large		540,000	25,000
Capital Costs (SCC_{spi})	Small	$	2,069,829	639,000
	Medium		7,862,044	7,851,000
	Large		25,526,292	38,868,000
Unit Cost (USC_{spi})	Small	$ d^{-1}	0.02698	0.27926
	Medium		0.00635	0.18972
	Large		0.00569	0.18712

Table E7 Parameters for filling stations.

Parameter	Unit	Size	LH_2 (Tanker)	GH_2 (Trailer)	GH_2 (Distributed)
Maximum Capacity ($FCAP_{fpi}^{max}$)	kg d^{-1}	Small	325	325	n.a.
		Medium	750	750	n.a.
		Large	1,500	1,500	1,500
Capital costs ($FSCC_{fpi}$)	$	Small	318,000	234,000	n.a.
		Medium	637,000	499,000	n.a.
		Large	1,274,000	998,000	2,607,000

Table E8 Technological specifications of filling stations.

	LH_2 (Tanker)			**GH_2 (Distr)**	**GH_2 (Trailer)**		
	Small	Medium	Large	Large	Small	Medium	Large
Maximum throughput (kg d^{-1})	325	750	1,500	1,500	325	750	1,500
Served cars per day	72	167	333	333	72	167	333
Dispensers	2	3	6	6	2	3	6
Gas compressors required	0	0	0	2	1	1	2
Gas compressor throughput (kg/h per compressor)	0	0	0	63	27	63	63
High pressure storage (kg)	38	75	150	150	0	0	0
Low pressure storage (kg)	0	0	0	1,500	0	0	0
Liquid H_2 storage (kg)	2,250	4,500	9,000	0	0	0	0
Evaporator unit (kg d^{-1})	375	750	1,500	0	0	0	0
Cryogenic compressors	1	1	1	0	0	0	0
Cryogenic compressor power (kW)	17.5	35	70	0	0	0	0

E.3 CCS Parameters

Table E9 CO_2 emissions from electricity (Dodds and McDowall, 2012).

Year	Emission Factors (gCO_2/kWh)
2020	391
2025	235
2030	168
2035	102
2040	69
2045	45
2050	26
2055	26
2060	26

Table E10 Reservoirs modelled in this study and related collection points (DECC, 2010b).

Reservoir	Collection Points
UK Northern and Central North	North Eastern
UK Southern North Sea	East Anglia
East Irish Sea	Merseyside

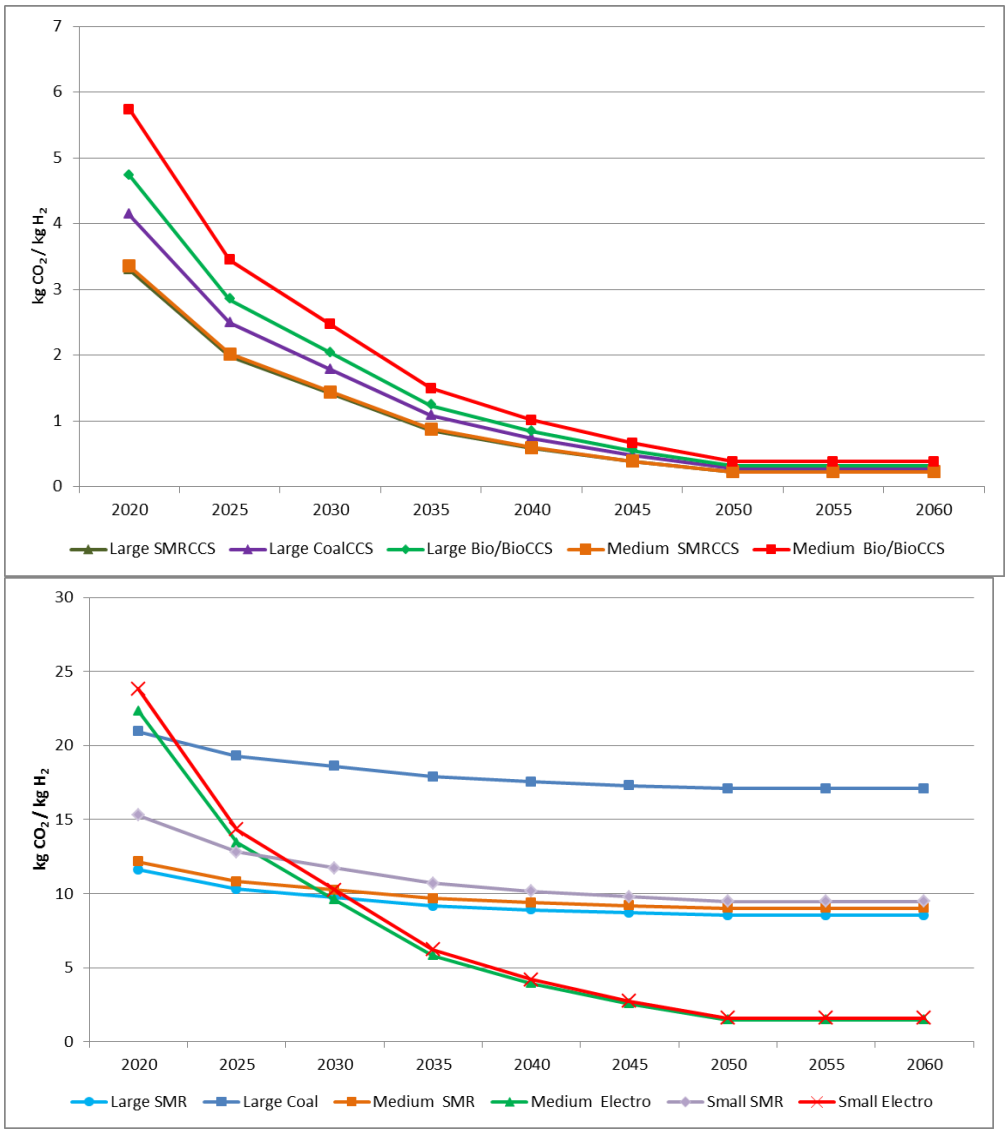

Figure E1 CO_2 emissions from technologies producing hydrogen in liquid form (ye_{jpit}) (Dodds and McDowall, 2012; NRC and NAE, 2004).

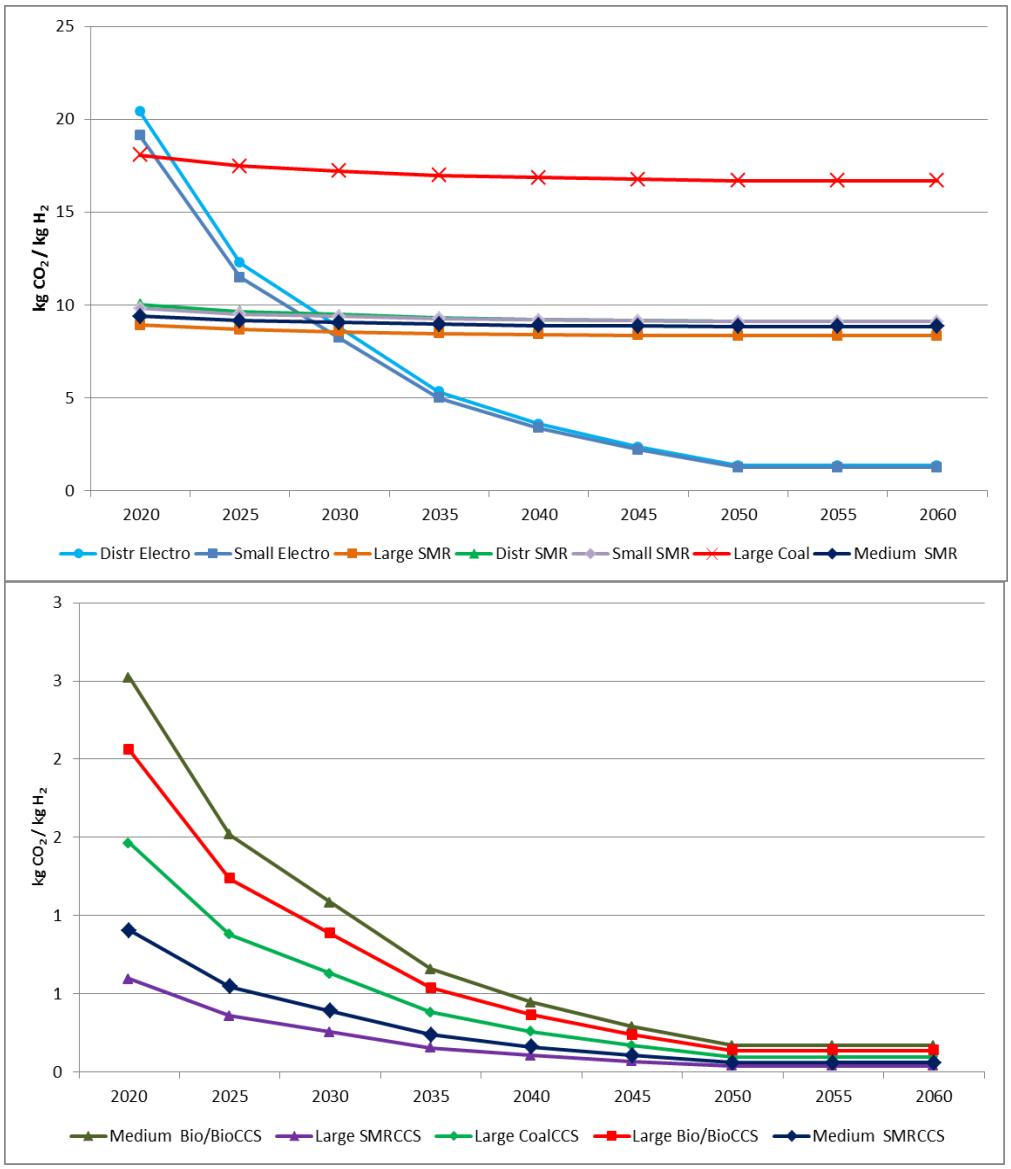

Figure E2 CO_2 emissions from technologies producing hydrogen in gaseous form (ye_{jpit}) (Dodds and McDowall, 2012; NRC and NAE, 2004).

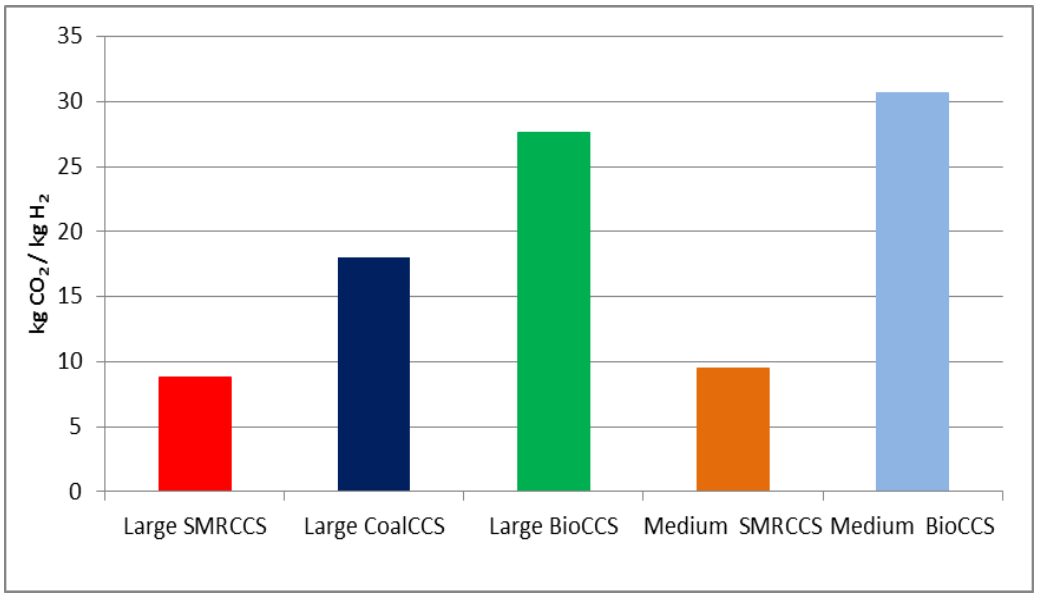

Figure E3 CO_2 sequestered from technologies producing hydrogen (γc_{jpit}) (Dodds and McDowall, 2012; NRC and NAE, 2004).

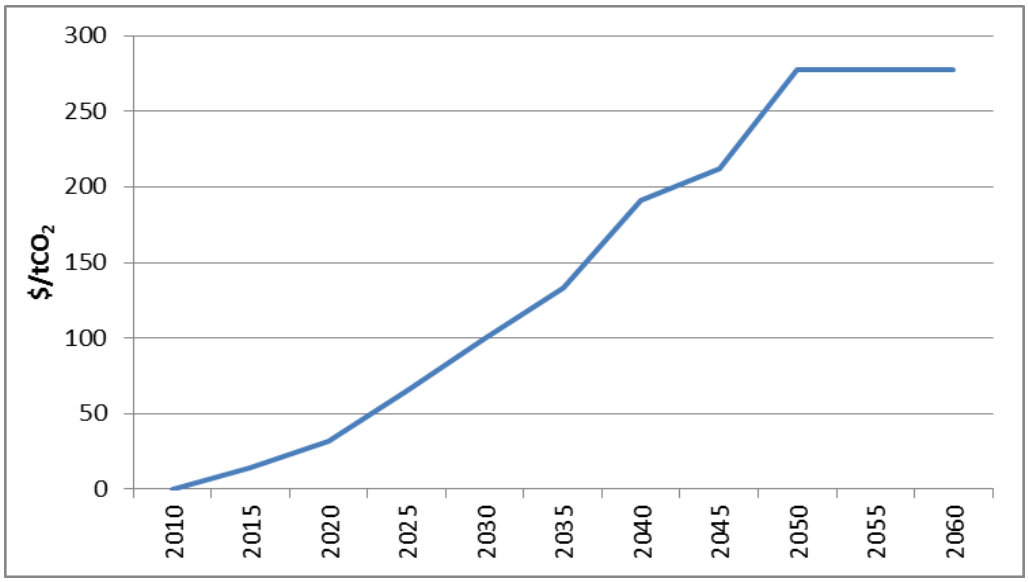

Figure E4 CO_2 tax, in £/t CO_2, used in this study (CT_t).

E.4 Economic Parameters

In this study, it is assumed that capital investment costs are incurred at the beginning of each time period whereas the operating costs are discounted on a yearly basis. Therefore the discount factors for the plant capital costs ($DFCAP_t$) and for the operating costs is given by ($DFOC_t$):

$$DFCAP_t = \frac{1}{(1+r)^{5t-5}} \quad \forall t \in T \tag{E.1}$$

$$DFOC_t = \frac{1}{(1+r)^{5t-5}} + \frac{1}{(1+r)^{5t-4}} + \frac{1}{(1+r)^{5t-3}} + \frac{1}{(1+r)^{5t-2}} + \frac{1}{(1+r)^{5t-1}} \quad \forall t \in T \tag{E.2}$$

where r is the interest rate and t is the time period. The interest rate used in this study is 5%.

Appendix F Publications

The following is the list of the publications arising from the work in this thesis:

Articles in Refereed Journals

[1] Akgul, O., Zamboni, A., Bezzo, F., Shah, N., Papageorgiou, L. G. (2011) Optimization-based approaches for bioethanol supply chains. *Industrial Engineering & Chemistry Research*, 50 (9), 4927–4938.

[2] Akgul, O., Shah, N., Papageorgiou, L. G. (2012) Economic optimisation of a UK advanced biofuel supply chain. *Biomass and Bioenergy*, 41, 57-72.

[3] Akgul, O., Shah, N., Papageorgiou, L. G. (2012) An optimisation framework for a hybrid first/second generation bioethanol supply chain. *Computers & Chemical Engineering*, 42, 101-114.

[4] Agnolucci, P., Akgul, O., McDowall, W., Papageorgiou, L. G. (2013) The importance of economies of scale, transport costs and demand patterns in optimising hydrogen fuelling infrastructure: an exploration with SHIPMod (spatial hydrogen infrastructure planning model). *International Journal of Hydrogen Energy*, 38 (26), 11189–11201.

[5] Akgul, O., Mac Dowell, N., Shah, N., Papageorgiou, L. G. (2013) Carbon negative electricity production in the UK - can UK power generation become a carbon sink?. *International Journal of Greenhouse Gas Control*, Submitted for publication.

Articles in Refereed Conference Proceedings

[6] Akgul, O., Shah, N., Papageorgiou, L. G. (2010) Optimisation-based approaches for bioethanol supply chains. *7th International Conference on Computational Management Science*, Austria.

[7] Akgul, O., Shah, N., Papageorgiou, L. G. (2011) An MILP model for the strategic design of the UK bioethanol supply chain. In: Pistikopoulos, E. N. and Georgiadis, M. C. and Kokossis, A. C. (eds.) *21st European Symposium on Computer*

Aided Process Engineering, Computer Aided Chemical Engineering, vol. 29. Greece: Elsevier. pp. 1799-1803.

[8] Akgul, O., Shah, N., Papageorgiou, L. G. (2011) Optimisation of hybrid first/second generation biofuel supply chains. *10th International Conference on Sustainable Energy Technologies*, Turkey.

[9] Akgul, O., Shah, N., Papageorgiou, L. G. (2012) Optimisation of integrated first/second generation biofuel supply chains. *9th International Conference on Computational Management Science*, UK.

[10] Akgul, O., Mac Dowell, N., Shah, N., Papageorgiou, L. G. (2012) Optimisation of bioelectricity supply chains. *AIChE Annual Meeting*, *USA.*

[11] Akgul, O., Shah, N., Papageorgiou, L. G. (2012) A spatially-explicit, multi-period MILP modelling framework for the optimal design of a hybrid biofuel supply chain. *22nd European Symposium on Computer Aided Process Engineering*, UK.

References

Achour, M. H., Haroun, A. E., Schult, C. J., Gasem, K. A. M. (2005) A new method to assess the environmental risk of a chemical process. *Chemical Engineering and Processing*, 44 (8), 901-909.

Acquaye, A. A., Wiedmann, T., Feng, K., Crawford, R. H., Barrett, J., Kuylenstierna, J., Duffy, A. P., Koh, S. C. L., McQueen-Mason, S. (2011) Identification of 'carbon hot-spots' and quantification of GHG intensities in the biodiesel supply chain using hybrid LCA and structural path analysis. *Environmental Science & Technology*, 45 (6), 2471-2478.

Agnolucci, P., McDowall, W. (2013) Designing future hydrogen infrastructure: insights from analysis at different spatial scales. *International Journal of Hydrogen Energy*, 38 (13), 5181-5191.

Allen, D., Shonnard, D. (2001) Green engineering: environmentally conscious design of chemical processes and products. *AlChE Journal*, 47 (9), 1906-1910.

Almansoori, A. (2006) Design and operation of a future hydrogen supply chain. Thesis (Ph.D.), Imperial College London.

Almansoori, A., Shah, N. (2006) Design and operation of a future hydrogen supply chain: snapshot model. *Chem. Engineering Research and Design*, 84 (6), 423-438.

Almansoori, A., Shah, N. (2009) Design and operation of a future hydrogen supply chain: multi-period model. *International Journal of Hydrogen Energy*, 34 (19), 7883–7897

Almansoori, A., Shah, N. (2012) Design and operation of a stochastic hydrogen supply chain network under demand uncertainty. *International Journal of Hydrogen Energy*, 37 (5), 3965-3977.

Bai, Y., Hwang, T., Kang, S., Ouyang, Y. (2011) Biofuel refinery location and supply chain planning under traffic congestion. *Transportation Research Part B: Methodological*, 45 (1), 162-175.

References

Bake, J. D. W., Junginger, M., Faaij, A., Poot, T., Walter, A. (2009) Explaining the experience curve: cost reductions of Brazilian ethanol from sugarcane. *Biomass & Bioenergy*, 33 (4), 644-658.

Bakshi, B. R. (2002) Explaining the experience curve: cost reductions of Brazilian ethanol from sugarcane. *Computers & Chemical Engineering*, 26, 269-282.

BBC (2010) EU considers general carbon tax. **[**online]. Available from: http://news.bbc.co.uk/1/hi/8552604.stm [Accessed September 2013].

Beamon, B. M. (2005) Environmental and sustainability ethics in supply chain management. *Science and Engineering Ethics*, 11 (2), 221-234.

Bersani, C., Minciardi, R., Sacile, R., Trasforini, E. (2009) Network planning of fuelling service stations in a near-term competitive scenario of the hydrogen economy. *Socio-Economic Planning Sciences*, 43 (1), 55-71.

BFIN Bioenergy conversion factors. [online]. Available from: https://bioenergy.ornl.gov/papers/misc/energy_conv.html [Accessed September 2013].

Bowling, I. M., Ponce - Ortega, J. M., El-Halwagi, M. M. (2011) Facility location and supply chain optimization for a biorefinery. *Industrial & Engineering Chemistry Research*, 50 (10), 6276-6286.

Brey, J. J., Brey R., Carazo A. F., Contreras I., Hernandez-Diaz, A. G., Gallardo, V. (2006) Designing gradual transition to hydrogen economy in Spain. *Journal of Power Sources*, 159 (2), 1231-1240.

Bryngelsson, D. K., Lindgren, K. (2013) Why large-scale bioenergy production on marginal land is unfeasible: a conceptual partial equilibrium analysis. *Energy Polic*y, 55, 454-466.

BusinessGreen (2010) UK carbon tax could reach £40 a tonne by 2020. **[**online]. Available from: http://www.businessgreen.com/bg/news/1933187/uk-carbon-taxreach-gbp40-tonne-2020 [Accessed September 2013].

References

CEBR (2010) The economic value of the woodfuel industry to the UK economy by 2020. **[**online]. Available from: http://www.biomassenergycentre.org.uk/portal/page?_pageid=75,517181&_dad=portal&_schema=PORTAL [Accessed September 2013].

Chan, H.K., Wang, X., White, G.R.T., Yip,N. (2013) An extended fuzzy-AHP approach for the evaluation of green product designs. *IEEE Ttansactions on Engineering Management*, 60 (2), 327-339.

Chen, C. W., Fan, Y. Y. (2012) Bioethanol supply chain system planning under supply and demand uncertainties. *Transportatıon Research Part E-Logıstıcs And Transportatıon Revıew*, 48 (1), 150-164.

Cherubini, F., Bird, N. D., Cowie, A., Jungmeier, G., Schlamadinger, B., Woess-Gallasch, S. (2009) Energy- and greenhouse gas-based LCA of biofuel and bioenergy systems: key issues, ranges and recommendations. *Resources, Conservation and Recycling*, 53 (8), 434-447.

Cherubini, F., Jungmeier, G. (2010) LCA of a biorefinery concept producing bioethanol, bioenergy, and chemicals from switchgrass. *Internatıonal Journal Of Life Cycle Assessment*, 15 (1), 53-66.

Chunshan, L Zhang, X., Zhang, S., Suzuki, K. (2009) Environmentally conscious design of chemical processes and products: multi-optimization method. *Chemical Engineering Research & Design*, 87 (2), 233-243.

Clarke, D., Jablonski, S., Moran, B., Anandarajah, G., Taylor, G. (2009) How can accelerated development of bioenergy contribute to the future UK energy mix? Insights from a MARKAL modelling exercise. *Biotechnology for Biofuels*, 2:13.

CMU Integrated Environmental Control Model (IECM). **[**online]. Available from: http://www.cmu.edu/epp/iecm [Accessed September 2013].

Corbiere-Nicollier T., Blanc I., Erkman S. (2011) Towards a global criteria based framework for the sustainability assessment of bioethanol supply chains: application

to the Swiss dilemma: is local produced bioethanol more sustainable than bioethanol imported from Brazil?. *Ecological Indicators*, 11 (5), 1447-1458.

Corsano, G., Vecchietti, A. R., Montagna, J. M. (2011) Optimal design for sustainable bioethanol supply chain considering detailed plant performance model. *Computers & Chemical Engineering*, 35 (8), 1384-1398.

Cucek, L., Varbanov, P. S., Klemes, J., Kravanja, Z. (2012) Total footprints-based multi-criteria optimisation of regional biomass energy supply chains. *Energy*, 44 (1), 135-145.

Dal-Mas M., Giarola S., Zamboni A., Bezzo F. (2011) Strategic design and investment capacity planning of the ethanol supply chain under price uncertainty. *Biomass and Bioenergy*, 35 (5), 2059–2071.

Davidon, W.C. (1959) Variable metric method for minimization. *Argonne National Laboratory Report* ANL-5990.

DECC (2010a) Biomass prices in the heat and electricity sectors in the UK. **[**online]. Available from: http://www.rhincentive.co.uk/library/regulation/100201Biomass_prices.pdf [Accessed September 2013].

DECC (2010b) CO_2 storage in the UK - ındustry potential. **[**online]. Available from: http://www.ukccsrc.ac.uk/system/files/10D512.pdf [Accessed September 2013].

DECC (2010c) Guidance on estimating carbon values beyond 2050: an interim approach. **[**online]. Available from: https://www.gov.uk/government/publications/guidance-on-estimating-carbon-values-beyond-2050-an-interim-approach [Accessed September 2013].

DECC (2011a) DECC coal price projections. **[**online]. Available from: http://www.ukccsrc.ac.uk/system/files/11D875.pdf [Accessed September 2013].

DECC (2011b) Planning our electric future: a white paper for secure, affordable and low‑carbon electricity. **[**online]. Available from:

https://www.gov.uk/government/uploads/system/uploads/attachment_data/file/48129/2176-emr-white-paper.pdf [Accessed September 2013].

DECC (2012a) Digest of United Kingdom energy statistics. **[**online]. Available from: https://www.gov.uk/government/uploads/system/uploads/attachment_data/file/65881/5949-dukes-2012-exc-cover.pdf [Accessed September 2013].

DECC (2012b) Quarterly Energy Prices. **[**online]. Available from: https://www.gov.uk/government/organisations/department-of-energy-climatechange/series/quarterly-energy-prices [Accessed September 2013].

DECC (2012c) Technology innovation needs assessments: carbon capture and storage in the power sector summary report, Available from: http://www.lowcarboninnovation.co.uk/working_together/technology_focus_areas/carbon_capture_and_storage/ [Accessed September 2013].

DECC (2012d) UK Renewable energy roadmap update. **[**online]. Available from: https://www.gov.uk/government/uploads/system/uploads/attachment_data/file/80246/11-02-13_UK_Renewable_Energy_Roadmap_Update_FINAL_DRAFT.pdf [Accessed September 2013].

DEFRA (2007) Change in the area and disrtibution of set-aside in England and its environmental impact. **[**online]. Available from: http://archive.defra.gov.uk/evidence/statistics/foodfarm/enviro/observatory/research/documents/observatory08.pdf [Accessed September 2013].

DEFRA (2009) Solid recovered fuel regional assessments. **[**online]. Available from: http://archive.defra.gov.uk/environment/waste/residual/widp/documents/SRF-Hull-East-Riding.pdf [Accessed September 2013].

DEFRA (2010) Cereals and oilseed rape production. **[**online]. Available from: http://webarchive.nationalarchives.gov.uk/20130123162956/http:/www.defra.gov.uk/evidence/statistics/foodfarm/food/cereals/documents/cyield_c.xls [Accessed September 2013].

References

DEFRA (2012) UK bioenergy strategy. [online]. Available from: https://www.gov.uk/government/uploads/system/uploads/attachment_data/file/48337/5142-bioenergy-strategy-.pdf [Accessed September 2013].

DFT (2012) Road traffic estimates 2011. **[**online]. Available from: https://www.gov.uk/government/publications/road-traffic-estimates-2011 [Accessed September 2013].

Diabat, A, Simchi-Levi, D. (2009) A carbon-capped supply chain network problem. *International Conference on Industrial Engineering and Engineering Management (IEEM)*, 523-527.

Diabat, A., Abdallah, T., Al-Refaie, A., Svetinovic, D., Govindan, K. (2013) Strategic closed-loop facility location problem with carbon market trading. *IEEE Ttansactions on Engineering Management*, 60 (2), 398-408.

Dodds, P. E., McDowall, W. A. S. (2012) Hydrogen transitions in the UK: an economic appraisal from an energy systems perspective. *Proceedings of World Hydrogen Energy Conference*.

DRDNI (2009) Traffic and Travel Information Report 2009. **[**online]. Available from: http://www.drdni.gov.uk/index/freedom_of_information/customer_information/doc-details.htm?docid=7271 [Accessed September 2013].

DTI (2003) Technology status review and carbon abatement potential of renewable transport fuels in the UK. **[**online]. Available from: http://www.fcrn.org.uk/sites/default/files/DTI_Technology_status_review.pdf [Accessed September 2013].

DTI (2006) Industrial carbon dioxide emissions and carbon dioxide storage potential in the UK. **[**online]. Available from: http://nora.nerc.ac.uk/4837/1/CR06185N.pdf [Accessed September 2013].

Duer, H., Christensen, P. O. (2010) Socio-economic aspects of different biofuel development pathways. *Biomass & Bioenergy*, 34 (2), 237-243.

References

Dunnett, A., Adjiman, C., Shah, N. (2007) Biomass to heat supply chains: applications of process optimization. *Process Safety and Environmental Protection*, 85 (5), 419-429.

Dunnett, A., Shah, N. (2007) Prospects for Bioenergy. *Biobased Materials and Bioenergy*, 1, 1-18.

Dunning, J. H. (1980) Towards an eclectic theory of ınternational production: some empirical tests. *Journal of International Business Studies*, 11 (1), 9-31

Dyken, S. V., Bakken, B. H., Skjelbred, H. I. (2010) Linear mixed-integer models for biomass supply chains with transport, storage and processing. *Energy*, 35 (3), 1338-1350.

E.ON UK Ratcliffe-on-Soar. **[**online]. Available from: http://www.eon-uk.com/560.aspx [Accessed September 2013].

EC (2008) HyWays The European Hydrogen Roadmap. **[**online]. Available from: ftp://ftp.cordis.europa.eu/pub/fp7/energy/docs/hyways-roadmap_en.pdf [Accessed September 2013].

EC (2003) Directive 2003/30/EC of the European Parliament and of the Council of 8 May 2003 on the Promotion of the Use of Biofuels or Other Renewable Fuels for Transport.
[online]. Available from: http://eurlex.europa.eu/LexUriServ/LexUriServ.do?uri=OJ:L:2003:123:0042:0042:EN:PDF [Accessed September 2013].

EC (2009) Directive 2009/28/EC of the European Parliament and of the Council of 23 April 2009 on the Promotion of the Use of Energy from Renewable Sources and Amending and Subsequently Repealing Directives 2001/77/EC and 2003/30/EC. **[**online]. Available from: http://eurlex.europa.eu/LexUriServ/LexUriServ.do?uri=OJ:L:2009:140:0016:0062:EN:PDF [Accessed September 2013].

EC (2010) Communication from the Commission on the Practical Implementation of

the EU Bioliquids Sustainability Scheme and on Counting Rules for Biofuels. **[**online]. Available from: http://eurlex.europa.eu/LexUriServ/LexUriServ.do?uri=OJ:C:2010:160:0008:0016:EN:PDF [Accessed September 2013].

EC Joint Research Centre (2006) Well-to-Wheels analysis of future automotive fuels and powertrains in the European context. **[**online]. Available from: http://ies.jrc.ec.europa.eu/uploads/media/WTT_Report_010307.pdf [Accessed September 2013].

Edgar, T. F., Himmelblau, D. M., Lasdon, L. S. (2001) Optimization of chemical processes. 2nd ed. New York: McGraw-Hill.

Eksioglu, S. D., Acharya, A., Leightley, L. E., Arora, S. (2009) Analyzing the design and management of biomass-to-biorefinery supply chain. *Computers & Industrial Engineering*, 57 (4), 1342-1352.

Elia, J. A., Baliban, R. C., Floudas, C. A., Gurau, B., Weingarten, M. B., Klotz, S. D. Hardwood biomass to gasoline, diesel, and jet fuel: 2. Supply chain optimization framework for a network of thermochemical refineries. *Energy & Fuels*, 2013, 27 (8), 4325-4352.

EPA (2006) Life cycle assessment: principles and practice. **[**online]. Available from: http://www.epa.gov/nrmrl/std/lca/pdfs/chapter1_frontmatter_lca101.pdf [Accessed September 2013].

EPI (2011) Climate, energy, and transportation. [online]. Available from: http://www.earth-policy.org/datacenter/xls/book_wote_energy_biofuels.xls [Accessed September 2013].

Ericsson, K., Rosenqvist, H., Nilsson, L.J. (2009) Energy crop production costs in the EU. *Biomass and Bioenergy*, 33 (11), 1577-1586.

ETSAP (2004) Documentation for the MARKAL family of models. **[**online]. Available from:

http://www.iea-etsap.org/web/MrklDoc-I_StdMARKAL.pdf [Accessed September 2013].

Eunomia Costs for municipal waste management in the EU. **[**online]. Available from: http://ec.europa.eu/environment/waste/studies/pdf/eucostwaste.pdf [Accessed September 2013].

Eurostat Population statistics. **[**online]. Available from: http://epp.eurostat.ec.europa.eu/portal/page/portal/hicp/introduction [Accessed September 2013].

Ewing, G., Sarigollu, E. (2000) Assessing consumer preferences for clean-fuel vehicles: a discrete choice experiment. *Journal of Public Policy and Marketing*,19 (1), 106-118.

Farmers Guardian (2008) UK has capacity to produce extra 15.7 million tonnes of biomass. **[**online]. Available from: http://www.farmersguardian.com/uk-has-capacity-to-produce-extra-157million-tonnes-of-biomass/20848.article [Accessed September 2013].

Fuss, S. (2012) BECCS status and gaps: results from the IEA-IIASA Workshop on BECCS. [online]. Available from: http://www.iea.org/media/workshops/2012/bioenergyccsandbeccs/1IIASA_BECCS_wksp_Laxenburg.pdf [Accessed September 2013].

Gan, J., Smith, C. T. (2011) Optimal plant size and feedstock supply radius: a modelling approach to minimize bioenergy production costs. *Biomass and Bioenergy*, 35 (8), 3350-3359.

Giarola S., Zamboni A., Bezzo F. (2011) Spatially explicit multi-objective optimisation for design and planning of hybrid first and second generation biorefineries. *Computers & Chemical Engineering*, 35 (9), 1782-1797.

References

Giarola, S., Shah, N., Bezzo, F. (2012a) A comprehensive approach to the design of ethanol supply chains including carbon trading effects. *Bioresource Technology*, 107, 175-185.

Giarola, S., Zamboni, A., Bezzo, F. (2012b) Environmentally conscious capacity planning and technology selection for bioethanol supply chains. *Renewable Energy*, 43, 61-72.

Gnansounou, E., Dauriat A., Villegas J., Panichelli L. (2009) Life cycle assessment of biofuels: energy and greenhouse gas balances. *Bioresource Technology*, 100 (21), 4919-4930.

Gomory, R.E. (1958) Outline of an algorithm for integer solutions to linear programs. *Bulletin of the American Mathematical Society*, 64, 275–278.

Gough, C., Upham, P. (2011) Biomass energy with carbon capture and storage (BECCS or Bio-CCS). *Greenhouse gases: Science and Technology*, 1 (4), 324-334.

Grubler, A., Nakicenovic, N., Victor, D. G. (1999) Dynamics of energy technologies and global change. *Energy Policy*, 27, 247-280.

Guillen-Gosalbez, G., Grossmann, I. E. (2009) Optimal design and planning of sustainable chemical supply chains under uncertainty. *AlChE Journal*, 55 (1), 99-121.

Guillen-Gosalbez, G., Mele, F. D., Grossmann, I. E. (2010) A bi-criterion optimization approach for the design and planning of hydrogen supply chains for vehicle use. *AIChE Journal*, 56 (3), 650–667.

Gurel S, Akturk M. S. (2007) Optimal allocation and processing time decisions on non-identical parallel CNC machines: ε-constraint approach. *European Journal of Operational Research*, 183 (2), 591-607.

Han, J. H., Ryu, J. H., Lee I. B. (2012) Modeling the operation of hydrogen supply networks considering facility location. *International Journal of Hydrogen Energy*, 37 (6), 5328-5346.

References

Harvard Green Campus Initiative Biomass fact sheet. **[**online]. Available from: http://green.harvard.edu/sites/default/files/attachments/renewables/biomass-fact-sheet.pdf [Accessed September 2013].

Helm, D. (2012) The carbon crunch: how we're getting climate change wrong - and how to fix it. New Haven: Yale University Press.

Hettinga, W. G., Junginger, H. M., Dekker, S. C., Hoogwijk, M., McAloon, A.J., Hicks, K.B. (2009) Understanding the reductions in US corn ethanol production costs: an experience curve approach. *Energy Policy*, 37 (1), 190-203.

HGCA (2010) Outlook for the UK grain market. **[**online]. Available from: http://smartstore.bpex.org.uk/articles/dodownload.asp?a=smartstore.bpex.org.uk.15.4.2010.14.27.0.pdf&i=300206 [Accessed September 2013].

Huang, Y., Chen, C., Fan, Y. (2010) Multistage optimization of the supply chains of biofuels. *Transportation Research Part E: Logistics and Transportation Review*, 46 (6), 820–830**.**

Hugo, A., Rutter, P., Pistikopoulos, S., Amorelli, A., Zoia, G. (2005) Hydrogen infrastructure strategic planning using multi-objective optimization. *International Journal of Hydrogen Energy*, 30 (15), 1523-1534.

Hydrogen Analysis Resource Center (2008) Lower and higher heating values of hydrogen and fuels. **[**online]. Available from: http://hydrogen.pnl.gov/cocoon/morf/projects/hydrogen/datasheets/lower_and_higher_heating_values.xls [Accessed September 2013].

Iaquaniello, G., Giacobbe, F., Morico, B., Cosenza, S., Farace, A. (2008) Membrane reforming in converting natural gas to hydrogen: production costs, Part II. *International Journal of Hydrogen Energy*, 33 (22), 6595-6601.

IEA (2006) IEA Bioenergy Task 40-Sustainable international bioenergy trade: securing supply and demand. **[**online]. Available from: http://www.fao.org/uploads/media/0611_IEA_Task_40_-_Technology_report.pdf [Accessed September 2013].

References

IEA (2007) Energy security and climate policy. **[**online]. Available from: http://www.iea.org/publications/freepublications/publication/energy_security_climate_policy.pdf [Accessed September 2013].

IEA (2008) From 1st- to 2nd- generation biofuel technologies. [online]. Available from: http://www.iea.org/publications/freepublications/publication/2nd_Biofuel_Gen.pdf [Accessed September 2013].

IEA (2010a) Roadmap background information: biofuels for transport **[**online]. Available from: http://www.iea.org/Papers/2010/biofuels_roadmap.pdf [Accessed September 2013].

IEA (2010b) World Energy Outlook 2010-Chapter 7 Renewable energy outlook. **[**online]. Available from: http://www.iea.org/publications/freepublications/publication/weo2010.pdf [Accessed September 2013].

IEA (2011) Technology roadmap biofuels for transport. **[**online]. Available from: http://www.iea.org/publications/freepublications/publication/biofuels_roadmap.pdf [Accessed September 2013].

IEA (2012a) IEA Bioenergy - Task 42 Biorefinery: biobased chemicals - value added products from biorefineries. **[**online]. Available from: http://www.nnfcc.co.uk/tools/iea-bioenergy-task-42-biorefinery-biobased-chemicals-value-added-products-from-biorefineries [Accessed September 2013].

IEA (2012b) Key world energy statistics. **[**online]. Available from: http://www.iea.org/publications/freepublications/publication/kwes.pdf [Accessed September 2013].

IEA (2012c) Renewable energy outlook. **[**online]. Available from: http://www.worldenergyoutlook.org/media/weowebsite/2012/WEO2012_Renewables.pdf [Accessed September 2013].

References

IEA (2012d) Technology roadmap bioenergy for heat and power. **[**online]. Available from: http://www.iea.org/publications/freepublications/publication/bioenergy.pdf [Accessed September 2013].

IEF (2010) Assessment of biofuels potential and limitations. **[**online]. Available from: http://www.ief.org/_resources/files/content/news/presentations/ief-report-biofuels-potentials-and-limitations-february-2010.pdf [Accessed September 2013].

Ingason, H. T., Ingolfsson, H. P., Jensson P. (2008) Optimizing site selection for hydrogen production in Iceland. *International Journal of Hydrogen Energy*, 33 (14), 3632-3643.

IPCC (2005) Carbon dioxide capture and storage. **[**online]. Available from: http://www.ipcc-wg3.de/special-reports/special-report-on-carbon-dioxide-capture-and-storage [Accessed September 2013].

IPCC (2007) Climate change 2007: synthesis report. **[**online]. Available from: http://www.ipcc.ch/publications_and_data/publications_ipcc_fourth_assessment_report_synthesis_report.htm [Accessed September 2013].

Iriarte, A., Rieradevall, J., Gabarrell, X. (2012) Transition towards a more environmentally sustainable biodiesel in South America: the case of Chile. *Applied Energy*, 91 (1), 263-273.

ITF (2010) Reducing transport greenhouse gas emissions. **[**online]. Available from: http://www.internationaltransportforum.org/Pub/pdf/10GHGTrends.pdf [Accessed September 2013].

Johnson, N., Ogden, J. (2012) A spatially-explicit optimisation model for long-term hydrogen pipeline planning, *International Journal of Hydrogen Energy*, 37 (6), 5421-5433.

Kamarudin, S. K., Daud W. R. W., Yaakub, Z., Misron, Z., Anuar, W., Yusuf, N. N. A. N. (2009) Synthesis and optimization of future hydrogen energy infrastructure

planning in Peninsular Malaysia. *International Journal of Hydrogen Energy*, 2009, 34 (5), 2077-2088.

Karmarkar, N. (1984) A new polynomial-time algorithm for linear programming. *Combinatorica*, 4, 373–395.

Kelloway, A., Marvin, W. A., Daoutidis, P. (2012) Optimization of a distributed small scale biodiesel production system in Greater London**.** *22nd European Symposium on Computer Aided Process Engineering*, 30, 322-326.

Kim J., Lee Y, Moon, I. (2008a) Optimisation of a hydrogen supply chain under demand uncertainty. *International Journal of Hydrogen Energy*, 33 (18), 4715–4729.

Kim J., Moon, I. (2008b) Strategic design of hydrogen infrastructure considering cost and safety using multiobjective optimization. *International Journal of Hydrogen Energy*, 33 (21), 5887–5896.

Kim J., Realff M. J., Lee J. H. (2011a) Optimal design and global sensitivity analysis of biomass supply chain networks for biofuels under uncertainty. *Computers & Chemical Engineering*, 35 (9), 1738-1751.

Kim J., Realff M. J., Lee J. H., Whittaker C., Furtner L. (2011b) Design of biomass processing network for biofuel production using an MILP model. *Biomass Bioenergy*, 35 (2), 853-871.

Kim, J., Realff, M. J., Lee, J. H. (2010) Simultaneous design and operation decisions for biorefinery supply chain networks: centralized vs. distributed system. *Proceedings of the 9th International Symposium on Dynamics and Control of Process Systems*, 73-78.

Klemes, J., Pierucci, S., Worrell, E. (2007) Sustainable processes thorough LCA, process integration and optimal design. *Resources, Conservation and Recycling*, 50 (2), 115-121.

Kostin A. M., Guillen-Gosalbez G., Mele F. D., Bagajewicz, M. J., Jimenez L. (2012) Design and planning of infrastructures for bioethanol and sugar production

under demand uncertainty. *Chemical Engineering Research & Design*, 90 (3), 359-376.

Kretschmer, B., Narita, D., Peterson, S. (2009) The economic effects of the EU biofuel target. *Energy Economics*, 31 (2), S285-S294.

Krewitt, W., Schmid, S.A. (2005) Fuel cell technologies and hydrogen production/distribution options. **[**online]. Available from: http://www.dlr.de/fk/Portaldata/40/Resources/dokumente/publikationen/2005-09-02_CASCADE_D1.1_fin.pdf [Accessed September 2013].

Kuby, M., Lines, L., Schultz, R., Xie, Z., Kim, J. G., Lim, S. (2009) Optimization of hydrogen stations in Florida using the flow-refuelling location model. *International Journal of Hydrogen Energy*, 34 (15), 6045-6064.

Lam, H. L., Varbanov, P., Klemes, J. (2010) Minimising carbon footprint of regional biomass supply chains. *Resources, Conservation and Recycling*, 54 (5), 303-309.

Land, A. H., Doig, A. G. (1960) An automatic method of solving discrete programming problems. *Econometrica*, 28 (3), 497-520.

Larsen, H. N., Solli, C., Pettersena, J. (2012) Supply chain management - how can we reduce our energy/climate footprint?. *Energy Procedia*, 20, 354-363.

Leduc, S., Starfelt, F., Dotzauer, E., Kindermann, G., McCallum, I., Obersteiner, M., Lundgren, J. (2010) Optimal location of lignocellulosic ethanol refineries with polygeneration in Sweden. *Energy*, 35 (6), 2709–2716.

Li Z., Gao D., Chang L., Liu P., Pistikopoulos, E. N. (2008) Hydrogen infrastructure design and optimization: a case study of China. *International Journal of Hydrogen Energy*, 33 (20), 5275–5286.

Lin, Z. H., Ogden, J., Fan, Y. Y., Chen, C. W. (2008) The fuel-travel-back approach to hydrogen station siting. *International Journal of Hydrogen Energy*, 33 (12), 3096-3101.

References

Linton, J. D., Klassen, R., Jayaraman, V. (2007) Sustainable supply chains: an introduction. *Journal of Operations Management*, 25 (6), 1075-1082.

Mac Dowell, N., Florin, N., Buchard, A., Hallett, J., Galindo, A., Jackson, G., Adjiman, C. S., Williams, C. K. Shah, N., Fennell, P. (2010) An overview of CO_2 capture technologies. *Energy & Environmental Science*, 3 (11), 1645-1669.

Mann, M. K., Spath, P. L. (2001) A life cycle assessment of biomass cofiring in a coal-fired power plant. *Clean Products and Processes*, 3, 81−91.

Marvin W. A., Schmidt L. D., Benjaafar S., Tiffany D. G., Daoutidis P. (2012) Economic optimization of a lignocellulosic biomass-to-ethanol supply chain. *Chemical Engineering Sci*ence, 67 (1), 68-79.

Marvin, W. A., Schmidt, L. D., Daoutidis, P. (2013) Biorefinery location and technology selection through supply chain optimization**.** *Industrial & Engineering Chemistry Research*, 52 (9), 3192-3208.

McCartney, C. (2007) A feasibility study for small-scale wood pellet production in the Scottish Borders. **[**online]. Available from: http://www.energyfarming.org.uk/resources/Wood%20Pellet%20final%20report%20CM%20Nov07.pdf [Accessed September 2013].

McDowall, W. Validating hydrogen transitions with lessons from the past. Forthcoming.

McDowall, W., Dodds, P. E. (2012) A review of hydrogen end-use technologies for energy system models. *UKSHEC Working Paper*, UCL Energy Institute.

McGlashan, N., Shah, N., Caldecott, B., Workman, M. (2012) High-level techno-economic assessment of negative emissions technologies. *Process Safety & Environmental Protection*, 90 (6), 501-510.

McKechnie, J., Colombo, S., Chen, J., Mabee, W., MacLean, H. L. (2011) Forest bioenergy or forest carbon? Assessing trade-offs in greenhouse gas mitigation with wood-based fuels. *Environmental Science & Technology*, 45 (2), 789-795.

References

Melendez M., Milbrandt, A. (2006) Geographically based hydrogen consumer demand and infrastructure analysis. **[**online]. Available from: http://www.nrel.gov/hydrogen/pdfs/40373.pdf [Accessed September 2013].

Morrow, W. R., Griffin, W.M., Matthews, H. S. (2006) Modeling switchgrass derived cellulosic ethanol distribution in the United States. *Environmental Science and Technology*, 40 (9), 2877-2886.

Morrow, W. R. Griffin, W. M., Matthews, H. S. (2007) State-level infrastructure and economic effects of switchgrass cofiring with coal in existing power plants for carbon mitigation. *Environmental Science & Technology*, *41* **(**19), 6657-6662.

Murthy Konda, N. V. S. N., Shah, N., Brandon, N. P. (2011) Optimal transition towards a large-scale hydrogen infrastructure for the transport sector: the case for the Netherlands. *International Journal of Hydrogen Energy*, 36 (8), 4619-4635.

Naik, S. N., Goud, V. V., Rout, P. K., Dalai, A. K. (2010) Production of first and second generation biofuels: a comprehensive review. *Renewable & Sustainable Energy Reviews*, 14 (2), 578-597.

NEP (2010) Coordinated use of energy system models in energy and climate policy analysis. **[**online]. Available from: www.nordicenergyperspectives.org/modellrapport.pdf [Accessed September 2013].

NNFCC (2005) The biorefinery concept: a platform for the delivery of renewable chemicals. **[**online]. Available from: http://www.nnfcc.co.uk/publications/nnfcc-position-paper-the-biorefinery-concept-a-platform-for-the-delivery-of-renewables/at_download/file [Accessed September 2013].

NNFCC (2008a) Addressing the land use issues for non-food crops, in response to ıncreasing fuel and energy generation opportunities. **[**online]. Available from: http://www.nnfcc.co.uk/tools/addressing-the-land-use-issues-for-non-food-crops-in-response-to-increasing-fuel-and-energy-generation-opportunities-nnfcc-08-004 [Accessed September 2013].

References

NNFCC (2008b) Lignocellulosic ethanol plant in the UK-feasibility study. **[**online]. Available from: http://www.nnfcc.co.uk/tools/lignocellulosic-ethanol-plant-in-the-uk-feasibility-study-nnfcc-08-007 [Accessed September 2013].

NRC (2008) Transitions to alternative transportation technologies-a focus on hydrogen. Washington, D.C.: The National Academies Press.

NRC, NAE (2004) The hydrogen economy: opportunities, costs, barriers, and R&D needs. Washington, D.C.: The National Academies Press.

OFID (2009) Biofuels and food security. **[**online]. Available from: http://www.ofid.org/LinkClick.aspx?fileticket=4PjzcrL3584%3D&tabid=112&mid=552 [Accessed September 2013].

ONS (2012) Neighbourhood statists. **[**online]. Available from: http://neighbourhood.statistics.gov.uk/dissemination [Accessed September 2013].

Papageorgiou, L. G. (2009) Supply chain optimisation for the process industries: advances and opportunities. *Computers & Chemical Engineering*, 33 (12), 1931-1938.

Papageorgiou, L. G., Bogle, D., Dua, V. (2010) Advanced process engineering lecture notes, University College London.

Parker , N., Fan, Y., Ogden, J. (2010a) From waste to hydrogen: an optimal design of energy production and distribution network. *Transportation Research Part E*, 46 (4), 534-545.

Parker, N., Tittmann, P., Hart, Q., Nelson, R., Skog, K., Schmidt, A., Gray, E., Jenkins, B. (2010b) Development of a biorefinery optimized biofuel supply curve for the Western United States. *Biomass & Bioenergy*, 34 (11), 1597-1607.

Perez-Fortes, M., Laínez-Aguirre, J. M., Arranz-Piera, P., Velo, E., Puijganer L. (2012) Design of regional and sustainable bio-based networks for electricity generation using a multi-objective MILP approach. *Energy*, 44 (1), 79-95.

References

Ping, H., Zhang, D. K. (2008) The approach of green supply chain management for modern enterprises. *Logistics Research and Practice in China*, 104-109.

Ramudhin, A., Chaabane, A., Kharoune, M., Paquet, M. (2008) Carbon market sensitive green supply chain network design. *International Conference on Industrial Engineering and Engineering Management (IEEM)*, 1093-1097.

Rangaiah, G. P. (2009) Multi-objective optimization: techniques and applications in chemical engineering (Chapter 1). [online]. Available from: http://www.worldscientific.com/doi/suppl/10.1142/7088/suppl_file/7088_chap01.pdf [Accessed September 2013].

Rentizelas, A. A., Tatsiopoulos, I. P., Tolis A. (2009) An optimization model for multi-biomass tri-generation energy supply. *Biomass and Bioenergy*, 33 (2), 223-233.

RFA (2011) Carbon reporting - default values and fuel chains. **[**online]. Available from: http://webarchive.nationalarchives.gov.uk/20110407094507/http://www.renewablefuelsagency.gov.uk/page/guidance-v4 [Accessed September 2013].

Rogers, E. M. (2003) Diffusion of innovations. 5th ed. New York: Free Press.

Sabio N., Kostin A., Guillen-Gosalbez G., Jimenez, L. (2012) Holistic minimization of the life cycle environmental impact of hydrogen infrastructures using multi-objective optimisation and principal component analysis. *International Journal of Hydrogen Energy*, 37 (6), 5385-5405.

Sabio, N.; Gadalla, M., Guillen-Gosalbez, G., Jimenez, L. (2010) Strategic planning with risk control of hydrogen supply chains for vehicle use under uncertainty in operating costs: a case study of Spain. International Journal of Hydrogen Energy, 35 (13), 6836-6852.

Santibanez-Aguilar, J. E., Gonzalez-Campos, J. B., Ponce-Ortega, J. M., Serna-Gonzalez, M., El-Halwagi, M. M. (2011) Optimal planning of a biomass conversion

system considering economic and environmental aspects. *Industrıal & Engıneerıng Chemıstry Research* 50 (14), 8558-8570.

Savaskan, R. C., Bhattacharya, S., Van Wassenhove, L.N. (2004) Closed loop supply chain models with product remanufacturing. *Management Science*, 50 (2), 239-252.

Savills Research (2009) Agricultural land market survey. **[**online]. Available from: http://docs.savills.co.uk/campaign/research/SavillsAgriculturalLandMarketSurvey2009.pdf [Accessed September 2013].

Schulze, E., Korner, C., Law, B. E., Haberl, H., Luyssaert, S. (2012) Large-scale bioenergy from additional harvest of forest biomass is neither sustainable nor greenhouse gas neutral. *GCB Bioenergy*, 4 (6), 611-616.

SCROL (2012) Scotland‘s Census results online. **[**online]. Available from: http://www.scrol.gov.uk/scrol/common/home.jsp [Accessed September 2013].

Shah, N. (2005) Process industry supply chains: advances and challenges. *Computers & Chemical Engineering*, 29, 1225-1235.

Singh, A., Pant, D., Korres, N. E., Nizami, A. S., Prasad, S., Murphy, J. D. (2010) Key issues in life cycle assessment of ethanol production from lignocellulosic biomass: challenges and perspectives. *Bioresource Technology*, 101 (13), 5003-5012.

Srivastava, S. K. (2007) How green supply chain management: a state-of-the-art literature review. *International Journal of Management Reviews*, 9 (1), 53-80.

Steward, D., Ramsden, T. (2008) H2A production model, version 2 user guide. **[**online]. Available from: https://apps1.hydrogen.energy.gov/cfm/h2a_active_folder/h2a_production/04P_H2A_Hydrogen_Production_Model_User_Guide,_Version_2.pdf [Accessed September 2013].

Tan R. R., Aviso K. B., Barilea I. U., Culaba, A. B., Cruz, Jr. J. B. (2012) A fuzzy multi-regional input–output optimization model for biomass production and trade under resource and footprint constraints. *Applied Energy*, 90 (1), 154-60.

References

Tay, D. H. S., Ng, D. K. S., Sammons, N. E., Eden, M. R. (2011) Fuzzy optimization approach for the synthesis of a sustainable integrated biorefinery. *Industrial & Engineering Chemistry Research*, 50 (3), 1652-1665.

Tittmann, P. W., Parker , N. C., Hart, Q. J., Jenkins, B. M. (2010) A spatially explicit techno-economic model of bioenergy and biofuels production in California. *Journal of Transport Geography*, 18 (6), 715-728.

UKERC (2009) Decarbonising the UK energy system: accelerated development of low carbon energy supply technologies. **[**online]. Available from: www.ukerc.ac.uk/support/tiki-download_file.php?fileId=166 [Accessed September 2013].

UKPIA (2008) Briefing: Renewable Transport Fuels Obligation. **[**online]. Available from: http://www.ukpia.com/Libraries/Download/UKPIA-Briefing-Paper-RTFO.sflb.ashx [Accessed September 2013].

UNEP (2009) Towards sustainable production and use of biofuels: assessing biofuels. **[**online]. Available from: http://www.unep.org/pdf/Assessing_Biofuels-full_report-Web.pdf [Accessed September 2013].

Wallquist, L., Seigo, S. L., Visschers, V. H. M., Siegrist, M. (2012) Public acceptance of CCS system elements: a conjoint measurement. *International Journal of Greenhouse Gas Control*, 6, 77-83.

Wianwiwat, S. and Asafu-Adjaye, J. (2013) Is there a role for biofuels in promoting energy self-sufficiency and security? A CGE analysis of biofuel policy in Thailand. *Energy Policy*, 55, 543-555.

Wiesenthal, T., Leduc, G., Christidis, P., Schade, B., Pelkmans, L., Govaerts, L., Georgopoulos, P. (2009) Biofuel support policies in Europe: lessons learnt for the long way ahead. *Renewable & Sustainable Energy Reviews*, 13 (4), 789-800.

References

Winrock International (2009) The impact of expanding biofuel production on GHG emissions. [online]. Available from: http://www.indiaenvironmentportal.org.in/files/GHG_implications_biofuel_0.pdf [Accessed September 2013].

Wit, M., Junginger, M., Lensink, S., Londo, M., Faaij, A. (2010) Competition between biofuels: modeling technological learning and cost reductions over time. *Biomass & Bioenergy*, 34 (2), 203-217.

Yang, C., Ogden, J. (2007) Determining the lowest-cost hydrogen delivery mode. *International Journal of Hydrogen Energy*, 32 (2), 268-286.

You, F. Q., Wang, B. (2011) Life cycle optimization of biomass-to-liquid supply chains with distributed-centralized processing networks. *Industrial & Engineering Chemistry Research*, 50 (17), 10102-10127.

You, F., Tao, L., Graziano, D. J., Snyder, S. W. (2012) Optimal design of sustainable cellulosic biofuel supply chains: multiobjective optimization coupled with life cycle assessment and input–output analysis. *AIChE Journal*, 58 (4), 1157-1180.

Yu, Y., Bartle, J., Li, C., Wu, H. (2009) Mallee biomass as a key bioenergy source in Western Australia: importance of biomass supply chain. *Energy & Fuels*, 23 (6), 3290-3299.

Zamboni A., Murphy R. J., Woods J., Bezzo F., Shah N. (2011) Biofuels carbon footprints: whole-systems optimisation for GHG emissions reduction. *Bioresource Technology*, 102 (16), 7457-7465.

Zamboni, A., Shah, N., Bezzo, F. (2009a) Spatially explicit static model for the strategic design of future bioethanol production systems: 1. Cost minimisation. *Energy & Fuels*, 23, 5121-5133.

Zamboni, A., Bezzo, F., Shah, N. (2009b) Spatially explicit static model for the strategic design of future bioethanol production systems. 2. Multi-objective environmental optimization. *Energy & Fuels*, 23, 5134-5143.

References

Zhang, Y., McKechnie, J., Cormier, D., Lyng, R., Mabee, W., Ogino, A., MacLean, H. L. (2010) Life cycle emissions and cost of producing electricity from coal, natural gas, and wood pellets in Ontario, Canada. *Environmental Sciemce & Technology*, 44 (1), 538-544.